Some properties of maximum likelihood estimators of Weibull parameters with Type I censored data.

Finselbach, Hannah K

Some Properties Of Maximum Likelihood Estimators Of Weibull Parameters With Type I Censored Data

by

Hannah K Finselbach, BSc (University of Wales Swansea)

Thesis submitted to the University of Wales Swansea

in candidature for the degree of

PHILOSOPHIÆ DOCTOR

School of Business and Economics
University of Wales Swansea
Swansea SA2 8PP
United Kingdom

September 2007

Declaration

This work has not previously been accepted in substance for any degree and is not being concurrently submitted in candidature for any degree.

HANNAH K FINSELBACH
28 September 2007

Statement

This thesis is the result of my own investigation, except where acknowledgement of other sources is given.

HANNAH K FINSELBACH
28 September 2007

Statement

I hereby give consent for my thesis, if accepted, to be available for photocopying and for inter-library loan (subject to the law of copyright), and for the title and summary to be made available to outside organisations.

HANNAH K FINSELBACH
28 September 2007

Acknowledgements

First and foremost, I would like to thank my supervisor Dr. Alan Watkins. For your continual help and advice, I will be eternally grateful.

I would like to thank the EPSRC for their financial support, as well as my colleagues at ONS for the flexibility and understanding they have shown during the completion of this thesis.

Many thanks also go out to all of the friends I have made at the School of Business and Economics over the past few years for providing a sound and enjoyable environment to work in.

Finally, I would like to thank my family and friends for their constant encouragement and support.

HANNAH K FINSELBACH

University of Wales Swansea
September 2007

Summary

This thesis looks at extending previous work in the field of Type I censored reliability experiments. Due to its popularity and wide use, we use the Weibull distribution, and provide formulae on asymptotically valid variances and covariance of the maximum likelihood estimates and quantiles. We also examine the effect that sample size and censoring levels have on such properties. Theoretical results are validated with simulation studies throughout.

These results are then used to obtain measures of precision in the Weibull parameter and quantile estimates given the assumption of asymptotic Normality. The suitability of using this large sample Normal theory in finite samples is consequently studied, and we provide an alternative measure of precision using relative likelihood methods. Confidence regions for each method are compared using published data.

We investigate the concept of undertaking interim analysis of reliability data, where maximum likelihood estimates are calculated at successive times during an experiment, but the experiment is only stopped when adequate precision in the censored estimate is obtained. That is, when the censored estimate can provide a reliable guide to the complete estimate.

Finally we summarise our results and conclusions, and some ideas for future research are discussed.

To my family

Contents

List of Figures

List of Tables

Chapter 1

Introduction

This thesis is concerned with various aspects of the analysis of reliability data. We start with a brief description of reliability data, and summarise some of its unusual features.

Although data available for statistical analysis is typically regarded as fixed once collected, reliability analysis is an exception, as data generally accrues with time, and it is possible to conduct one or more interim analyses in addition to a final analysis; successive analyses are then based on increasing sample sizes. There is the additional feature that the status of items (for instance, whether operational or not) can vary with time, even when the sample size is fixed at the outset of an experiment.

The data collected for such reliability studies is a measure of use until failure of, say, n, similar items that are being tested under the same conditions. Throughout this thesis, as in the wider literature, we will refer to the *time to failure*, even though the actual measurement may relate to some other aspect of use, such as the number of operations, breaking strength, or the number of complete cycles. We note here the underlying assumption that items are entered to the trial at the same time (*at time* 0).

Examples of such data include, the lifetimes of electrical insulators, remission times related to a drug for treating cancer, and the number of revolutions until failure of ball bearings. It is usual for these times to failure to be modelled, and some commonly used lifetime distributions have been developed, as will be discussed later. The motivation and emphasis of these studies are usually not simply to estimate the model parameters, but other, related factors such as failure rates, quantiles and probabilities are of interest. In practical terms, these can be interpreted by, say, a probability that an item survives beyond a time, t, or the determination of guarantee periods.

Reliability data is also commonly known as life data, failure-time data, and survival data, and there are numerous texts and journals that cover all aspects of the analysis; some of these are listed in Table 1.1. In the 1950's and 1960's reliability engineering advanced, mainly due to rapid advances in technology and application in a military setting, or with increasing customer expectations. Nelson (1982) gives some applications of reliability studies to many fields other than engineering and manufacturing, such as economists studying the length of

Reliability Journals
Technometrics (1959-present)
IEEE Transactions in Reliability (1961-present)
Reliability Engineering & System Safety (1981-present)
Int. Journal of Reliability, Quality and Safety Engineering (1994-present)
Lifetime Data Analysis (1996-present)
Other journals
Journal of the Royal Statistical Society (1887-present)
Journal of the American Statistical Society (1888-present)
Biometrika (1901-present)
Books
Methods of Statistical Analysis of Reliability and Life Data, Mann et al. (1974)
The Statistical Analysis of Failure Time Data, Kalbfleisch & Prentice (1980)
Statistical Models and Methods of Lifetime Data, Lawless (1982)
Applied Life Data Analysis, Nelson (1982)
Statistical Analysis of Reliability Data, Crowder et al. (1991)
Practical Methods for Reliability Analysis, Ansell & Phillips (1994)

Table 1.1: Key journals and texts in the field of reliability data

time people are in the workforce; wildlife managers using mortality tables to predict wildlife population sizes and determine hunting seasons; or the success of medical treatments of certain diseases being measured by the length of patient survival. Insurance companies have long used actuarial methods to estimate survivorship of both medical patients and various equipment.

Many other examples of the use of reliability analysis are discussed in publications listed in Table 1.1, and key contributions also appear in more mainstream statistical journals.

Like other areas of statistics, reliability analysis is concerned with estimates and confidence limits for population parameters, and with predictions and prediction limits for future items and samples. However, in reliability, the practitioner has some influence on the nature of data to be analysed, as experiments are often stopped before all items have failed, and so the data are incomplete in some way. The analyst then uses the information in the (unfinished or *censored*) lifetimes of survivors as well as the information in the observed times to failure.

We next briefly review the practice of censoring.

1.1 Censored Data

Censoring is common in reliability because of time limits or other restrictions on data collection. To allow all of the items in some reliability studies to fail can often take a great deal of time, and could therefore be a very expensive process. Although some information is lost during a censoring regime, often the loss is small compared with the time or money saved (and it is always better - in statistical terms - to know the individual failure times of

17.88	28.92	33.00	41.52	42.12	45.60
48.48	51.84	51.96	54.12	55.56	67.80
68.64	68.64	68.88	84.12	93.12	98.64
105.12	105.84	127.92	128.04	173.40	

Table 1.2: Lifetimes (in millions of revolutions) of 23 ball bearings; from Lieblein and Zelen (1956)

each item in the sample).

Two common censoring techniques (Type I and Type II) are described below, and a more detailed discussion can be found in Cohen (1991). In this thesis we will be primarily interested in Type I censoring.

1.1.1 Example of Complete and Censored Data

Table 1.2 shows the lifetimes (in millions of revolutions) of $n = 23$ ball bearings. The data was introduced by Lieblein & Zelen (1956) and has been widely discussed by others, including Kalbfleisch (1979); Caroni (2002) reports that the famous data set is misquoted, and proposes corrections, but we will analyse the data as originally presented. In particular, we will use this data set to illustrate the different types of censoring, and also, in later sections, as an example of fitting the Weibull distribution to sample data. We note here that, historically, relatively few real life data sets were published in the field of reliability, probably due to commercial confidentiality restrictions.

Type I Censoring

Type I, sometimes referred to as "time censoring", is used to describe an experiment that will end at a prespecified time, c, and lifetimes will only be known for those items that have failed by time c - the remaining (surviving) items will have a censored failure time equal to the stopping time c. In the ball bearing failure times, if we had stopped the experiment at time, $c = 70$, instead of allowing all of the items to fail, then the Type I censored sample would be as follows

17.88	28.92	33.00	41.52	42.12	45.60
48.48	51.84	51.96	54.12	55.56	67.80
68.64	68.64	68.88	70*	70*	70*
70*	70*	70*	70*	70*	

where, as is conventional, the starred values denote the censored times.

This technique has the advantage that time duration of the experiment is fixed from the onset, and thus can be planned practically, but the number of items that will fail, M say, is random, and so may be less useful statistically if there are too few failure times to analyse.

Type II Censoring

A Type II censored sample is one for which only the first m failure times of a random sample of n items are observed. The number of observations, m, is decided before the data is collected, and the time of failure of the m^{th} item is then recorded as the censored time of failure for the remaining $n - m$ items. Using the ball bearing data again, and suppose that we choose $m = 15$; then the Type II censored sample would be

17.88	28.92	33.00	41.52	42.12	45.60
48.48	51.84	51.96	54.12	55.56	67.80
68.64	68.64	68.88	68.88*	68.88*	68.88*
68.88*	68.88*	68.88*	68.88*	68.88*	

where again the starred values denote the censored times. Here, there is the statistical advantage that the number of failures is known in advance of the analysis, but the duration of the experiment is not known, and therefore less favorable in practical terms, as the experiment may be more difficult to plan and monitor.

We will be investigating when we could, in theory, or should, in practice, censor in such a way to maximise the practical benefits while minimising the loss of statistical information arising from curtailing an experiment or trial in some way.

The above summary has already indicated some random aspects of experiments and the data generated from them, and it is now appropriate to review briefly some of the mathematical funcations, and statistical background which we will use when discussing these aspects in further detail.

1.2 Mathematical Functions

We will use various properties of well-known mathematical functions in the discussion in this thesis, and refer to Abramowitz & Stegun (1972) and Gradshteyn & Ryzhik (2000) for further details.

1.2.1 Gamma and related functions

Gamma Function

The gamma function is denoted by Γ, and defined by

$$\Gamma(z) = \int_0^\infty t^{z-1} \exp(-t) dt \tag{1.1}$$

or, equivalently,

$$\Gamma(z+1) = \int_0^\infty t^z \exp(-t) dt. \tag{1.2}$$

The gamma function satisfies the recurrence relationship

$$\Gamma(z+1) = z\Gamma(z) \tag{1.3}$$

and, for integer z, we have

$$\Gamma(z+1) = z!. \tag{1.4}$$

Psi (Digamma) Function

The psi function is the derivative of the natural logarithm of the gamma function, and is given by

$$\Psi(z) = \frac{d\ln\Gamma(z)}{dz} = \frac{\Gamma^{(1)}(z)}{\Gamma(z)} \tag{1.5}$$

Some important results are

$$\Psi(z+1) = \Psi(z) + \frac{1}{z} \tag{1.6}$$

for $z > 0$, and

$$\Psi(1) = -\gamma \tag{1.7}$$

where $\gamma = 0.577215\cdots$ is called Euler's constant.

Incomplete Gamma Function

The incomplete gamma function arises in the context of Type I censored data and is defined as

$$\gamma(z,x) = \int_0^x t^{z-1}\exp(-t)\,dt, \tag{1.8}$$

and as $x \to \infty$, the incomplete Gamma function tends to the Gamma function. It also satisfies the recurrence relationship

$$\gamma(z+1,x) = z\gamma(z,x) - x^z\exp(-x). \tag{1.9}$$

We use the following notation for derivatives:

$$\gamma^{(j)}(z,x) = \frac{d^j\gamma(z,x)}{dz^j}. \tag{1.10}$$

Beta and Incomplete Beta function

The beta function is defined in terms of the gamma function as

$$B(a,b) = \frac{\Gamma(a)\Gamma(b)}{\Gamma(a+b)}, \tag{1.11}$$

and can be written as the integrals

$$B(a,b) = \int_0^1 t^{a-1}(1-t)^{b-1}dt = \int_0^\infty \frac{t^{a-1}}{(1+t)^{a+b}}dt.$$

The incomplete beta function is defined as

$$B_x(a,b) = \int_0^x t^{a-1}(1-t)^{b-1}dt, \tag{1.12}$$

for $0 \leq x \leq 1$.

1.2.2 Hypergeometric functions

The generalised hypergeometric function is defined as

$$F_{p,q}(a_1,...,a_p;b_1,...,b_q;z) = \sum_{k=0}^{\infty} \frac{(a_1)_k...(a_p)_k}{(b_1)_k...(b_q)_k}\frac{z^k}{k!} \tag{1.13}$$

where $(x)_k$ is Pochhammer's symbol for the product of k successive integers starting at x_j, in terms of gamma functions we have

$$(x)_k = \frac{\Gamma(x+k)}{\Gamma(x)}. \tag{1.14}$$

A specific case of (1.13), often used has $p = 2$, $q = 1$; which is

$$F_{2,1}(a_1,a_2;b_1;z) = \frac{\Gamma(b_1)}{\Gamma(a_1)\Gamma(a_2)} \sum_{k=0}^{\infty} \frac{\Gamma(a_1+k)\Gamma(a_2+k)}{\Gamma(b_1+k)}\frac{z^k}{k!}. \tag{1.15}$$

Further properties and results on the generalised hypergeometric function can be found in Slater (1966).

1.2.3 Order statistics

We arrange a random sample $Y_1, Y_2, ..., Y_n$ into ascending order. We write $Y_{(1:n)} = \min_i\{Y_i\}$, and $Y_{(n:n)} = \max_i\{Y_i\}$, with corresponding definitions for

$$Y_{(1:n)} \leq Y_{(2:n)} \leq ... \leq Y_{(n-1:n)} \leq Y_{(n:n)}$$

in which we refer to $Y_{(i:n)}$ as the i^{th} order statistic.

Order statistics occur naturally in Type II censored samples (and hence make relatively few appearances in this thesis), as the sample consists of the m smallest lifetimes (i.e., the first m order statistics)

$$Y_{(1:n)} \leq Y_{(2:n)} \leq ... \leq Y_{(m:n)},$$

which will each have their own distribution, depending on their order, whilst the remaining

$n-m$ will be censored with distribution function equal to $Y_{(m:n)}$. Balakrishnan & Rao (1997) and David & Nagaraja (2003) give discussions, further properties, and results on order statistics.

1.3 Statistical Background

1.3.1 General Concepts

Let Y be a continuous random variable representing the time to failure, so $Y \geq 0$. The probability density function (pdf) $f(y)$ of Y is defined via

$$\Pr\{t < Y < t + dt\} = \int_t^{t+dt} f(y)dy \simeq f(t)dt, \tag{1.16}$$

for $t \geq 0$, and the cumulative distribution (cdf), F of Y, which is based on aggregating probabilities, is given by

$$F(t) = \Pr\{Y \leq t\} = \int_0^t f(y)dy, \tag{1.17}$$

again for $t \geq 0$.

Any reliability distribution can also be characterised by its survivor function, $S(t)$, and the hazard function, $h(t)$. The survival function is the probability that an individual survives at least time t, so that

$$S(t) = 1 - F(t), \tag{1.18}$$

for $t \geq 0$. The hazard (or instant hazard) function is defined in terms of the probability that, given its survival until t, an item then fails in the interval $(t, t+dt)$. Since this probability is, via the conditioning argument,

$$\frac{f(t)dt}{1-F(t)} = \frac{f(t)dt}{S(t)},$$

we see that

$$h(t) = \frac{f(t)}{S(t)}; \tag{1.19}$$

Thus the hazard function is sometimes called a "conditional failure rate", since the denominator reflects the conditional probability given survival to time t. The cumulative hazard function is given by

$$H(t) = \int_0^t h(u)du \tag{1.20}$$

from which

$$S(t) = \exp\{-H(t)\}. \tag{1.21}$$

In a reliability context, the discussion will often focus on the time by which a percentage p of the population has failed. The $100p^{th}$ percentile of the distribution of Y is defined by

$$B_{100p} = F^{-1}(p), \tag{1.22}$$

which introduces the quantile function of Y, as the inverse of its cdf.

The 10^{th} percentile B_{10} concentrates on early failures, and is commonly used in engineering. Of more interest in medical statistics is the median, or the 50^{th} percentile, which gives the time at which half the observations or items have failed.

1.4 Lifetime Models

1.4.1 Negative Exponential Distribution

The negative exponential distribution is the simplest distribution used in the analysis of reliability data, and is a popular choice for some types of electronic components, for example capacitors. For parameter θ (> 0), it has pdf

$$f(y;\theta) = \frac{1}{\theta}\exp\left\{-\left(\frac{y}{\theta}\right)\right\} \tag{1.23}$$

and cdf,

$$F(y;\theta) = 1 - \exp\left\{-\left(\frac{y}{\theta}\right)\right\}.$$

The negative exponential distribution hazard function is constant, given by

$$h(y;\theta) = \frac{1}{\theta},$$

so that the cumulative hazard function has the form

$$H(y;\theta) = \frac{y}{\theta}.$$

It is straight forward to obtain the mean and variance of a negative exponential random variable, Y as

$$E[Y] = \theta,$$

and

$$Var(Y) = \theta^2.$$

Finally, the quantile function is

$$B_{100p} = -\theta \ln(1-p); \tag{1.24}$$

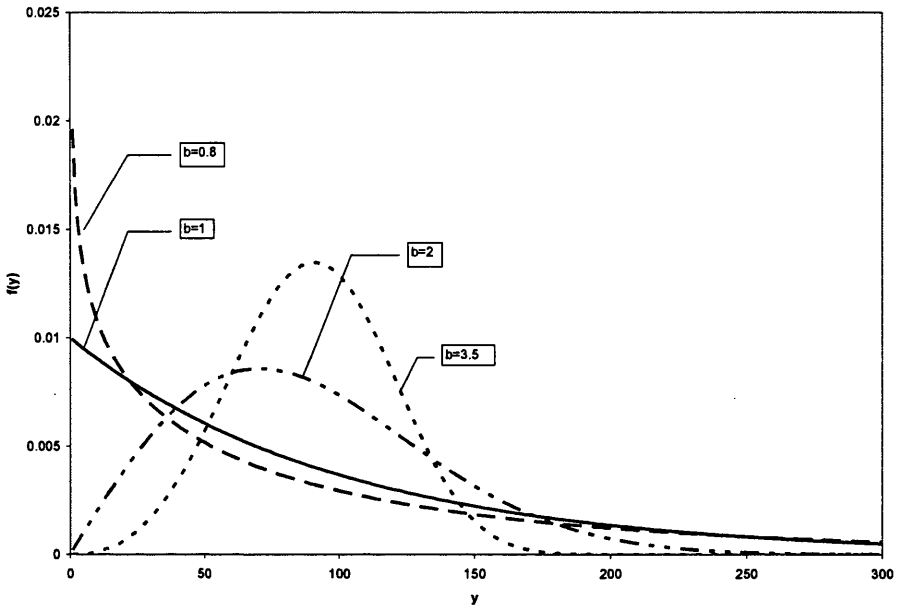

Figure 1.1: Weibull pdf for varying β; $\theta = 100$.

here, as throughout this thesis, $\ln(x) \equiv Log_e(x)$ denotes the natural logarithm of the positive quantity x.

The negative exponential distribution also has the unique lack of memory property; in practical terms, future failures are not influenced by survival to the present.

1.4.2 Weibull Distribution

The Weibull distribution, see Weibull (1951), is the most frequently used lifetime distribution model in all areas of engineering (Ansell & Phillips, 1994), and is also widely used in biomedical applications; see Gross & Clark (1975). With scale parameter θ, and shape parameter β (both positive), the Weibull distribution has pdf

$$f(y;\theta,\beta) = \beta\theta^{-\beta}y^{\beta-1}\exp\left\{-\left(\frac{y}{\theta}\right)^{\beta}\right\} \tag{1.25}$$

for which the corresponding cdf is,

$$F(y;\theta,\beta) = 1 - \exp\left\{-\left(\frac{y}{\theta}\right)^{\beta}\right\}. \tag{1.26}$$

Figure 1.1 shows (1.25) for various values of β, and indicates that this distribution can model a large variety of data and life characteristics, as simply changing the value of β affects the shape of the distribution.

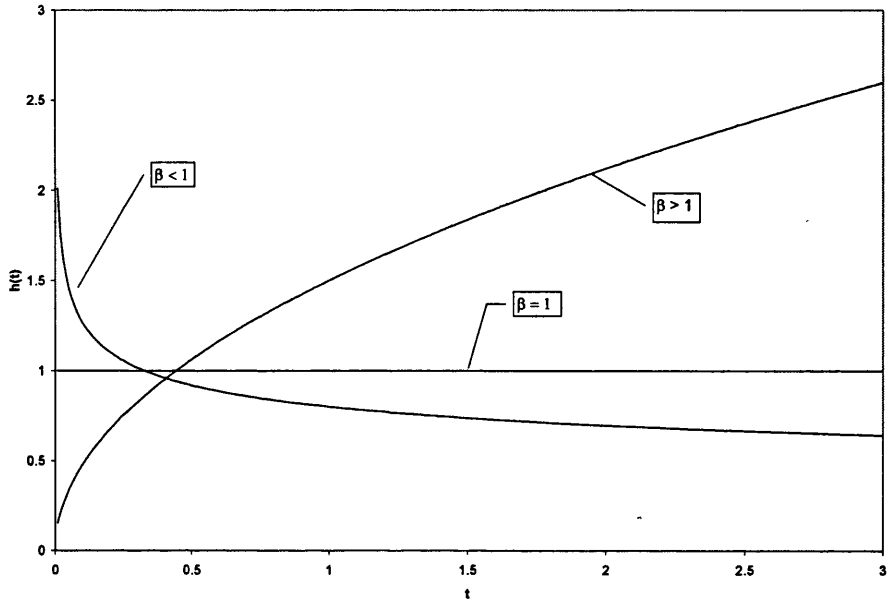

Figure 1.2: Weibull hazard function for varying β; $\theta = 1$.

Wolstenholme (1999) notes that the variance of the Weibull random variable is inversely related to β; from Figure 1.1 we can see that there is less variability in the distribution for larger values of β. The hazard function for the Weibull distribution is defined as

$$h(y;\beta,\theta) = \frac{\beta y^{\beta-1}}{\theta^{\beta}} \tag{1.27}$$

and, via (1.20), we obtain the cumulative hazard function

$$H(y;\beta,\theta) = \left(\frac{y}{\theta}\right)^{\beta}. \tag{1.28}$$

The expression for the hazard function shows that the shape parameter β also determines whether the hazard function is an increasing $(\beta > 1)$, a constant $(\beta = 1)$, or a decreasing $(\beta < 1)$ function of time y, and we illustrate the Weibull hazard function in these three cases in Figure 1.2.The mean and variance of a Weibull random variable can be expressed in terms of the Gamma function, (1.2), as

$$E[Y] = \theta\Gamma\left(1+\frac{1}{\beta}\right),$$

and

$$Var(Y) = \theta^2\left[\Gamma\left(1+\frac{2}{\beta}\right) - \Gamma^2\left(1+\frac{1}{\beta}\right)\right].$$

Finally, the quantile function for the Weibull distribution takes the form

$$B_{100p} = F^{-1}(p) = \theta\{-\ln(1-p)\}^{\frac{1}{\beta}}. \tag{1.29}$$

The Weibull distribution has received considerable attention - and, compared to other reliability distributions, has been applied to many reliability problems, particularly dealing with material strength and durity. Some examples for the use of this distribution are the analysis of failure in electronic components, ball bearings, motors and capacitors, and various biological organisms situations, as well as for the study of breaking strength and fatigue in textiles.

It is clear that the negative exponential distribution is equivalent to the Weibull distribution with parameter $\beta = 1$. As well as the negative exponential distribution, we also know that the Weibull distribution includes the Rayleigh distribution as a special case (when $\beta = 2$), and we have an approximately Normal distribution when $\beta = 3.5$; see Mann et al. (1974) for further discussion.

1.4.3 Alternative Reliability Distributions

In addition to the Weibull and its related distributions there are many other lifetime models, some of which are described briefly below; see Richards & McDonald (1987) for further details.

The Burr XII distribution

The three-parameter Burr XII distribution, introduced by Burr (1942) has cdf

$$F(y;\tau,\alpha,\phi) = 1 - \left\{1 + \left(\frac{y}{\phi}\right)^{\tau}\right\}^{-\alpha}$$

for $y > 0$, where the positive parameters α and τ control the shape of the distribution and $\phi > 0$ is a scale parameter. The Burr XII distribution has the property of including the Weibull model as a limiting case; see Watkins (2001).

The Extreme Value distribution

The Extreme Value distribution has cdf

$$F(u;\varepsilon,\delta) = 1 - \exp\{-\exp[(u-\varepsilon)/\delta]\}$$

for $-\infty \leq u \leq \infty$, with location parameter $\infty \leq \varepsilon \leq \infty$ and positive scale parameter δ. This distribution is closely connected with the Weibull distribution; if Y has a Weibull distribution,

$$U = \ln(Y)$$

has an extreme value distribution. For further details on the relationship between Weibull and Extreme Value parameters, see Nelson (1982).

The Lognormal distribution

This distribution is closely related to the Normal distribution, in the sense that if $\ln(Y)$ is Normally distributed, then Y follows a lognormal distribution with cdf

$$F(y;\mu,\sigma) = \Phi\left(\frac{\ln y - \mu}{\sigma}\right)$$

for $y \geq 0$, where Φ is the usual standard Normal cdf. This distribution is often useful if the range of data is several powers of 10, and thus has a large range of applications (see Johnson et al., 1994). Of particular interest is its use for certain types of life data, for example metal fatigue and electrical insulation life.

1.5 Modelling Lifetime Distribution

The first step in the process of modelling reliability data is identifying a suitable model. Model selection is often based upon graphical representation of the sample data, and advice on the choice of model is given in Chapter 1 of Lawless (1982).

In practice, the parameters of the distribution being fitted are usually unknown, and so an estimate must be calculated from the sample. A good estimator has to be consistent and efficient in giving valid and precise estimates in practice (ideally, we require the estimator to be unbiased, and to have the smallest possible variance). Several methods for estimating distribution parameters have been established, such as methods of moments, maximum likelihood, least squares, and Bayes estimator; see Mann et al. (1974) for an overview of estimation methods.

1.5.1 Maximum Likelihood Estimation

We will be using the method of maximum likelihood estimation for the reasons as discussed in Crowder et al. (1991), namely the method's generality and relative ease of programming computation. Many texts also agree that, for small samples, the maximum likelihood estimates generally compare well with other estimates; see Nelson (1982), for instance. As well as reliability analysis, maximum likelihood extends to most statistical topics, including areas like time series, categorical data analysis, variance components, spatial analysis, to name a few. The properties of maximum likelihood estimates (from now on referred to as MLEs) will be discussed in further detail in succeeding Chapters, with particular emphasis on asymptotic Normality. We note here that the asymptotic covariance matrix of the MLEs is easily obtainable, as it is the inverse of the expected Fisher information matrix, where elements are based on expected values of second partial derivatives of the log-likelihood

function. We discuss this further in the following chapter, and refer to Cox & Hinkley (1974) for a detailed discussion of MLE properties.

However, in many cases, the analyst has to deal with small or moderate samples, and here, such large sample theory results may not hold. The bias and standard deviation of these small data sets may be larger than such results would imply, and as we will see in Chapter 2, these will also depend on the size and censoring level applied to the sample. Ross (1996) discusses two methods to reduce the bias of the Weibull shape parameter MLE, $\hat{\beta}$, as well as defining an "Asymptotic Function", that measures the difference between expected values of estimators from finite and infinite sample size. Encouragingly, however, the overall conclusion is that the maximum likelihood methods provide a good fit to Weibull data, even for small samples and censored data.

1.6 Computational issues

We use SAS for most computational tasks related to the generation and analysis of data. In particular, by writing a suitable algorithm in the statistical software package SAS, (see Der & Everitt, 2002), we can simulate observed values from reliability distributions using the quantile function

$$y_i = F^{-1}(u_i),$$

where the u_i are independently and uniformly distributed on $[0, 1]$. Thus, to simulate a set of data from the Weibull distribution with known specified parameters β and θ, we use (1.29) and compute

$$y_i = \theta(-\ln[1 - u_i])^{\frac{1}{\beta}} \tag{1.30}$$

Using further SAS/IML® commands we can then apply a censoring regime to generalised data, and then compute the maximum likelihood estimates at successive censoring levels, and also when all simulated items have failed, *i.e.* after the last failure time, when the data set is complete. In order to obtain robust results and conclusions when assessing agreement with asymptotic results, our simulation exercises are based on 10,000 replications. Consequently the production of 10,000 replications, particularly for large sample sizes greater than 1000, say, can take up to six hours to run for each set of parameter values. More information on SAS/IML® can be found in SAS (2004).

Throughout this thesis we will need to maximise functions based on likelihoods, where no analytical solutions are available. We will therefore need to employ a numerical method to perform the maximisation. Our approach is to use the Newton-Raphson computational procedure. Although other methods are available, this is a straightforward iterative process that is easily programmable in SAS/IML®. More details are given in relevant sections.

Mathematica will also be used to evaluate some of the assumptions made in our theoretical considerations. Further details and specific code are given in relevant sections.

1.7 Structure of thesis

In this chapter we have briefly reviewed the background theory required for analysing reliability data using reliability distributions to model the time to failure. We have discussed the practical considerations, and the censoring techniques used to overcome these problems in experiments. In Chapter 2, we will outline the method of maximum likelihood estimation and use this to fit the Weibull distribution to complete and censored data.

This thesis will consider three distinct problems regarding ML estimation under a Type I censoring regime:

- The property of asymptotic Normality of MLEs is well known, see Nelson (1982), for example, and can be used to obtain approximate confidence limits around parameters. Chapter 3 will find the extent to which the assumption of Normality of Weibull parameters and B_{10} are suitable for finite samples, in particular smaller and Type I censored data sets. We are interested in the effects of varying the censoring level on the convergence to asymptotic Normality.

- For the asymptotic theory to give good approximations, the sample, n, should be large, but for practical purposes, in general, the asymptotic methods are applied to small samples. In Chapter 4 we introduce an alternative method to measure the precision of the Weibull MLEs, that intuitively, may be more suitable for small, or highly censored samples.

- Chapter 5 will establish a method to measure the precision of Type I censored MLEs as estimates of the complete MLEs, and investigate the use of information from interim analyses, to predict the complete estimate. For simplicity, we will initially concentrate on the negative exponential distribution, and Chapter 6 will extend the methods developed for this case to the Weibull distribution, which has the added complications of an extra parameter and the quantile function B_{10}.

Chapter 2

Maximum Likelihood Estimation in the Weibull Distribution

2.1 Introduction

This Chapter details the method of maximum likelihood, specifically for the Weibull distribution. We also demonstrate how the size and nature of the data being analysed can affect the accuracy and precision of the MLEs.

Since we will not, in general, be able to study the sampling distribution of the MLE analytically, we must in practice either

- use asymptotic theory, from which the MLE is regarded as Normally distributed about the true, unknown parameter, with variance-covariance matrix given by the Expected Fisher information (as will be discussed in further detail, below), or
- use some alternative approach, such as the method of relative likelihood; see for instance, Kalbfleisch (1979).

2.2 The Method of ML in Complete Samples

We first outline the framework for fitting models from the Weibull distribution, and then apply this method to an example. Likelihood may be defined as the joint pdf based on a specified distribution at the observed sample points. The MLEs of the parameters are the values that maximise the likelihood function, or equivalently the natural logartihm of the likelihood function (the log-likelihood). From (1.25), the likelihood for a complete data set $y_1, y_2, ..., y_n$ is

$$L = \prod_{i=1}^{n} f(y_i; \beta, \theta) = \left(\beta\theta^{-\beta}\right)^n \left(\prod_{i=1}^{n} y_i\right)^{\beta-1} \exp\left(-\theta^{-\beta}\sum_{i=1}^{n} y_i^{\beta}\right) \tag{2.1}$$

and the log-likelihood is

$$l = n\ln\beta - n\beta\ln\theta + (\beta-1)\sum_{i=1}^{n}\ln y_i - \theta^{-\beta}\sum_{i=1}^{n} y_i^{\beta}. \tag{2.2}$$

It is convenient to define,

$$S_e = \sum_{i=1}^{n}\ln y_i,$$

and

$$S_j(\beta) = \sum_{i=1}^{n} y_i^{\beta}(\ln y_i)^j \tag{2.3}$$

for integer $j \geq 0$, taking $0^0 = 1$ if necessary, and note that for $j \geq 1$ we have

$$S_j(\beta) = \frac{d^j S_0(\beta)}{d\beta^j} = \frac{dS_{j-1}(\beta)}{d\beta}.$$

Then (2.2) can be written as

$$l = n\ln\beta - n\beta\ln\theta + (\beta-1)S_e - \theta^{-\beta}S_0(\beta).$$

We then find the partial derivatives of l to be

$$\frac{\partial l}{\partial\beta} = n\beta^{-1} - n\ln\theta + S_e + \theta^{-\beta}\ln\theta S_0(\beta) - \theta^{-\beta}S_1(\beta), \tag{2.4}$$

and

$$\frac{\partial l}{\partial\theta} = -n\beta\theta^{-1} + \beta\theta^{-(\beta+1)}S_0(\beta). \tag{2.5}$$

2.2.1 Profile likelihood and an iterative method

There are no analytical solutions to these equations, but, we can equate (2.5) to zero, and then solve for θ in terms of β. This gives

$$\tilde{\theta} = \left(n^{-1}S_0(\beta)\right)^{1/\beta}. \tag{2.6}$$

We can now substitute (2.6) into (2.2) and (2.4) to obtain the *profile* log-likelihood, denoted with an asterisk,

$$l^* = n\ln\beta - n\ln S_0(\beta) + n(\ln n - 1) + (\beta-1)S_n \tag{2.7}$$

with first derivative

$$\frac{dl^*}{d\beta} = n\beta^{-1} + S_n - n\left(\frac{S_1(\beta)}{S_0(\beta)}\right), \tag{2.8}$$

and second derivative

$$\frac{d^2l^*}{d\beta^2} = -n\beta^{-2} - n\left\{\frac{S_0(\beta)S_2(\beta) - S_1(\beta)^2}{[S_0(\beta)]^2}\right\}. \tag{2.9}$$

We can now solve equation (2.7) for $\hat{\beta}$ using the Newton-Raphson iteration method, with a starting value $\beta^{[0]}$ "close" to the ML estimate in order for the method to converge. Farnum & Booth (1997) suggest

$$\beta^{[0]} = 2\left(\ln(y_{(n:n)}) - n^{-1}S_e\right)^{-1} \tag{2.10}$$

as an initial starting value. The iterative process is outlined below:

- Calculate the next approximation to β

$$\beta^{[1]} = \beta^{[0]} - \frac{\frac{dl^*(\beta^{[0]})}{d\beta}}{\frac{d^2l^*(\beta^{[0]})}{d\beta^2}} \tag{2.11}$$

- Repeat this step replacing $\beta^{[k]}$ with $\beta^{[k+1]}$, and continue repeating this until convergence is achieved. We stop when successive values are close together, when $\frac{dl^*(\beta)}{d\beta}$ is close to 0.

We can then substitute our estimate $\hat{\beta}$ into (2.6), and solve for $\hat{\theta}$.

2.2.2 Example: Ball bearings data

We now obtain the Weibull MLEs for the Ball Bearings dataset; see Table 1.2. For the $n = 23$ failure times, the above procedure, using

$$\beta^{[0]} = 1.9898$$

yields convergence in five iterations (see Table 2.1) to

$$\hat{\beta} = 2.1021,$$

which consequently gives

$$\hat{\theta} = 81.8783,$$

and together these allow us to calculate, using (1.29), the 10^{th} percentile

$$\hat{B}_{10} = 28.0694. \tag{2.12}$$

Table 2.1 shows the rate at which the profile score function reaches zero.

Iteration	$\hat{\beta}$	$\frac{dl^*}{d\beta}$	$\frac{d^2l^*}{d\beta^2}$
1	1.9898	1.07968	−9.9891
2	2.0978	0.03905	−9.2820
3	2.1021	0.00005	−9.2563
4	2.1021	1.042×10^{-10}	−9.2562
5	2.1021	0	−9.2562

Table 2.1: Summary of iterations for fitting the Weibull distribution to the Ball Bearings data

1.2	7.0	23.9	47.9	62.7	95.1	128.7	151.6	185.2	253.1
2.2	12.1	24.3	48.4	72.4	97.9	133.6	152.6	187.1	304.1
4.9	13.7	25.1	49.3	73.6	99.6	144.1	164.2	203.0	341.7
5.0	15.1	35.8	53.2	76.8	102.8	147.6	166.8	204.3	354.4
6.8	15.2	38.9	55.6	83.8	108.5	150.6	178.6	229.5	

Table 2.2: 49 failure times, given in Epstein (1960), thought to follow a negative exponential distribution

2.2.3 Example: Epstein's Data (49 failure times)

Finselbach & Watkins (2006) consider a dataset of 49 failure times, originally discussed by Epstein (1960), and displayed in Table 2.2. The failure times (unit unknown) are thought to follow a negative exponential distribution, and so, if we were to perform Weibull analysis, we would expect an estimate of β to be approximately 1. With a starting value for the Newton-Raphson method being

$$\beta^{[0]} = 0.6667$$

the MLE analysis outlined above provides us with the following estimates,

$$\hat{\beta} = 1.0300,$$

$$\hat{\theta} = 106.0505$$

and

$$\hat{B}_{10} = 11.9312. \tag{2.13}$$

Table 2.3 summarises the iteration process, and we see that we have convergence to $\hat{\beta}$ after just 6 iterations. We remark that $\hat{\beta}$ is appropriately close to 1, and we can compare the estimate of θ to the value calculated in Finselbach & Watkins (2006) using the exponential analysis, $\hat{\theta} = 104.89$ (for which $\hat{B}_{10} = 11.0513$). It may be of interest to perform some formal goodness of fit tests for the suitability of fitting the Weibull distribution to this data, but such considerations will be omitted here as the purpose is simply to illustrate the procedure of obtaining the MLEs.

Iteration	$\hat{\beta}$	$\frac{dl^*}{d\beta}$	$\frac{d^2l^*}{d\beta^2}$
1	0.6667	35.8643	−144.0329
2	0.9157	8.6381	−83.4887
3	1.0191	0.7521	−69.6338
4	1.0299	0.0067	−68.4059
5	1.0300	5.314×10^{-7}	−68.395
6	1.0300	0.0000	−68.395

Table 2.3: Summary of iterations for fitting the Weibull distribution to Epstein's 49 Failures data

2.2.4 Simulation: Fitting a Weibull Distribution to Weibull Data

So far we have looked at two examples of failure data and fitted a Weibull distribution to them, but there are limitations when analysing single sets of data. We want to investigate the effect of censoring and sample size on the bias and standard deviations of the estimates, and therefore require a simulation study to enable the study of the sampling distribution of $\left(\hat{\beta}, \hat{\theta}\right)$, with known true parameters β and θ.

The Weibull parameters are set at

$$\beta = 2, \quad \theta = 100,$$

and we run the program for $n = 50, 100, 300, 500$, and 1000. The process is then repeated 10,000 times. We can compare the estimated value $\widehat{B}_{10}$, obtained from the MLEs $\hat{\theta}$ and $\hat{\beta}$, with the true value calculated below:

$$B_{10} = 100\{-\ln(0.9)\}^{\frac{1}{2}} = 32.4593 \tag{2.14}$$

Results for the complete sample are summarised in Table 2.4.

We observe excellent agreement between the true and estimated parameter values, and this improves as n increases. It is also clear that the precision of the MLEs improve as n gets bigger. Following from these results on the moments of MLEs, we note that it would be of interest to investigate the distribution of the Weibull MLEs and $\hat{B}_{10}$, for both large samples (where the asymptotic properties, such as the variance, are known), and smaller samples (to see the extent to which the asymptotic Normality can be regarded appropriate). This will be addressed in Chapter 3.

2.3 The Method of ML in Type I Censored Samples

As outlined in section 1.1, an experiment terminated at some prespecified time, c, say, is subject to Type I censoring, and we only have the exact lifetimes $y_1, ...y_M$ of the m items that have failed before c, with the other $n - m$ items having a censored operational life of

n	50	100	300	500	1000
$\widehat{\beta}$: *mean*	2.0553	2.0269	2.0093	2.0053	2.0026
(*st.dev.*)	(0.2341)	(0.1600)	(0.0905)	(0.0705)	(0.0496)
$\widehat{\theta}$: *mean*	99.8834	99.9956	99.9783	99.9766	100.0301
(*st.dev.*)	(7.3980)	(5.3344)	(3.0623)	(2.3614)	(1.6666)
$\widehat{B}_{10}$: *mean*	33.2983	32.8945	32.6048	32.5382	32.5113
(*st.dev.*)	(5.3652)	(3.7956)	(2.1688)	(1.6763)	(1.1852)

Table 2.4: MLE summaries for the Weibull distribution fitted to simulated Weibull complete data with $\beta = 2, \theta = 100$

c. Thus, M (> 0), is a random variable, with

$$\Pr\{\text{any item fails in } (0,c)\} = 1 - \exp\left\{-\left(\frac{c}{\theta}\right)^{\beta}\right\} = q_c, \tag{2.15}$$

say, so that M follows a binomial distribution with parameters n and q_c. The observed times to failure Y, follow the truncated Weibull distribution with pdf

$$\frac{\beta y^{\beta-1}}{\theta^{\beta} q_c} \exp\left\{-\left(\frac{y}{\theta}\right)^{\beta}\right\} \tag{2.16}$$

for $0 \leq y \leq c$. We point out here that letting $c \to \infty$ will lead to a complete sample, with $M = n$, and $q_c = 1$.

2.3.1 The Likelihood and fitting a Weibull distribution to censored data

Without loss of generality, the likelihood for Weibull data under a Type I censoring regime is

$$L_c = \left[\prod_{i=1}^{M} \beta\theta^{-\beta} Y_i^{\beta-1} \exp\left\{-Y_i^{\beta}\theta^{-\beta}\right\}\right] \prod_{i=1}^{n-M} \exp\left\{-c^{\beta}\theta^{-\beta}\right\} \tag{2.17}$$

Taking logarithms of (2.17), the log-likelihood for censored Weibull data is

$$l_c = M\ln(\beta) - M\beta\ln(\theta) + (\beta-1)\sum_{i=1}^{M}\ln(Y_i) - \theta^{-\beta}\left\{\sum_{i=1}^{M} Y_i^{\beta} + (n-M)\,c^{\beta}\right\} \tag{2.18}$$

We now find it convenient to define

$$S_{M,e} = \sum_{i=1}^{M} \ln Y_i,$$

and

$$S_{M,j}(\beta) = \sum_{i=1}^{M} Y_i^{\beta}(\ln Y_i)^j + (n-M)\,c^{\beta}(\ln c)^j$$

for integer $j \geq 0$, taking $0^0 = 1$ if necessary, and note that for $j \geq 1$ we have

$$S_{M,j}(\beta) = \frac{d^j S_{M,0}(\beta)}{d\beta^j} = \frac{dS_{M,j-1}(\beta)}{d\beta}.$$

The log-likelihood, (2.18), can now be written as

$$l_c = M \ln \beta - M\beta \ln \theta + (\beta - 1) S_{M,e} - \theta^{-\beta} S_{M,0}(\beta).$$

We then equate the partial derivatives

$$\frac{\partial l_c}{\partial \beta} = M\beta^{-1} - M \ln \theta + S_{M,e} - \theta^{-\beta} \{S_{M,1}(\beta) - \ln \theta S_{M,0}(\beta)\}, \tag{2.19}$$

and

$$\frac{\partial l_c}{\partial \theta} = -M\beta\theta^{-1} + \beta\theta^{-1-\beta} S_{M,0}(\beta), \tag{2.20}$$

to zero. From (2.20) we obtain

$$\theta = \left(\frac{S_{M,0}(\beta)}{M}\right)^{\frac{1}{\beta}}, \tag{2.21}$$

so we can now substitute (2.21) into (2.18) to obtain the profile log-likelihood

$$l_c^* = M \ln \beta - M \ln S_{M,0}(\beta) + (\beta - 1) S_{M,e} - M. \tag{2.22}$$

with first and second derivatives

$$\frac{dl_c^*}{d\beta} = M\beta^{-1} + S_{M,e} - M\frac{S_{M,1}(\beta)}{S_{M,0}(\beta)} \tag{2.23}$$

and

$$\frac{d^2 l_c^*}{d\beta^2} = -M\beta^{-2} - M\left\{\frac{S_{M,2}(\beta) S_{M,0}(\beta) - S_{M,1}(\beta)}{[S_{M,0}(\beta)]^2}\right\}.$$

We can now solve equation (2.22) for $\hat{\beta}_c$ using the Newton-Raphson iteration method with starting value, suggested by Farnum & Booth (1997), as

$$\beta^{[0]} = \left[\left(1 - \frac{M}{2n}\right)(\ln c - M S_{M,e})\right]^{-1}; \tag{2.24}$$

we note that (2.24) simplifies to (2.10) for the complete case, where $M \longrightarrow n$ and $c \longrightarrow y_{(n,n)}$. This censored MLE of β can then be substituted into (2.21) to find $\hat{\theta}_c$.

2.3.2 Example: Ball Bearings data with Type I censoring

Under the assumption that the continual monitoring of the ball bearings was possible, Table 2.5 summarises the MLEs, and maximum profile log likelihood, obtained at times

c	50	75	100	125	150	∞
M	7	15	18	20	22	23
$\widehat{\beta}_c$	3.0866	2.7634	2.2398	2.0731	2.1268	2.1021
$\widehat{\theta}_c$	69.4707	72.8142	80.3151	82.4301	81.5604	81.8783
$\hat{B}_{10,c}$	33.5100	32.2517	29.4066	27.8393	28.3111	28.0694

Table 2.5: Summary of MLEs for various censoring levels in a Type I censoring regime applied to the Ball Bearings data

$c = 50, 75, 100, 125, 150$. These can be compared to the complete results when $c \to \infty$, and all the items have failed; see section 2.2.2 above.

Somewhat more generally, we can repeat this process for a longer sequence of values for c, and plot each MLE against c. Figure 2.1 displays $\hat{\beta}_c$ versus c (for $c = 19$, increasing to $c = 174$ by intervals of 0.05), with observed failure times plotted along the horizontal axis. We observe sharp rises in the estimator at the actual times of failures; this follows directly from the increase in M increases as another failure occurs, and reflects the increasing failure rate, which contrasts against the decrease in the MLE between failures, where the general trend is for $\hat{\beta}_c$ to decrease with increasing c, as seen in Table 2.5.

The opposite trend is seen for $\hat{\theta}_c$ in Figure 2.2, where sharp drops now occur in the MLE obtained at failure times. This can be explained by consideration of (2.21); a failure occurring increases the denominator M, and causes the estimate to decrease, which contrasts with a general increase in $\hat{\theta}_c$ with c between failures.

Finally, Figure 2.3 shows that for small c, $\hat{B}_{10,c}$ is generally increasing with c, with a sharp drop at each failure, but at around $c = 50$, this pattern changes, and the estimate begins to decrease between failures, with sudden rises with the occurrence of a failure. This seems to be explained by the dominance and size of the sharp increases seen in $\hat{\theta}_c$ for early c. This then lessens with the increased censoring time, and, after $c = 50$, it is the change in $\hat{\beta}_c$ that dominates.

Clearly for each parameter and the quantile, the stability in the estimate obtained is relative to c, and, as c increases, the size of the respective jumps or drops reduce, and the observed estimates level off. These graphs may also benefit from smoothing and plotting of pointwise confidence intervals, and although these ideas are not considered further in this thesis, we note the possibility for future research.

2.3.3 Example: Epstein's data

We can perform a similar analysis on Epstein's 49 failure times data, and compare the results, shown in Table 2.6, with the complete data analysis, in section 2.2.3. We see as the censoring time increases and more items are left to fail, the estimates generally become closer to the complete estimates.

As with the ball bearings example, on plotting each MLE against c (now calculated from $c = 2$ to $c = 355$, by 0.05), we observe the same jumps or drops, and eventual levelling, of

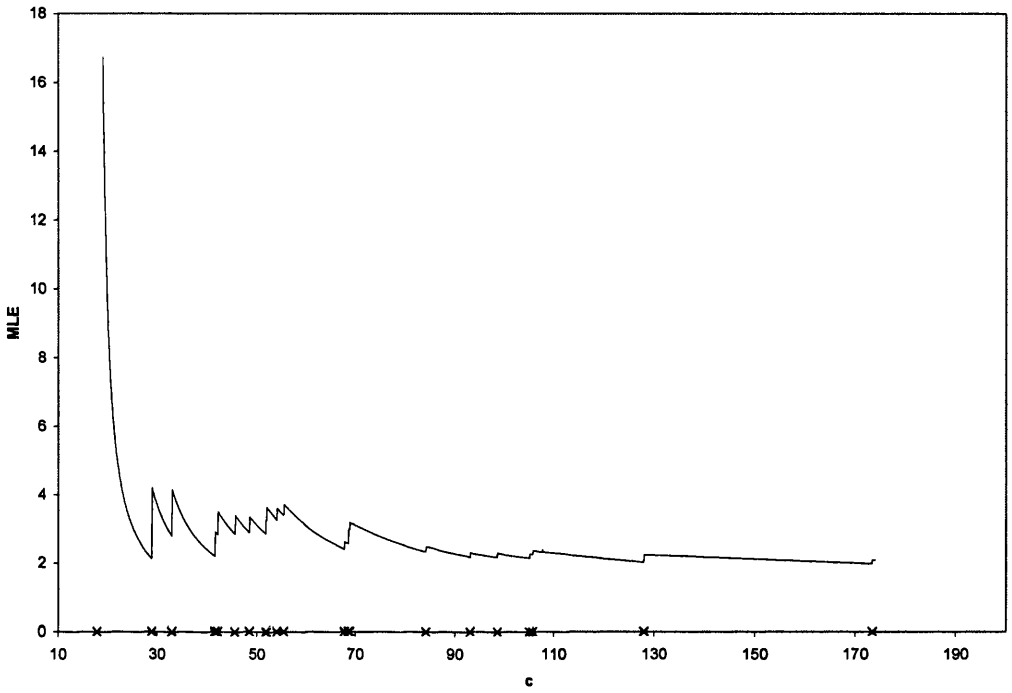

Figure 2.1: $\hat{\beta}_c$ versus c for the Ball Bearings data (Table 1.2), plotted with failure times ($\times$)

c	50	100	150	200	∞
M	18	28	34	42	49
$\widehat{\beta}_c$	0.8569	0.8709	0.8625	0.9656	1.0300
$\widehat{\theta}_c$	124.0083	122.4351	124.7209	110.1130	106.0505
$\hat{B}_{10,c}$	8.9736	9.2401	9.1789	10.7083	11.9312

Table 2.6: Summary of MLEs for various censoring levels in a Type I censoring regime applied to Epstein's 49 failure times data

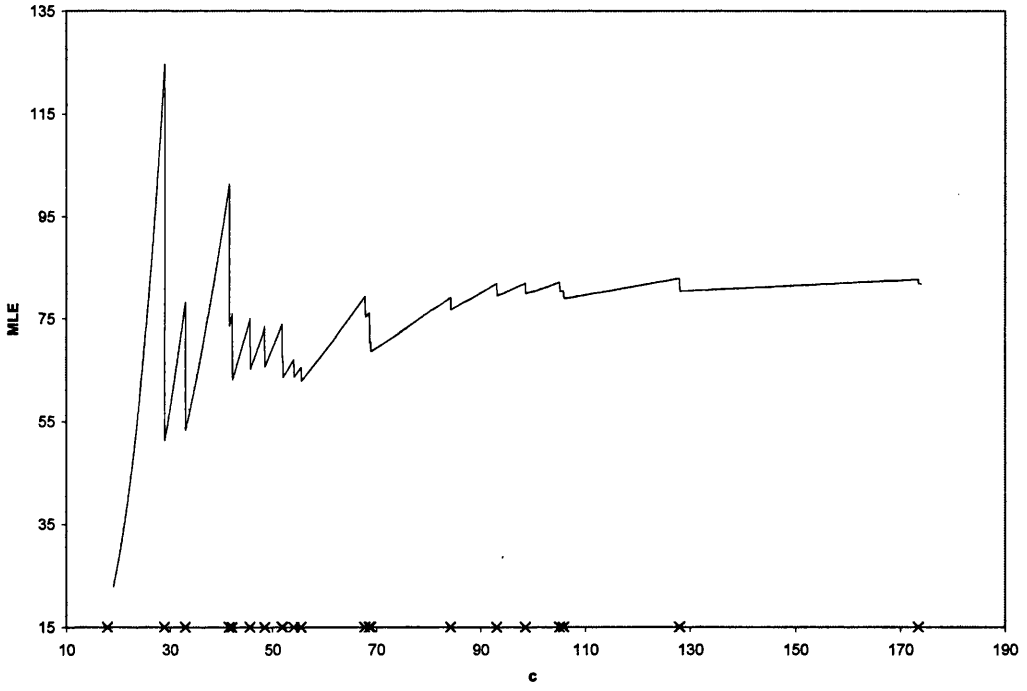

Figure 2.2: $\hat{\theta}_c$ versus c for the Ball Bearings data, plotted with failure times ($\times$)

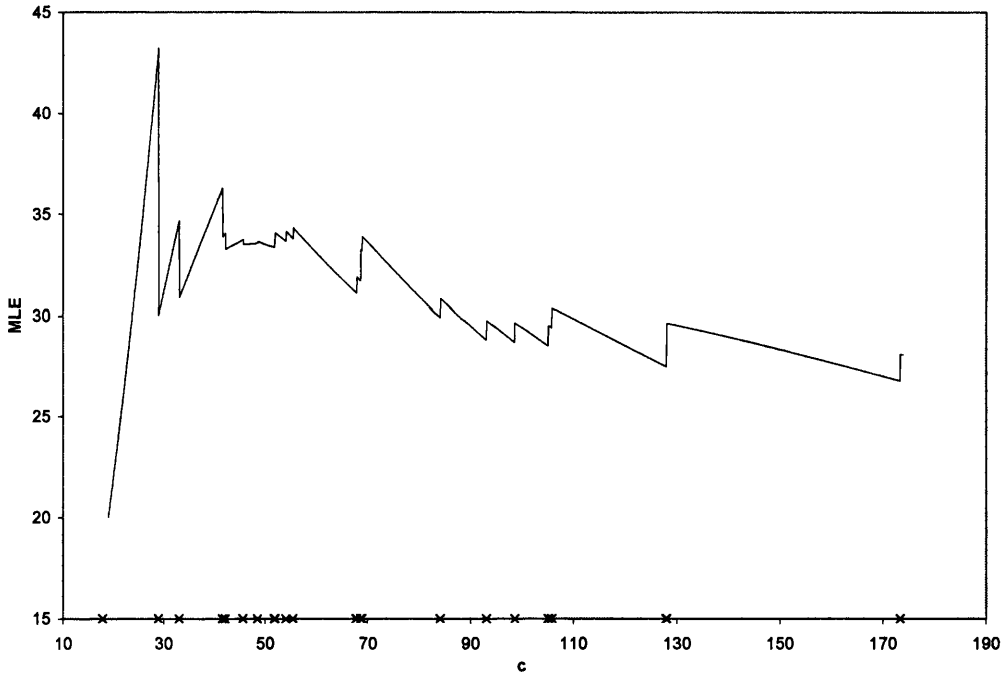

Figure 2.3: $\hat{B}_{10}$ versus c for the Ball Bearings, plotted with failure times ($\times$)

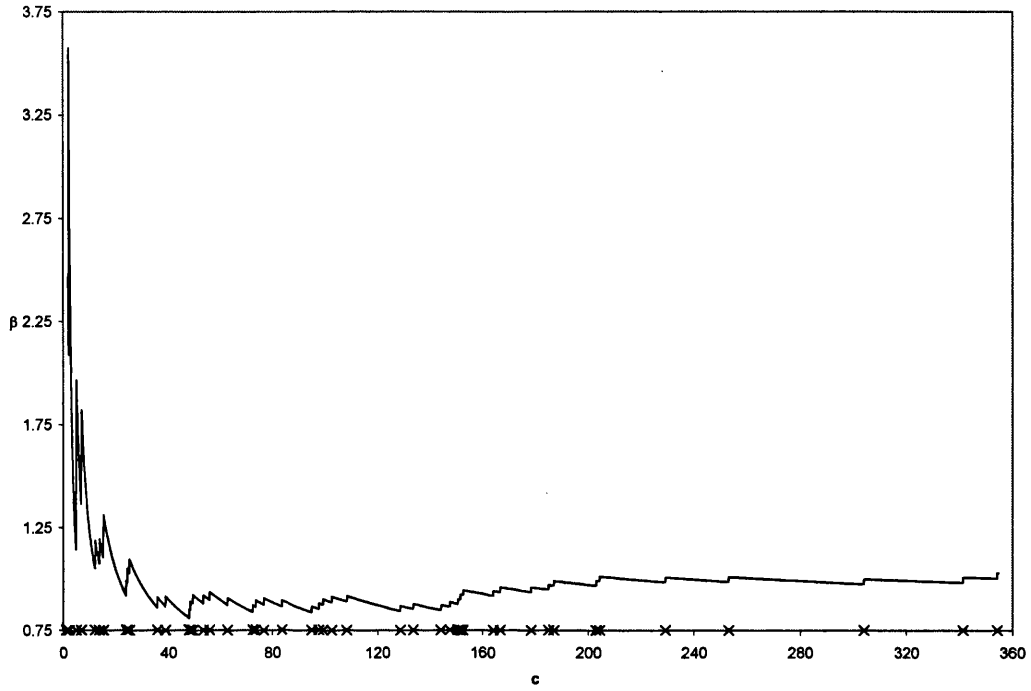

Figure 2.4: $\hat{\beta}_c$ versus c for Epstein's data, plotted with failure times ($\times$)

the estimate at the point of a failure; see Figure 2.4, 2.5, and 2.6 for plots of $\hat{\beta}_c$, $\hat{\theta}_c$, and $\hat{B}_{10,c}$ respectively. It would be of interest to assess the size and nature of these jumps, as related to the censoring level; this is not our main focus, however, and it will not be considered here.

We see from both examples that the estimates level off as c increases, and when c reaches 100 in the ball bearings example (or 200 in the 49 failure times data), the censored estimate does not appear to differ greatly from the complete estimate, hence censoring at these times may give a reasonable guide to the outcome of the experiment if c was large enough to allow all items to fail. We will return to this concept of using interim analysis to predict final MLEs in Chapter 5.

2.3.4 Simulations: Fitting a Weibull distribution to Censored Weibull data

Using SAS, we simulate a set number of Weibull random variables, again with $\beta = 2$ and $\theta = 100$, and, using a Type I censoring regime, we censor at several different levels, including leaving a complete sample with no censoring, that is, $c \to \infty$.

Leech & Watkins (1990) discuss the effect of censoring and sample size on the precision in parameter estimation, and we now investigate these factors separately. Table 2.8 sum-

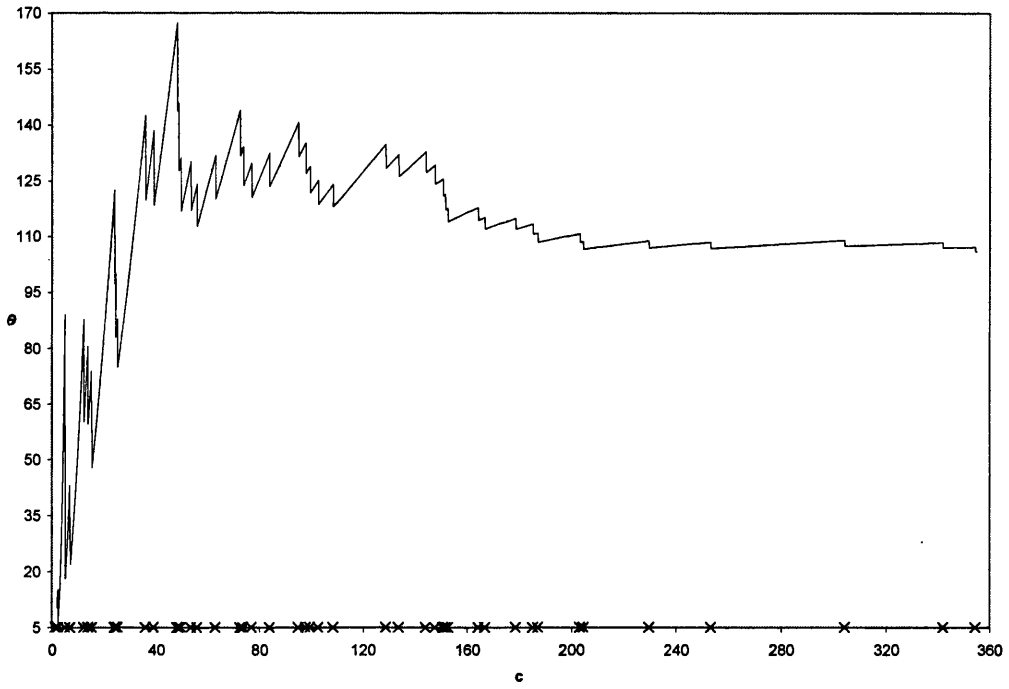

Figure 2.5: $\hat{\theta}_c$ versus c for Epstein's data, plotted with failure times ($\times$)

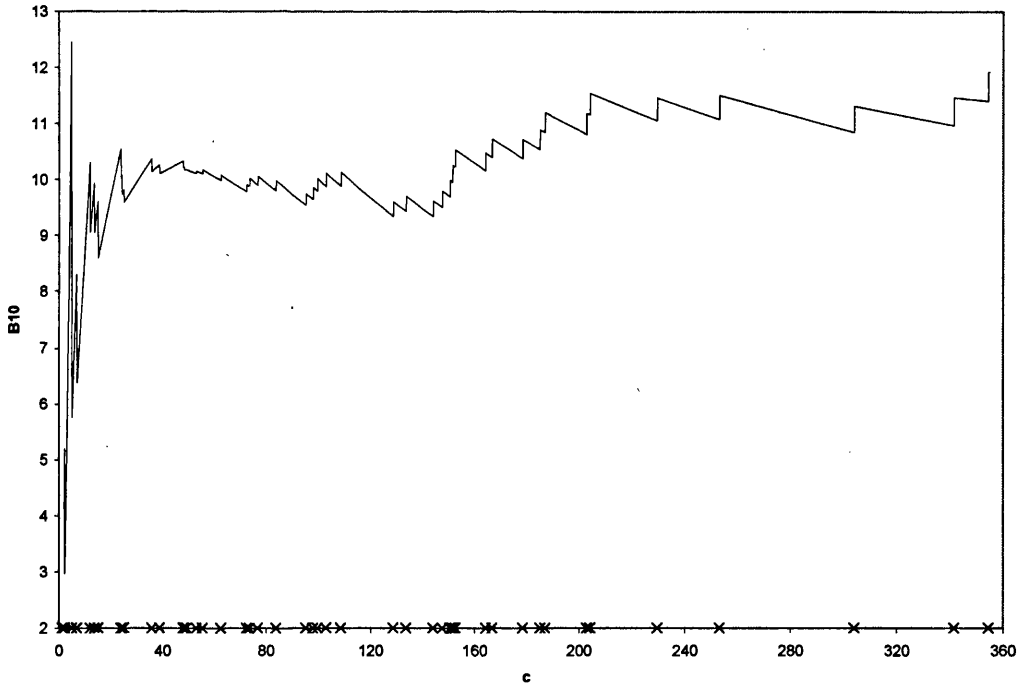

Figure 2.6: $\hat{B}_{10,c}$ versus c for Epstein's data, plotted with failure times ($\times$)

n	50	100	1000	
$\frac{sd(\hat{\beta}_c)}{sd(\hat{\beta})}$	$\frac{0.3405}{0.2341}$	$\frac{0.2307}{0.1600}$	$\frac{0.0718}{0.0496}$	$\simeq 1.4$
$\frac{sd(\hat{\theta}_c)}{sd(\hat{\theta})}$	$\frac{9.4899}{7.3980}$	$\frac{6.6752}{5.3344}$	$\frac{2.0672}{1.6666}$	$\simeq 1.2$
$\frac{sd(\hat{B}_{10,c})}{sd(\hat{B}_{10})}$	$\frac{5.9666}{5.3652}$	$\frac{4.2066}{3.7956}$	$\frac{1.3212}{1.1852}$	$\simeq 1.1$

Table 2.7: Ratio of standard deviations from censored and complete estimates

marises the results for varying censoring level, keeping the sample size fixed at $n = 1000$, and we can compare these results with the final column of Table 2.4. Table 2.9 shows the results for varying sample sizes, keeping the censoring, or stopping, time fixed at $c = 100$; each column can be compared with the corresponding column of Table 2.4. In each case, the summaries are based on 10,000 replications.

When we vary the censoring level the standard deviations of the MLEs and quantile function decreases as c increases. By comparing these results to those in Table 2.4, we see that censoring as early at $c = 100$ on a large sample of 1000 units gives an approximately equal standard deviation of $\hat{\beta}_c$ to that of obtained for a complete sample with $n = 500$, but the standard deviations are considerably more for $\hat{\theta}$ and $\hat{B}_{10}$ under the Type I censored experimental design (with $n = 1000$) compared to the $n = 500$ complete data. We also note that direct comparison of standard deviations between the complete estimates in Table 2.4 and the censored estimates in Table 2.9 (for the various n considered) give the following ratios, shown in Table 2.7.

So, there are larger differences between the precision of censored and complete estimates of β, and this reduces for estimates of θ. The precision of complete and censored estimates of B_{10} is very close, which is promising, as it is often the percentiles that are of more interest to practitioners than the parameters themselves. Investigation into these results could be extended to compare the precision between complete and censored estimates at further censoring levels, but this is not the focus of this thesis.

In practice, the costs of running an experiment would be the determining factor in deciding whether to use a larger sample size with early censoring, or a smaller sample with a higher level of censoring, if any at all. Usually, it would depend on which was most expensive, the running costs of an experiment with unknown duration, or a larger number of items to be tested.

2.4 Complete MLEs and the EFI Matrix

The expected Fisher information matrix, from now on referred to as the EFI matrix, is known to yield asymptotically valid variances and covariances of the Weibull distribution parameters; see, for example, Lawless (1982). This section will provide these theoretical EFI matrix, which will be checked to assess the extent to which asymptotic results apply

c	50	100	150	200	∞
$\hat{\beta}_c$: *mean*	2.0052	2.0023	2.0021	2.0024	2.0026
(*St dev*)	(0.1326)	(0.0718)	(0.0559)	(0.0509)	(0.0496)
$\hat{\theta}_c$: *mean*	100.4770	100.0751	100.0751	100.0415	100.0301
(*St dev*)	(6.0025)	(2.0672)	(1.6957)	(1.6678)	(1.6666)
$\hat{B}_{10,c}$: *mean*	32.5216	32.4995	32.5013	32.5071	32.5113
(*St dev*)	(1.3807)	(1.3212)	(1.2435)	(1.2001)	(1.1852)

Table 2.8: MLE summaries for Type I censored Weibull data, varying c, with fixed $n = 1000$

n	50	100	300	500	1000
$\hat{\beta}_c$: *mean*	2.0599	2.0282	2.0093	2.0052	2.0023
(*St dev*)	(0.3405)	(0.2307)	(0.1335)	(0.1018)	(0.0718)
$\hat{\theta}_c$: *mean*	100.5839	100.3429	100.1056	100.0612	100.0751
(*St dev*)	(9.4899)	(6.6752)	(3.7926)	(2.9274)	(2.0672)
$\hat{B}_{10,c}$: *mean*	33.1581	32.8139	32.5704	32.5193	32.4995
(*St dev*)	(5.9666)	(4.2066)	(2.4351)	(1.8662)	(1.3212)

Table 2.9: MLE summaries for Type I censored Weibull data, varying n, with fixed $c = 100$

in finite samples. For a complete sample from the Weibull distribution, we can obtain the EFI matrix,

$$\mathbf{A} = -E\begin{bmatrix} \frac{\partial^2 l}{\partial \beta^2} & \frac{\partial^2 l}{\partial \beta \partial \theta} \\ & \frac{\partial^2 l}{\partial \theta^2} \end{bmatrix},$$

and since the matrix is symmetric, only the upper half is given. Hence, we have the inverse EFI matrix

$$\mathbf{A}^{-1} = \begin{pmatrix} Var\left(\hat{\beta}\right) & Cov\left(\hat{\beta}, \hat{\theta}\right) \\ & Var\left(\hat{\theta}\right) \end{pmatrix} \tag{2.25}$$

This, in turn, will provide the asymptotic distribution of any function of β, θ, in particular the quantile $\hat{B}_{10}$, see Watkins & John (2008) for further details.

2.4.1 Expectations of second derivatives

Watkins (1998) computes expectations of the second derivatives of the Weibull distribution, which, from (2.4) and (2.5), are given by

$$\frac{\partial^2 l}{\partial \beta^2} = -n\beta^{-2} + 2\theta^{-\beta}(\ln\theta) S_1(\beta) - \theta^{-\beta}(\ln\theta)^2 S_0(\beta) - \theta^{-\beta} S_2(\beta),$$

$$\frac{\partial^2 l}{\partial \theta^2} = -n\beta\theta^{-2} - \beta(\beta+1)\theta^{-(\beta+2)} S_0(\beta),$$

and

$$\begin{aligned}\frac{\partial^2 l}{\partial\beta\partial\theta} &= \frac{\partial^2 l}{\partial\theta\partial\beta} \\ &= -n\theta^{-1} + \theta^{-(\beta+1)} S_0(\beta)\{1 - \beta\ln\theta\} + \theta^{-(\beta+1)} S_1(\beta).\end{aligned}$$

From (2.3), we see that the second derivatives are functions of

$$z = g(y) = \left(\frac{y}{\theta}\right)^{i\beta} \ln\left(\frac{y}{\theta}\right)^{j},$$

for integers $i, j \leq 2$. Hence we approach the expectations using the transformed variable

$$Z = \left(\frac{Y}{\theta}\right)^{\beta}, \tag{2.26}$$

which follows the standard negative exponential distribution, with probability density function for $z \geq 0$ given by

$$\exp(-z); \tag{2.27}$$

The expectations required, in terms of the random variable Z are

$$E\left[-\frac{\partial^2 l}{\partial\beta^2}\right] = n\beta^{-2}\left(1 + E\left[Z(\ln Z)^2\right]\right),$$

$$E\left[-\frac{\partial^2 l}{\partial\theta^2}\right] = -n\beta\theta^{-2}(1 - (\beta+1)E[Z]),$$

and

$$E\left[-\frac{\partial^2 l}{\partial\beta\partial\theta}\right] = -n\theta^{-1}(-1 + E[Z] + E[Z\ln Z]).$$

By exploiting the connection between the Gamma functions outlined in Chapter 1, Watkins (1998) provides expressions for the expectations required; since

$$E[Z^r] = \int_0^\infty z^r \exp(-z)\, dz = \Gamma(1+r),$$

we have

$$E[Z^r(\ln Z)^s] = \Gamma^{(s)}(1+r).$$

and specifically

$$E_Y[Z] = \Gamma(2) = 1, \tag{2.28}$$

$$E_Y[\ln Z] = \Gamma^{(1)}(1) = -\gamma, \tag{2.29}$$

$$E_Y[Z\ln Z] = \Gamma^{(1)}(2) = 1 - \gamma \tag{2.30}$$

and

$$E_Y\left[Z\left(\ln Z\right)^2\right] = \Gamma^{(2)}\left(2\right) = \frac{\pi^2}{6} + \gamma^2 - 2\gamma. \tag{2.31}$$

2.4.2 Asymptotic standard deviations

These allow us to obtain the EFI matrix as follows

$$\mathbf{A} = n\begin{pmatrix} \beta^{-2}\left[\frac{\pi^2}{6} + (\gamma-1)^2\right] & -\theta^{-1}(1-\gamma) \\ & \beta^2\theta^{-2} \end{pmatrix}.$$

On taking the inverse we have the variance covariance matrix

$$\mathbf{A}^{-1} = 6n^{-1}\pi^{-2}\begin{pmatrix} \beta^2 & \theta(1-\gamma) \\ & \beta^{-2}\theta^2\left[\frac{\pi^2}{6} + (\gamma-1)^2\right] \end{pmatrix}. \tag{2.32}$$

Taking the square roots of elements of the diagonal elements of the inverse EFI matrix, (2.32), we obtain the approximate standard deviations. With $\beta = 2$, and $\theta = 100$, (2.32) becomes

$$\begin{aligned} \mathbf{A}^{-1} &= 6n^{-1}\pi^{-2}\begin{pmatrix} 2^2 & 100(1-\gamma) \\ & 2^{-2}100^2\left[\frac{\pi^2}{6} + (\gamma-1)^2\right] \end{pmatrix} \\ &= 6n^{-1}\pi^{-2}\begin{pmatrix} 4 & 100(1-\gamma) \\ & 2500\left[\frac{\pi^2}{6} + (\gamma-1)^2\right] \end{pmatrix}, \end{aligned}$$

and hence we obtain the inverse EFI matrix elements, to 4 decimal places as,

$$\mathbf{A}^{-1} = n^{-1}\begin{pmatrix} 2.4317 & 25.7022 \\ & 2771.6623 \end{pmatrix}.$$

Table 2.10 and Table 2.11 display the theoretical asymptotic standard deviations of $\hat{\beta}$ and $\hat{\theta}$ respectively, for various n, along with the simulated counterparts (based on 10,000 repetitions). We repeat this check for consistency between theory and simulated results for several values of the shape parameter, β, to allow coverage of a suitable portion of the parameter space and various failure rates. Those additional parameter values of particular interest are $\beta = 1$ and 3.5. At $\beta = 1$ the hazard function, or failure rate changes from a decreasing function to an increasing function, and we focus on this change by exploring what happens at $\beta = 0.9$ and $\beta = 1.1$. We see that for most cases, simulated values get closer to their theoretical counterparts with increasing sample size.

We have shown that for a complete sample, our asymptotic approximations to the variance of the MLEs hold in finite samples, and the next section will assess the asymptotic variances in censored samples. An obvious extension to checking these asymptotic theoretical variances would be to assess the assumption of asymptotic Normality of the MLEs in

β	n				
	50	100	300	500	1000
0.9	0.0992	0.0702	0.0405	0.0314	0.0222
	0.1060	0.0740	0.0414	0.0317	0.0221
1	0.1103	0.0780	0.0450	0.0349	0.0247
	0.1194	0.0802	0.0449	0.0344	0.0249
1.1	0.1213	0.0858	0.0495	0.0384	0.0271
	0.1274	0.0897	0.0501	0.0388	0.0273
2	0.2205	0.1559	0.0900	0.0700	0.0490
	0.2341	0.1600	0.0905	0.0705	0.0496
3.5	0.3859	0.2729	0.1576	0.1220	0.0863
	0.4065	0.2823	0.1590	0.1241	0.0869

Table 2.10: Theoretical (upper) and simulated (lower) standard deviations of complete $\hat{\beta}$ for various β, n, and $\theta = 100$.

β	n				
	50	100	300	500	1000
0.9	16.5452	11.6992	6.7546	5.2321	3.6996
	16.5078	11.7093	6.8252	5.2277	3.6948
1	14.8907	10.5293	6.0791	4.7089	3.3297
	14.8247	10.4643	5.9579	4.7314	3.3435
1.1	13.5370	9.5721	5.5265	4.2808	3.0270
	13.4953	9.5773	5.5945	4.2213	3.0643
2	7.4453	5.23476	3.0396	2.3544	1.6648
	7.3980	5.3344	3.0623	2.3614	1.6666
3.5	4.2545	3.0084	1.7359	1.3454	0.9513
	4.2376	2.9925	1.7465	1.3493	0.9511

Table 2.11: Theoretical (upper) and simulated (lower) standard deviations of complete $\hat{\theta}$ with various β, n, and $\theta = 100$.

finite samples. This will be considered in a later chapter.

2.5 Type I Censored MLEs and the EFI Matrix

Watkins & John (2004) provides formulae for the elements of the EFI, and we follow the same techniques in this section to obtain the censored data variance-covariance matrix, now denoted as

$$\mathbf{A}_c^{-1} = \begin{pmatrix} Var\left(\hat{\beta}_c\right) & Cov\left(\hat{\beta}_c, \hat{\theta}_c\right) \\ & Var\left(\hat{\theta}_c\right) \end{pmatrix} \tag{2.33}$$

We again use the transformation (2.26), where Z now follows the truncated negative exponential distribution with pdf

$$q_c^{-1} \exp\left(-z\right) \tag{2.34}$$

for $0 \leq z \leq z_c$, where we write

$$z_c = \left(\frac{c}{\theta}\right)^{\beta}.$$

2.5.1 Expectations of second derivatives

By taking derivatives of the score functions ((2.19) and (2.20)), with respect to β and θ, and applying the transformation from Y to Z, we obtain

$$\begin{aligned} -\frac{\partial^2 l_c}{\partial \beta^2} &= \beta^{-2}\left[M + \left\{ \begin{array}{c} \sum_{i=1}^{M} Y_i^{\beta}\theta^{-\beta}\beta^2\left\{\ln\left(Y_i\theta^{-1}\right)\right\}^2 \\ +\left(n-M\right)c^{\beta}\theta^{-\beta}\beta^2\left(\ln\left(c\theta^{-1}\right)\right)^2 \end{array} \right\}\right] \\ &= \beta^{-2}\left[M + \left\{\sum_{i=1}^{M} Z_i\left(\ln Z_i\right)^2 + \left(n-M\right)z_c\left(\ln z_c\right)^2\right\}\right], \end{aligned} \tag{2.35}$$

$$\begin{aligned} -\frac{\partial^2 l_c}{\partial \theta^2} &= \beta\theta^{-2}\left[\left(\beta+1\right)\left\{\sum_{i=1}^{M} Y_i^{\beta}\theta^{-\beta} + \left(n-M\right)c^{\beta}\theta^{-\beta}\right\} - M\right] \\ &= \beta\theta^{-2}\left[\left(\beta+1\right)\left\{\sum_{i=1}^{M} Z_i + \left(n-M\right)z_c\right\} - M\right], \end{aligned} \tag{2.36}$$

and

$$\begin{aligned} -\frac{\partial^2 l_c}{\partial \beta \partial \theta} &= -\frac{\partial^2 l_c}{\partial \theta \partial \beta} \\ &= -\theta^{-1}\left[\sum_{i=1}^{M} Y_i^{\beta}\theta^{-\beta}\left\{1+\beta\ln\left(Y_i\theta^{-1}\right)\right\} + \left(n-M\right)c^{\beta}\theta^{-\beta}\left\{1+\beta\ln\left(c\theta^{-1}\right)\right\} - M\right] \\ &= -\theta^{-1}\left[\sum_{i=1}^{M} Z_i\left\{1+\ln Z_i\right\} + \left(n-M\right)z_c\left\{1+\ln z_c\right\} - M\right]. \end{aligned} \tag{2.37}$$

The form of these second derivatives, written in terms of Z, show that the EFI matrix requires the expectations

$$E\left[Z^i (\ln Z)^j\right] = \mu_{ij},$$

say, for integer $i, j \leq 2$. From (2.34), we have

$$E[Z^i] = \int_0^{z_c} \frac{z^i \exp(-z)}{q_c} dz = q_c^{-1} \gamma(i+1, z_c)$$

where $\gamma(i+1, z_c)$ is the incomplete gamma function defined in (1.8). Differentiating j times with respect to i then gives

$$E\left[Z^i (\ln Z)^j\right] = q_c^{-1} \gamma^{(j)}(i+1, z_c).$$

The computation of this function will be given below.

2.5.2 Expectations involved

We recall that M follows a Binomial distribution, with

$$E[M] = nq_c,$$

so that

$$E[n - M] = n(1 - q_c) = nr_c q_c,$$

where

$$r_c = \frac{1 - q_c}{q_c} \tag{2.38}$$

is the odds-ratio of the probability of survival beyond c to failure before c.

In general, we can obtain the expectations in derivatives via a conditionality argument on M, in which we write

$$E\left[\sum_{i=1}^{M} g(Y_i)\right] = nq_c E[g(Y)], \tag{2.39}$$

where the expectation $E[g(Y)]$ is with respect to the truncated Weibull distribution, and can be expressed as an expectation in Z following the truncated negative exponential distribution. It is suitable to here summarise the expectations required for the following analysis, and use notation that will simplify formulae in further chapters. We also plot these as functions of c, in Figures 2.7 to 2.14. The expectations will use the recurrence relation of the incomplete gamma distribution, given in (1.9).

$$\mu_{10} = E[Z] = \gamma(2, z_c) q_c^{-1} = \gamma(1, z_c) q_c^{-1} - z_c r_c = 1 - z_c r_c \tag{2.40}$$

$$\mu_{20} = E[Z^2] = \gamma(3, z_c) q_c^{-1} = 2\gamma(2, z_c) q_c^{-1} - z_c^2 r_c = 2 - 2z_c r_c - z_c^2 r_c \tag{2.41}$$

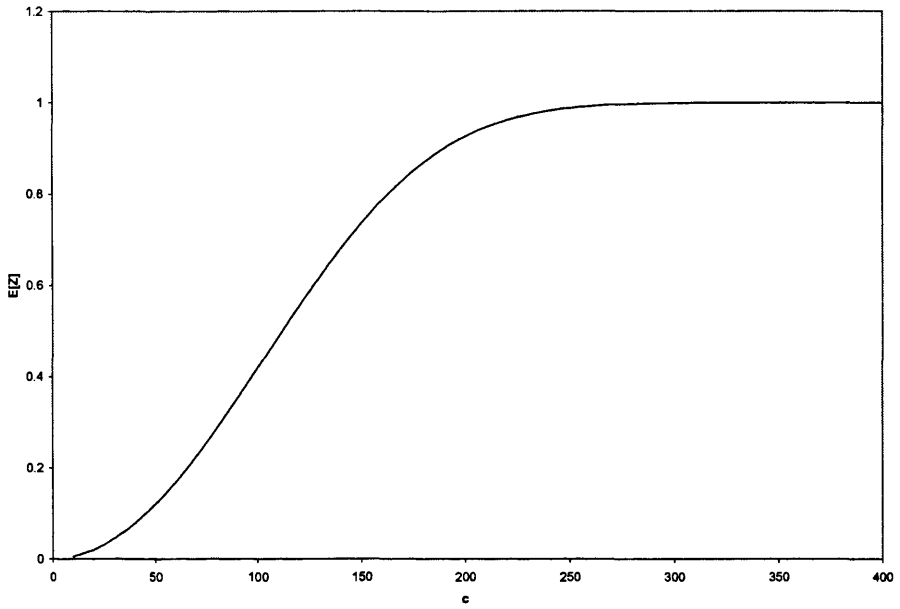

Figure 2.7: Plot of $\mu_{10} = E[Z]$ versus c, for $\beta = 2$ and $\theta = 100$.

$$\mu_{01} = E[\ln Z] = \gamma^{(1)}(1, z_c)\, q_c^{-1} \tag{2.42}$$

$$\begin{aligned} \mu_{11} &= E[Z \ln Z] = \gamma^{(1)}(2, z_c)\, q_c^{-1} = \mu_{01} + 1 - z_c \ln z_c r_c \\ &= \gamma^{(1)}(1, z_c)\, q_c^{-1} + 1 - z_c \ln z_c r_c \end{aligned} \tag{2.43}$$

$$\begin{aligned} \mu_{21} &= E[Z^2 \ln Z] = 2\mu_{11} + 1 - z_c r_c - z_c^2 \ln z_c r_c \\ &= 2\gamma^{(1)}(1, z_c)\, q_c^{-1} + 3 - z_c r_c - 2 z_c \ln z_c r_c - z_c^2 \ln z_c r_c \end{aligned} \tag{2.44}$$

$$\mu_{02} = E[(\ln Z)^2] = \gamma^{(2)}(1, z_c)\, q_c^{-1} \tag{2.45}$$

$$\begin{aligned} \mu_{12} &= E\left[Z (\ln Z)^2\right] = \mu_{02} + 2\mu_{01} - z_c (\ln z_c)^2 r_c \\ &= \gamma^{(2)}(1, z_c)\, q_c^{-1} + 2\gamma^{(1)}(1, z_c)\, q_c^{-1} - z_c (\ln z_c)^2 r_c \end{aligned} \tag{2.46}$$

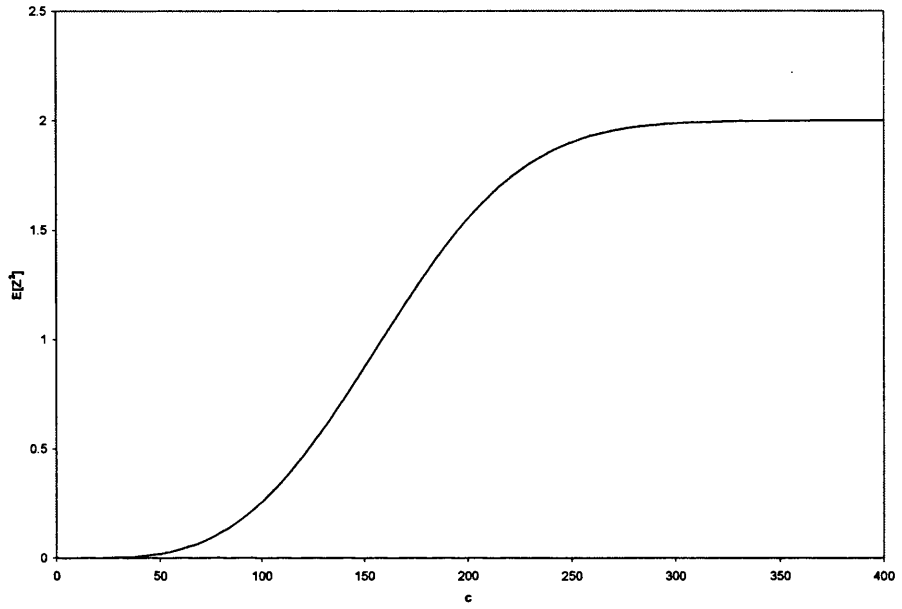

Figure 2.8: Plot of $\mu_{20} = E\left[Z^2\right]$ versus c, for $\beta = 2$ and $\theta = 100$.

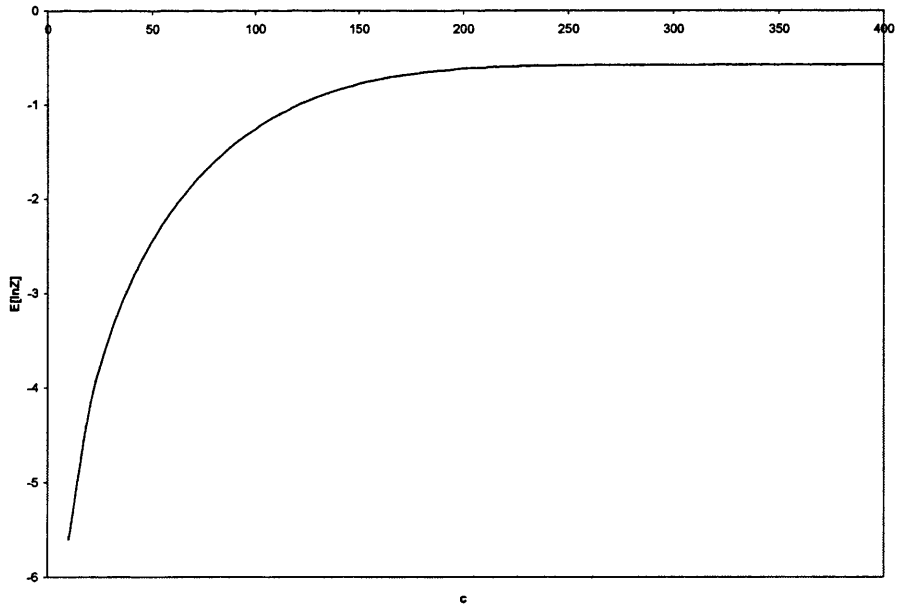

Figure 2.9: Plot of $\mu_{01} = E\left[\ln Z\right]$ versus c, for $\beta = 2$ and $\theta = 100$.

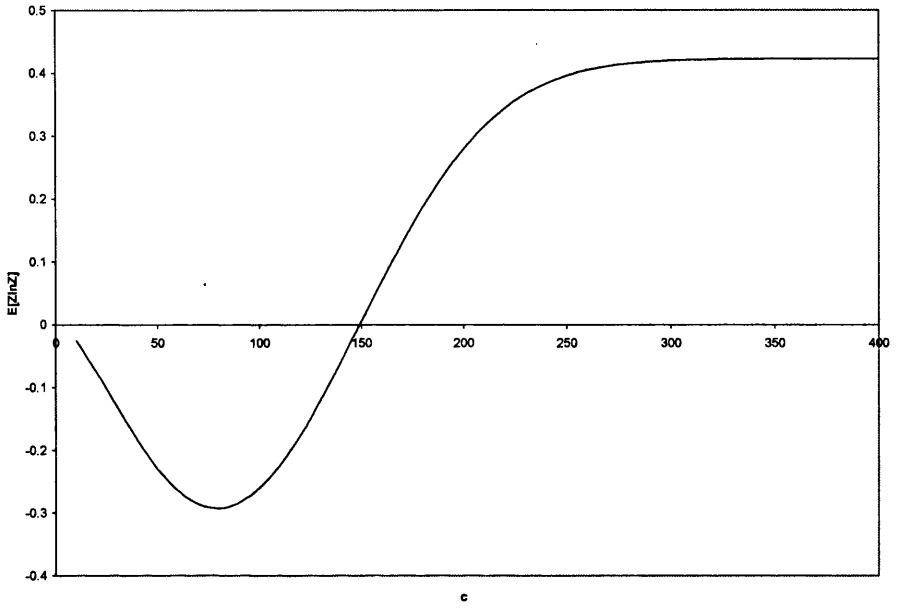

Figure 2.10: Plot of $\mu_{11} = E[Z \ln Z]$ versus c, for $\beta = 2$ and $\theta = 100$.

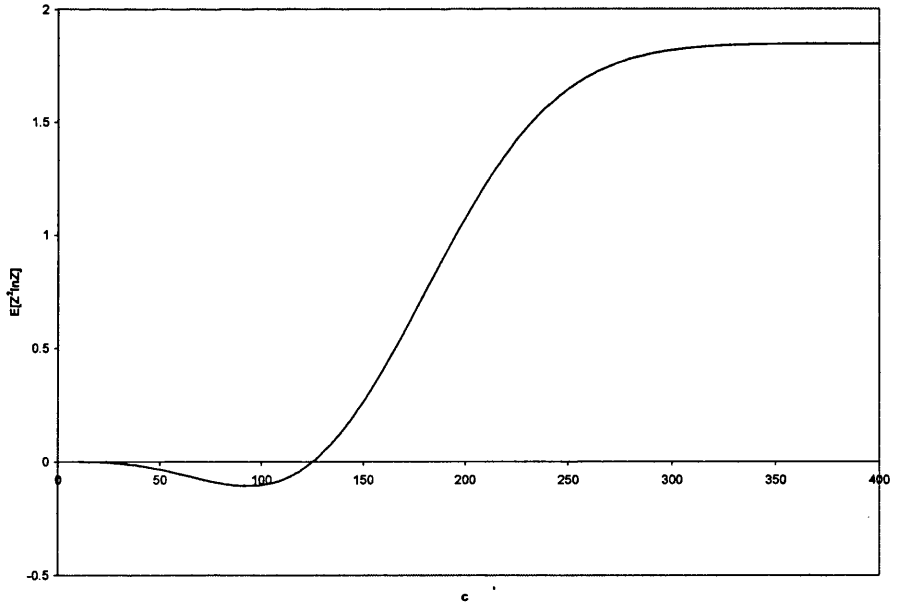

Figure 2.11: Plot of $\mu_{21} = E\left[Z^2 (\ln Z)\right]$ versus c, for $\beta = 2$ and $\theta = 100$.

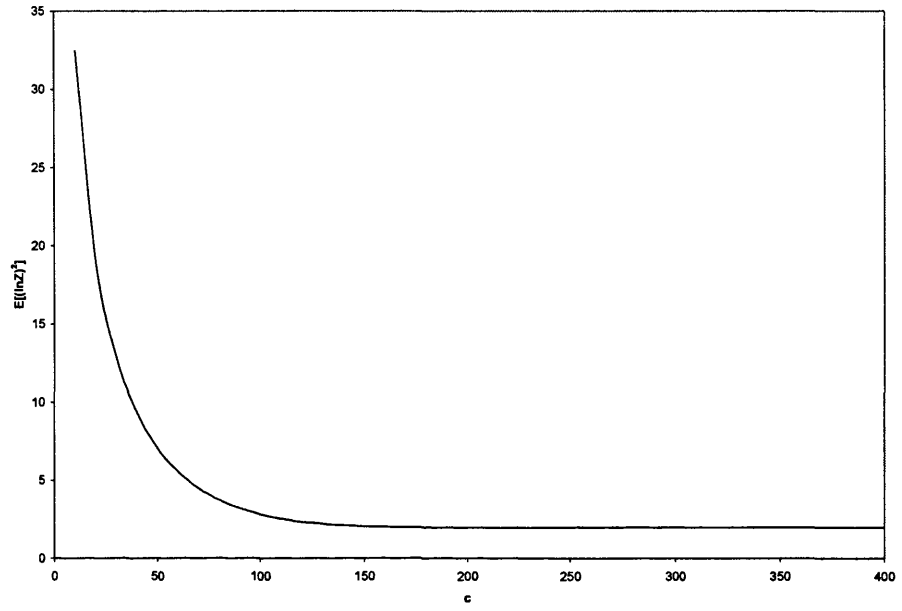

Figure 2.12: Plot of $\mu_{02} = E\left[(\ln Z)^2\right]$ versus c, for $\beta = 2$ and $\theta = 100$.

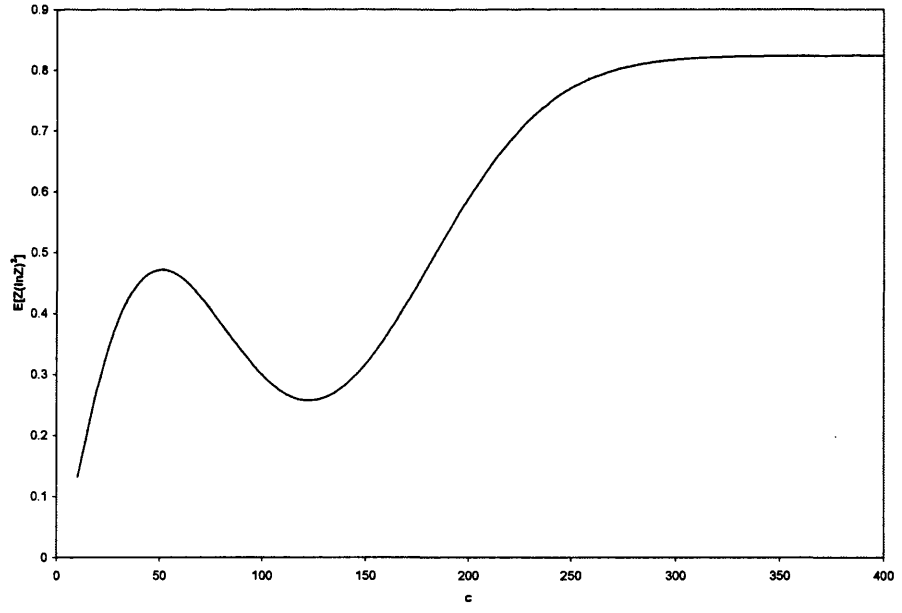

Figure 2.13: Plot of $\mu_{12} = E\left[Z\,(\ln Z)^2\right]$ versus c, for $\beta = 2$ and $\theta = 100$.

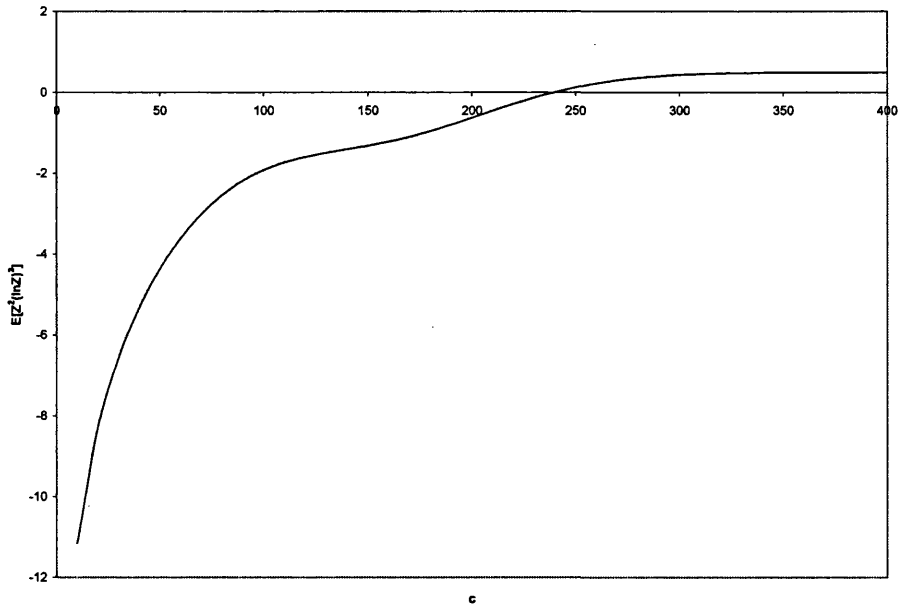

Figure 2.14: Plot of $\mu_{22} = E\left[Z^2 (\ln Z)^2\right]$ versus c, for $\beta = 2$ and $\theta = 100$.

$$\begin{aligned}
\mu_{22} &= E\left[Z^2 (\ln Z)^2\right] = \gamma^{(2)}(3, z_c)\, q_c^{-1} = 2\mu_{12} + 2\mu_{11} - z_c^2 (\ln z_c)^2 r_c \\
&= 2\gamma^{(2)}(1, z_c)\, q_c^{-1} + 6\gamma^{(1)}(1, z_c)\, q_c^{-1} + 2 \\
&\quad -z_c (\ln z_c)\, r_c (2 + 2\ln z_c + z_c \ln z_c) \qquad (2.47)
\end{aligned}$$

We note that, in general, these functions are relatively constant for $c \geq 200$, and from Figures 2.7, 2.9, 2.10 and 2.13 it is clear that these functions approach their counterparts from in the complete case, given in equations (2.28), (2.29), (2.30), and (2.31).

Thus, on taking the expectations of the above second derivatives, we have

$$\begin{aligned}
E\left[-\frac{\partial^2 l_c}{\partial \beta^2}\right] &= n\beta^{-2}\left\{q_c + q_c\mu_{12} + z_c (\ln z_c)^2 q_c r_c\right\} \\
&= n\beta^{-2}\left\{\begin{array}{c} q_c + \gamma^{(2)}(1, z_c) + 2\gamma^{(1)}(1, z_c) - z_c (\ln z_c)^2 q_c r_c \\ +z_c (\ln z_c)^2 q_c r_c \end{array}\right\} \\
&= n\beta^{-2}\left\{q_c + \gamma^{(2)}(1, z_c) + 2\gamma^{(1)}(1, z_c)\right\},
\end{aligned}$$

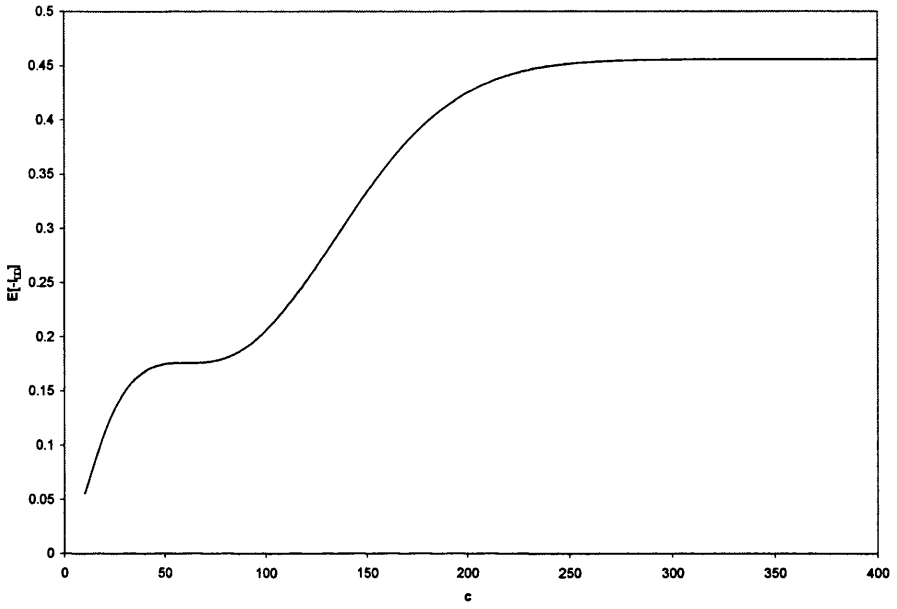

Figure 2.15: Plot of $n^{-1}E\left[-\frac{\partial^2 l_c}{\partial\beta^2}\right]$ versus c, for $\beta = 2$, $\theta = 100$ and $n = 1000$.

$$\begin{aligned} E\left[-\frac{\partial^2 l_c}{\partial\theta^2}\right] &= n\beta\theta^{-2}\left[(\beta+1)\left\{q_c\mu_c + z_c r_c q_c\right\} - q_c\right] \\ &= n\beta\theta^{-2}\left[(\beta+1)\left\{q_c\left(1 - z_c r_c\right) + z_c r_c q_c\right\} - q_c\right] \\ &= n\beta\theta^{-2}\left[(\beta+1)\, q_c - q_c\right] \\ &= n\beta^2\theta^{-2} q_c, \end{aligned}$$

and finally,

$$\begin{aligned} E\left[-\frac{\partial^2 l_c}{\partial\beta\partial\theta}\right] &= E\left[-\frac{\partial^2 l_c}{\partial\theta\partial\beta}\right] \\ &= -n\theta^{-1}\left\{q_c\left(\mu_c + \mu_{11}\right) + z_c\left(1 + \ln z_c\right) r_c q_c - q_c\right\} \\ &= -n\theta^{-1}\left\{\begin{array}{c} q_c\left(1 - z_c r_c + \gamma^{(1)}\left(1, z_c\right) q_c^{-1} + 1 - z_c \ln z_c r_c\right) \\ +z_c\left(1 + \ln z_c\right) r_c q_c - q_c \end{array}\right\} \\ &= -n\theta^{-1}\left\{q_c + \gamma^{(1)}\left(1, z_c\right)\right\}. \end{aligned}$$

Again, we conclude that these expectations of the second derivatives also approach their complete counterparts as $c \to \infty$, and Figures 2.15, 2.16 and 2.17 show these expectations, suitably standardised by multiplication by n^{-1}, for $\beta = 2$, $\theta = 100$, over $0 < c \leq 400$.

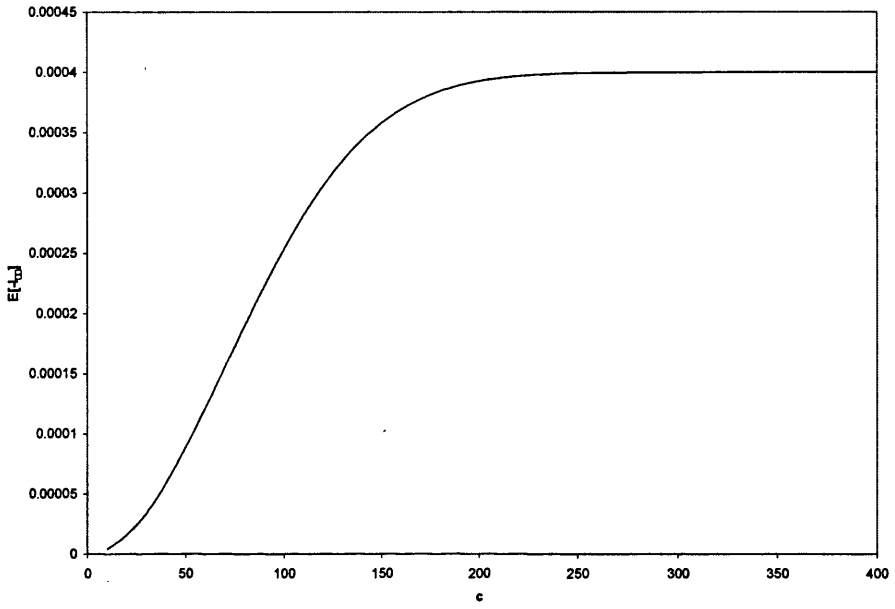

Figure 2.16: Plot of $n^{-1}E\left[-\frac{\partial^2 l_c}{\partial\theta^2}\right]$ versus c, for $\beta = 2$, $\theta = 100$ and $n = 1000$.

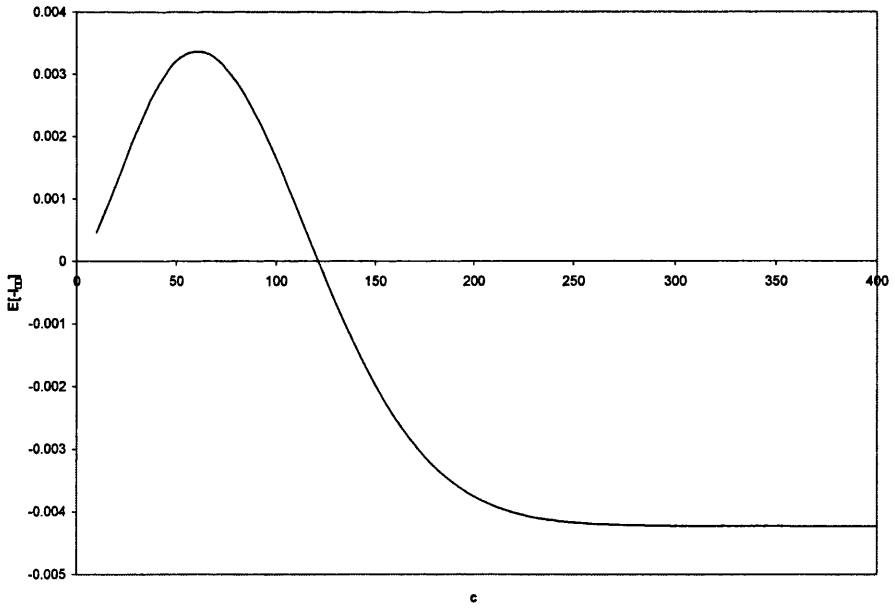

Figure 2.17: Plot of $n^{-1}E\left[-\frac{\partial^2 l_c}{\partial\beta\partial\theta}\right]$ versus c, for $\beta = 2$, $\theta = 100$ and $n = 1000$.

2.5.3 Asymptotic standard deviations

Substituting these expectations into the elements of (2.33), we obtain our required symmetric matrix

$$n\begin{pmatrix}\beta^{-2}\left\{q_c+\gamma^{(2)}(1,z_c)+2\gamma^{(1)}(1,z_c)\right\} & -\theta^{-1}\left\{q_c+\gamma^{(1)}(1,z_c)\right\}\\ & \beta^2\theta^{-2}q_c\end{pmatrix}$$

and, with inverse it becomes,

$$\mathbf{A}_c^{-1} = n^{-1}\left[q_c\gamma^{(2)}(1,z_c)-\left\{\gamma^{(1)}(1,z_c)\right\}^2\right]^{-1}\times \begin{pmatrix}\beta^2q_c & \theta\left\{q_c+\gamma^{(1)}(1,z_c)\right\}\\ & \beta^{-2}\theta^2\left\{q_c+\gamma^{(2)}(1,z_c)+2\gamma^{(1)}(1,z_c)\right\}\end{pmatrix}. \tag{2.48}$$

2.5.4 Computational issues

It is now convenient to exploit the connection between the incomplete gamma function and the confluent hypergeometric function in order to calculate the elements of the inverse EFI matrix required. This approach uses

$$\gamma(r,z)=z^rS_1(r,z)$$

where

$$S_i(r,z)=\sum_{n=0}^{\infty}\frac{(-z)^n}{(r+n)^in!}$$

and satisfies

$$\frac{\partial S_i}{\partial r}=-iS_{i+1},$$

with

$$S_i(1,z)=F_{i,i}[\{1,...,1\},\{2,...,2\};-z] \tag{2.49}$$

where $F_{i,i}$ is the usual hypergeometric function; see (1.13). We therefore have

$$\gamma^{(1)}(r,z)=z^r(\ln z)S_1(r,z)-z^rS_2(r,z), \tag{2.50}$$

and

$$\gamma^{(2)}(r,z)=z^r(\ln z)^2S_1(r,z)-2z^r(\ln z)S_2(r,z)+2z^rS_3(r,z). \tag{2.51}$$

These functions can then be computed using Mathematica's HypergeometricPFQ[$\{a_1,\ldots,a_p\}$, $\{b_1,\ldots,b_q\}$, z], and our variance-covariance matrix, (2.48), is constructed. For example, in Mathematica, if we specify a value of β (`beta`), θ (`theta`), and c (`c`), then we can use the

following code to compute the above functions

```
zc=N[(c/theta)^beta]
lc=Log[zc]
s1=HypergeometricPFQ[{1},{2},-zc]
s2=HypergeometricPFQ[{1,1},{2,2},-zc]
s3=HypergeometricPFQ[{1,1,1},{2,2,2},-zc]
g1=zc*lc*s1-zc*s2
g2=lc*lc*qc-2*zc*lc*s2+2*zc*s3
```
(2.52)

So, for a Weibull distribution with $\beta = 2$ and $\theta = 100$, the elements of the censored EFI matrix (2.48) at $c = 100$, can be calculated in Mathematica as follows,

```
In[1] :=beta=2;
In[2] :=theta=100;
In[3] :=c=100;
In[4] :=zc=N[(c/theta)^beta]
Out[4] :=1.
In[5] :=qc=1-Exp[-zc]
Out[5] :=0.632121
In[6] :=lc=Log[zc]
Out[6] :=0.
In[7] :=s1=HypergeometricPFQ[{1},{2},-zc]
Out[7] :=0.632121
In[8] :=s2=HypergeometricPFQ[{1,1},{2,2},-zc]
Out[8] :=0.7966
In[9] :=s3=HypergeometricPFQ[{1,1,1},{2,2,2},-zc]
Out[9] :=0.891213
In[10] :=g1=zc*lc*s1-zc*s2
Out[10] :=-0.7966
In[11] :=g2=lc*lc*qc-2*zc*lc*s2+2*zc*s3
Out[11] :=1.78243
```

$$\text{In}[12] := \text{vbc} = \frac{\texttt{beta*beta*qc}}{\texttt{n*(qc*g2-g1*g1)}}$$

$$\text{Out}[12] := n^{-1}5.1378$$

$$\text{In}[13] := \text{vtc} = \frac{\texttt{theta*theta*(qc+g2+2*g1)}}{\texttt{n*(qc*g2-g1*g1)*beta*beta}}$$

$$\text{Out}[13] := n^{-1}4172.3496$$

$$\text{In}[14] := \text{vbtc} = \frac{\texttt{theta*(qc+g1)}}{\texttt{n*(qc*g2-g1*g1)}}$$

$$\text{Out}[14] := -n^{-1}33.4214.$$

Thus, we obtain

$$\mathbf{A}_c^{-1} = n^{-1}\begin{pmatrix} 5.1378 & -33.4214 \\ & 4172.3496 \end{pmatrix}.$$

It is then straightforward to then obtain the theoretical standard deviations of $\hat{\beta}_c$ and $\hat{\theta}_c$ as the square root of the diagonal elements.

2.5.5 Effect of the censoring level

Using the above expectations, we can also obtain the standardised asymptotic variances

$$Var\left(\frac{\sqrt{n}}{\beta} \times \hat{\beta}\right) = \frac{q_c}{q_c\gamma^{(2)}(1, z_c) - \left\{\gamma^{(1)}(1, z_c)\right\}^2}$$

and

$$Var\left(\frac{\sqrt{n}\beta}{\theta} \times \hat{\theta}\right) = \frac{q_c + \gamma^{(2)}(1, z_c) + 2\gamma^{(1)}(1, z_c)}{q_c\gamma^{(2)}(1, z_c) - \left\{\gamma^{(1)}(1, z_c)\right\}^2},$$

as discussed in Watkins & John (2004). Using the square root of standardised quantities - that is, the asymptotic standardised standard deviations - we will assess the effect that the level censoring has on the precision of the estimate, as well as comparing these asymptotic results to their practical counterparts from simulated Weibull data, with $\beta = 2$ and $\theta = 100$. Watkins & John (2004) presented these results for simulated data from a Weibull distribution with $\beta = \theta = 1$, and one, large sample size, $n = 2500$; we extend their work with the inclusion of several (much smaller) sample sizes, ranging from $n = 50$ to $n = 1000$, given below.

We plot the theoretical and simulated standard deviations versus c, at various sample sizes. We denote the theoretical standard deviations with a smooth line, unbroken (—) for $\hat{\beta}_c$, and dashed (- - -) for $\hat{\theta}_c$. The simulated results are represented by markers, with a diamond (♦) for $\hat{\beta}_c$, and a square (■) for $\hat{\theta}_c$.

- Figure 2.18 shows the theoretical and simulated standard deviations for $\hat{\beta}_c$ and $\hat{\theta}_c$, for a sample size of 50, at increasing censoring levels. We see at early censoring levels there are quite large discrepancies between the theoretical and simulated values, but agreement improves as the censoring time is allowed to increase. Figure 2.19 again

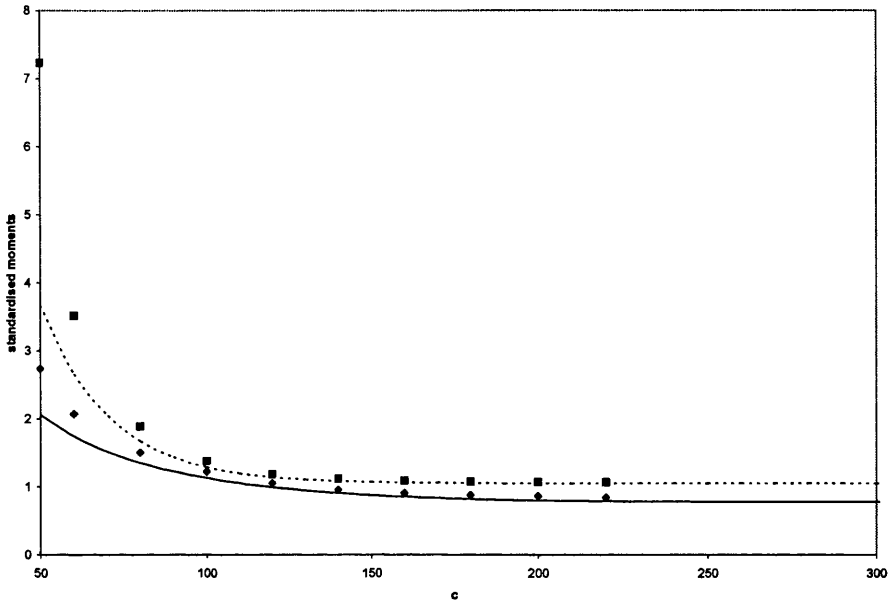

Figure 2.18: Theoretical and simulated standardised standard deviations of $\hat{\beta}_c$ (—♦—) and $\hat{\theta}_c$ (- -■- -) versus c, for $\beta = 2$, $\theta = 100$, and $n = 50$. Simulated values are based on 10,000 replications.

shows some discrepancies between theoretical and simulated standard deviations for $n = 100$ at early censoring levels, which improve as more items are left to fail.

- We see that for larger sample sizes, $n = 300$ (Figure 2.20), and $n = 500$ (Figure 2.21), there is good agreement between the simulated and theoretical standard deviations of $\hat{\beta}_c$ and $\hat{\theta}_c$, with much improvement at early censoring levels when n increases to 500.

- and for large samples, $n = 1000$ (Figure 2.22), we see excellent agreement between the simulated and theoretical standard deviations of $\hat{\beta}_c$ and $\hat{\theta}_c$, even with very early censoring.

For all sample sizes, we see excellent agreement between theory and simulations at $c \geq 140$. We note that the standard deviations are reduced as c increases, this is expected, as more failure information is observed with later censoring levels, which, in turn will improve the precision of the estimates yielded. These censored results clearly level off to the corresponding complete standard deviations as $c \to \infty$.

2.5.6 Effect of the shape parameter

As in the complete case, the theoretical standard deviations obtained from the EFI matrix, see (2.48), need to be checked against finite simulated samples to assure the suitability of

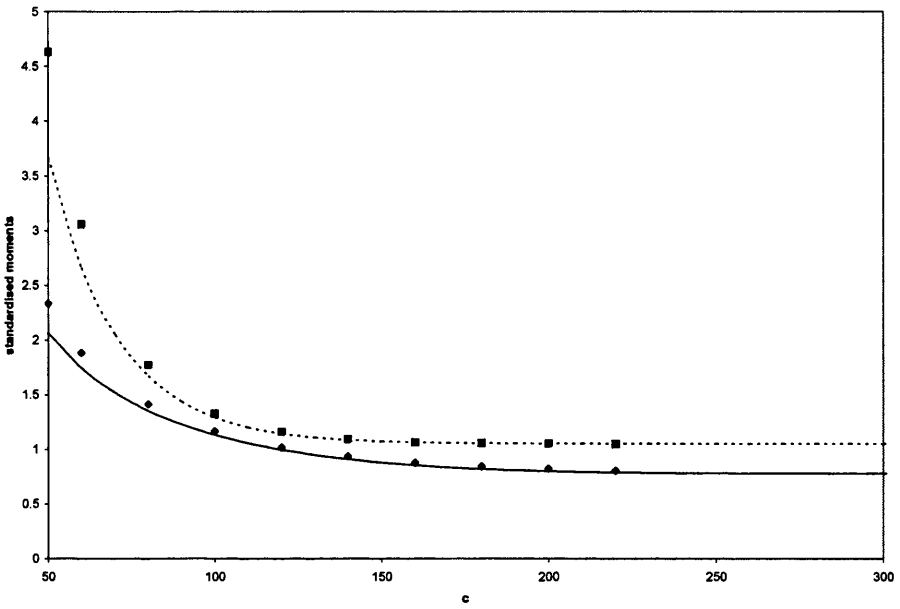

Figure 2.19: Theoretical and simulated standardised standard deviations of $\hat{\beta}_c$ (—♦—) and $\hat{\theta}_c$ (- -■- -) versus c, for $\beta = 2$, $\theta = 100$, and $n = 100$. Simulated values are based on 10,000 replications.

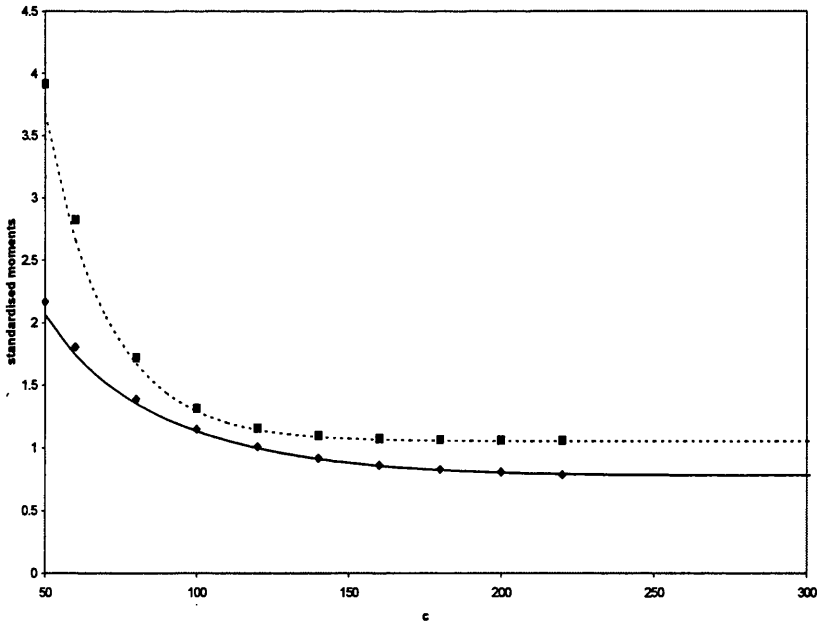

Figure 2.20: Theoretical and simulated standardised standard deviations of $\hat{\beta}_c$ (—♦—) and $\hat{\theta}_c$ (- -■- -) versus c, for $\beta = 2$, $\theta = 100$, and $n = 300$. Simulated values are based on 10,000 replications.

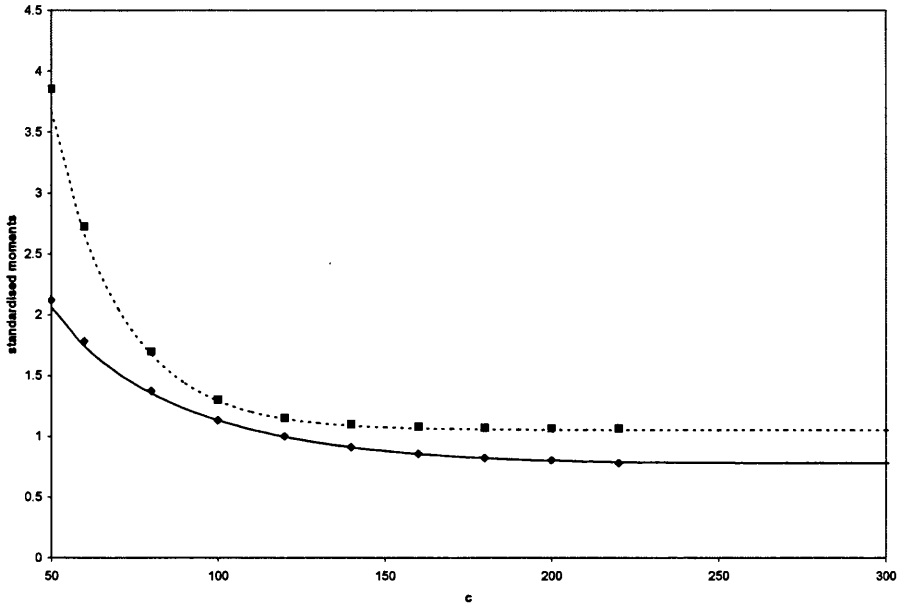

Figure 2.21: Theoretical and simulated standardised standard deviations of $\hat{\beta}_c$ (—♦—) and $\hat{\theta}_c$ (- -■- -) versus c, for $\beta = 2$, $\theta = 100$, and $n = 500$. Simulated values are based on 10,000 replications.

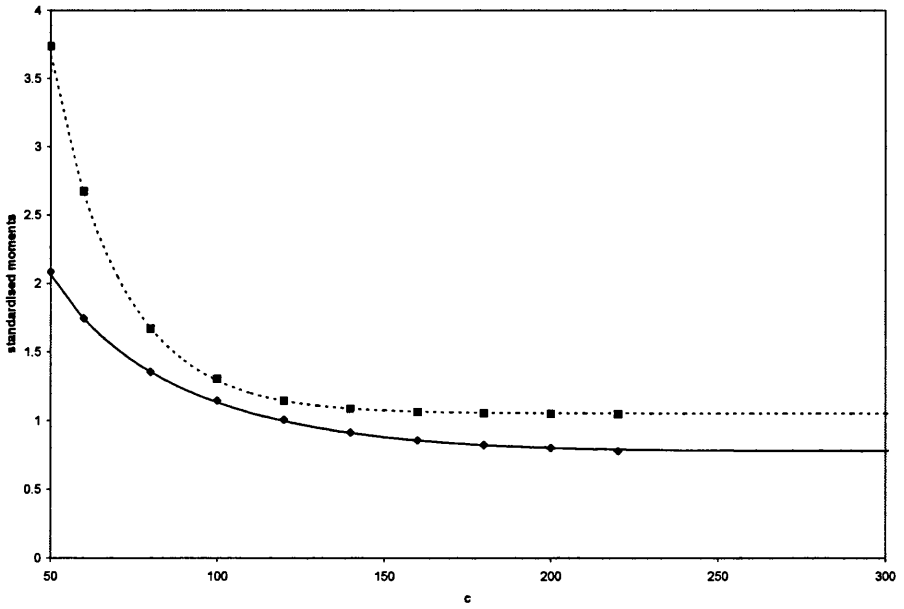

Figure 2.22: Theoretical and simulated standardised standard deviations of $\hat{\beta}_c$ (—♦—) and $\hat{\theta}_c$ (- -■- -) versus c, for $\beta = 2$, $\theta = 100$, and $n = 1000$. Simulated values are based on 10,000 replications.

β	c				
	50	100	150	200	∞
0.9	0.0416	0.0323	0.0284	0.0263	0.0222
	0.0415	0.0323	0.0285	0.0264	0.0224
1	0.0476	0.0358	0.0311	0.0291	0.0247
	0.0478	0.0362	0.0314	0.0288	0.0247
1.1	0.0540	0.0394	0.0338	0.0310	0.0271
	0.0546	0.0394	0.0340	0.0313	0.0274
2	0.1305	0.0717	0.0557	0.0507	0.0470
	0.1326	0.0718	0.0559	0.0509	0.0496
3.5	0.3764	0.1254	0.0884	0.0863	0.0863
	0.3887	0.1260	0.0892	0.0869	0.0869

Table 2.12: Theoretical (upper) and simulated (lower) standard deviations of $\hat{\beta}_c$ with varying c and β, and fixed $\theta = 100$, $n = 1000$.

the asymptotic approximations. These checks should also be extended to the asymptotic Normal distribution of the MLEs, which we will study in the next chapter.

The above plots clearly illustrate the effect censoring has on the standardised theoretical and simulated standard deviations, summarised for $\beta = 2$ and $\theta = 100$. We now want to expand these checks on the theoretical and simulated standard deviations, numerically, for alternative shape parameter values. This should confirm the agreement between theory and practice for $\beta = 2$, when the hazard function is increasing, still holds for decreasing ($\beta < 1$) or constant ($\beta = 1$) hazard functions. We restrain our parameter value options and keep θ fixed, because, although varying θ (with β fixed) will change the spread and peak of the distribution, it should not affect the characteristics of the hazard function, or the nature of the failure data itself, hence, we do not expect that a change in the scale parameter will affect the asymptotic approximations used throughout this thesis.

Results for varying the censoring level with sample size fixed at $n = 1000$ are shown in Tables 2.12 for $\hat{\beta}_c$, and Table 2.14 for $\hat{\theta}_c$; and varying the sample sample size with a fixed censoring level of $c = 100$, are shown in Tables 2.13 for $\hat{\beta}_c$, and Table 2.15 for $\hat{\theta}_c$.

We observe good agreement between these theoretical results and those obtained in simulation experiments, for all true values β considered here. This agreement improves as the sample size increases, and at $n = 1000$, we see that even for early censored estimates the results for theory and practice are consistent.

2.6 The Weibull Quantile Function B_{10}

We can now use the EFI matrix found in the previous section to derive the asymptotic distribution of $\hat{B}_{10,c}$. A first order Taylor series about the true parameters (β, θ) is used to express the estimated 10^{th} percentile as

$$\hat{B}_{10,c} \simeq B_{10} + \mathbf{b}'(\hat{\beta}_c - \beta, \hat{\theta}_c - \theta)$$

β	n				
	50	100	300	500	1000
0.9	0.1443	0.1020	0.0589	0.0456	0.0323
	0.1510	0.1035	0.0594	0.0455	0.0323
1	0.1603	0.1133	0.0654	0.0507	0.0358
	0.1682	0.0510	0.0663	0.0510	0.0362
1.1	0.1763	0.1247	0.0720	0.0558	0.0394
	0.1833	0.1292	0.0717	0.0567	0.0394
2	0.3206	0.2267	0.1309	0.1014	0.0717
	0.3405	0.2307	0.1335	0.1018	0.0718
3.5	0.6490	0.3967	0.2290	0.1774	0.1254
	0.5797	0.4065	0.2315	0.1791	0.1260

Table 2.13: Theoretical (upper) and simulated (lower) standard deviations of $\hat{\beta}_c$ with varying n and β, and fixed $\theta = 100$, $c = 100$.

β	c				
	50	100	150	200	∞
0.9	6.7102	4.5392	4.0223	3.8461	3.6996
	6.8553	4.5631	4.0251	3.8659	3.7088
1	6.3797	4.0853	3.5880	3.4344	3.3297
	6.4348	4.0621	3.5516	3.4077	3.3093
1.1	6.1358	3.7139	3.2353	3.1020	3.0270
	6.1782	3.7260	3.2286	3.0846	2.9989
2	5.8028	2.0426	1.6996	1.6678	1.6648
	6.0025	2.0672	1.6957	1.6678	1.6666
3.5	8.1390	1.1672	0.9527	0.9513	0.9513
	8.5130	1.1789	0.9615	0.9603	0.9603

Table 2.14: Theoretical (upper) and simulated (lower) standard deviations of $\hat{\theta}_c$ with varying c and β, and fixed $\theta = 100$, $n = 1000$.

β	n				
	50	100	300	500	1000
0.9	20.2999	14.3542	8.2874	6.4194	4.5392
	22.6960	15.0484	8.4719	6.4555	4.5631
1	18.2699	12.9187	7.4586	5.7774	4.0853
	19.9034	5.8677	7.5142	5.8677	4.0621
1.1	16.6090	11.7443	6.7806	5.2522	3.7139
	17.9513	12.4299	6.8495	5.2733	3.7260
2	9.1349	6.4593	3.7293	2.8887	2.0426
	9.4899	6.6752	3.7926	2.9274	2.0672
3.5	5.2200	3.6912	2.1310	1.6507	1.1672
	5.4687	3.7858	2.1486	1.6592	1.1789

Table 2.15: Theoretical (upper) and simulated (lower) standard deviations of $\hat{\theta}_c$ with varying n and β, and fixed $\theta = 100$, $c = 100$.

where

$$\mathbf{b} = \begin{pmatrix} \frac{\partial B_{10}}{\partial \beta} \\ \frac{\partial B_{10}}{\partial \theta} \end{pmatrix} = \begin{pmatrix} -\theta\beta^{-2}\lambda^{\frac{1}{\beta}} \ln\lambda \\ \lambda^{\frac{1}{\beta}} \end{pmatrix},$$

and

$$\lambda = -\ln 0.9. \tag{2.53}$$

Hence, for large samples we have

$$E\left[\hat{B}_{10,c}\right] \simeq B_{10} + \mathbf{b}'E\left[(\hat{\beta}_c - \beta, \hat{\theta}_c - \theta)\right] \simeq B_{10}$$

$$\begin{aligned} Var\left(\hat{B}_{10,c}\right) &\simeq \mathbf{b}'\mathbf{A}_c^{-1}\mathbf{b} \\ &= n^{-1}\left[q_c\gamma^{(2)}(1,z_c) - \left\{\gamma^{(1)}(1,z_c)\right\}^2\right]^{-1} \\ &\quad \left(-\theta\beta^{-2}\lambda^{\frac{1}{\beta}}\ln\lambda \quad \lambda^{\frac{1}{\beta}}\right)\begin{pmatrix} \beta^2 q_c & \theta\left\{q_c + \gamma^{(1)}(1,z_c)\right\} \\ & \beta^{-2}\theta^2\left\{q_c + \gamma^{(2)}(1,z_c) + 2\gamma^{(1)}(1,z_c)\right\} \end{pmatrix} \\ &\quad \begin{pmatrix} -\theta\beta^{-2}\lambda^{\frac{1}{\beta}}\ln\lambda \\ \lambda^{\frac{1}{\beta}} \end{pmatrix}. \end{aligned}$$

Expanding the quadratic form then gives,

$$\left\{\begin{array}{c} -\beta^{-2}\theta^2\left(\lambda^{\frac{1}{\beta}}\right)^2\ln\lambda\left[q_c + \gamma^{(1)}(1,z_c) - q_c\ln\lambda\right] + \\ \beta^{-2}\theta^2\left(\lambda^{\frac{1}{\beta}}\right)^2\left[q_c + \gamma^{(2)}(1,z_c) + 2\gamma^{(1)}(1,z_c) - q_c\lambda - \gamma^{(1)}(1,z_c)\ln\lambda\right] \end{array}\right\},$$

which then simplifies to

$$\beta^{-2}\theta^2\left(\lambda^{\frac{1}{\beta}}\right)^2\left\{\begin{array}{c} q_c(\ln\lambda)^2 - 2\ln\lambda\left(q_c + \gamma^{(1)}(1,z_c)\right) \\ +q_c + \gamma^{(2)}(1,z_c) + 2\gamma^{(1)}(1,z_c) \end{array}\right\},$$

and so we have

$$\begin{aligned} Var\left(\hat{B}_{10,c}\right) \doteq\ & n^{-1}\left[q_c\gamma^{(2)}(1,z_c) - \left\{\gamma^{(1)}(1,z_c)\right\}^2\right]^{-1} \times \\ & \beta^{-2}\theta^2\left(\lambda^{\frac{1}{\beta}}\right)^2\left\{\begin{array}{c} q_c(\ln\lambda)^2 - 2\ln\lambda\left(q_c + \gamma^{(1)}(1,z_c)\right) \\ +q_c + \gamma^{(2)}(1,z_c) + 2\gamma^{(1)}(1,z_c) \end{array}\right\}. \end{aligned} \tag{2.54}$$

We note that the asymptotic distribution of $\hat{B}_{10,c}$ is Normal with the above mean and variance; we refer to Mardia et al. (1979), for example, for further details on the asymptotic distribution of non-linear functions of MLEs. As with the MLEs of β and θ, we will need to assess the extent to which these asymptotic properties hold in finite samples. We further

note that allowing all items to fail ($c \to \infty$) we will obtain, for the complete case

$$E\left[\hat{B}_{10}\right] \doteq B_{10}$$

and

$$\begin{aligned} Var\left(\hat{B}_{10}\right) &\doteq \mathbf{b}'\mathbf{A}^{-1}\mathbf{b} \\ &= 6n^{-1}\pi^{-2}\beta^{-2}\theta^2\left(\lambda^{\frac{1}{\beta}}\right)^2\left[(\ln\lambda)^2 - 2\ln\lambda\,(1-\gamma) + \frac{\pi^2}{6} + (\gamma-1)^2\right] \quad (2.55) \end{aligned}$$

2.6.1 Effect of censoring level and shape parameter

As for the estimators $\hat{\beta}_c$ and $\hat{\theta}_c$, we will once again need to assess the agreement between these asymptotic results and their simulated counterparts on finite sample data. First, we can observe the effect that the level censoring has on the precision of the estimate $\hat{B}_{10,c}$, as well as comparing these asymptotic results to their practical counterparts from our simulated Weibull data, with $\beta = 2$ and $\theta = 100$. More thorough numerical checks of the asymptotic theory for Weibull data with various censoring levels, sample sizes, and shape parameter values, will follow below.

In Figures 2.23, 2.24, 2.25, 2.26 and 2.27, we plot the theoretical and simulated standard deviations versus c, at sample sizes $n = 50, 100, 300, 500$ and 1000 respectively. We denote the theoretical standard deviations with a smooth line, (—) the simulated results are represented by a diamond (♦). We see that when n is small there are noticeable differences between theoretical and simulated standard deviations at early censoring times, but this is small at $n = 300$, and has effectively disappeared when the sample size increases to $n = 500$.

As we would expect, the standard deviations are smaller for later censoring levels, reaching the standard deviations for the complete sample, obtained from (2.55), as $c \to \infty$.

Tables 2.16 and 2.17 show the theoretical and simulated standard deviations of $\hat{B}_{10,c}$ for various censoring levels and sample sizes. When we vary the sample size and keep the censoring level fixed at $c = 100$, we see that the simulated sample standard deviations are closer to their theoretical counterparts as n increases. We can see that for large sample size ($n = 1000$) we have excellent agreement between theory and practice at all censoring levels, but we note that for small n, observed values are slightly higher. This was illustrated for $\beta = 2$ in Figure 2.27. Tables 2.16 and 2.17 confirm that the general pattern seen for $\beta = 2$ holds for all shape parameter values.

2.7 Practical Considerations

From an experimental point of view, consideration must be given to the choice of how many items to test (n), and the time, c, at which we stop the experiment. From a statistical perspective, we would prefer to test as many items as possible, and allow all of these items to

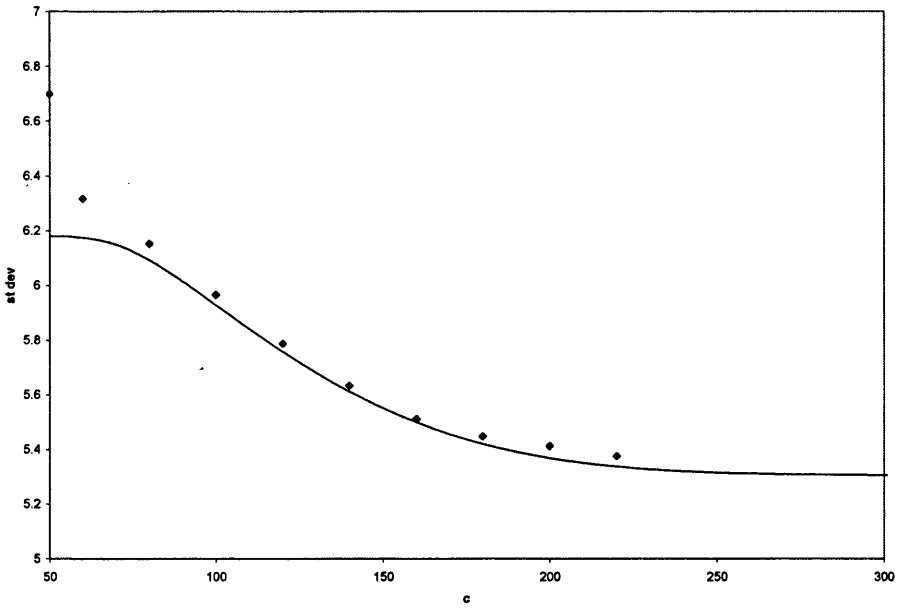

Figure 2.23: Theoretical (—) and simulated (♦) standard deviations of $\hat{B}_{10,c}$ versus c, for $\beta = 2$, $\theta = 100$, and $n = 50$. Simulated values are based on 10,000 replications.

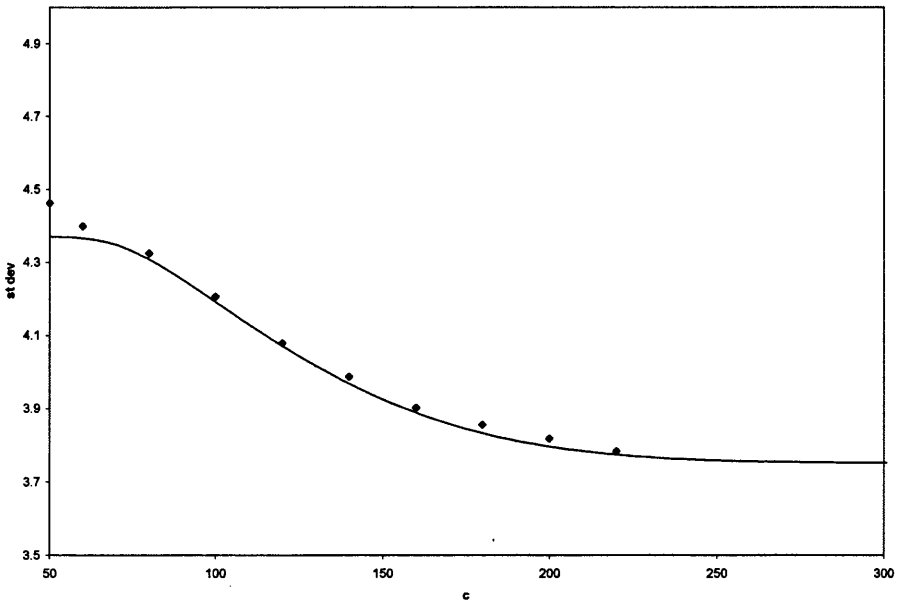

Figure 2.24: Theoretical (—) and simulated (♦) standard deviations of $\hat{B}_{10,c}$ versus c, for $\beta = 2$, $\theta = 100$, and $n = 100$. Simulated values are based on 10,000 replications.

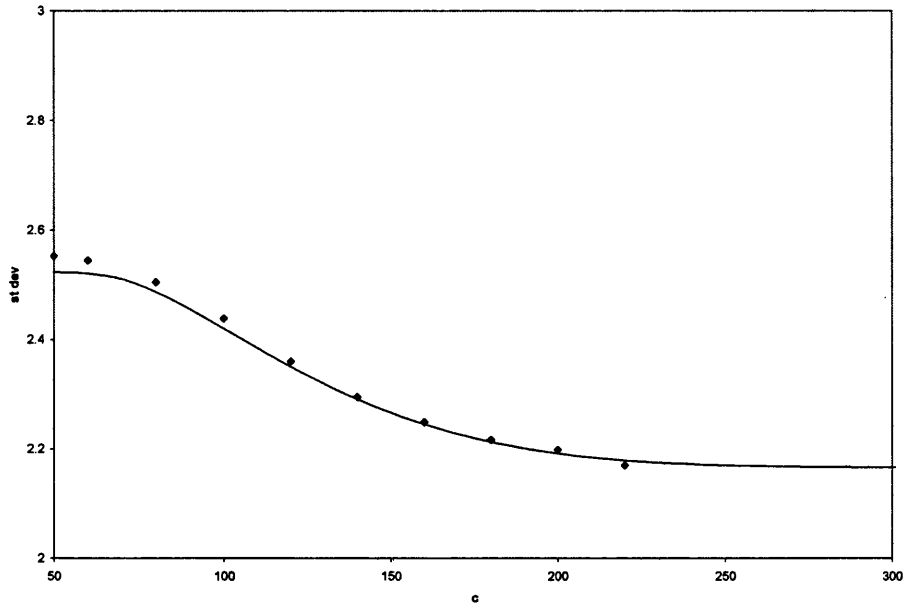

Figure 2.25: Theoretical (—) and simulated (♦) standard deviations of $\hat{B}_{10,c}$ versus c, for $\beta = 2$, $\theta = 100$, and $n = 300$. Simulated values are based on 10,000 replications.

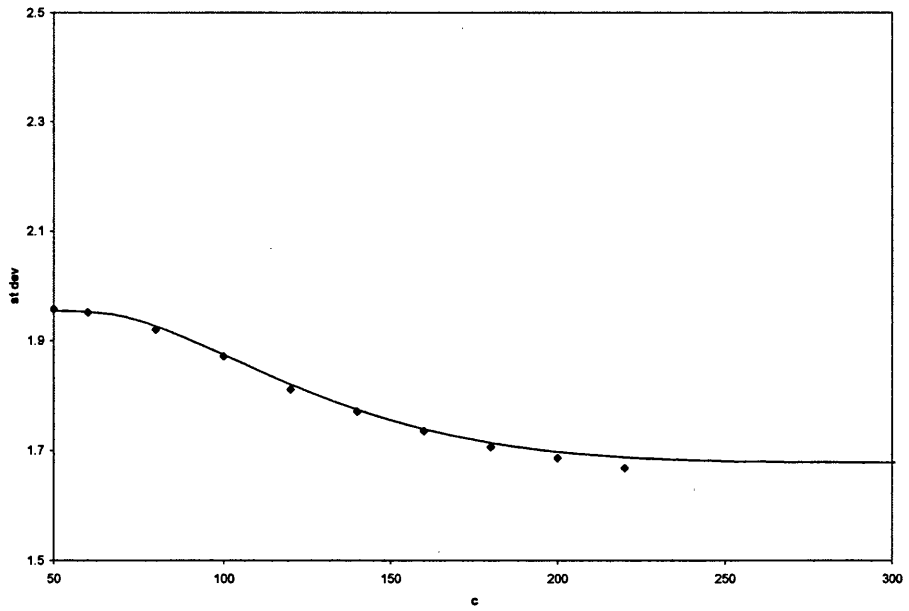

Figure 2.26: Theoretical (—) and simulated (♦) standard deviations of $\hat{B}_{10,c}$ versus c, for $\beta = 2$, $\theta = 100$, and $n = 500$. Simulated values are based on 10,000 replications.

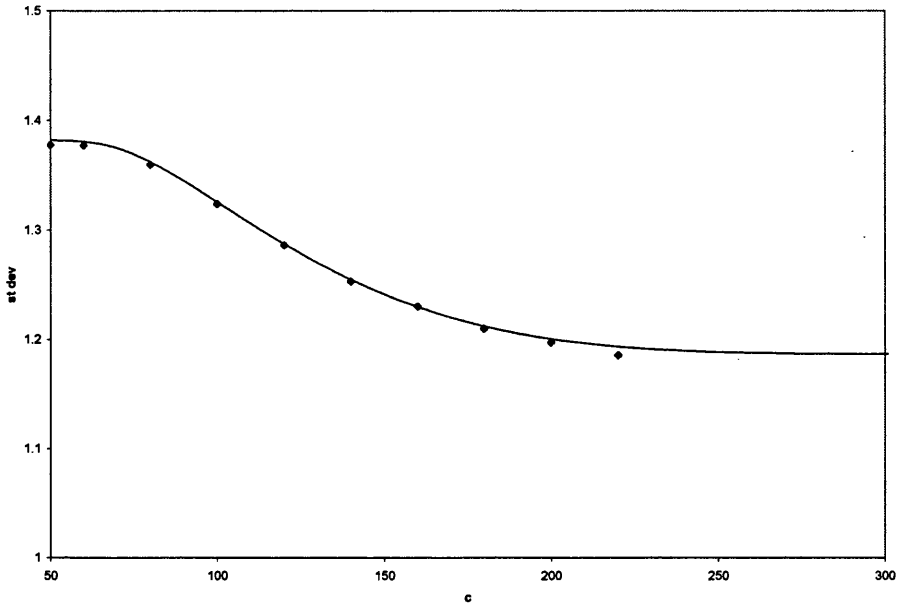

Figure 2.27: Theoretical (—) and simulated (♦) standard deviations of $\hat{B}_{10,c}$ versus c, for $\beta = 2$, $\theta = 100$, and $n = 1000$. Simulated values are based on 10,000 replications.

β	c				
	50	100	150	200	∞
0.9	0.7705	0.7445	0.7231	0.7077	0.6665
	0.7703	0.7443	0.7193	0.7024	0.6608
1	0.8922	0.8604	0.8328	0.8133	0.7702
	0.8924	0.8586	0.8324	0.8127	0.7737
1.1	0.9969	0.9598	0.9258	0.9023	0.8592
	1.0001	0.9654	0.9356	0.9092	0.8689
2	1.3820	1.3254	1.2414	1.2049	1.1864
	1.3807	1.3212	1.2435	1.2001	1.1852
3.5	1.6641	1.2267	1.1098	1.0981	1.0981
	1.6785	1.2318	1.1169	1.1054	1.1055

Table 2.16: Theoretical (upper) and simulated (lower) standard deviations of $\hat{B}_{10,c}$ with varying c and β, and fixed $\theta = 100$, $n = 1000$.

β	n				
	50	100	300	500	1000
0.9	3.3297	2.3544	1.3593	1.0529	0.7445
	3.5726	2.5045	1.4048	1.0652	0.7443
1	3.8480	2.7209	1.5709	1.2168	0.8604
	4.1481	2.7858	1.5595	1.2176	0.8586
1.1	4.2923	3.0351	1.7523	1.3573	0.9598
	4.5038	3.1436	1.7813	1.3669	0.9654
2	5.9274	4.1913	2.4199	1.8744	1.3254
	5.9666	4.2066	2.4351	1.8662	1.3212
3.5	5.4860	3.8792	2.2396	1.7348	1.2267
	5.4522	3.8915	2.2539	1.7344	1.2318

Table 2.17: Theoretical (upper) and simulated (lower) standard deviations of $\hat{B}_{10,c}$ with varying n and β, and fixed $\theta = 100$, $c = 100$.

fail, but clearly limited resources will generally restrict both sample size and censoring time. We have investigated the theoretical standard deviations for Weibull parameter estimates $\hat{\beta}_c$ and $\hat{\theta}_c$ as well as the quantile estimate $\hat{B}_{10,c}$, at various sample sizes and censoring levels, and have shown that these asymptotic results hold in finite samples.

We can conclude that for β and θ, large sample sizes will generally yield more precise estimates, but, when using a censoring regime, gains can be made in the precision if we reduce the sample size, as long as the censoring time is then increased.

However, B_{10} is often a more useful quantity to estimate, in particular for establishing warranty periods, and, in fact Figures 2.23 to 2.27 show that the same benefits cannot be achieved here. At $n = 1000$, even for the earliest censoring time studied, $c = 50$, the estimate is more precise than those yielded from any smaller, complete, sample. It seems that in circumstances where the running costs of the experiment are more expensive than the cost of the items put to test, it would be more beneficial to increase the sample size being tested, and lower the censoring time, as this would yield the most precise estimate at the lowest cost.

We have only looked at selected sample sizes and censoring times, and, for the purpose of assessing the suitability of the asymptotic approximations, these are, we argue, sufficient. However, further simulation experiments would be beneficial in finding an optimal level of censoring, and sample size, and evaluating the balance between obtaining adequate precision and experiment expenditure, in terms of a cost function. This will not be considered as part of this thesis, but is noted as a topic for further research.

2.8 Summary

In this chapter we have examined examples of fitting the Weibull distribution to both complete and censored data. We have employed the EFI matrix to yield asymptotically valid

variances and covariances of MLEs of the shape and scale parameters, as well as variances of functions of the parameters, in particular B_{10}. These parameter results feature widely in statistical inference, but published discussions generally give the observed information, see Nelson (1982) for example, or leave the EFI in terms of general integrals. This chapter provides formulae for the elements of the matrix, discusses their computation and behaviour, and assesses the worth of these asymptotic variances in finite samples. We have compiled the results of extensive simulation studies in order to check such approximations to the moments of the Weibull parameter MLEs, and have shown that there is good agreement between the theoretical approximations and simulated values, even for small sample sizes, which is somewhat contrary to assertions made in Nelson (1982).

Further to the study of moments of MLEs, in Chapter 3 we conduct an investigation to the distribution of the MLEs, which due to the asymptotic properties we know to be Normal for large samples, see Ansell & Phillips (1994) for example, but there is no reference to how large a sample needs to be for this to hold. We consider the rate at which the MLEs reach Normality, with increasing n, and also indicate the effect Type I censoring has on this. This progress should confirm the suitability of the asymptotic approximations in small to moderate samples. This extends the work introduced by Chua et al. (2007), where the emphasis concentrated on Type II censored Weibull data.

Obviously, where the sample size is too small for Normality to be assumed, a different method to measure the precision of the MLEs must be used. Several papers have discussed alternative approaches to the "Normal-theory" to obtain confidence regions, using the relative likelihood function, see Meeker & Escobar (1995) for example. As well as being asymptotically equivalent to the Normal confidence regions, studies by Watkins (2004) and Chua et al. (2007), for example, have shown that relative likelihood contours reflect more accurately the behaviour of the distributions of MLEs for small sample sizes. This will be the focus of Chapter 4.

The final strand of the thesis is to use these asymptotic theoretical results discussed hitherto, to explain the relationship between the time of censoring and the value of the MLE. Using the ball bearings data, Kalbfleisch (1979), computed MLEs for the complete data, and then worked backwards, imagining the experiment had been censored at 75 millions revolutions, recalculated the censored MLEs and compared the results. We, on the other hand, would like to work along the same time line as the experiment, and, as discussed using Figures 2.1, 2.2 and 2.3, we wish to find the extent to which the censored estimate obtained in an interim analysis, can be regarded as a reliable guide to the complete estimate, obtained when the last item fails.

Chapter 3

Asymptotic Normality of MLEs

The general property of asymptotic Normality of the MLEs is discussed in all of the key texts available in the field of reliability and statistical inference generally; we refer to Cox & Hinkley (1974) for a detailed discussion, based on the theoretical proof in Cramer (1946). Due to the assumptions and asymptotic approximations made in the previous chapters, a larger scale investigation seems appropriate. We consider the implications of asymptotic Normality, and more importantly, are any of these conditions met in finite samples?

3.1 Approximate Confidence Regions

We know that, asymptotically, $\left(\hat{\beta}_c, \hat{\theta}_c\right)$ follows the Normal distribution with mean (β, θ) and covariance matrix equal to the inverse of the EFI matrix, given in (2.48). This, in turn, gives the approximate confidence regions for the sampling distribution of $\left(\hat{\beta}_c, \hat{\theta}_c\right)$; for example, the $(1-\alpha)100\%$ confidence limits for β is

$$\hat{\beta}_c \pm s_{\alpha/2}\sqrt{Var\left(\hat{\beta}_c\right)}.$$

for $s_{\alpha/2}$ satisfying

$$\Pr\left\{S < s_{\alpha/2}\right\} = 1 - \frac{\alpha}{2},$$

where S follows the standard Normal distribution, and $s_{\alpha/2}$ is easily obtained from a Normal table, see for example Murdoch & Barnes (1974). So, for $\alpha = 0.05$, our 95% confidence intervals for the true Weibull parameters are

$$\beta = \hat{\beta}_c \pm 1.96\sqrt{Var\left(\hat{\beta}_c\right)} \tag{3.1}$$

and

$$\theta = \hat{\theta}_c \pm 1.96\sqrt{Var\left(\hat{\theta}_c\right)}, \tag{3.2}$$

where, from (2.48), we have the approximate variances,

$$Var\left(\hat{\beta}_c\right) \doteqdot \frac{\beta^2 q_c}{n\left[q_c\gamma^{(2)}\left(1,z_c\right) - \left\{\gamma^{(1)}\left(1,z_c\right)\right\}^2\right]}$$

and

$$Var\left(\hat{\theta}_c\right) \doteqdot \frac{\beta^{-2}\theta^2\left\{q_c + \gamma^{(2)}\left(1,z_c\right) + 2\gamma^{(1)}\left(1,z_c\right)\right\}}{n\left[q_c\gamma^{(2)}\left(1,z_c\right) - \left\{\gamma^{(1)}\left(1,z_c\right)\right\}^2\right]}$$

where β, θ, and therefore q_c and z_c, are unknown (except in simulation experiments), and have to be replaced by the estimates $\hat{\beta}_c$ and $\hat{\theta}_c$ in practice. We expect to see symmetric confidence intervals for a single parameter.

Revisiting the ball bearings in Table 1.2, if censored at $c = 100$, via (3.1) and (3.2) we obtain the approximate confidence intervals for β and θ to be

$$\begin{aligned} \beta &= \hat{\beta}_c \pm 1.96\sqrt{Var\left(\hat{\beta}_c\right)} \\ &= 2.2400 \pm 1.96\sqrt{0.2007} \\ &= (1.3620, 3.1180) \end{aligned} \tag{3.3}$$

and

$$\begin{aligned} \theta &= \hat{\theta}_c \pm 1.96\sqrt{Var\left(\hat{\theta}_c\right)} \\ &= 80.3159 \pm 1.96\sqrt{69.6458} \\ &= (63.9589, 96.6729) \end{aligned} \tag{3.4}$$

In practice, the s value, $s_{\alpha/2} = 1.96$ would be replaced by t value, and we refer to Montgomery & Runger (1994) for further details.

Similarly for bivariate $\left(\hat{\beta}_c, \hat{\theta}_c\right)$, asymptotic Normality implies that the sampling distribution of $\left(\hat{\beta}_c, \hat{\theta}_c\right)$ is characterised by ellipses of constant density, defined by

$$\begin{pmatrix} \beta - \beta_0 \\ \theta - \theta_0 \end{pmatrix}' \mathbf{A}_c \begin{pmatrix} \beta - \beta_0 \\ \theta - \theta_0 \end{pmatrix} = c$$

for arbitrary non-negative c. Since, asymptotically,

$$\begin{pmatrix} \beta - \hat{\beta}_c \\ \theta - \hat{\theta}_c \end{pmatrix}' \mathbf{A}_c \begin{pmatrix} \beta - \hat{\beta}_c \\ \theta - \hat{\theta}_c \end{pmatrix} \sim \chi^2_2,$$

Watkins (2004) illustrates that due to the convergence of observed and expected Fisher information matrices, an approximate $100\,(1-\alpha)\,\%$ confidence region for (β, θ) can be obtained

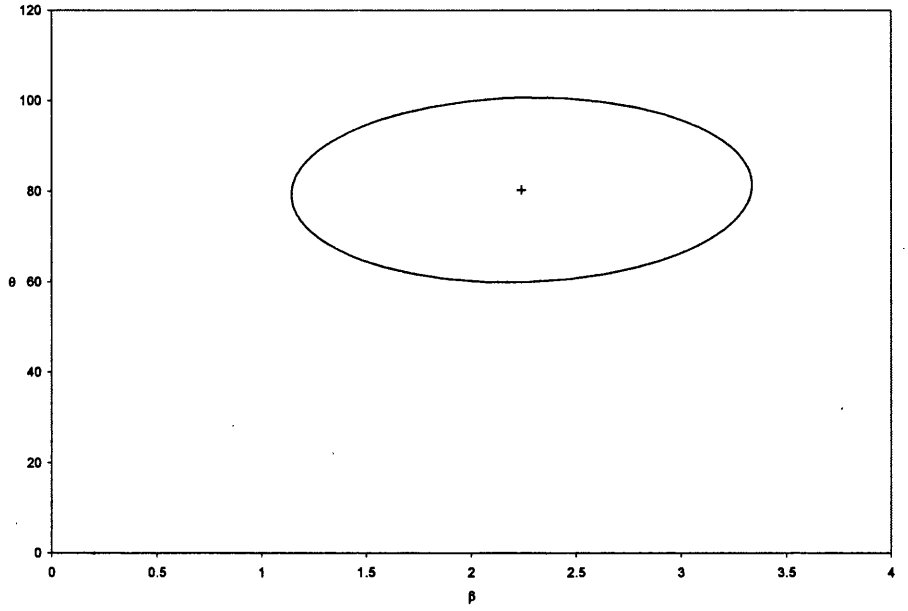

Figure 3.1: 95% Confidence Ellipse around the MLEs for the Ball Bearings data at $c = 100$.

by calculating the ellipse

$$\begin{pmatrix} \beta - \hat{\beta}_c \\ \theta - \hat{\theta}_c \end{pmatrix}' \hat{\mathbf{J}}_c \begin{pmatrix} \beta - \hat{\beta}_c \\ \theta - \hat{\theta}_c \end{pmatrix} = -2 \ln \alpha$$

where $\mathbf{J}_c$ is the *observed* Fisher information matrix. This result depends on unknown β and θ, therefore in practice we use the estimates $\left(\hat{\beta}_c, \hat{\theta}_c\right)$, and the notation $\hat{\mathbf{J}}_c$.

We can therefore construct the 95% confidence ellipse for the ball bearings data, censored at $c = 100$, and this is shown in Figure 3.1. From a brief investigation of the ellipse, we see that the limits deduced above in (3.3) and (3.4) for β and θ provide a rough guide to the scope of the confidence ellipse of (β, θ).

3.1.1 Asymptotic assumptions in small sample sizes

Are these asymptotic approximations suitable in the inference of small to moderate samples, such as the ball bearings data? There seems to be a consensus within these key texts, that these large sample theory approximations do not hold very well for small to moderate sample sizes, see for example, Shenton & Bowman (1977). However, there appears to be no referenced information suggesting how big a sample should be before these asymptotic assumptions may hold. In this chapter we will not be looking to test Normality at any given sample size, but instead to show, using our simulated estimates, that at a small sample size the MLEs are non-Normal, and eventually when the sample size gets larger, the MLEs

become Normally distributed. Our interest is the rate at which this occurs for different shape parameter values and censoring levels. As always, we simulate $N = 10,000$ failure times from a Weibull distribution, for various sample sizes and censoring levels. We set $\theta = 100$ and vary the shape parameter β, as the value of this parameter will affect the hazard function, and therefore has a large influence on the nature of the data.

We use the properties of the bivariate Normal distribution, in particular the necessary, but not sufficient, condition that each marginal distribution is univariate Normal, and so an initial conclusion of non-Normality of $\hat{\beta}_c$ and $\hat{\theta}_c$ would confirm multivariate non-Normality. We will therefore begin by checking the distribution of the MLEs for individual parameters, and then will extend our testing to the multivariate Normal tests described below.

Another interesting aspect for study is the rate at which the quantile function $\hat{B}_{10}$, approaches Normality, and we will explore the estimates of B_{10} further on in this chapter.

3.2 Tests and Measures of Univariate Normality

There are many discussions of tests of normality, and we refer to D'Agostino & Stephens (1986), and more recently, Khattree & Rao (2003) (Chapter 24), and Thode (2002) for a detailed outline on such tests. We will discuss some of the best known tests and review the literature advice and recommendations.

3.2.1 Basic Statistical Summaries

This section introduces moment based tests, that is, tests for skewness, $\sqrt{b_1}$, and tests of kurtosis, b_2. More details, and suggestions for using these tests, are discussed in D'Agostino et al. (1990). We let $\hat{\phi}$ be a Normal random variable with mean μ, and standard deviation σ, then we define the skewness and kurtosis using the third and fourth standardised moments

$$\sqrt{\beta_1} = \frac{E\left[\hat{\phi}-\mu\right]^3}{\left(E\left[\hat{\phi}-\mu\right]^2\right)^{\frac{3}{2}}} = \frac{E\left[\hat{\phi}-\mu\right]^3}{\sigma^3}$$

$$\beta_2 = \frac{E\left[\hat{\phi}-\mu\right]^4}{\left(E\left[\hat{\phi}-\mu\right]^2\right)^2} = \frac{E\left[\hat{\phi}-\mu\right]^4}{\sigma^4}$$

and for the Normal distribution these are equal to 0 and 3 respectively. D'Agostino & Stephens (1986) shows that the sample estimates of $\sqrt{\beta_1}$ and β_2 can be used to describe non-Normal distributions, by using the standardised third and fourth moments, given by

$$\sqrt{b_1} = \frac{m_3}{m_2^{\frac{3}{2}}}$$

β	$\sqrt{b_1}$	b_2	$\%\ in\ CI$	$\% < CI$	$\% > CI$
0.8	0.54	3.51	93.67	5.65	0.68
1	0.61	3.64	93.37	6.13	0.50
2	0.69	4.00	92.98	6.36	0.66
3.5	0.50	3.33	94.26	5.09	0.65

Table 3.1: Tests of skewness and kurtosis of $\hat{\beta}_c$ yielded from a Weibull distribution with various β, and fixed $\theta = 100$, $c = 100$, and $n = 50$.

and

$$b_2 = \frac{m_4}{m_2^2}$$

where

$$m_k = \frac{\sum_{i=1}^{n} \left(\hat{\phi}_i - \overline{\hat{\phi}}\right)^k}{N}, \qquad k = 2,3,4$$

and $\overline{\hat{\phi}}$ is the sample mean. Under Normality, these statistics would then have expected values of 0 and $\frac{3(N-1)}{(N+1)} = 3\frac{2}{N+1}$.

For each estimate, we can investigate the symmetry around the calculated confidence intervals, again with the focus on the effect of censoring and the nature of the data, determined by the shape parameter β of the sampling distribution of $\left(\hat{\beta}_c, \hat{\theta}_c\right)$. Via the asymptotically derived confidence limits, (3.1) and (3.2), for each simulated MLE, we can obtain the corresponding 95% confidence interval. By counting how many of these confidence intervals contain the true parameter value, as well as the percentage of confidence limits with MLEs that fall either below the lower limit, or above the upper limit, we can judge the effectiveness of the Normal assumption We would expect symmetric intervals, with 95% of true parameter values to lie within the intervals, and thus 2.5% to lie below and 2.5% to lie above the limits.

Results and discussion

As we see from Tables 3.1 and 3.2, this is far from the case at $n = 50$. The coverage of the confidence intervals are good (close to 95%), but a much higher proportion of the true values that are not within the interval are below the lower limit, again suggesting right skewness of the MLEs, which is confirmed by the values of $\sqrt{b_1}$ yielded (all greater than 0). A slight improvement is noticed as n increases to 500, see Tables 3.3 and 3.4. In fact we do not see symmetry until $n = 5000$, for both parameters, in Tables 3.5 and 3.6. This is consistent across the various values of the shape parameter β investigated.

3.2.2 Probability Plots

A $Q - Q$ (Quantile-Quantile) plot involves plotting the sample order statistics against the "expected" quantiles from a standard Normal distribution. The first step is to sort the

β	$\sqrt{b_1}$	b_2	$\%\ in\ CI$	$\% < CI$	$\% > CI$
0.8	1.44	7.69	92.99	6.80	0.21
1	1.13	5.64	93.64	5.89	0.47
2	0.70	4.42	94.14	4.80	1.06
3.5	0.56	3.91	94.26	5.09	0.65

Table 3.2: Tests of skewness and kurtosis of $\hat{\theta}_c$ yielded from a Weibull distribution with various β, and fixed $\theta = 100$, $c = 100$, and $n = 50$.

β	$\sqrt{b_1}$	b_2	$\%\ in\ CI$	$\% < CI$	$\% > CI$
0.8	0.19	3.09	94.81	3.56	1.63
1	0.21	3.16	94.72	3.68	1.60
2	0.18	3.14	95.39	3.09	1.52
3.5	0.16	3.01	94.88	3.28	1.84

Table 3.3: Tests of skewness and kurtosis of $\hat{\beta}_c$ yielded from a Weibull distribution with various β, and fixed $\theta = 100$, $c = 100$, and $n = 500$.

β	$\sqrt{b_1}$	b_2	$\%\ in\ CI$	$\% < CI$	$\% > CI$
0.8	0.32	3.36	95.18	3.24	1.58
1	0.34	3.28	94.72	3.59	1.69
2	0.21	3.17	95.12	3.15	1.73
3.5	0.16	3.09	94.70	3.23	2.07

Table 3.4: Tests of skewness and kurtosis of $\hat{\theta}_c$ yielded from a Weibull distribution with various β, and fixed $\theta = 100$, $c = 100$, and $n = 500$.

β	$\sqrt{b_1}$	b_2	$\%\ in\ CI$	$\% < CI$	$\% > CI$
0.8	0.00	3.02	95.11	2.51	2.38
1	0.06	3.04	94.90	2.88	2.22
2	0.04	2.98	95.14	3.00	1.86
3.5	0.10	3.13	95.25	2.80	1.95

Table 3.5: Tests of skewness and kurtosis of $\hat{\beta}_c$ yielded from a Weibull distribution with various β, and fixed $\theta = 100$, $c = 100$, and $n = 5000$.

β	$\sqrt{b_1}$	b_2	$\%\ in\ CI$	$\% < CI$	$\% > CI$
0.8	0.11	3.10	94.94	2.85	2.21
1	0.05	2.99	95.16	2.66	2.18
2	0.02	3.01	95.16	2.48	2.36
3.5	0.04	2.94	95.05	2.63	2.32

Table 3.6: Tests of skewness and kurtosis of $\hat{\theta}_c$ yielded from a Weibull distribution with various β, and fixed $\theta = 100$, $c = 100$, and $n = 5000$.

observations to obtain order statistics

$$\hat{\phi}_{(1)}, \hat{\phi}_{(2)}, ..., \hat{\phi}_{(N)}$$

these are the empirical quantiles used as the ordinates on the plot. Values for the abscissa of the empirical quantiles must now be chosen, and a commonly used plotting position is

$$p_i = \frac{i - \frac{1}{2}}{N}.$$

The pairs

$$\left(\Phi^{-1}(p_i), \hat{\phi}_{(i)}\right)$$

are then plotted. The $Q - Q$ plot allows us to see if the two cdfs differ only in scale and location; if the cdfs are in good agreement then the plotted points will lie on a straight line, any systematic deviation from linearity in the plot indicates that the data is not Normal. Kalbfleisch (1979) comments that $Q-Q$ plots are widely used in goodness of fit tests, hence we use this graphical method as an initial guide to the suitability of the assumed Normal distribution in our finite simulated samples of MLEs, for various shape parameter values and sample sizes. A formal test will follow to provide further confirmation and information to the $Q-Q$ plots. We refer to Thode (2002) for a more detailed discussion on probability plotting, including an outline of standardised $P - P$ (Percentile-Percentile) plots, which allow some goodness-of-fit tests based on the correlation between sample and theoretical probabilities; these plots are more sensitive to detecting discrepancies in the middle of the distribution.

Output and discussion

Each $Q-Q$ plot (Figure 3.2 to 3.17) gives the quantiles plotted for a sample obtained from complete failure data, $(\times)$, and the sample when failures are censored at $c = 100$, $(\circ)$. We start with a sample of 10,000 MLEs calculated from a generated Weibull distribution with parameters $\beta = 0.8$ and $\theta = 100$; we first examine the distribution of $\hat{\beta}_c$ for increasing n, and then repeat for $\hat{\theta}_c$.

At $n = 50$, Figure 3.2 shows a clear curved pattern with slope increasing from left to right, indicating that the distribution of $\hat{\beta}_c$ is skewed to the right. The same pattern is seen in both the complete and censored plots, with a larger range of expected and observed value indicated for the censored estimate, particularly in the right hand tail. There also seems to be a levelling effect at the tails of the censored plot, which can indicate truncation.

As n increases to 500 (see Figure 3.3), the right skewness is reduced, and both the censored and complete estimate plots are more symmetric, lying on the 45° line. As expected, a wider range of values are observed in the censored estimates, and there are more outliers present.

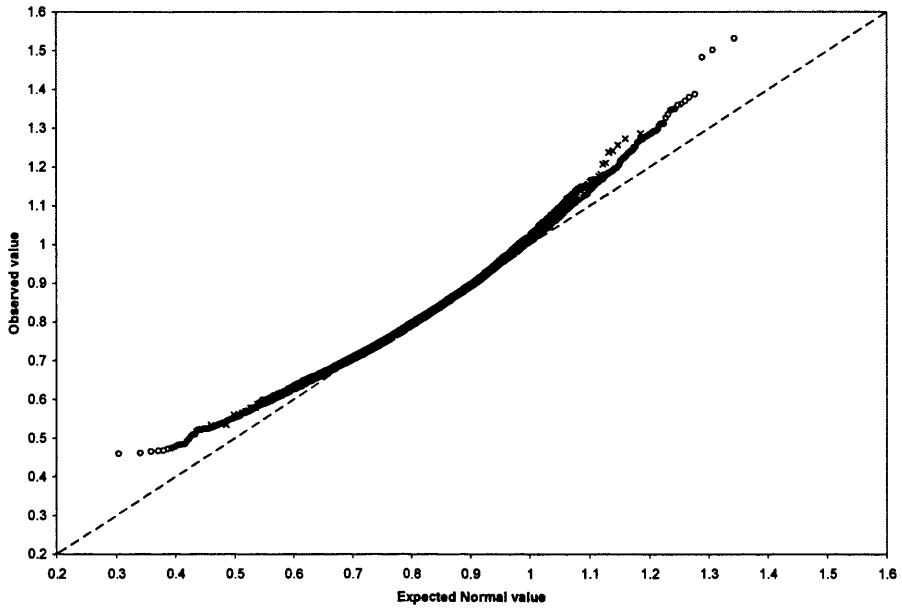

Figure 3.2: $Q-Q$ plot for $\hat{\beta}_c$, based on data generated from a Weibull distribution with $(\beta, \theta) = (0.8, 100)$ and $n = 50$.

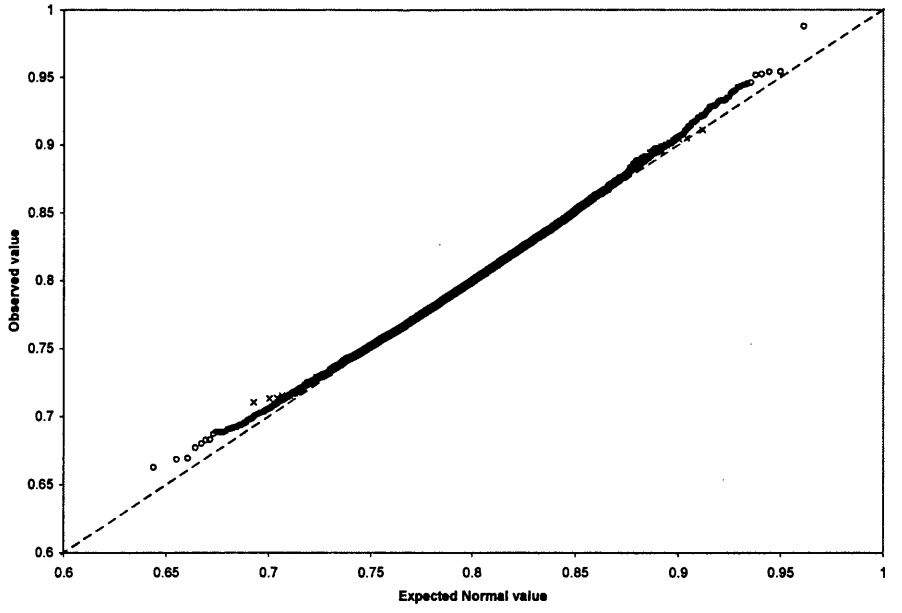

Figure 3.3: $Q-Q$ plot for $\hat{\beta}_c$, based on data generated from a Weibull distribution with $(\beta, \theta) = (0.8, 100)$ and $n = 500$.

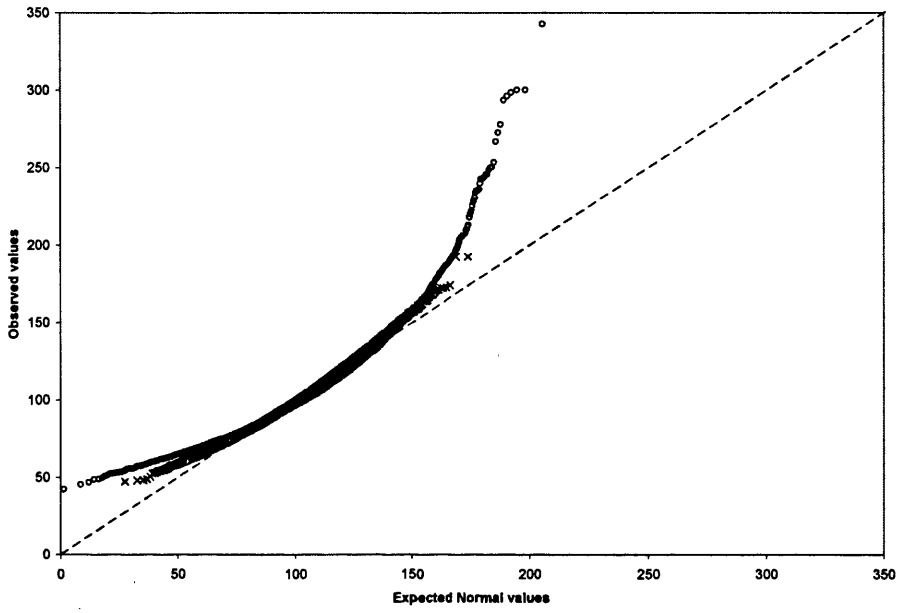

Figure 3.4: $Q-Q$ plot for $\hat{\theta}_c$, based on data generated from a Weibull distribution with $(\beta, \theta) = (0.8, 100)$ and $n = 50$.

The $Q-Q$ plot of $\hat{\theta}_c$ at $\beta = 0.8$ differs from the corresponding plot for $\hat{\beta}_c$. There are now noticeable differences between the complete data estimates and those obtained at $c = 100$. The complete plot is much less skewed, and there appear to be many more observed outliers to the right in the censored case. These outliers reduce as n reaches 500, and the censored plot is a closer reflection of the complete MLEs.

The same pattern is displayed for the $Q-Q$ plots for $\beta = 1$, shown in Figures 3.6, 3.7, 3.8 and 3.9. More outliers are present in the plot of $\hat{\theta}_c$ than $\hat{\beta}_c$, and the MLEs become more Normally distributed as n increases.

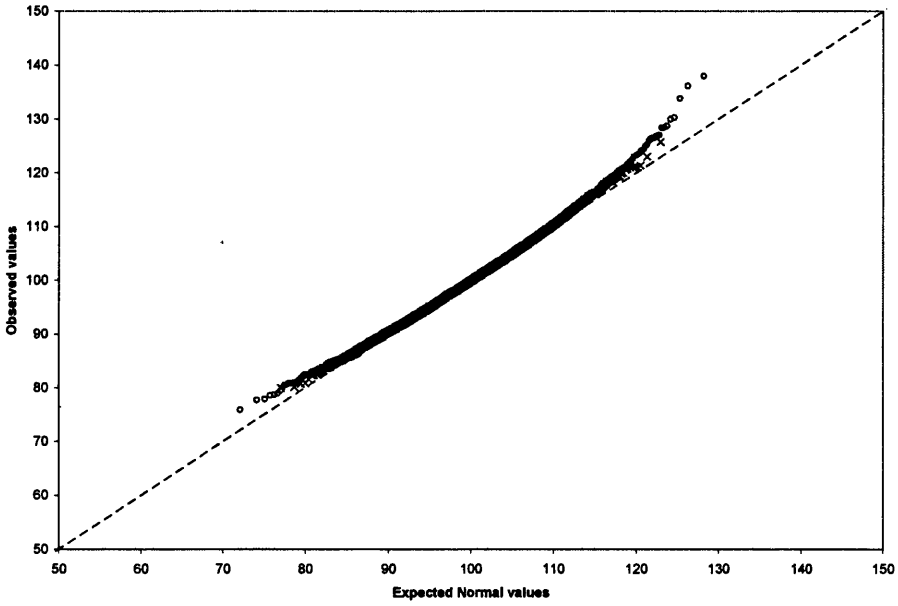

Figure 3.5: $Q-Q$ plot for $\hat{\theta}_c$, based on data generated from a Weibull distribution with $(\beta, \theta) = (0.8, 100)$ and $n = 500$.

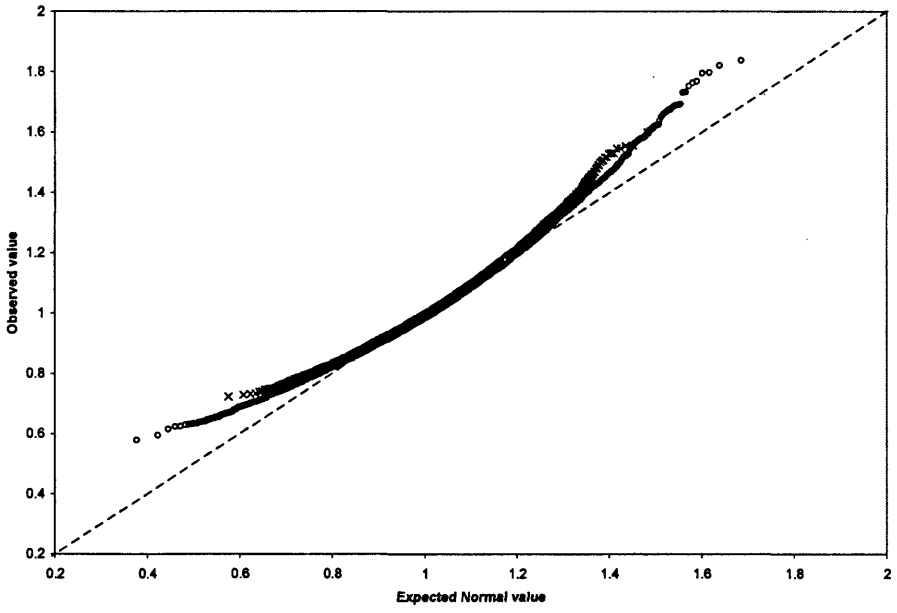

Figure 3.6: $Q-Q$ plot for $\hat{\beta}_c$, based on data generated from a Weibull distribution with $(\beta, \theta) = (1, 100)$ and $n = 50$.

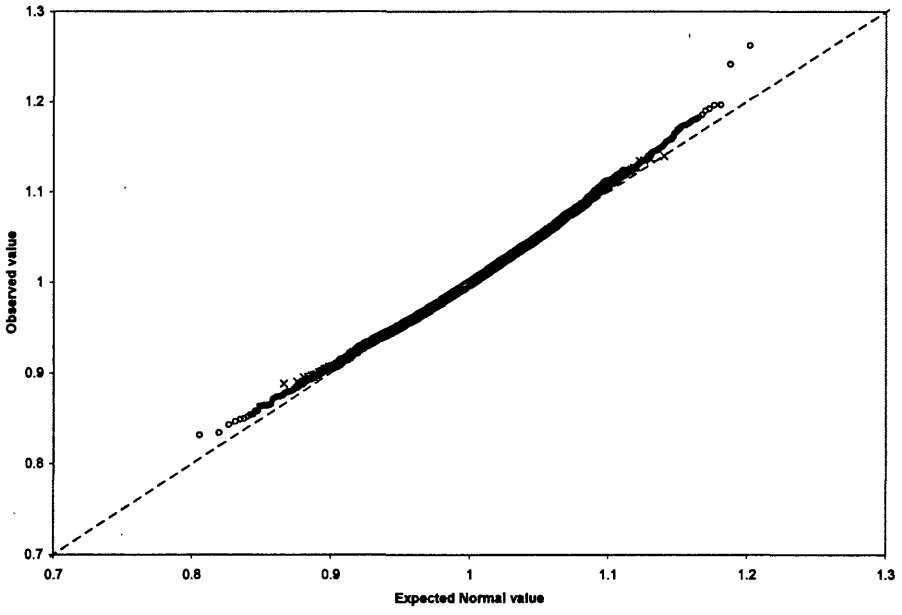

Figure 3.7: $Q-Q$ plot for $\hat{\beta}_c$, based on data generated from a Weibull distribution with $(\beta, \theta) = (1, 100)$ and $n = 500$.

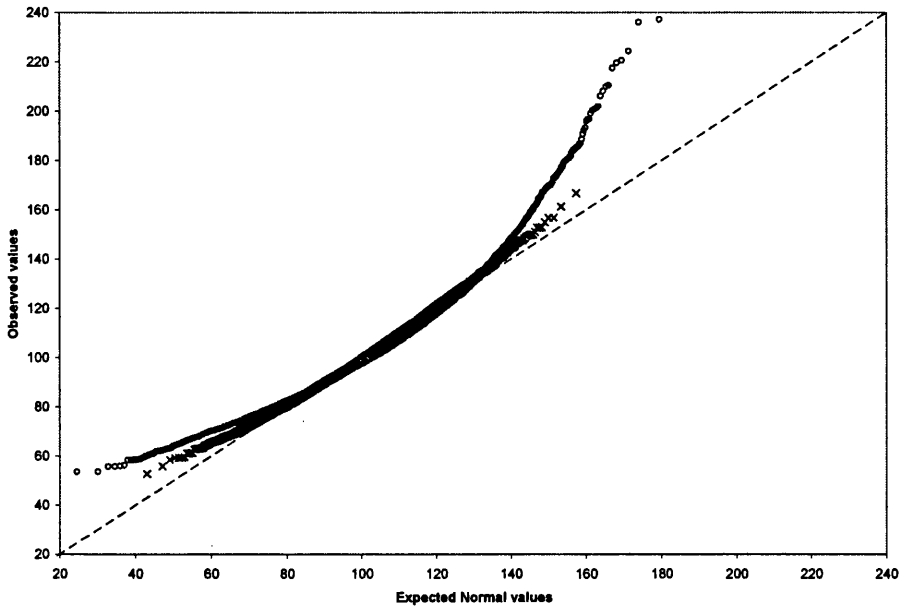

Figure 3.8: $Q-Q$ plot for $\hat{\theta}_c$, based on data generated from a Weibull distribution with $(\beta, \theta) = (1, 100)$ and $n = 50$.

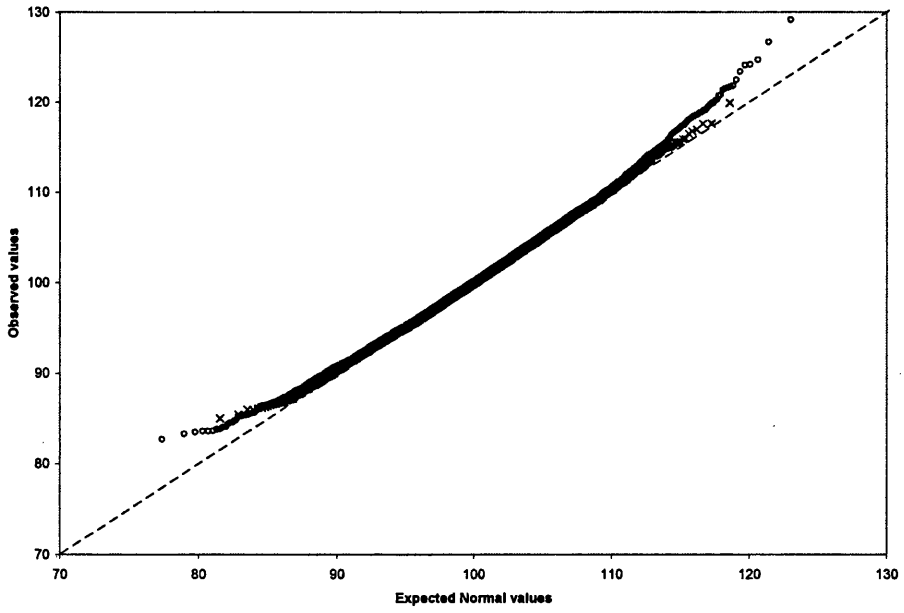

Figure 3.9: $Q-Q$ plot for $\hat{\theta}_c$, based on data generated from a Weibull distribution with $(\beta, \theta) = (1, 100)$ and $n = 500$.

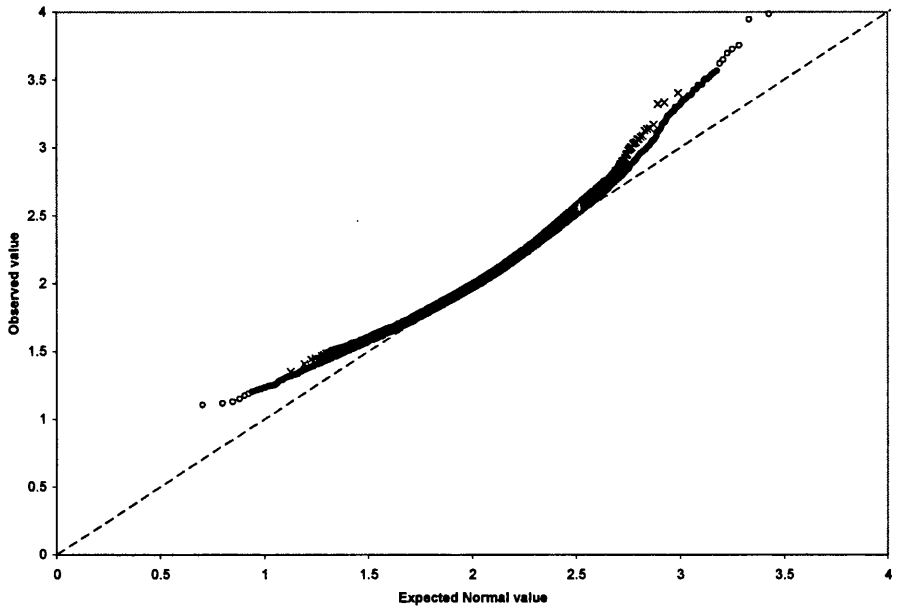

Figure 3.10: $Q-Q$ plot for $\hat{\beta}_c$, based on data generated from a Weibull distribution with $(\beta, \theta) = (2, 100)$ and $n = 50$.

Clearly from the Weibull pdf, Figure 1.1, $\beta = 2$ has a completely different shape to the distribution when $\beta \leq 1$. The $Q-Q$ plots for $\hat{\beta}_c$, Figures 3.10 and 3.11, however, are not dissimilar. The $Q-Q$ plots for $\hat{\theta}_c$, Figures 3.12 and 3.13, show a larger discrepancy between censored and complete estimates.

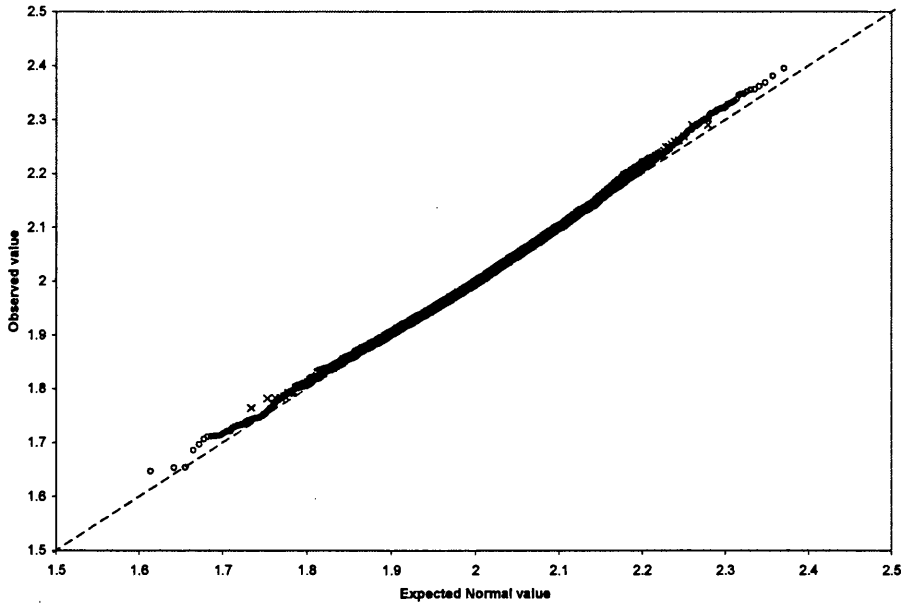

Figure 3.11: $Q-Q$ plot for $\hat{\beta}_c$, based on data generated from a Weibull distribution with $(\beta, \theta) = (2, 100)$ and $n = 500$.

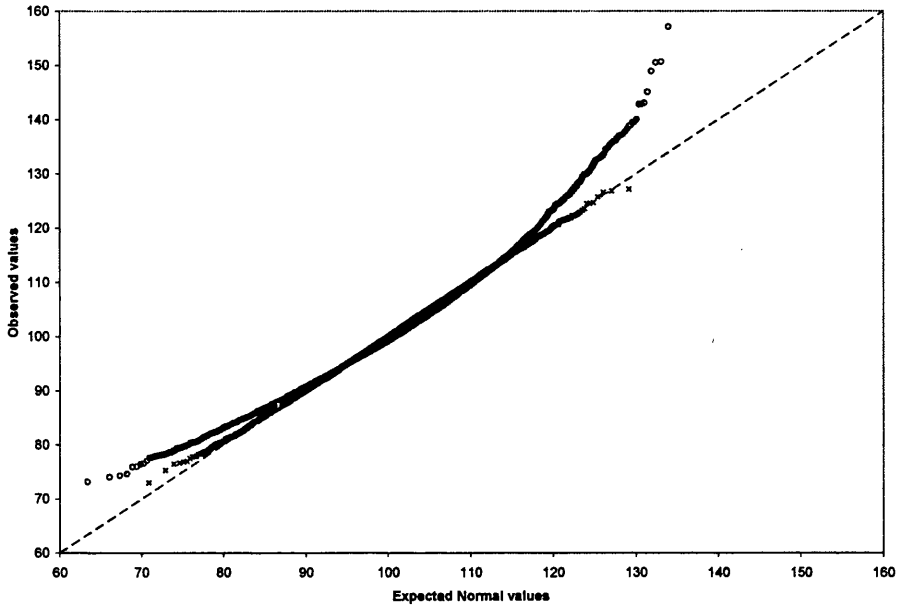

Figure 3.12: $Q-Q$ plot for $\hat{\theta}_c$, based on data generated from a Weibull distribution with $(\beta, \theta) = (2, 100)$ and $n = 50$.

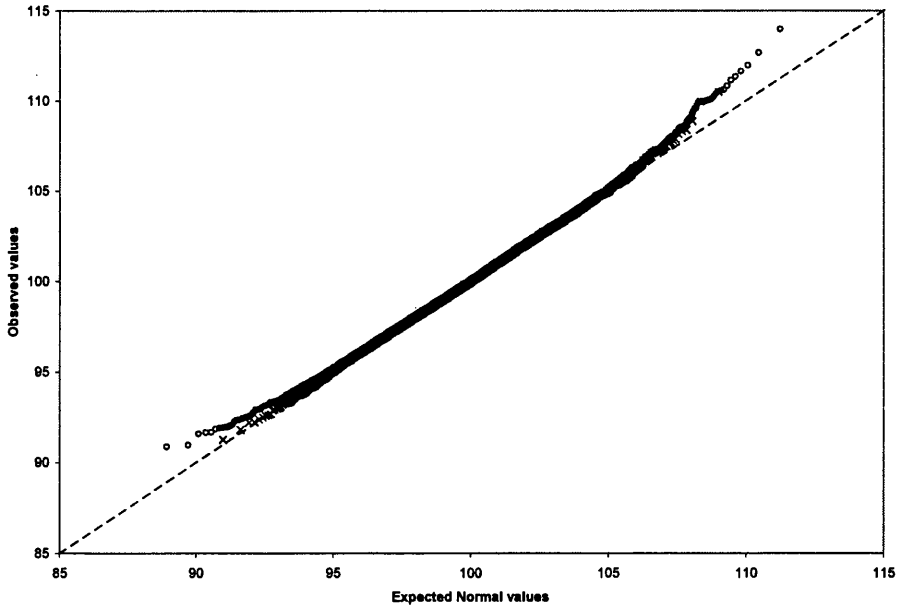

Figure 3.13: $Q-Q$ plot for $\hat{\theta}_c$, based on data generated from a Weibull distribution with $(\beta, \theta) = (2, 100)$ and $n = 500$.

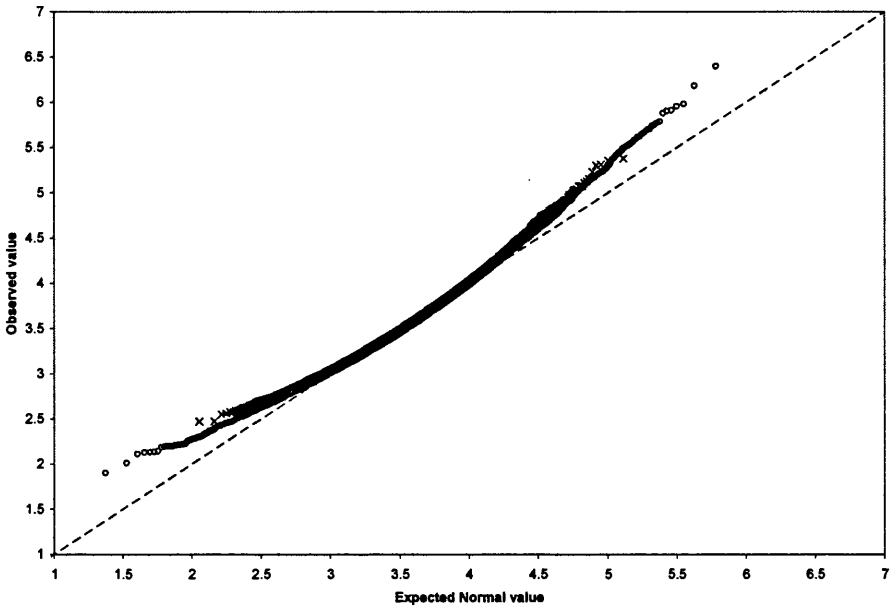

Figure 3.14: $Q-Q$ plot for $\hat{\beta}_c$, based on data generated from a Weibull distribution with $(\beta, \theta) = (3.5, 100)$ and $n = 50$.

Once again the same pattern of right skewness is present in the $Q-Q$ plots of the MLEs generated from a shape parameter $\beta = 3.5$ (Figures 3.14, 3.15, 3.16 and 3.17), becoming more symmetric in $\hat{\beta}_c$ as both n and c increases, and a near normal (close to the 45° line) plot for complete $\hat{\theta}$, even at small sample sizes.

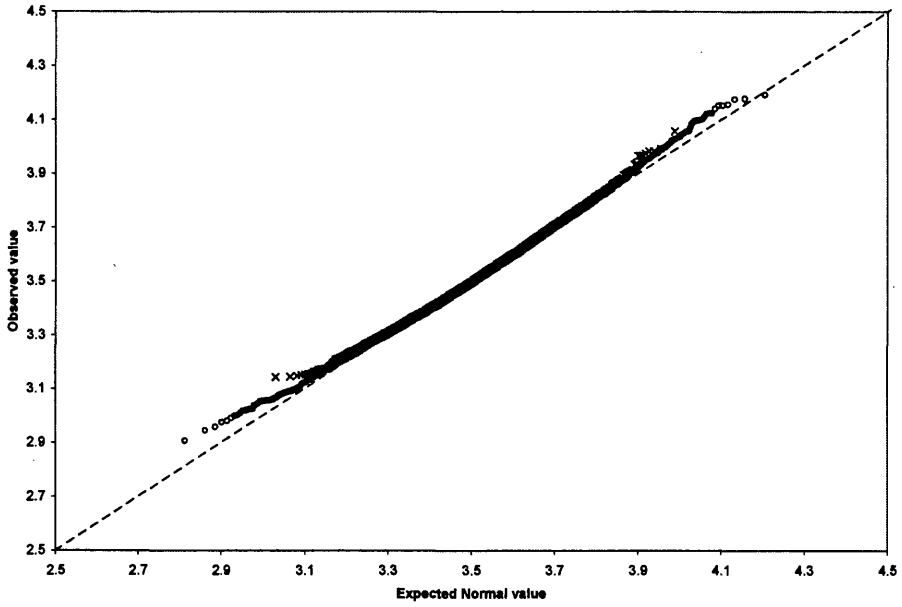

Figure 3.15: $Q-Q$ plot for $\hat{\beta}_c$, based on data generated from a Weibull distribution with $(\beta, \theta) = (3.5, 100)$ and $n = 500$.

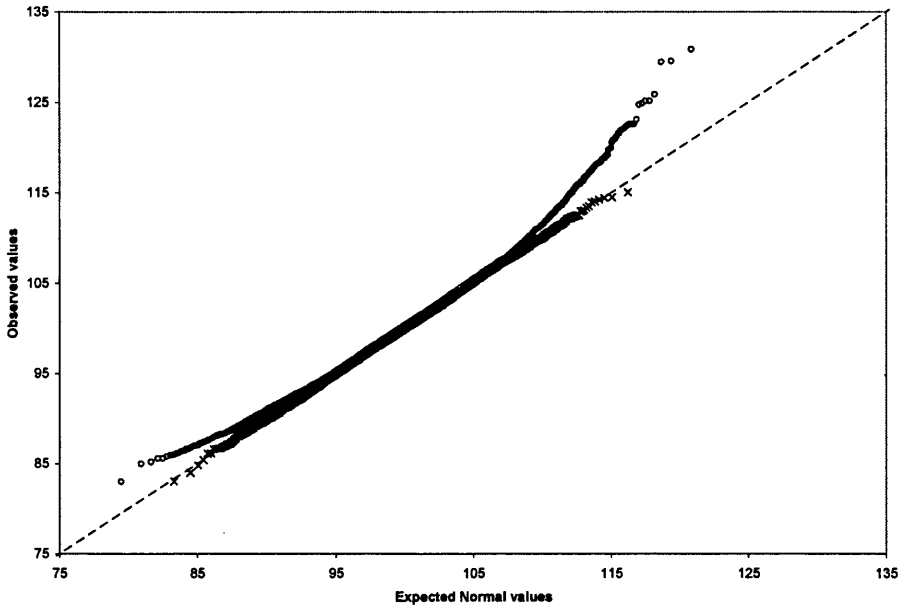

Figure 3.16: $Q-Q$ plot for $\hat{\theta}_c$, based on data generated from a Weibull distribution with $(\beta, \theta) = (3.5, 100)$ and $n = 50$.

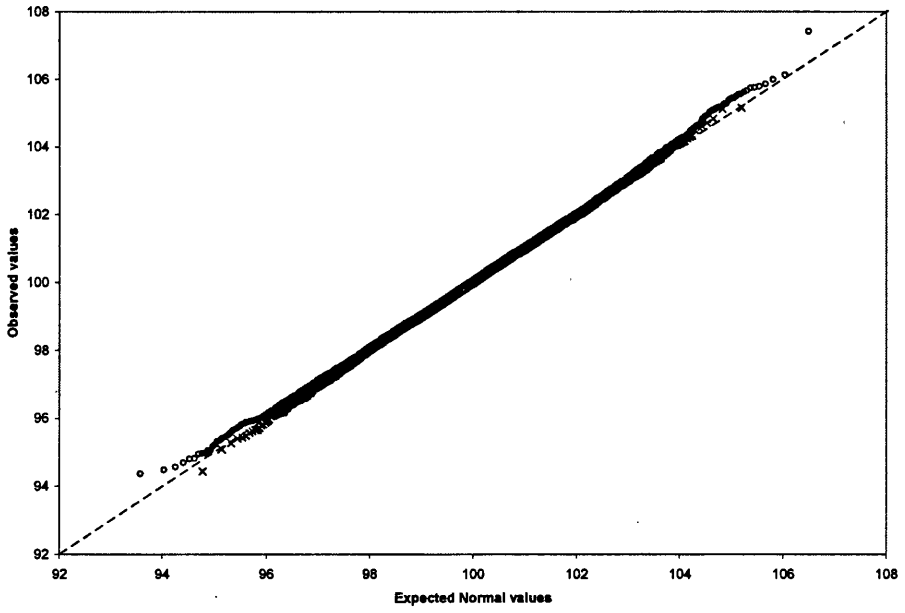

Figure 3.17: $Q-Q$ plot for $\hat{\theta}_c$, based on data generated from a Weibull distribution with $(\beta, \theta) = (3.5, 100)$ and $n = 500$.

3.2.3 Formal Normality Tests

The formal tests that have been developed can be classified as graphical tests, EDF tests, moment based tests, and Shapiro-Wilk regression tests.

EDF Tests

Empirical distribution function (EDF) tests essentially enable us to test the hypothesis that the data comes from a proposed distribution, and are based on the differences between the observed and theoretical ecdf. For a random sample $\hat{\phi}_1, \hat{\phi}_2, ..., \hat{\phi}_N$, under the hypothesis that the data is Normal, we have

$$p_{(i)} = \Phi\left(\frac{\left[\hat{\phi}_{(i)} - \hat{\mu}\right]}{\hat{\sigma}}\right),$$

where $\hat{\mu}$ and $\hat{\sigma}$ are the sample mean and standard deviation, respectively. EDF tests reject the null hypothesis (Normality) when discrepancies between the EDF of a sample, defined as

$$F_N\left(\hat{\phi}\right) = \frac{i}{N},$$

and $p_{(i)}$ are too large.

The Kolmogorov-Smirnov test statistic, D, is defined as the maximum vertical distance between the ecdf, $F_N\left(\hat{\phi}\right)$, and the proposed (in our case, normal) cdf, $p_{(i)}$. The larger D is, the worse the fit between the theoretical distribution and data set, and so significantly large values of D lead us to reject the hypothesis that the underlying data is adequately modelled using the proposed distribution. We also have the goodness of fit test statistics denoted by

$$W^2 = \sum_i \left(p_{(i)} - \frac{2i-1}{2n}\right)^2 + \frac{1}{12n}.$$

and

$$A^2 = -n - \frac{1}{n}\sum_{i=1}^{n}\left[(2i-1)\left(\log p_{(i)} + \log\left(1 - p_{(n+1-i)}\right)\right)\right]$$

where W^2 is the Cramer-von Mises tests statistic, and A^2 is the Anderson-Darling statistic. If these numbers are too large then the hypothesis of normality is rejected. Modifications to the EDF test statistics are derived in Stephens (1974), so that the critical values for each test are independent of the sample size, and that source provides further information on goodness of fit tests.

Moment based tests

The $\sqrt{b_1}$ and b_2 statistics are very useful in indicating the type of non-Normality, and can judge if the non-Normality will affect any inferences to be made with the data, for example,

if a $t-test$ is to be applied to the data or a prediction is to be made. Omnibus tests, which have good power properties over a range of non-Normal distributions, have been developed using a combination of the sample estimates$\sqrt{b_1}$ and b_2, and will be discussed in a later section. A detailed review of skewness and kurtosis tests is given in D'Agostino et al. (1990). They also describe a method to implement the tests into available statistical packages, that is, it shows how to calculate the normal approximations to $\sqrt{b_1}$ and b_2, $Z\left(\sqrt{b_1}\right)$ and $Z\left(b_2\right)$, and then uses these approximations to calculate the D'Agostino-Pearson K^2 omnibus test, discussed in D'Agostino & Pearson (1973), as below

$$K^2 = Z^2\left(\sqrt{b_1}\right) + Z^2\left(b_2\right).$$

The K^2 statistic has approximately a χ^2 distribution with 2 degrees of freedom when the population is normally distributed. Since χ^2_2 is the negative exponential distribution, pdf (1.23), with $\theta = 2$, the critical value for an upper tail probability of p is

$$-2\ln(p).$$

Therefore, for $p = 0.05$ we obtain the critical value 5.9915.

Shapiro-Wilk Tests

The W tests statistic is the ratio of the square of a linear combination of the sample order statistics to the usual corrected sum of squares estimator of variance, s^2, Shapiro & Wilk (1965). We denote w_i the vector of expected value of the i^{th} order statistic, and V as the covariance matrix of the order statistics, $\phi_{(1)}, \phi_{(2)}, ..., \phi_{(N)}$. We then let ϕ' denote a vector of the ordered random observations, then the Shapiro-Wilk tests statistic is given by

$$W = \frac{(a'\phi)^2}{(n-1)s^2},$$

where we define

$$a' = (a_1, ..., a_n) = \frac{w'V^{-1}}{(w'V^{-1}V^{-1}w)^{\frac{1}{2}}}.$$

Small values of W lead to the rejection of the null hypothesis of Normality.

More details of the approximations associated with the W statistic are given in Shapiro & Wilk (1965). This test was initially derived for sample sizes of $n \leq 50$, and there is some literature covering the extension of this basic test to larger sample sizes, see D'Agostino (1971) and Shapiro & Francia (1972). However, the Shapiro-Wilk test, and its extensions, see Royston (1982), are only recommended for a sample size up to 2,000, and will therefore not be used to test our simulated samples of 10,000 MLEs, due to the extensive calculation that would be involved.

c	n					
	50	100	500	1000	2500	5000
50	1024.74	578.23	97.51	28.27	34.86	8.54
100	500.58	337.48	65.48	12.80	27.68	**0.17**
150	334.77	268.55	74.36	7.93	19.78	**1.19**
200	308.31	223.27	36.47	11.85	10.18	**2.89**
∞	448.32	162.40	28.62	16.96	13.34	**1.17**

Table 3.7: K^2 test statistics for $\hat{\beta}_c$ yielded from simulated Weibull data with $(\beta, \theta) = (0.8, 100)$ for various n and c.

c	n					
	50	100	500	1000	2500	5000
50	7503.46	3712.21	477.82	336.90	129.62	49.20
100	3023.02	1278.22	202.54	97.67	25.19	24.88
150	1525.78	562.97	118.68	49.77	22.66	**3.12**
200	775.14	291.23	82.05	23.87	17.12	**4.65**
∞	278.75	121.67	52.59	15.61	13.76	**1.17**

Table 3.8: K^2 test statistics for $\hat{\theta}_c$ yielded from simulated Weibull data with $(\beta, \theta) = (0.8, 100)$ for various n and c.

Power Comparisons and recommendations

We note here that comparative tests for univariate Normality are discussed more thoroughly in Shapiro et al. (1968), and literature shows that the recommendations for using specific tests are based on a number of factors, such as simplicity of calculation, power of the test, including the alternative options, and also the availability of critical values. Despite probably being the most well known EDF test, the Kolmogorov-Smirnov test gives the weakest results compared to the others, and recent texts are unanimous that this test should never be used, see Thode (2002) for example. Due to the power properties discussed above, we use the D'Agostino-Pearson K^2 omnibus test, D'Agostino & Pearson (1973), for our samples of MLEs.

3.2.4 Results and discussion

Tables 3.7 to 3.18 display the corresponding K^2 statistics, with bold values indicating a Normal distribution ($K^2 < 5.9915$). The indications of non-Normality in the Q-Q plots for $\beta = 0.8$ are confirmed by the K^2 statistics in Table 3.7. We see that Normality is not reached until $n = 5000$, and also that due to the nature (early failures) of the data at $\beta = 0.8$ there is not a substantial difference to the distribution of the MLEs after the censoring level increases past $c = 100$. Again, Table 3.8 shows that Normality is not detected until $n = 5000$, and then only for complete and late censoring levels.

As the hazard function changes dramatically around $\beta = 1$, we also include the K^2 statistics for $\beta = 0.9$ and $\beta = 1.1$ in Tables 3.9, 3.12, 3.11, and 3.14. For each shape

c	n					
	50	100	500	1000	2500	5000
50	1222.40	524.04	108.67	67.76	31.71	21.98
100	564.44	288.86	60.09	37.42	17.23	6.42
150	408.38	238.92	37.11	25.57	12.69	7.90
200	439.58	181.32	25.30	22.75	8.18	**2.22**
∞	540.49	233.02	38.94	18.87	19.26	**1.68**

Table 3.9: K^2 test statistics for $\hat{\beta}_c$ yielded from simulated Weibull data with $(\beta, \theta) = (0.9, 100)$ for various n and c.

c	n					
	50	100	500	1000	2500	5000
50	1605.82	725.74	124.45	63.21	13.15	15.27
100	638.50	395.93	81.07	30.71	16.05	6.28
150	421.96	303.20	51.95	15.72	17.99	6.61
200	359.18	236.21	51.34	10.46	7.23	6.53
∞	503.76	297.56	61.11	25.46	7.68	9.22

Table 3.10: K^2 test statistics for $\hat{\beta}_c$ yielded from simulated Weibull data with $(\beta, \theta) = (1, 100)$ for various n and c.

parameter, we see that K^2 statistics for $\hat{\beta}_c$ and $\hat{\theta}_c$ decrease for increasing n and c, thus indicating an approach to Normality. We also note that there are more $K^2 < 5.9915$ observed for the samples of $\hat{\theta}_c$ than $\hat{\beta}_c$.

We notice from the Weibull pdf (Figure 1.1) that for $\beta = 2$, the amount of failures occurring after time $y = 100$ begins to decrease, which is reflected in the K^2 statistics in Table 3.15, with Normality measures similar to the complete MLEs at censoring levels greater than 150. This is true for all sample sizes, and again, normality is only attained at large n. The larger discrepancy between censored and complete estimates, shown earlier in the $Q - Q$ plots for $\hat{\theta}_c$ (Figures 3.12 and 3.13), is confirmed by the K^2 statistics in Table 3.16. It is still true that the Normality measures become similar at censoring levels greater than 150, but there is a much bigger difference at early censoring. Normality is achieved at much smaller sample sizes in $\hat{\theta}_c$.

c	n					
	50	100	500	1000	2500	5000
50	1877.71	783.25	129.79	93.64	11.58	10.25
100	711.14	322.11	40.21	40.35	6.70	**4.43**
150	426.18	170.65	25.83	14.30	7.59	**0.41**
200	285.69	151.58	16.44	9.52	**4.33**	**0.74**
∞	454.99	200.86	35.70	18.43	6.40	**3.73**

Table 3.11: K^2 test statistics for $\hat{\beta}_c$ yielded from simulated Weibull data with $(\beta, \theta) = (1.1, 100)$ for various n and c.

c	n					
	50	100	500	1000	2500	5000
50	12978.40	3178.07	629.21	298.66	78.62	44.99
100	2508.50	1201.61	123.79	87.66	18.45	11.93
150	884.85	435.64	46.50	21.09	**4.04**	**2.41**
200	535.46	254.52	24.32	15.29	6.72	**2.42**
∞	184.01	129.47	15.75	**2.69**	**2.45**	**4.82**

Table 3.12: K^2 test statistics for $\hat{\theta}_c$ yielded from simulated Weibull data with $(\beta, \theta) = (0.9, 100)$ for various n and c.

c	n					
	50	100	500	1000	2500	5000
50	10901.33	3229.06	543.60	318.44	143.74	38.31
100	2043.07	773.16	207.71	84.43	31.54	**4.57**
150	557.71	382.88	65.29	22.57	15.00	**0.06**
200	254.43	184.89	37.91	14.39	6.28	**1.56**
∞	40.09	87.63	26.31	9.12	**2.94**	**1.65**

Table 3.13: K^2 test statistics for $\hat{\theta}_c$ yielded from simulated Weibull data with $(\beta, \theta) = (1, 100)$ for various n and c.

c	n					
	50	100	500	1000	2500	5000
50	9040.95	3952.98	601.61	287.78	82.94	40.54
100	2306.51	915.54	90.60	61.07	28.65	16.95
150	437.80	306.95	20.02	18.42	**5.52**	8.96
200	192.60	130.57	12.20	9.35	**4.77**	**5.07**
∞	92.61	72.10	6.58	**5.35**	**5.98**	**3.83**

Table 3.14: K^2 test statistics for $\hat{\theta}_c$ yielded from simulated Weibull data with $(\beta, \theta) = (1.1, 100)$ for various n and c.

c	n					
	50	100	500	1000	2500	5000
50	18119.57	1912.81	162.75	119.68	58.71	19.27
100	851.13	253.06	61.54	10.84	11.05	**2.36**
150	455.72	150.60	19.46	14.09	**1.03**	**0.64**
200	519.85	154.88	21.61	24.48	**3.52**	**2.76**
∞	619.99	208.56	33.17	28.58	**4.72**	**1.39**

Table 3.15: K^2 test statistics for $\hat{\beta}_c$ yielded from simulated Weibull data with $(\beta, \theta) = (2, 100)$ for various n and c.

c	n					
	50	100	500	1000	2500	5000
50	17447.69	4836.94	912.78	305.56	137.92	68.82
100	978.45	408.74	79.83	34.04	18.50	12.45
150	22.56	14.36	**2.00**	**2.57**	**1.47**	**0.75**
200	8.98	**1.97**	**0.30**	**1.67**	**0.48**	**0.22**
∞	8.91	**0.77**	**0.15**	**1.69**	**0.26**	**0.21**

Table 3.16: K^2 test statistics for $\hat{\theta}_c$ yielded from simulated Weibull data with $(\beta, \theta) = (2, 100)$ for various n and c.

c	n					
	50	100	500	1000	2500	5000
50	17201.16	12610.99	811.23	382.51	156.35	56.21
100	407.89	289.06	44.90	26.63	15.00	21.44
150	282.36	167.62	43.33	10.86	25.31	9.28
200	333.85	210.05	52.21	15.52	25.62	15.68
∞	334.41	210.89	52.76	15.60	25.87	15.73

Table 3.17: K^2 test statistics for $\hat{\beta}_c$ yielded from simulated Weibull data with $(\beta, \theta) = (3.5, 100)$ for various n and c.

The K^2 test results for $\beta = 3.5$ in Tables 3.17 and 3.18 show that in fact $\hat{\beta}_c$ does not reach Normality in this case, whereas $\hat{\theta}_c$ appears to follow a Normal distribution in samples as small as $n = 50$, provided the censoring level, c, is greater than 100.

3.2.5 Discussion

The simulation tests performed on $\hat{\beta}_c$ and $\hat{\theta}_c$ all agree that asymptotic Normality is implausible in small to moderate, or highly censored data sets. The rate of reaching Normality with increasing sample size depends on the true shape parameter, β, and this can affect the distribution of $\hat{\beta}_c$ and $\hat{\theta}_c$ differently.

For $\beta \leq 1.1$, the pattern of Normality in the distribution of $\hat{\beta}_c$ and $\hat{\theta}_c$ is similar, with sample sizes of $n = 2500$ (for $\hat{\theta}_c$) to $n = 5000$ (for $\hat{\beta}_c$) required before Normality is observed. For $\beta = 2$, we only observe Normality in the distribution of $\hat{\beta}_c$ when n reaches 2500, but $\hat{\theta}_c$

c	n					
	50	100	500	1000	2500	5000
50	39086.03	20628.42	1925.42	649.06	317.88	142.11
100	637.28	324.58	44.27	10.09	14.34	**3.99**
150	**0.14**	**0.67**	**3.28**	**0.39**	**0.42**	**0.20**
200	**0.71**	**1.51**	**4.26**	**0.38**	**0.32**	**0.13**
∞	**0.72**	**1.49**	**4.26**	**0.38**	**0.32**	**0.13**

Table 3.18: K^2 test statistics for $\hat{\theta}_c$ yielded from simulated Weibull data with $(\beta, \theta) = (3.5, 100)$ for various n and c.

follows a Normal distribution for samples as small as $n = 100$, providing there is only very late, or no censoring. This much faster rate of the distribution of $\hat{\theta}_c$ reaching Normality is also seen at $\beta = 3.5$; however, $\hat{\beta}_c$ fails to reach Normality even for a complete sample at $n = 5000$.

3.3 Tests for Bivariate Normality

There are several strategies suggested to assess multivariate Normality. As in the univariate case, probability plots can be a subjective test for bivariate Normality, and can also assess the directions of departure from Normality. We may also subjectively assess the marginal Normality via univariate tests described above, and then use the necessary, but not sufficient, condition that a multivariate Normal distribution is Normal in each of its marginal distributions. The extension of univariate procedures to the multivariate case is the approach taken by several researchers. For example, Healy (1968) suggested a method for multivariate normal plotting based upon the use of the squared radii, which, when ordered, are distributed as χ^2 with 2 degrees of freedom, which is in fact a plot of the unit Exponential order statistics. Finally, we can directly assess the bivariate Normality from the bivariate observations. A variety of tests are available for each of these strategies, see Thode (2002) or Khattree & Rao (2003) for a detailed review of available tests.

3.3.1 Graphical Methods

As we saw earlier, bivariate Normality implies that the scatter plot of $\left(\hat{\beta}_c, \hat{\theta}_c\right)$ will be elliptical in shape. We again use the MLEs obtained from 10,000 replicated set of data generated from Weibull distributions with various combinations of n and c. As before, we set $\theta = 100$, and look initially at $\beta = 2$. We display scatter plots of these estimates, and display these for samples censored at $c = 100$, for $n = 50, 100, 500, 1000$ and 5000, in Figures 3.18, 3.19, 3.20, 3.21, and 3.22, respectively.

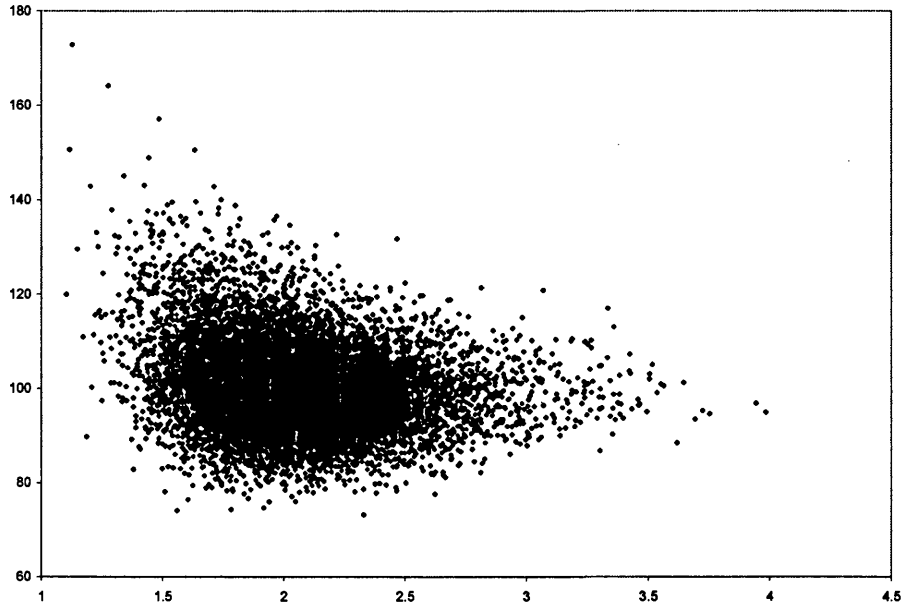

Figure 3.18: Scatter plots of $\left(\hat{\beta}_c, \hat{\theta}_c\right)$ generated from a Weibull distribution with $(\beta, \theta) = (2, 100)$ and $n = 50$, censored at $c = 100$.

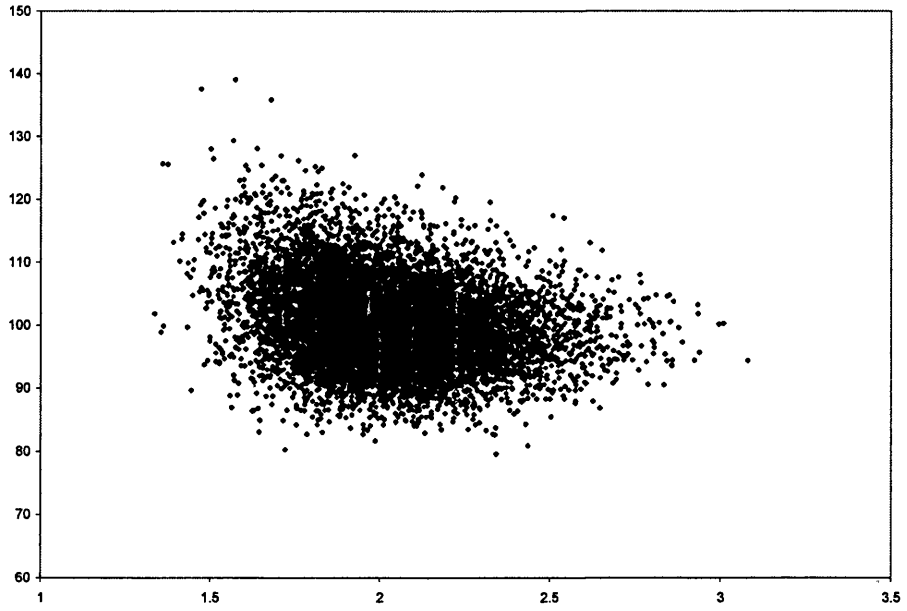

Figure 3.19: Scatter plots of $\left(\hat{\beta}_c, \hat{\theta}_c\right)$ generated from a Weibull distribution with $(\beta, \theta) = (2, 100)$ and $n = 100$, censored at $c = 100$.

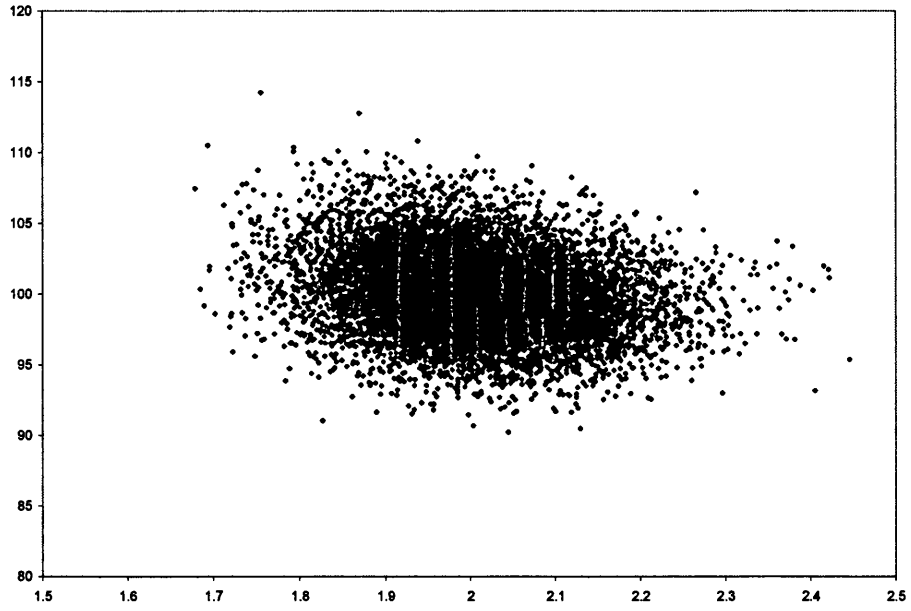

Figure 3.20: Scatter plots of $\left(\hat{\beta}_c, \hat{\theta}_c\right)$ generated from a Weibull distribution with $(\beta, \theta) = (2, 100)$ and $n = 500$, censored at $c = 100$.

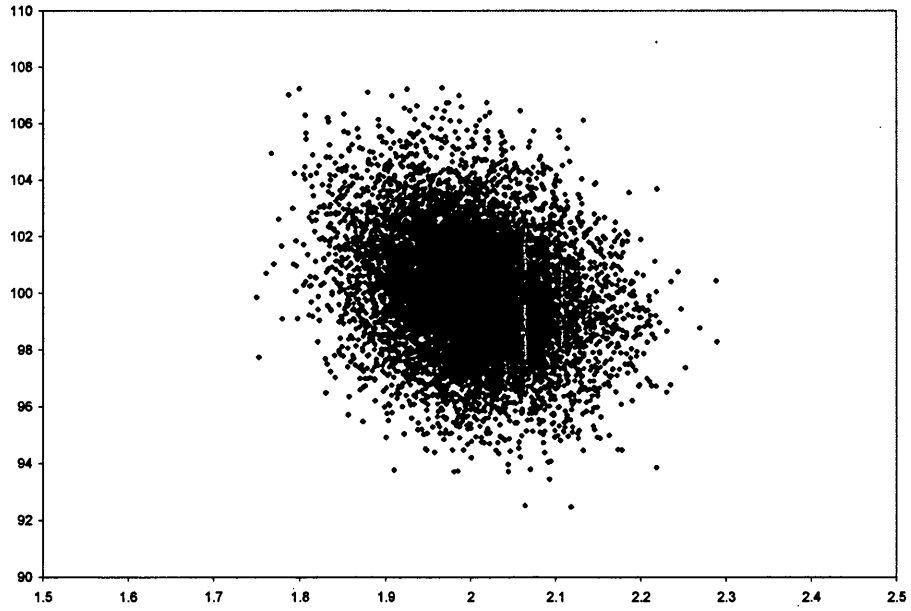

Figure 3.21: Scatter plots of $\left(\hat{\beta}_c, \hat{\theta}_c\right)$ generated from a Weibull distribution with $(\beta, \theta) = (2, 100)$ and $n = 1000$, censored at $c = 100$.

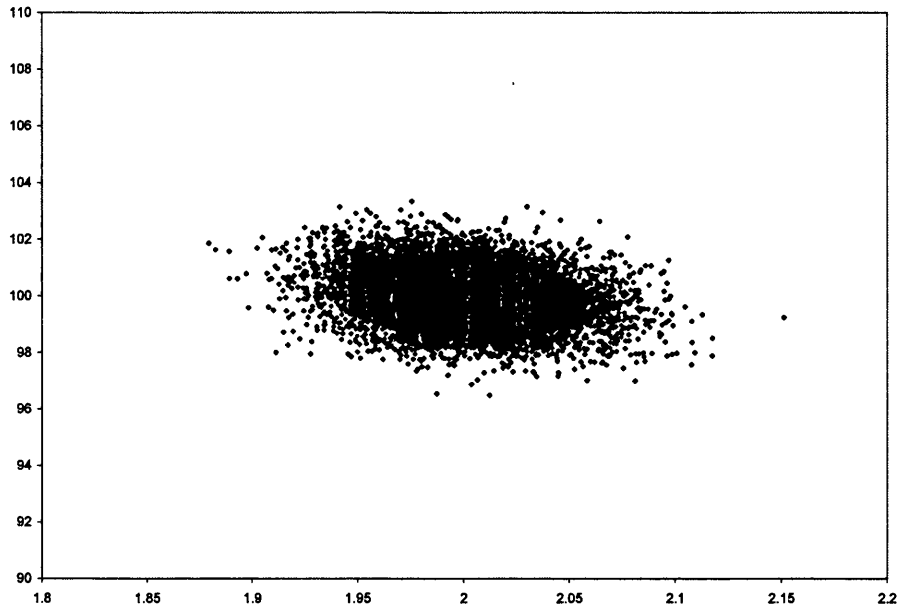

Figure 3.22: Scatter plots of $\left(\hat{\beta}_c, \hat{\theta}_c\right)$ generated from a Weibull distribution with $(\beta, \theta) = (2, 100)$ and $n = 5000$, censored at $c = 100$.

These plots show the increasing precision in $\left(\hat{\beta}_c, \hat{\theta}_c\right)$ as n increases, but clearly the distributional shape does not become elliptical until $n = 5000$, and so, as we would expect, bivariate Normality does not appear to hold in finite samples. We can observe the effect of a change in true shape parameter, by comparing the scatter plot with $\beta = 2$, in Figure 3.18, with various β values, at $n = 50$, in Figures 3.23, 3.24, and 3.25. At such small sample sizes, we see that there is a constraint on the lower limits of $\hat{\beta}_c$ and $\hat{\theta}_c$, resulting in the plots having what can be described as a "boomerang" shape. We also note that these lower limit constraints are more defined in the samples with true shape parameter $\beta \leq 1$, certainly at $c = 100$, as for our simulated data.

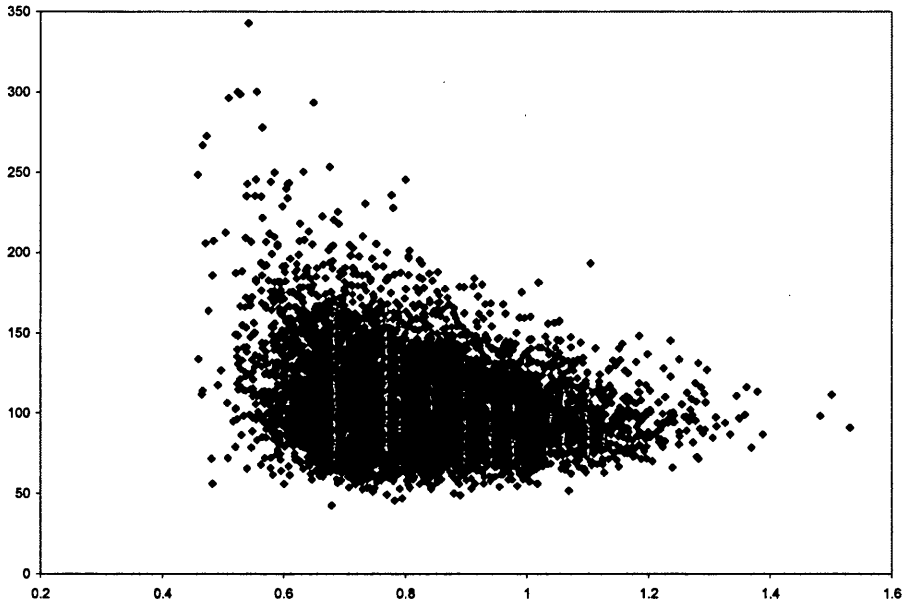

Figure 3.23: Scatter plots of $\left(\hat{\beta}_c, \hat{\theta}_c\right)$ generated from a Weibull distribution with $(\beta, \theta) = (0.8, 100)$ and $n = 50$, censored at $c = 100$.

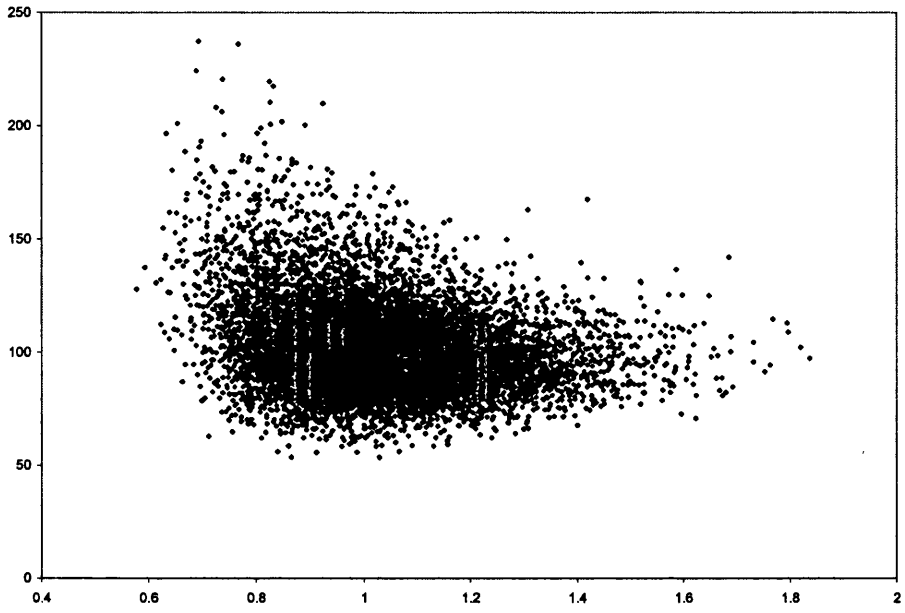

Figure 3.24: Scatter plots of $\left(\hat{\beta}_c, \hat{\theta}_c\right)$ generated from a Weibull distribution with $(\beta, \theta) = (1, 100)$ and $n = 50$, censored at $c = 100$.

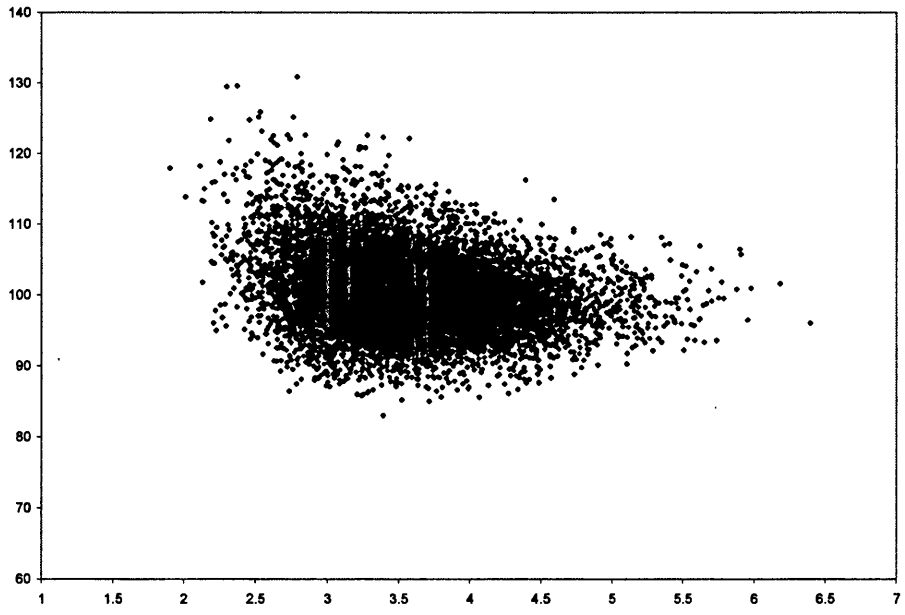

Figure 3.25: Scatter plots of $\left(\hat{\beta}_c, \hat{\theta}_c\right)$ generated from a Weibull distribution with $(\beta, \theta) = (3.5, 100)$ and $n = 50$, censored at $c = 100$.

3.3.2 Multivariate Test Statistics

As well as the in-depth study of the marginal distributions, we have chosen to use a method proposed by Mardia & Foster (1983), which is similar to the approach used in the D'Agostino and Pearson K^2 statistic, using multivariate measure of skewness and kurtosis, $b_{1,m}$ and $b_{m,2}$. The test statistics are calculated from generalised versions of the squared radii,

$$r_{ij} = (\mathbf{y}_i - \bar{\mathbf{y}})' \mathbf{S}^{-1} (\mathbf{y}_j - \bar{\mathbf{y}}),$$

and given as

$$b_{1,2} = \frac{1}{n^2} \sum_{i,j=1}^{n} r_{ij}^3$$

and

$$b_{2,2} = \frac{1}{n} \sum_{i=1}^{n} r_{ii}^2.$$

As for the univariate case, we can now perform a formal test of Normality on the bivariate sample. Mardia & Foster (1983) propose a test statistic S_W^2, defined as

$$S_W^2 = \{W(b_{1,2})\}^2 + \{W(b_{2,2})\}^2$$

in which $W(b_{1,p})$ and $W(b_{2,p})$, the Wilson-Hilferty transformations of a χ^2 variate, are standardised multivariate measures of skewness and kurtosis for the p-variate sample, defined as

$$W(b_{1,p}) = \frac{1}{6\sqrt{2f}} \left\{ 6 \left(\frac{4nf^2}{3} b_{1,p} \right)^{1/3} - 18f + 4 \right\},$$

where

$$f = \frac{\{p(p+1)(p+2)\}}{6};$$

and

$$W(b_{2,p}) = 3 \left(\frac{f_1}{2} \right)^{1/2} \left[1 - \left(\frac{2}{9f_1} \right) - \left\{ \frac{(1-(2/f_1))}{\left[1 + b_{2,p} \{2/(f_1-4)\}^{1/2} \right]^{1/3}} \right\} \right],$$

where

$$\begin{aligned} f_1 &= 6 + \left\{ 8p(p+2)/(p+8)^2 \right\}^{1/2} n^{1/2} \\ &\times \left[\begin{array}{l} \{p(p+2)/2\}^{1/2} (p+8)^{-1} n^{1/2} + \\ \left\{ 1 + \left(np(p+2)(p+8)^{-2} \right)/2 \right\}^{1/2} \end{array} \right]. \end{aligned}$$

For further details we refer to the paper.

Again, under the hypothesis that the joint distribution of the estimators is multivariate Normal, we have $S_W^2 \sim \chi_2^2$, and hence the same critical value, 5.9915, as the corresponding

c	n					
	50	100	500	1000	2500	5000
50	6275.55	2428.66	173.71	99.87	41.47	12.30
100	1643.99	578.00	72.31	20.95	10.82	**4.51**
150	785.44	295.83	53.30	11.62	7.31	**0.83**
200	425.98	161.51	29.89	**5.82**	**4.81**	**0.07**
∞	224.20	76.71	16.33	**4.30**	**3.71**	**1.79**

Table 3.19: S_W^2 test statistics for $\left(\hat{\beta}_c, \hat{\theta}_c\right)$ yielded from a Weibull distribution with $(\beta, \theta) = (0.8, 100)$, and various n and c.

c	n					
	50	100	500	1000	2500	5000
50	14801.86	1944.24	246.96	111.01	25.81	12.01
100	1361.68	553.24	47.77	29.94	**4.60**	**3.40**
150	511.91	221.51	28.82	8.41	**1.43**	**0.67**
200	391.44	139.56	13.10	7.16	**0.65**	**0.81**
∞	245.75	107.70	8.31	**1.46**	**2.91**	**0.28**

Table 3.20: S_W^2 test statistics for $\left(\hat{\beta}_c, \hat{\theta}_c\right)$ yielded from a Weibull distribution with $(\beta, \theta) = (0.9, 100)$, and various n and c.

univariate assessment of Normality, for an upper tail probability of $p = 0.05$.

Results and discussion

Tables 3.19 to 3.24 summarises the S_W^2 statistic for 10,000 simulated pairs of $\left(\hat{\beta}_c, \hat{\theta}_c\right)$, over a range of shape parameter values, with varying n and c. As we are investigating the variation of three factors (β, n, c), a series of tables is the only way in which these results can be displayed.

These results confirm the lack of Normality in small and early censored samples. The rate of reaching joint Normality is more consistent across the range of shape parameters used, than those for the univariate tests; we see the test statistics reaching the critical value associated with Normality at samples at $n = 1000$, although only when censoring levels are greater than 100.

3.4 Normality of Functions of MLEs

The relevance and importance of the quantile B_{10} has been introduced in chapter one and two. Naturally, it is of interest to extend the Normality tests performed on $\hat{\beta}_c$ and $\hat{\theta}_c$ to $\hat{B}_{10,c}$. In this section we repeat the univariate tests, discussed for the Weibull MLEs, to the sets of 10,000 estimates of B_{10} yielded for the simulated data, for various shape parameters, sample sizes and censoring levels.

c	n					
	50	100	500	1000	2500	5000
50	11266.65	2253.13	226.11	104.43	40.07	11.11
100	1060.42	392.96	87.47	12.44	**3.06**	**1.77**
150	358.31	270.80	33.67	**4.15**	**0.97**	**0.68**
200	215.08	147.53	21.52	**3.60**	**0.21**	**3.52**
∞	183.72	116.09	18.29	**1.84**	**0.17**	**0.67**

Table 3.21: S_W^2 test statistics for $\left(\hat{\beta}_c, \hat{\theta}_c\right)$ yielded from a Weibull distribution with $(\beta, \theta) = (1, 100)$, and various n and c.

c	n					
	50	100	500	1000	2500	5000
50	9288.27	3128.89	293.28	123.70	23.23	11.24
100	1398.97	456.99	32.75	31.52	**5.51**	**3.66**
150	344.48	189.65	10.82	6.89	**0.06**	**0.66**
200	162.70	87.29	**5.43**	**3.68**	**0.11**	**0.44**
∞	189.78	69.99	8.46	**5.02**	**0.60**	**0.16**

Table 3.22: S_W^2 test statistics for $\left(\hat{\beta}_c, \hat{\theta}_c\right)$ yielded from a Weibull distribution with $(\beta, \theta) = (1.1, 100)$, and various n and c.

c	n					
	50	100	500	1000	2500	5000
50	36756.18	5371.70	704.91	224.37	96.89	55.94
100	727.26	228.87	55.25	11.49	**4.65**	**4.98**
150	144.31	57.92	8.40	**1.28**	**4.86**	**0.58**
200	146.50	38.38	7.68	**1.84**	**1.65**	**0.21**
∞	178.41	57.70	9.52	**3.03**	**1.78**	**0.65**

Table 3.23: S_W^2 test statistics for $\left(\hat{\beta}_c, \hat{\theta}_c\right)$ yielded from a Weibull distribution with $(\beta, \theta) = (2, 100)$, and various n and c.

c	n					
	50	100	500	1000	2500	5000
50	199995.88	30327.67	3623.99	1518.16	606.27	250.61
100	273.94	261.76	29.92	7.84	**3.70**	**3.14**
150	47.76	252.91	6.78	**0.91**	**2.07**	**0.35**
200	64.81	296.64	9.94	**1.29**	**2.30**	**0.76**
∞	65.11	296.66	10.08	**1.33**	**2.36**	**0.76**

Table 3.24: S_W^2 test statistics for $\left(\hat{\beta}_c, \hat{\theta}_c\right)$ yielded from a Weibull distribution with $(\beta, \theta) = (3.5, 100)$, and various n and c.

β	$\sqrt{b_1}$	b_2	% *in CI*	% < *CI*	% > *CI*
0.8	1.06	4.70	92.14	7.85	0.01
1	0.84	4.23	93.75	6.22	0.03
2	0.34	3.13	94.28	4.67	1.05
3.5	0.02	2.84	95.94	2.52	1.19

Table 3.25: Tests of skewness and kurtosis of $\hat{B}_{10,c}$ yielded from a Weibull distribution with various β, and fixed $\theta = 100$, $c = 100$ and $n = 50$.

3.4.1 Basic Statistical Summaries of $\hat{B}_{10,c}$

As for the parameters β and θ, we can calculate the moments $\sqrt{b_1}$ and b_2 to investigate the skewness and kurtosis of our samples of $\hat{B}_{10,c}$. For a Normal distribution we expect the values

$$\sqrt{b_1} = 0,$$

and

$$b_2 = 3 + \frac{2}{N+1}.$$

It is also possible to construct 95% confidence intervals around the true quantile function,

$$B_{10} = \hat{B}_{10,c} \pm 1.96\sqrt{Var\left(\hat{B}_{10,c}\right)} \tag{3.5}$$

where $Var\left(\hat{B}_{10,c}\right)$ is given in (2.54). As before, we investigate the symmetry around the calculated confidence intervals, again with the focus on the effect of censoring and the nature of the data, determined by the shape parameter β of the sampling distribution of $\left(\hat{\beta}_c, \hat{\theta}_c\right)$. By counting how many of these confidence interval contain the true percentile value, as well as the percentage of confidence limits with MLEs that fall either below the lower limit, or above the upper limit, we can judge the effectiveness of the Normal assumption.

Results and Discussion

This information is summarised in Tables 3.25, 3.26 and 3.27 for data censored at $c = 100$. As for the Weibull parameter estimators, we see the coverage of the confidence intervals are good (close to 95%), but a much higher proportion of the true values that are not within the interval are below the lower limit at $n = 50$, again confirming the right skewness of the MLEs. A reduction in skewness is noticed as n increases. This is consistent for values of the shape parameter β, and in general, the samples become more Normally distributed when the shape parameter value increases.

3.4.2 Probability Plots

We refer to the beginning of the chapter for details of the univariate plotting tests we intend to use, namely $Q - Q$ plots. We will display and discuss the tests for samples from a

β	$\sqrt{b_1}$	b_2	$\%$ *in CI*	$\%$ $<$ *CI*	$\%$ $>$ *CI*
0.8	0.39	3.32	94.94	3.51	1.55
1	0.30	3.16	94.67	4.05	1.28
2	0.01	3.23	95.25	2.90	1.85
3.5	0.04	2.98	95.16	2.74	2.10

Table 3.26: Tests of skewness and kurtosis of $\hat{B}_{10,c}$ yielded from a Weibull distribution with various β, and fixed $\theta = 100$, $c = 100$ and $n = 500$.

β	$\sqrt{b_1}$	b_2	$\%$ *in CI*	$\%$ $<$ *CI*	$\%$ $>$ *CI*
0.8	0.08	3.01	95.06	2.91	2.03
1	0.11	3.09	95.16	2.66	2.18
2	0.05	3.04	95.50	2.40	2.10
3.5	0.02	3.13	95.05	2.63	2.32

Table 3.27: Tests of skewness and kurtosis of $\hat{B}_{10,c}$ yielded from a Weibull distribution with various β, and fixed $\theta = 100$, $c = 100$ and $n = 5000$.

range of shape parameters below. Again, each $Q - Q$ plot (Figures 3.26 to 3.33) gives the quantiles plotted for a sample obtained from complete failure data, $(\times)$, and the sample when failures are censored at $c = 100$, $(\circ)$.

As for the Weibull parameter estimators, at $n = 50$, Figure 3.26 shows a clear curved pattern indicating right skewness for both the complete and censored simulated data when $\beta = 0.8$. We note that the expected normal values include negative values, which clearly are not present in the observed values, as by definition $B_{10} > 0$ for β, $\theta > 0$. When n increases to 500, we see in Figure 3.27, that the right skewness is reduced, but it is still evidently present in the distribution. In both sample sizes illustrated, there are a wider range of expected and observed values for the censored case, and more outliers present.

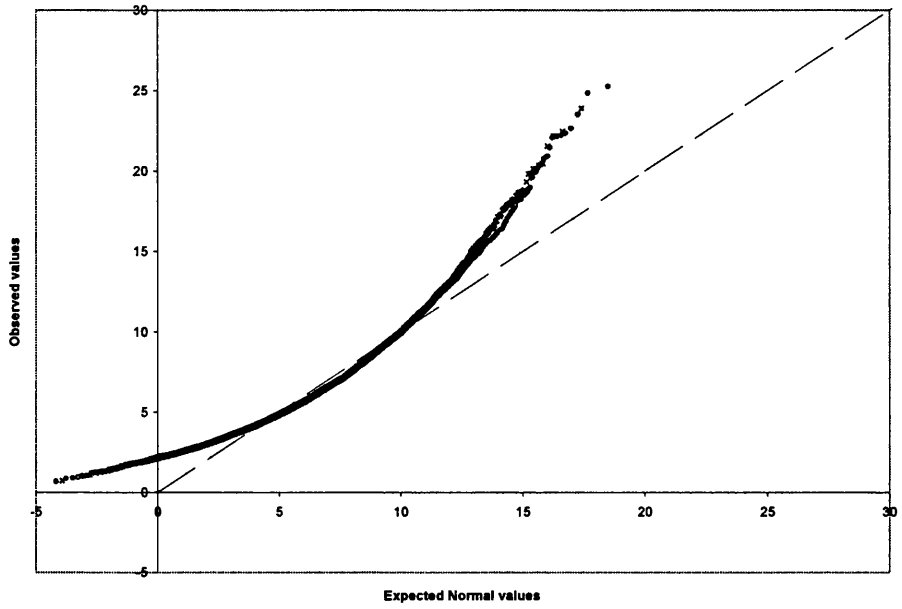

Figure 3.26: $Q-Q$ plot of $\hat{B}_{10,c}$, based on data generated from a Weibull distribution with $(\beta,\theta) = (0.8, 100)$ and $n = 50$.

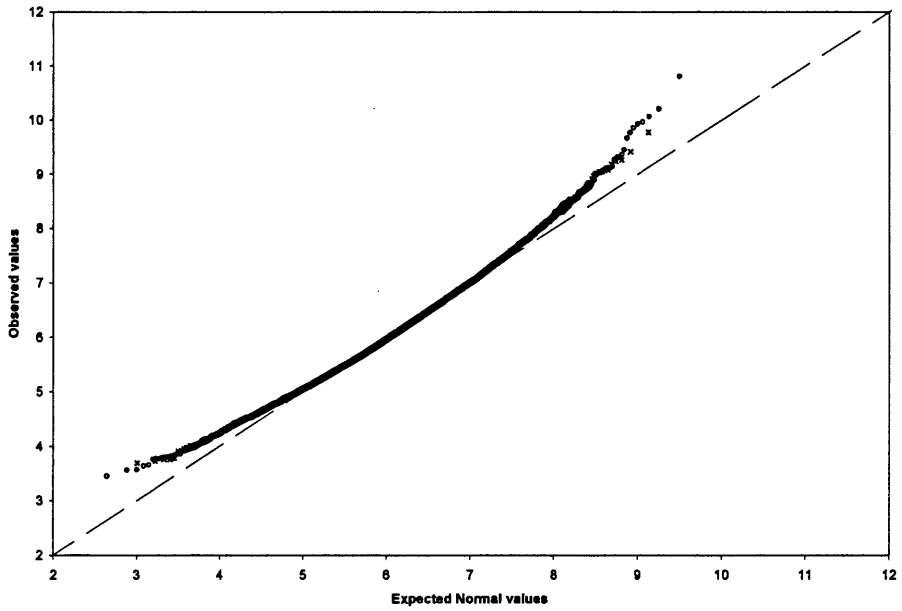

Figure 3.27: $Q-Q$ plot of $\hat{B}_{10,c}$, based on data generated from a Weibull distribution with $(\beta,\theta) = (0.8, 100)$ and $n = 500$.

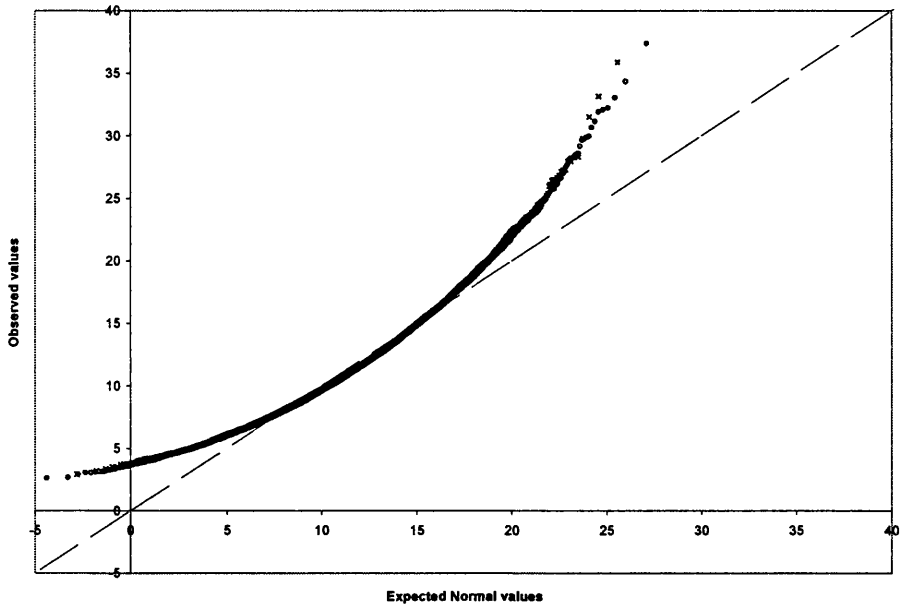

Figure 3.28: $Q-Q$ plot of $\hat{B}_{10,c}$, based on data generated from a Weibull distribution with $(\beta, \theta) = (1, 100)$ and $n = 50$.

The same pattern is seen for the $Q - Q$ plots for $\beta = 1$, in Figures 3.28 and 3.29. Although now we note a greater reduction of skewness with a sample size of $n = 500$ than that seen for $\beta = 0.8$.

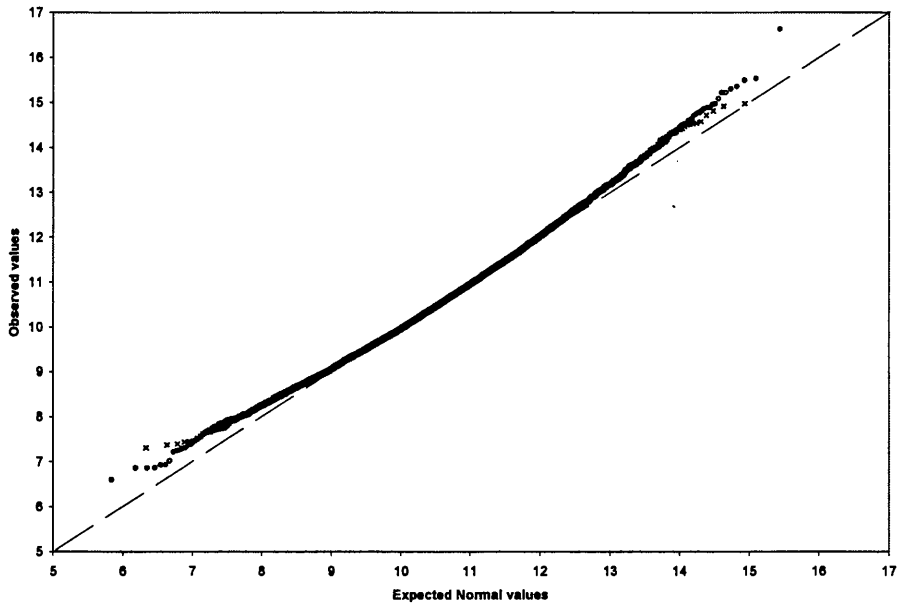

Figure 3.29: $Q-Q$ plot of $\hat{B}_{10,c}$, based on data generated from a Weibull distribution with $(\beta, \theta) = (1, 100)$ and $n = 500$.

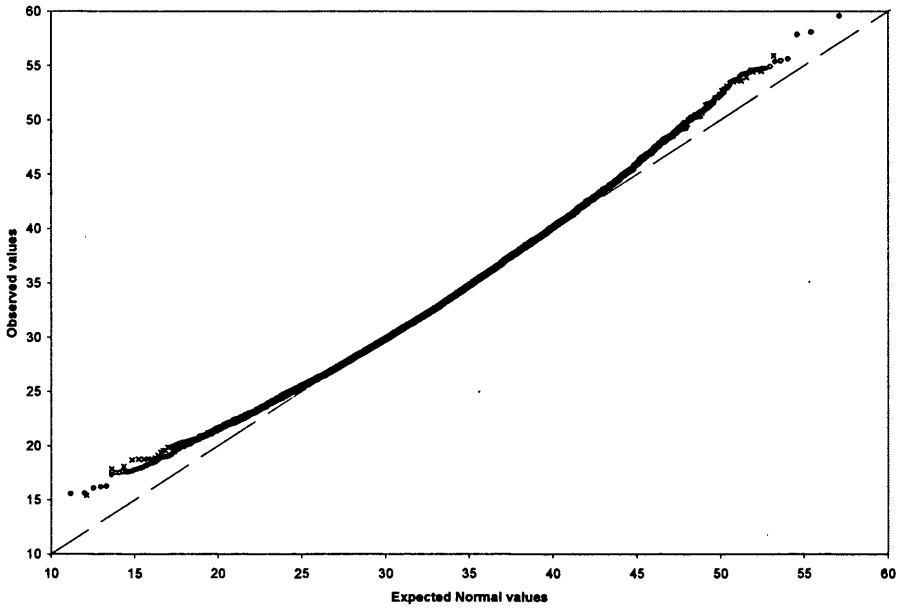

Figure 3.30: $Q-Q$ plot of $\hat{B}_{10,c}$, based on data generated from a Weibull distribution with $(\beta, \theta) = (2, 100)$ and $n = 50$.

We continue to see this reduction in the right skewness of the distribution of $B_{10,c}$ when the shape parameter increases to $\beta = 2$. The $Q-Q$ plot at $n = 50$, see Figure 3.30, lies much closer to the 45° line, and there is less upward curvature in the tails. From the $Q-Q$ plot in Figure 3.31, we might be prepared to accept that the sample in fact does follow a Normal distribution at $n = 500$.

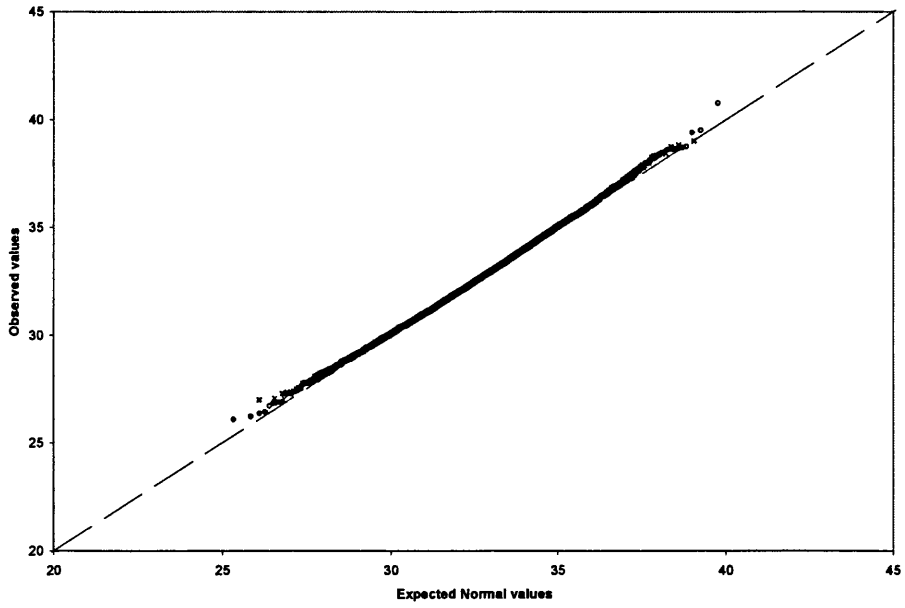

Figure 3.31: $Q-Q$ plot of $\hat{B}_{10,c}$, based on data generated from a Weibull distribution with $(\beta, \theta) = (2, 100)$ and $n = 500$.

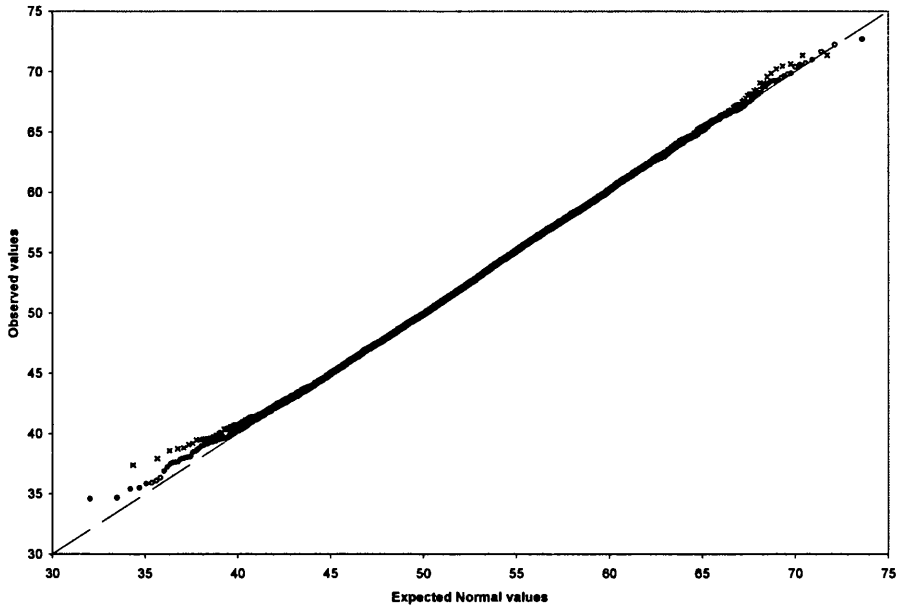

Figure 3.32: $Q-Q$ plot of $\hat{B}_{10,c}$, based on data generated from a Weibull distribution with $(\beta, \theta) = (3.5, 100)$ and $n = 50$.

Again, at $\beta = 3.5$ we see a much closer fit to Normality in Figures 3.32 and 3.33.

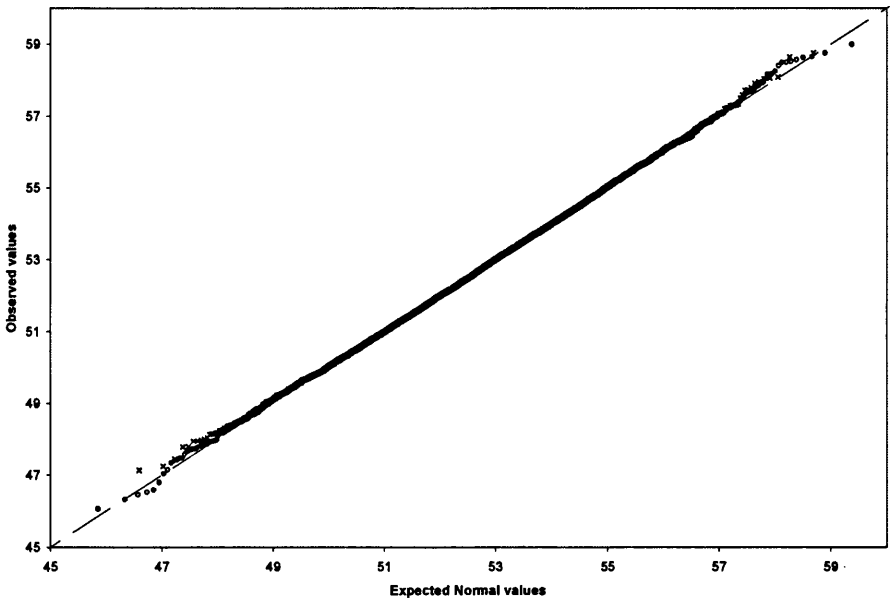

Figure 3.33: $Q-Q$ plot of $\hat{B}_{10,c}$, based on data generated from a Weibull distribution with $(\beta, \theta) = (3.5, 100)$ and $n = 500$.

c	n					
	50	100	500	1000	2500	5000
50	1705.30	1176.99	258.23	87.76	63.92	20.68
100	1679.16	1152.62	263.86	83.88	63.95	11.44
150	1654.20	1128.88	258.27	98.77	54.39	11.55
200	1707.64	1035.71	209.31	108.00	46.18	11.41
∞	1656.44	779.31	185.75	98.46	41.63	11.76

Table 3.28: K^2 test statistics for $\hat{B}_{10,c}$ yielded from simulated Weibull data with $(\beta, \theta) = (0.8, 100)$ for various n and c.

c	n					
	50	100	500	1000	2500	5000
50	1553.18	728.44	188.18	96.78	46.92	30.10
100	1493.54	745.78	178.19	90.83	39.75	28.64
150	1473.02	709.74	177.63	88.70	32.27	25.24
200	1474.12	674.58	168.29	86.32	24.63	19.10
∞	1478.42	659.54	149.71	71.50	30.18	15.59

Table 3.29: K^2 test statistics for $\hat{B}_{10,c}$ yielded from simulated Weibull data with $(\beta, \theta) = (0.9, 100)$ for various n and c.

3.4.3 Formal Normality Tests

Tables 3.28 to 3.33 display the corresponding K^2 statistics, with bold values indicating cases in which we would accept the hypothesis that the underlying distribution is Normal, as before, these correspond to $K^2 < 5.9915$.

The lack of Normality for $\beta = 0.8$ is confirmed in Table 3.28, where the K^2 statistic fails to fall below the critical value at any sample size, even a complete sample of $n = 5000$.

Again, due to the change in the nature of the hazard function around $\beta = 1$, we also summarise the K^2 test statistics for $\beta = 0.9$ and $\beta = 1.1$. These are seen in Tables 3.29, 3.30 and 3.31. We now see the effect of the shape parameter, and as β increases the K^2 test statistics decrease, thus approaching Normality. It is not until $\beta = 1.1$, for which the hazard function is increasing with time, do we see any samples reach Normality, and then it is only valid for $n = 5000$, with censoring levels $c > 100$.

c	n					
	50	100	500	1000	2500	5000
50	1236.12	715.12	148.35	52.69	29.24	18.46
100	1166.89	724.78	154.99	47.42	16.57	22.54
150	1129.82	711.80	137.28	43.22	15.51	21.69
200	1117.94	651.15	132.73	45.21	13.57	22.65
∞	1044.58	648.75	127.84	37.68	17.90	23.32

Table 3.30: K^2 test statistics for $\hat{B}_{10,c}$ yielded from simulated Weibull data with $(\beta, \theta) = (1, 100)$ for various n and c.

c	n					
	50	100	500	1000	2500	5000
50	1877.71	495.35	72.45	71.80	10.73	6.83
100	711.14	518.20	61.71	56.16	12.15	6.78
150	426.18	490.71	61.31	41.31	9.20	**2.60**
200	285.69	435.33	54.90	38.86	7.51	**3.79**
∞	454.99	451.46	60.22	46.52	8.96	**3.95**

Table 3.31: K^2 test statistics for $\hat{B}_{10,c}$ yielded from simulated Weibull data with $(\beta, \theta) = (1.1, 100)$ for various n and c.

c	n					
	50	100	500	1000	2500	5000
50	1556.74	146.98	35.68	8.17	**2.20**	**1.92**
100	185.34	78.32	22.34	6.25	**2.76**	**4.54**
150	158.85	63.80	9.50	13.11	**1.94**	**0.82**
200	151.42	53.59	9.87	14.59	**4.87**	**0.76**
∞	163.19	63.06	12.57	14.17	**5.83**	**1.38**

Table 3.32: K^2 test statistics for $\hat{B}_{10,c}$ yielded from simulated Weibull data with $(\beta, \theta) = (2, 100)$ for various n and c.

We recall that for $\beta = 2$ the $Q - Q$ plot indicated Normality at $n = 500$, the K^2 test statistics, in Table 3.32, however, show that that is not the case, and Normality is not observed until $n = 2500$, although it is now also seen for data censored as early as $c = 50$.

For $\beta = 3.5$, the K^2 test statistics, displayed in Table 3.33, now show that Normality is reached by $n = 100$, for censoring levels $c \geq 100$. It is also clear from the results, that at $c = 200$, in most simulations, all items have failed, and the test statistics are generally the same for $c = 200$ and complete data.

3.5 Summary

Exploiting the asymptotic properties of the Weibull parameter MLEs is a key step in applying results from statistical inference.

c	n					
	50	100	500	1000	2500	5000
50	26459.03	14292.25	1267.21	393.40	104.28	68.79
100	13.66	**0.02**	**2.31**	**2.41**	**2.78**	7.17
150	11.13	**4.41**	**4.25**	**3.12**	**1.79**	**0.96**
200	14.60	**5.89**	**5.40**	**1.79**	**2.02**	**1.56**
∞	14.60	**5.91**	**5.50**	**1.79**	**2.00**	**1.56**

Table 3.33: K^2 test statistics for $\hat{B}_{10,c}$ yielded from simulated Weibull data with $(\beta, \theta) = (3.5, 100)$ for various n and c.

The conclusions drawn from our large scale simulation study, is that asymptotic Normality assumptions on $\left(\hat{\beta}_c, \hat{\theta}_c\right)$ and functions of these estimators, such as $\hat{B}_{10,c}$, are implausible for sample sizes less than $n = 1000$, and then only for relatively late censoring times. As some compensation, if some prior information is known about items, and the true shape parameter is thought to be $\beta > 2$, then asymptotic assumptions may hold at smaller samples size, but these will often still be too large to become feasible for experiments.

Despite these poor approximations to the Normal distribution, precision and confidence intervals obtained in the simulation studies still provided good coverage of the MLEs, but the shape of the distribution is not well represented.

It seems appropriate, given these findings, that we consider alternative measures of precision in estimates.

Chapter 4

Properties of Weibull MLEs in Small Samples

Chapter 3 discussed the non-Normality in small to moderate samples of MLEs. Alternative approaches to asymptotic Normality are suggested by Lawless (1982), and in this section we will employ the relative likelihood function, mentioned in section 2.1.

4.1 Relative Likelihood

The relative likelihood function of Weibull parameters (β, θ) is defined as

$$R(\beta, \theta) = \frac{L(\beta, \theta)}{L\left(\hat{\beta}_c, \hat{\theta}_c\right)}$$

Since the regularity conditions of maximum likelihood theory hold, then under the hypothesis $H_0 : (\beta, \theta) = (\beta_0, \theta_0)$, the asymptotic distribution of

$$\Lambda = -2 \ln R(\beta_0, \theta_0)$$

is χ^2_2. Significance tests (the likelihood ratio test) can then be carried out, with large values of Λ indicating evidence against H_0. The test is known to possess some very desirable properties (see Kalbfleisch & Prentice (1980)), and can be used to construct confidence regions for parameter estimates. We refer to Wolstenholme (1999) for further discussion on the uses of the likelihood ratio test in the Weibull distribution.

Lawless (1982) outlines how to obtain approximate ρ confidence intervals for β and θ separately, by finding the appropriate set of values for each parameter for which H_0 is not rejected at the $1 - \rho$ level of significance. An alternative to looking at each parameter separately, via numerical procedures, is to consider an estimation of results by graphical means, using a contour map of (β, θ).

Kalbfleisch (1979) discussed the role of relative likelihood, including the possibility of censoring. The set of parameter values for which $R(\beta,\theta) \geq \rho$, can be described, or interpreted as a $100\rho\%$ likelihood region for (β,θ). By evaluating $R(\beta,\theta) = \rho$ over a lattice of values in the $\beta - \theta$ plane, he produces contours of constant relative likelihood in order to determine regions of plausible values for (β,θ). Values inside the $\rho = 0.5$ contour are quite plausible, while values outside the $\rho = 0.01$ contour are very implausible.

4.2 Drawing the contours

Kalbfleisch (1979) prepared his contour maps from tabulations of $R(\beta,\theta)$, and noted that the use of a computer programme to solve the equation $R(\beta,\theta) = \rho$ leads to a more accurate contour map, but usually at the expense of increased programming time and complexity. Watkins & Leech (1989) outline one approach to producing an accurate contour map. The algorithm has three main stages:

1. To locate the MLE of β and θ. This point $\left(\hat{\beta}_c, \hat{\theta}_c\right)$ lies at the centre of all contours. Chapter 2 outlines the procedure of locating the Weibull parameter MLEs for both complete and censored data.

2. To search the $\beta - \theta$ plane for a rectangular drawing area, within which the contour corresponding to ρ will lie.

3. To draw this contour by first finding, and then connecting a large number of points on it. This process is repeated for each contour.

4.2.1 Defining the drawing area

The next stage in the algorithm is to search the $\beta - \theta$ plane about $\left(\hat{\beta}_c, \hat{\theta}_c\right)$. This search introduces a rescaling argument, and we consider the relative likelihood at a series of fractions, and then multiples, of $\hat{\beta}_c$. The maximum value of the relative likelihood for β can be computed and we can search for maximum and minimum values of β that need to be considered; see Figure 4.1. For any given β, the value of θ that maximises the relative likelihood can be found from equation (2.21).

The same idea is used for θ, a series of fractions and multiples of $\hat{\theta}$ are considered and the β which maximises the relative likelihood for each value of θ is found. This maximum relative likelihood is computed, and we can search for the minimum and maximum values of θ that need to be considered; see Figure 4.2. All searches here must be numerical, using the Newton-Raphson method to locate a zero of the first derivative of the log-likelihood, (2.19), using $\hat{\beta}$ as the initial estimate.

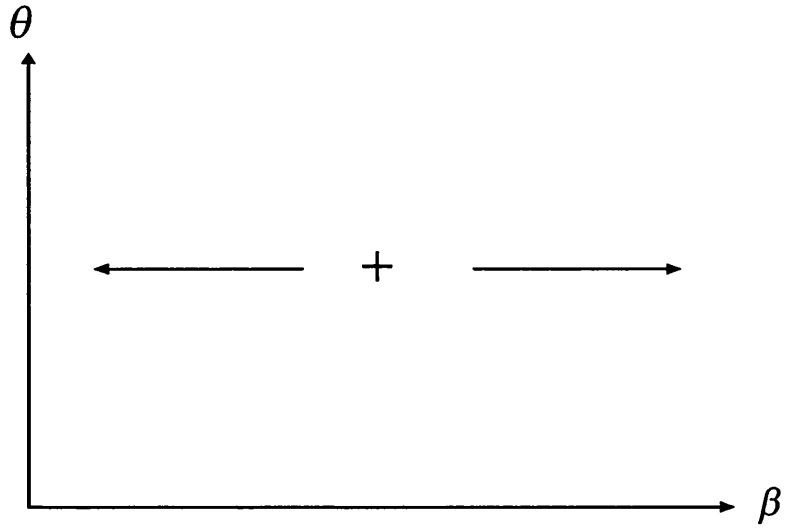

Figure 4.1: Search $\beta - \theta$ plane about $\left(\hat{\beta}_c, \hat{\theta}_c\right) = +$ for minumim and maximum values of β

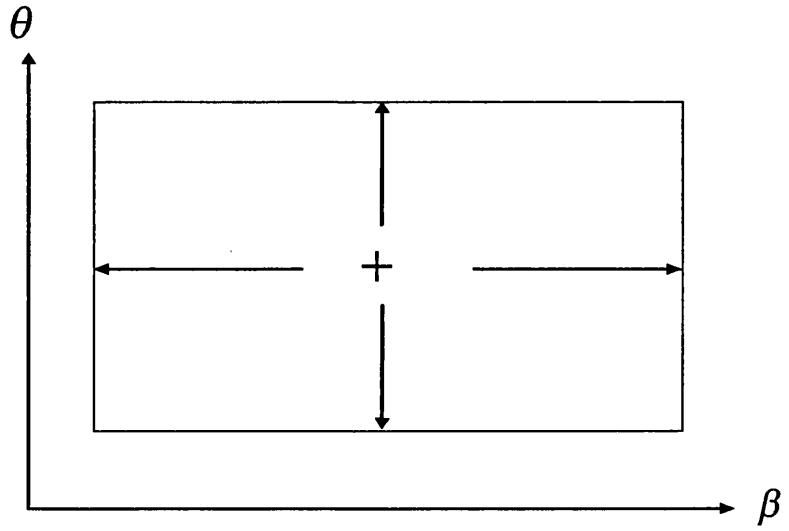

Figure 4.2: Search for the minimum and maximum values of θ

4.2.2 Drawing the contours

To draw the contour, we first find an initial point, and then try to move around the contour. We use $\beta = x\hat{\beta}_c$ and $\theta = y\hat{\theta}_c$ to define new working variables x and y, and we find it convenient to define

$$f(x,y) = \ln R\left(x\hat{\beta}_c, y\hat{\theta}_c\right). \tag{4.1}$$

The initial point on the contour

To find an initial point on a contour, we set $x = 1$ and search for a value of y, such that the relative likelihood at $\beta = x\hat{\beta} = \hat{\beta}$ and $\theta = y\hat{\theta}$ has the required value. Expressed mathematically, we have the logarithm of the relative likelihood, (4.1),

$$\begin{aligned} f(x,y) &= M\ln\left(x\hat{\beta}\right) - Mx\hat{\beta}\ln\left(y\hat{\theta}\right) + (x\hat{\beta}-1)\sum_{i=1}^{M}\ln(y_i) \\ &\quad - \left(y\hat{\theta}\right)^{-x\hat{\beta}}\left\{\sum_{i=1}^{M} y_i^{x\hat{\beta}} - (n-M)\,c^{x\hat{\beta}}\right\} - M\ln\left(\hat{\beta}\right) + M\hat{\beta}\ln\left(\hat{\theta}\right) \\ &\quad -(\hat{\beta}-1)\sum_{i=1}^{M}\ln(y_i) + \theta^{-\hat{\beta}}\left\{\sum_{i=1}^{M} y_i^{\hat{\beta}} - (n-M)\,c^{\hat{\beta}}\right\} \end{aligned} \tag{4.2}$$

and we search for y such that

$$f(x,y) - \ln(\rho_1) = 0 \tag{4.3}$$

with $x = 1$, which gives the first point on the contour $R\left(\hat{\beta},\hat{\theta}\right) = \rho_1$ (illustrated in Figure 4.3). Equation (4.3) is solved numerically, and the Newton-Raphson method requires the derivative

$$f_y(x,y) = Mx\hat{\beta}y^{-1} + x\hat{\beta}\left(y\hat{\theta}\right)^{-x\hat{\beta}}\left\{\sum_{i=1}^{M} y_i^{x\hat{\beta}} - (n-M)\,c^{x\hat{\beta}}\right\}y^{-1} \tag{4.4}$$

again with $x = 1$. The initial estimate of a solution to (4.3) can be

$$\frac{\theta_{\max}}{\hat{\theta}},$$

where $\theta_{\max}$ is the maximum value of θ in the drawing area.

Moving along the contour

We first calculate the gradient of the tangent to the contour at this initial point, that is

$$-\frac{f_x(x,y)}{f_y(x,y)}$$

where

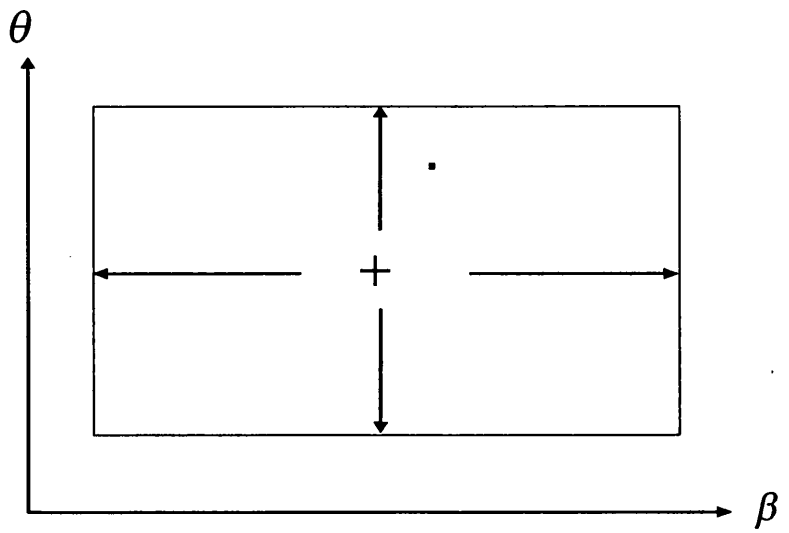

Figure 4.3: Find the first point on the contour $R\left(\hat{\beta}_c, \hat{\theta}_c\right) = \rho$

$$f_x(x,y) = Mx^{-1} - M\hat{\beta}\ln\left(y\hat{\theta}\right) + \hat{\beta}S_e + \left(y\hat{\theta}\right)^{-x\hat{\beta}}\hat{\beta}\left\{S_0\left(x\hat{\beta}\right)\ln(y\theta) - S_1\left(x\hat{\beta}\right)\right\} \quad (4.5)$$

again, when $x = 1$. The first estimate of the next point along the contour is now found by moving a distance, δ (> 0), in the $x - y$ plane along this tangent

$$x \to x + \frac{\delta f_y}{\left(f_x^2 + f_y^2\right)} \quad (4.6)$$

and

$$y \to y + \frac{\delta f_x}{\left(f_x^2 + f_y^2\right)} \quad (4.7)$$

For these new values of x and y, we fix x, and try and attempt to find a y that solves (4.3). This is the same method we used to find the initial point, but now we use the updated value of y in (4.7) is used as an initial estimate for the Newton-Raphson procedure, and $x = 1$ in (4.4) and (4.5) no longer applies. By iterating this process, recomputing the equations with the updated x and y values, we can move around the contour (Figure 4.4).

When this process approaches a turning point on the contour, we will fail to find a y value that solves equation (4.3), this is because the values of

$$f_y \text{ and } \frac{f_y}{\left(f_x^2 + f_y^2\right)}$$

are small near the extreme left or right edge of the contour. In such cases, we fix the value of y, and attempt to find a solution to (4.3) with a corresponding value of x; practically, we

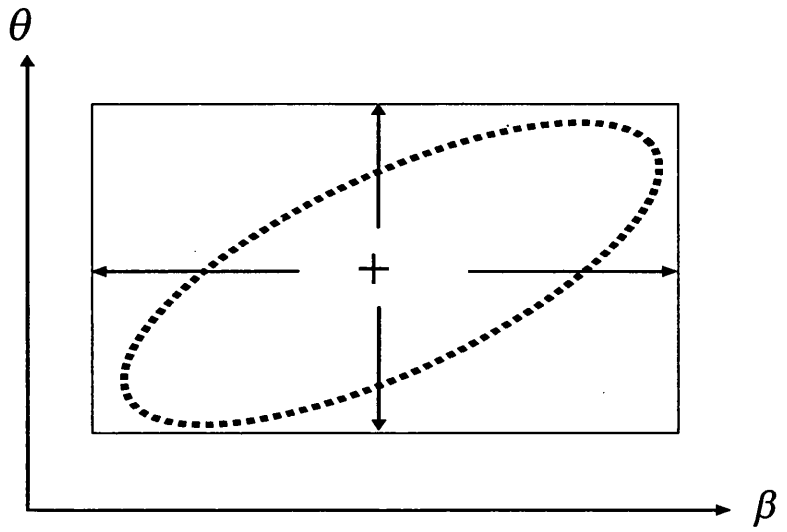

Figure 4.4: Moving around the contour with the iterative process

δ	Number of points
0.005	629
0.01	312
0.05	59
0.1	29

Table 4.1: Number of points of the RL contour $\rho = 0.05$ for the ball bearings data, censored at $c = 100$ for various values of δ.

are undergoing a change in slope, or direction, in the contour. This search must be carried out numerically, with the most updated value of x used as an initial estimate. The iterative Newton-Raphson method then uses $f_x(x, y)$ in (4.5) to improve this estimate.

Options for the algorithm

The contour drawing process can be done at various contour levels, $R\left(\hat{\beta}, \hat{\theta}\right) = \rho$. We can look at $\rho = 0.01, 0.05, 0.1, 0.25, 0.5, 0.75, 0.9, 0.95, 0.99$, with the first case yielding approximate 99% confidence regions, and so on.

We also note that the choice of distance δ in equations (4.6) and (4.7), will determine the smoothness of the contour. Table 4.1 compares the number of points of the contour $\rho = 0.05$, yielded from various values of δ choices using the ball bearings data, censored at $c = 100$. At $\delta = 0.01$, we have enough points for the contour to be sufficiently smooth without excessive computational time, and so for the purpose of the examples and work carried out in this chapter, we will set $\delta = 0.01$.

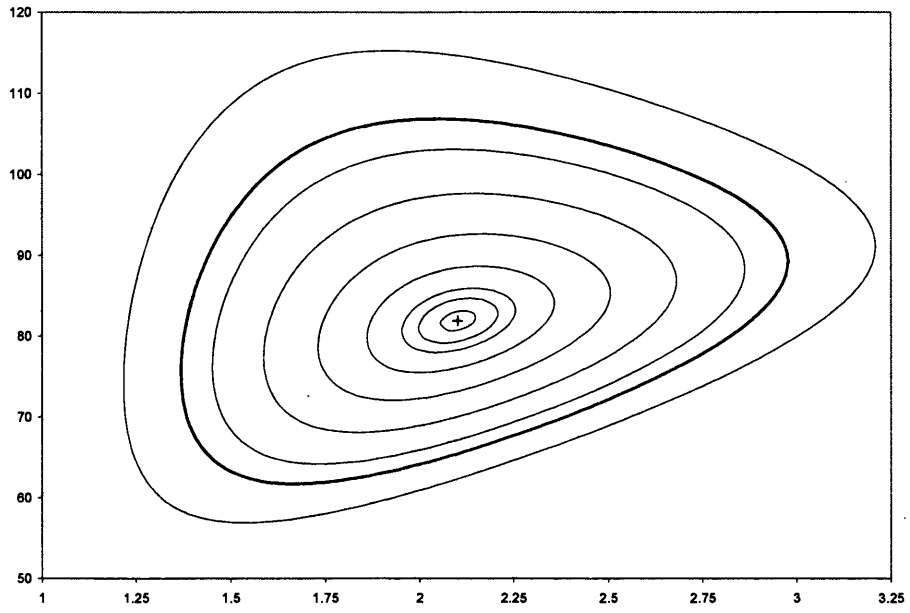

Figure 4.5: Relative likelihood contours of $\left(\hat{\beta}, \hat{\theta}\right)$ for complete ball bearings data.

4.2.3 Example: Ball bearings data

We revisit the concept of interim analysis of the failure times, we can return to the ball bearings data given in Table 1.2. The Watkins & Leech (1989) algorithm, outlined above, can construct the nine relative likelihood contours for various stopping times c. Figure 4.5 shows the contour plots for the complete ball bearings data. The outer contour is the curve along which $R\left(\hat{\beta}, \hat{\theta}\right) = 0.01$, and we highlight the next inward contour $R\left(\hat{\beta}, \hat{\theta}\right) = 0.05$ (the thicker line); this is of particular interest as it intuitively gives a 95% confidence region for $\left(\hat{\beta}, \hat{\theta}\right)$. We see that as ρ increases the contour area gets smaller, and its shape becomes more elliptical.

Consideration of a censoring regime causes distinct changes in the relative likelihood contours. Figures 4.6, 4.7, 4.8, and 4.9 are plots of the contour maps at increasing $c = 50, 75, 100$, and 125 respectively. We see that, at early censoring times, the shape of the contour extends over larger values in both the horizontal (β) and vertical (θ) axis, particularly for $\rho = 0.01$ and 0.05, where the contours are concave. Again, as ρ increases, the contour areas drop because the consistency rises, and the shape become more elliptical, reminiscent of bivariate Normality. We see that, as the c increases, the contour maps become similar to those obtained from the complete dataset.

The effect of c is more apparent in Figure 4.10, where for fixed $\rho = 0.05$, we have plotted the relative likelihood contour at various censoring levels; $c = 50$ being the outermost concave contour, and the innermost contour (dashed line) being that from the complete

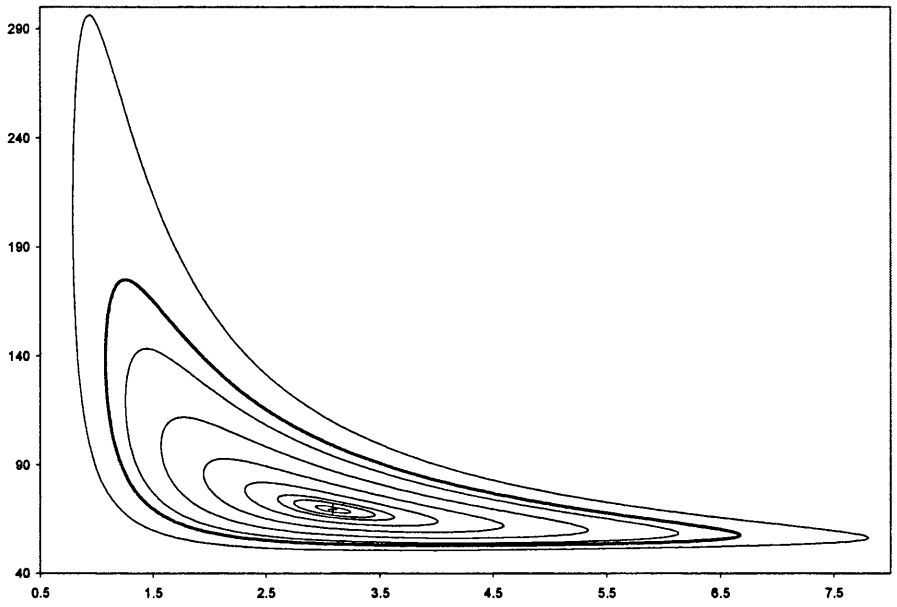

Figure 4.6: Relative likelihood contours of $\left(\hat{\beta}_c, \hat{\theta}_c\right)$ for ball bearings data censored at $c = 50$.

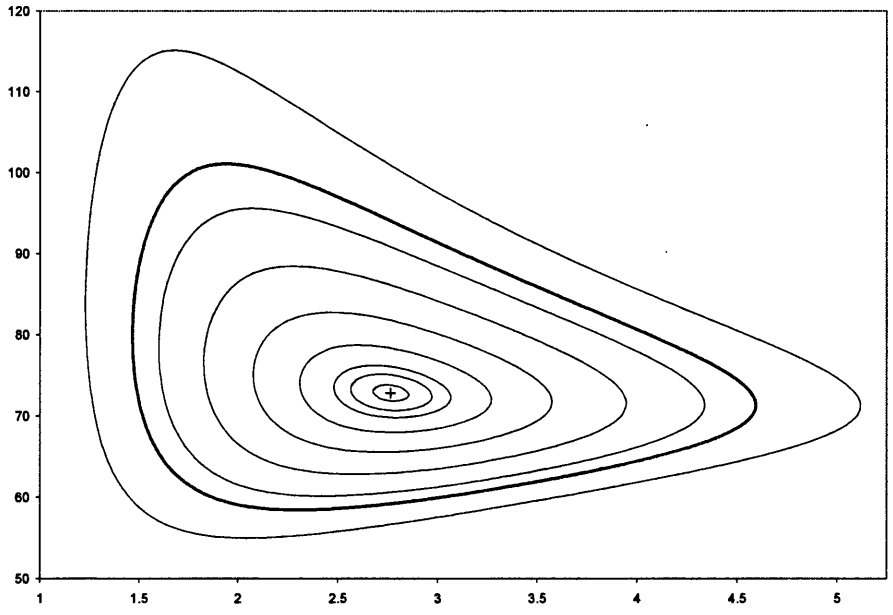

Figure 4.7: Relative likelihood contours of $\left(\hat{\beta}_c, \hat{\theta}_c\right)$ for ball bearings data censored at $c = 75$.

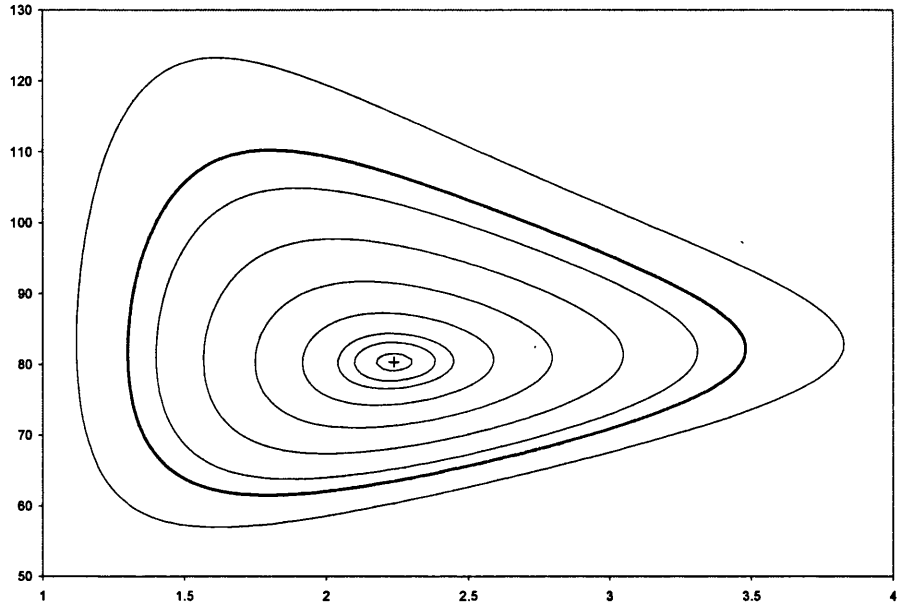

Figure 4.8: Relative likelihood contours of $\left(\hat{\beta}_c, \hat{\theta}_c\right)$ for ball bearings data censored at $c = 100$.

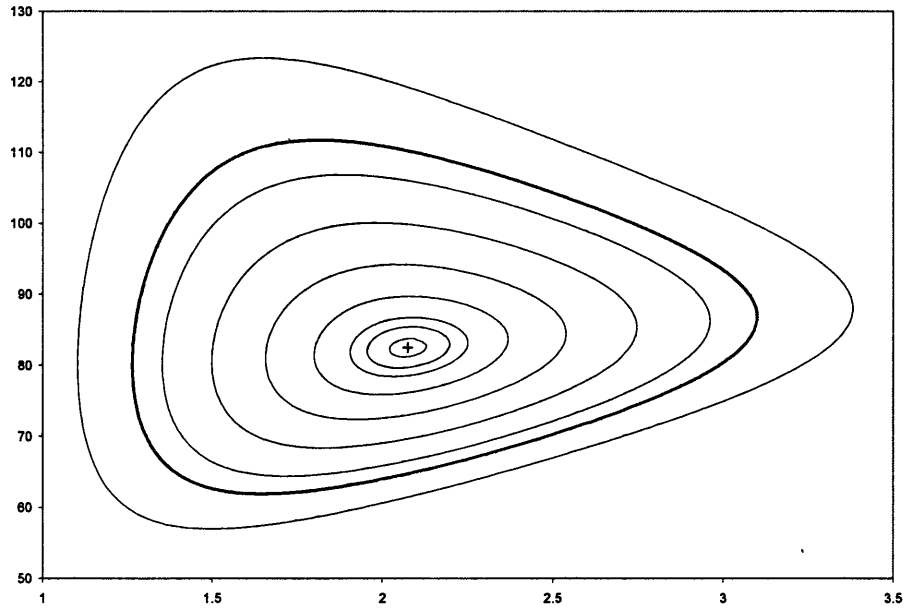

Figure 4.9: Relative likelihood contours of $\left(\hat{\beta}_c, \hat{\theta}_c\right)$ for ball bearings data censored at $c = 125$.

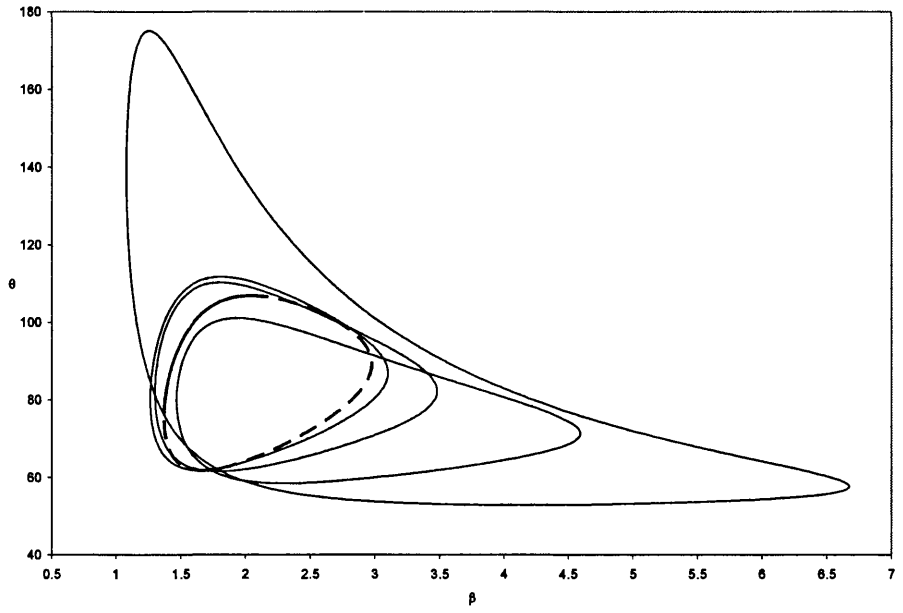

Figure 4.10: Relative likelihood contours, at $\rho = 0.05$, of $\left(\hat{\beta}_c, \hat{\theta}_c\right)$ for ball bearings data at various censoring levels. $c = 50$ is the outermost contour, $c = \infty$ is the innermost contour (dashed line).

data. We see here that the contours get smaller as c increases, which we expect, because the more failures we observe the more information we have to estimate the parameters. The contours also appear to move left along the horizontal (β) axis and shift up the vertical (θ) axis, as more items are allowed to fail.

These contours agree with those drawn in Kalbfleisch (1979), and then in Watkins & Leech (1989).

4.2.4 Example: 49 failure times

We can repeat the above process for our second example, in which we consider the 49 failure times; see Table 2.2. Once again, we can produce the relative likelihood contours around the MLEs obtained at time $c = 50, 100, 150, 200$ and then the final analysis when all items have failed; see Figures 4.11, 4.12, 4.13, 4.14 and 4.15.

We see similar patterns as in the ball bearings example, and note that, again, the shape of the contours become more elliptical, implying bivariate normality, when c increases, and when ρ is closer to 0.99. We can again look at fixed $\rho = 0.05$, and compare the contours at various censoring levels, Figure 4.16; $c = 50$ being the outermost concave contour, and the inner most contour (dashed line) being that from the complete data.

Again it is apparent that the contours become more precise as c increases, and for this example, as more items fail, we see a shift right along the horizontal (β) axis, and down the

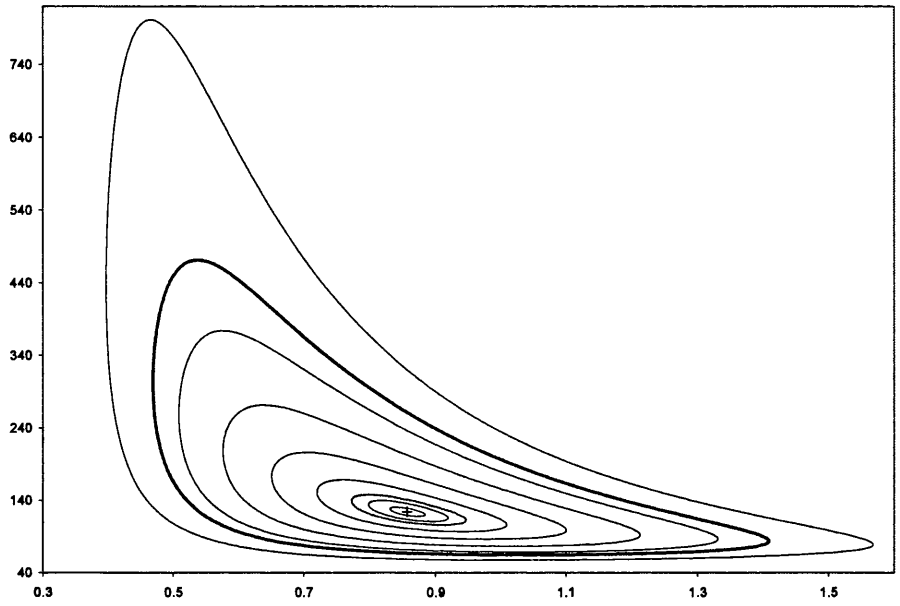

Figure 4.11: Relative likelihood contours of $\left(\hat{\beta}_c, \hat{\theta}_c\right)$ for 49 failures data censored at $c = 50$.

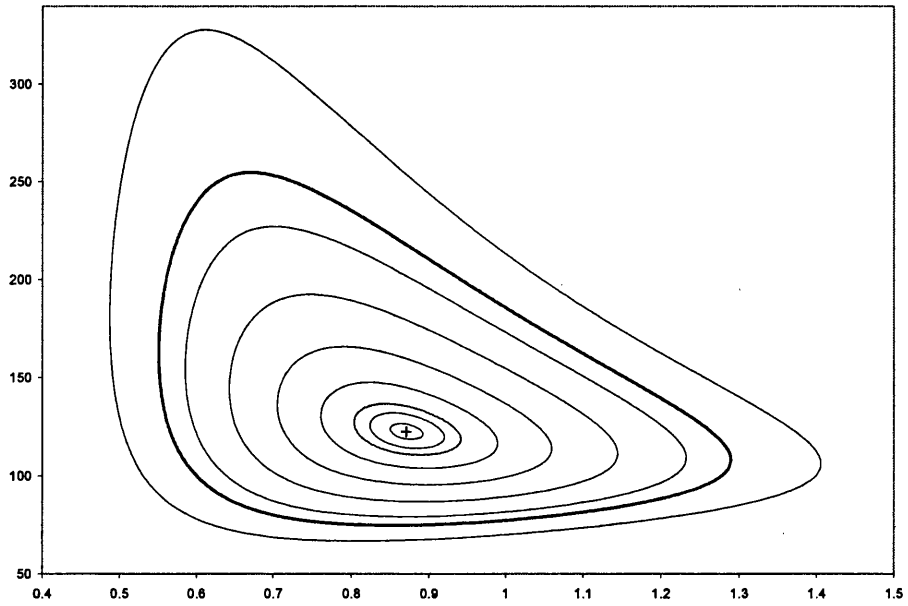

Figure 4.12: Relative likelihood contours of $\left(\hat{\beta}_c, \hat{\theta}_c\right)$ for 49 failures data censored at $c = 100$.

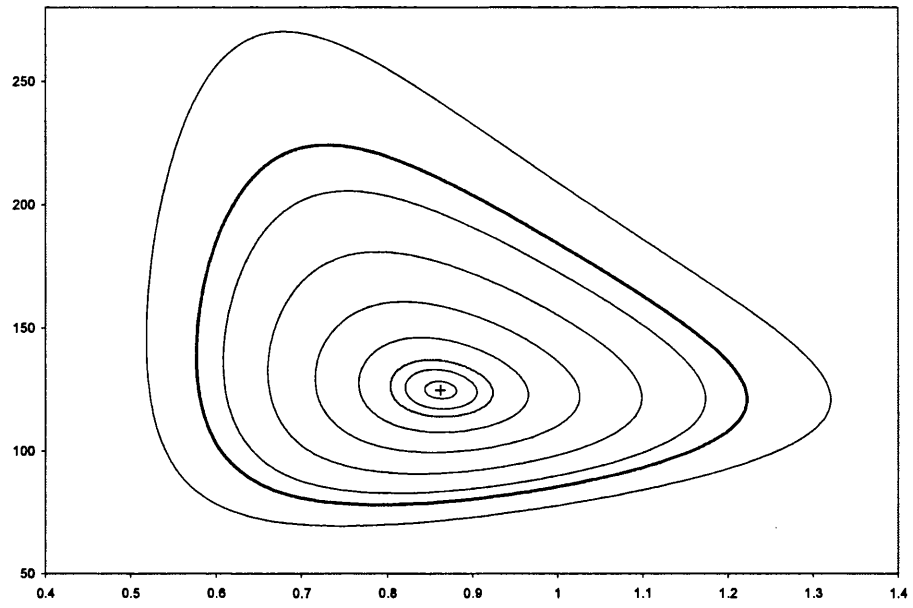

Figure 4.13: Relative likelihood contours of $\left(\hat{\beta}_c, \hat{\theta}_c\right)$ for 49 failures data censored at $c = 150$.

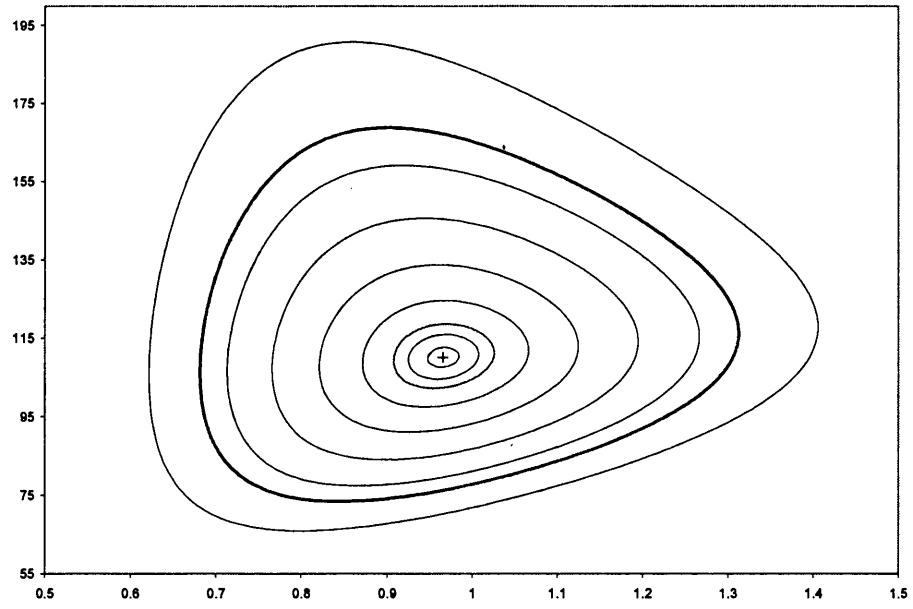

Figure 4.14: Relative likelihood contours of $\left(\hat{\beta}_c, \hat{\theta}_c\right)$ for 49 failures data censored at $c = 200$.

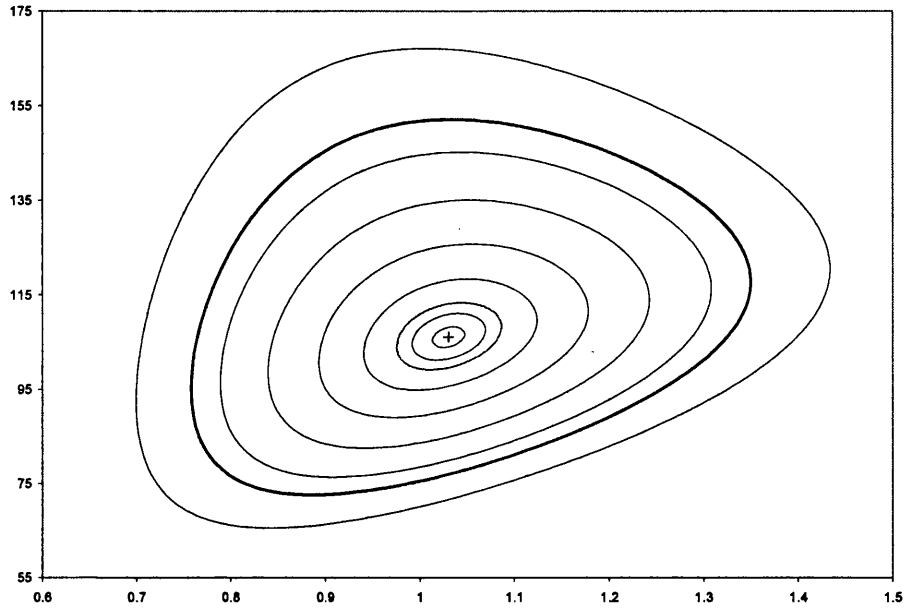

Figure 4.15: Relative likelihood contours of $\left(\hat{\beta}, \hat{\theta}\right)$ for complete 49 failures data.

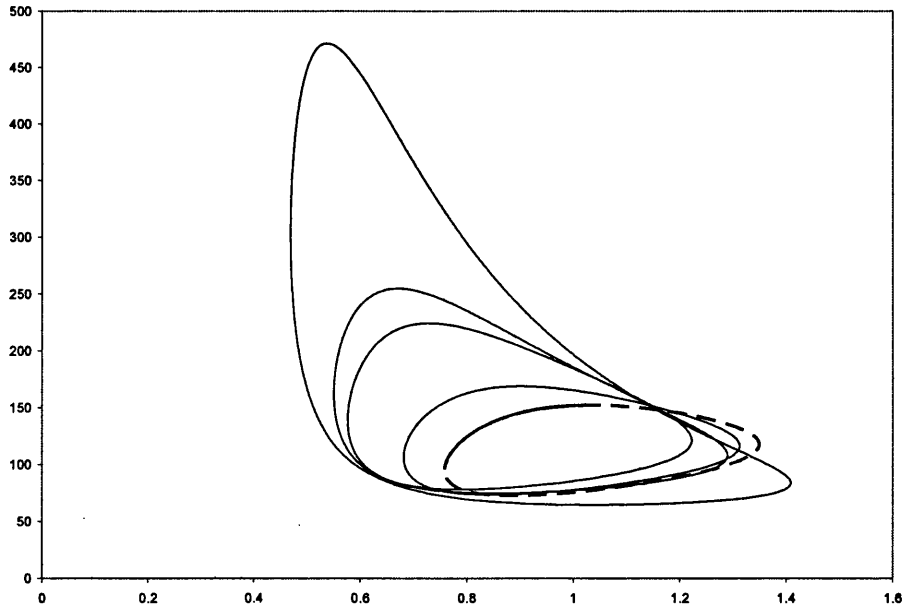

Figure 4.16: Relative likelihood contours, at $\rho = 0.05$, of $\left(\hat{\beta}_c, \hat{\theta}_c\right)$ for the 49 failure times data at various censoring levels. $c = 50$ is the outermost contour, $c = \infty$ is the innermost contour (dashed line).

vertical (θ) axis, opposite directions to the ball bearings example above (Figure 4.10). This agrees with the details given in Chapter 2, where, for the ball bearing data (Table 2.5), as c increases, $\hat{\beta}_c$ gets smaller, and $\hat{\theta}_c$ gets bigger; whereas for the 49 failure times data (Table 2.6), as c increases, $\hat{\beta}_c$ decreases, and $\hat{\theta}_c$ increases.

4.3 Comparison with Normal theory confidence intervals

Confidence regions based on relative likelihood methods are discussed in most reliability texts, see for instance Lawless (1982). Cox & Hinkley (1974) give an explicit proof that Normal theory and relative likelihood confidence regions are asymptotically equivalent, and, despite both methods using asymptotic theory, many authors have recognised the advantages of likelihood based inferences, see for example, Lawless (1982) and Meeker & Escobar (1995).

4.3.1 Example: Ball bearings data

For illustration, we will fix $\rho = 0.05$, and compare the confidence regions obtained via asymptotic Normality and relative likelihood theory for the ball bearings example. In the previous chapter, Figure 3.1 displayed the asymptotic Normal confidence ellipse for the MLEs of the ball bearings data at $c = 100$. We can now compare this region with that obtained using relative likelihood theory above; Figure 4.10.

Figures 4.17, 4.18, 4.19, 4.20 and 4.21 compare the confidence regions for the ball bearings data, at censoring levels, $c = 50, 75, 100, 125$, and the complete sample, respectively. We can see that there is an overlap between the two curves, and this overlap increases as $c \to \infty$. There are also points where the relative likelihood contour is almost tangential to the ellipse. On closer inspection we notice a small distance between the curves, but this distance appears to decrease as $c \to \infty$.

As already seen in Figure 4.10, as c increases, we observe the relative likelihood contour move towards the shrinking ellipse about $\left(\hat{\beta}_c, \hat{\theta}_c\right)$.

4.3.2 Example: 49 failure times data

Figures 4.22 to 4.26 confirm the same pattern in the curves for the 49 failure data as $c \to \infty$. The relative likelihood contour appears to be constrained at points to the asymptotic Normal confidence ellipse, and as c increases, the overlap between the curves increases, with the relative likelihood contour moving towards the central MLE.

Further research

There is obvious scope here to investigate the relative size of the two confidence regions, as well as the extent of the overlap in general, and the proximity between curves. For the purpose of this thesis however, we can conclude that the relative likelihood contours appear to reflect more accurately the nature of the distribution of small samples of MLEs, as seen

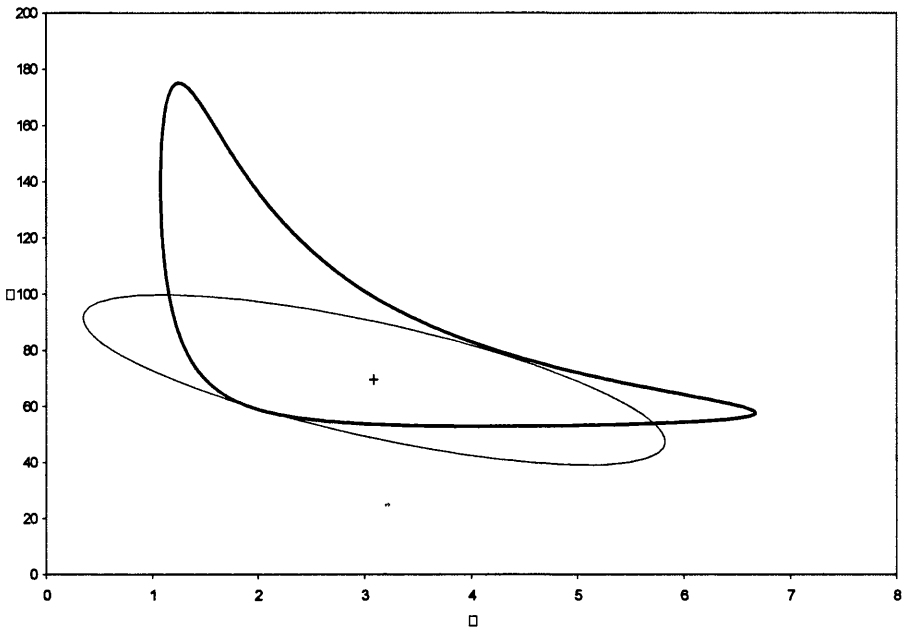

Figure 4.17: The MLE (+) together with 0.05 confidence regions based on asymptotic Normality and relative likelihood (bold line) for the ball bearings data at $c = 50$.

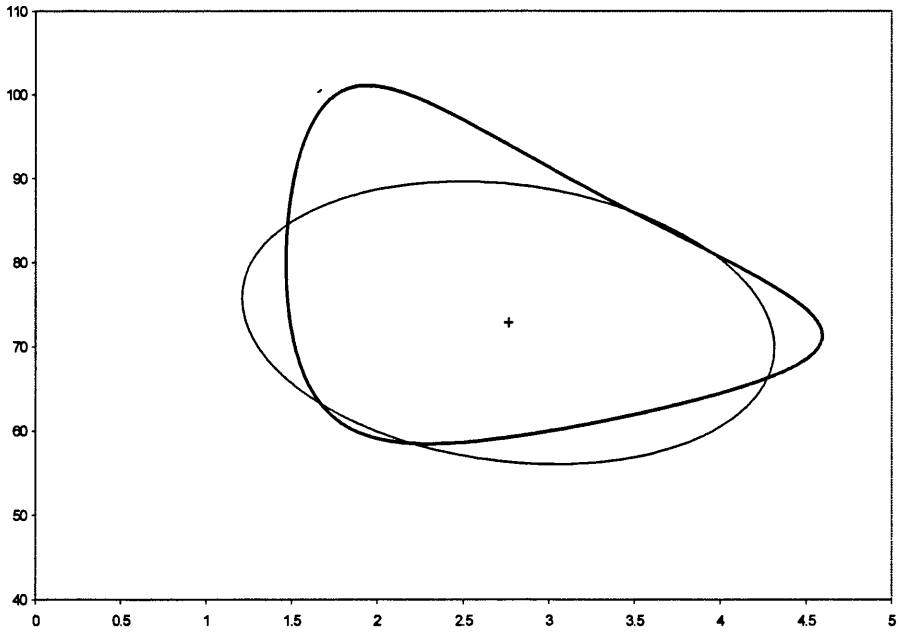

Figure 4.18: The MLE (+) together with 0.05 confidence regions based on asymptotic Normality and relative likelihood (bold line) for the ball bearings data at $c = 75$.

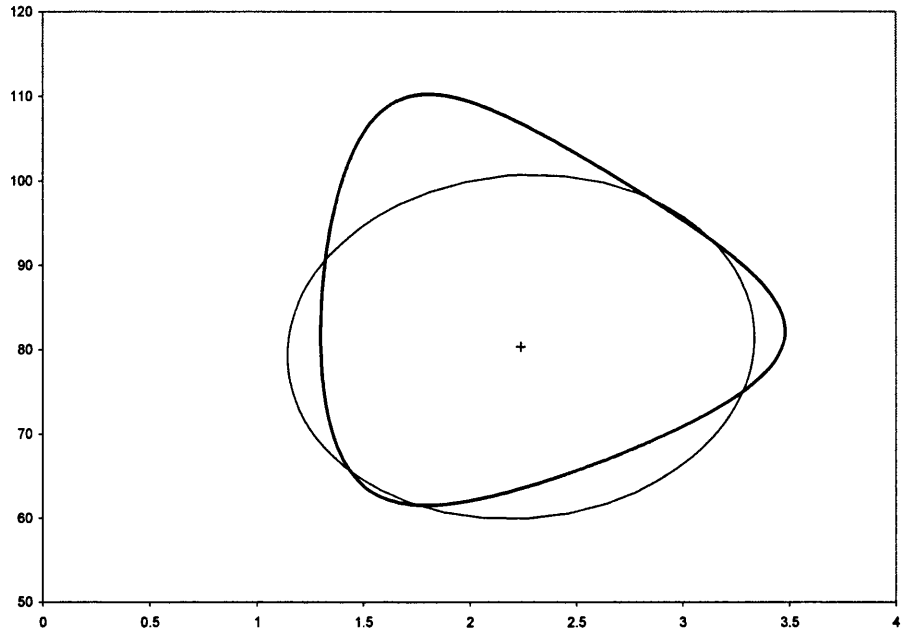

Figure 4.19: The MLE (+) together with 0.05 confidence regions based on asymptotic Normality and relative likelihood (bold line) for the ball bearings data at $c = 100$.

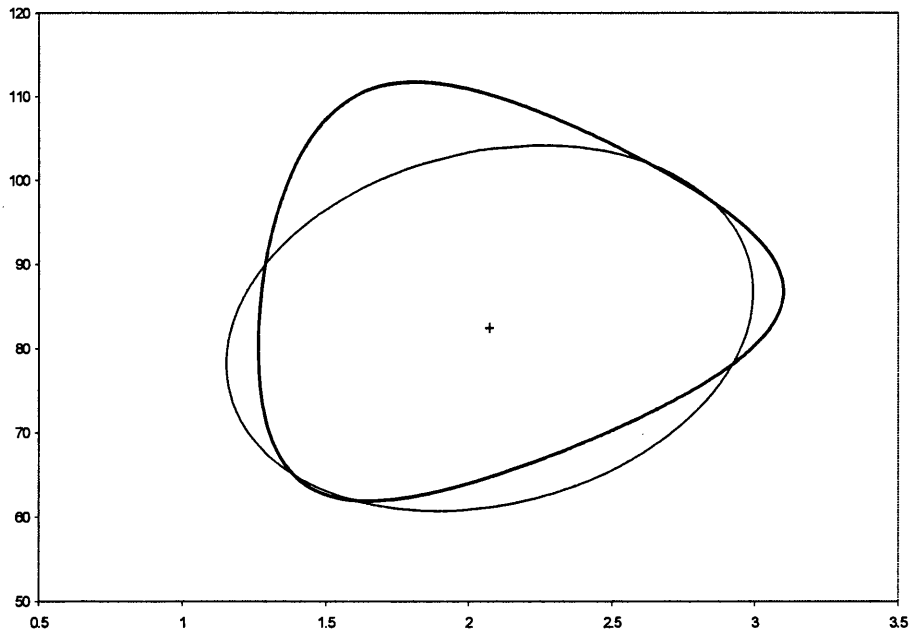

Figure 4.20: The MLE (+) together with 0.05 confidence regions based on asymptotic Normality and relative likelihood (bold line) for the ball bearings data at $c = 125$.

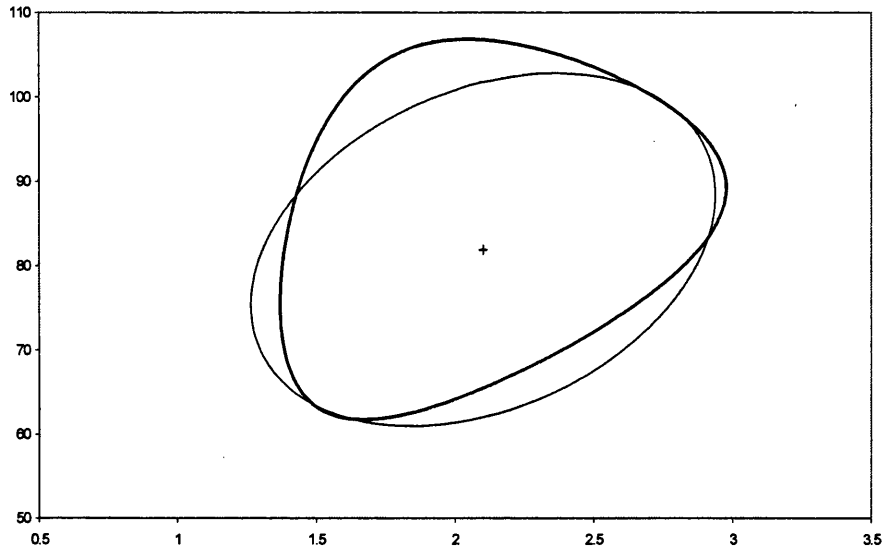

Figure 4.21: The MLE (+) together with 0.05 confidence regions based on asymptotic Normality and relative likelihood (bold line) for the ball bearings data at $c = \infty$.

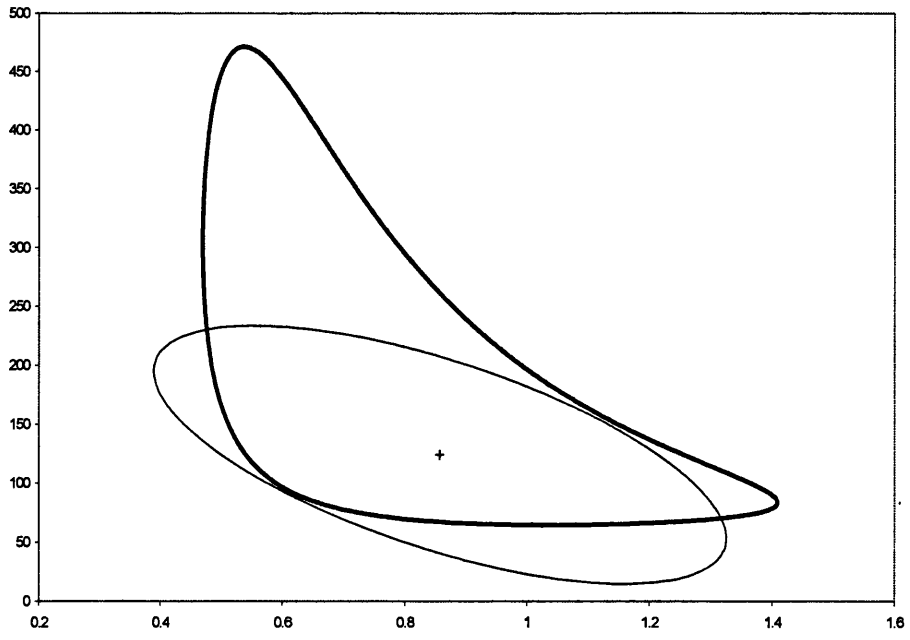

Figure 4.22: The MLE (+) together with 0.05 confidence regions based on asymptotic Normality and relative likelihood (bold line) for the 49 failures data from Epstein (1960), at $c = 50$.

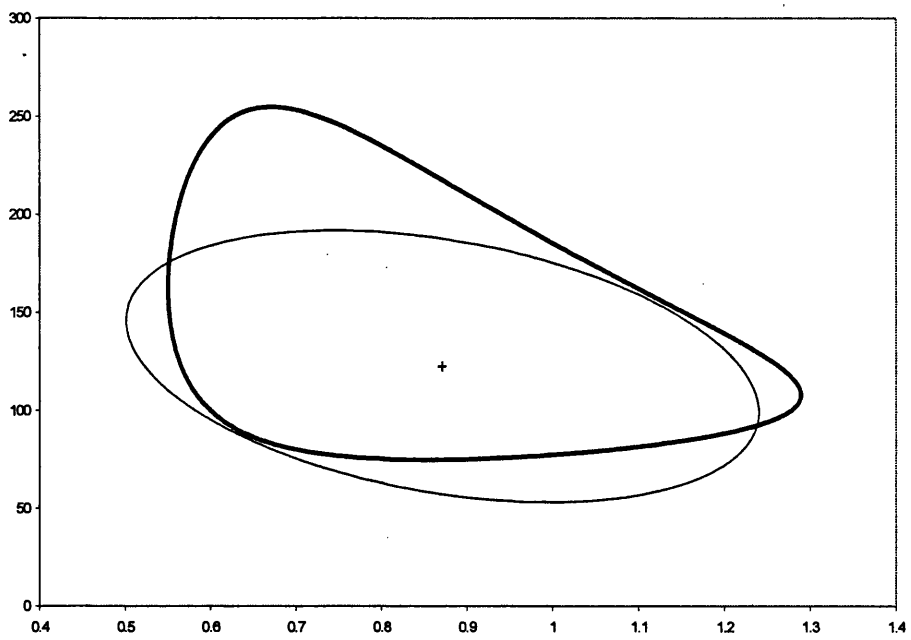

Figure 4.23: The MLE (+) together with 0.05 confidence regions based on asymptotic Normality and relative likelihood (bold line) for the 49 failures data from Epstein (1960), at $c = 100$.

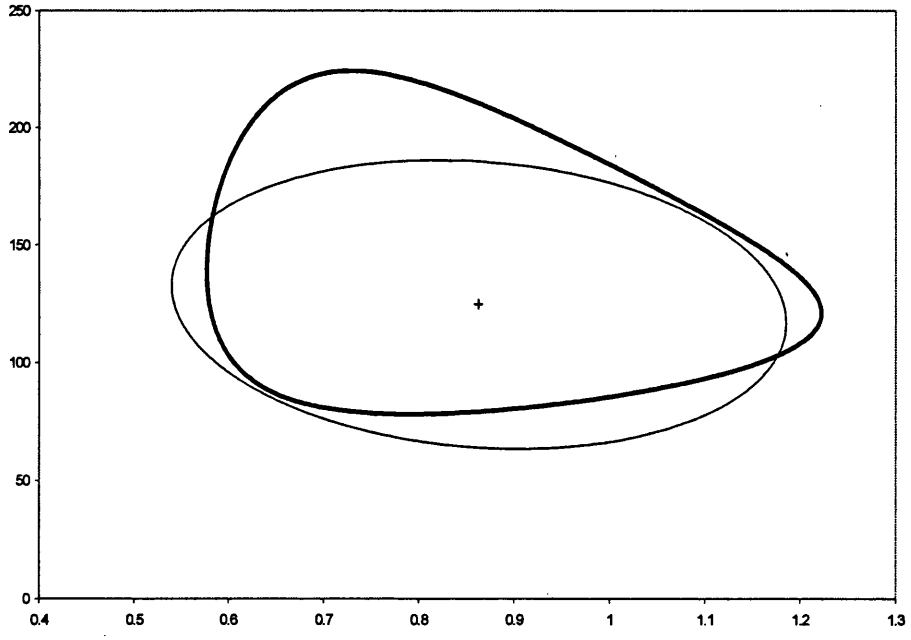

Figure 4.24: The MLE (+) together with 0.05 confidence regions based on asymptotic Normality and relative likelihood (bold line) for the 49 failures data from Epstein (1960), at $c = 150$.

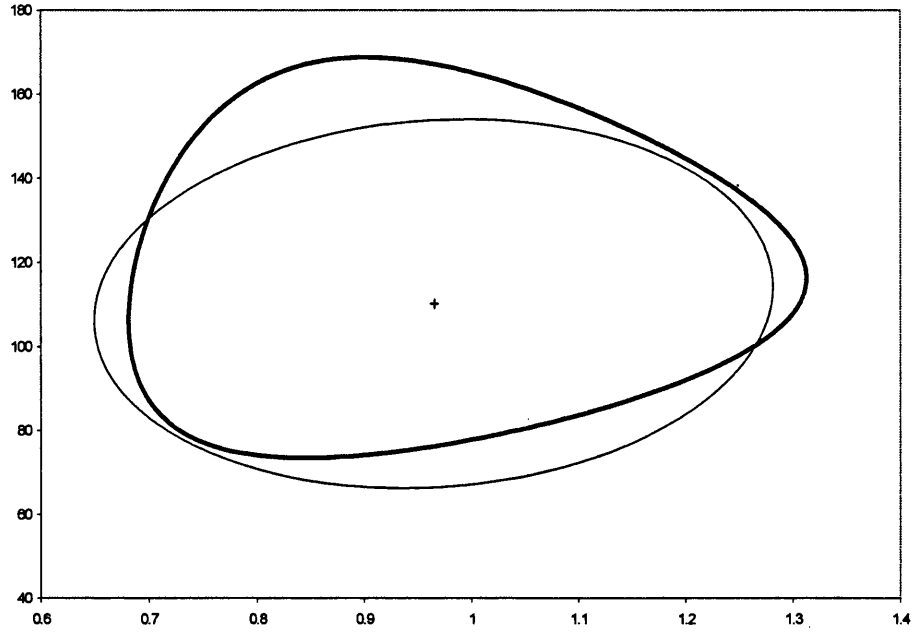

Figure 4.25: The MLE (+) together with 0.05 confidence regions based on asymptotic Normality and relative likelihood (bold line) for the 49 failures data from Epstein (1960), at $c = 200$.

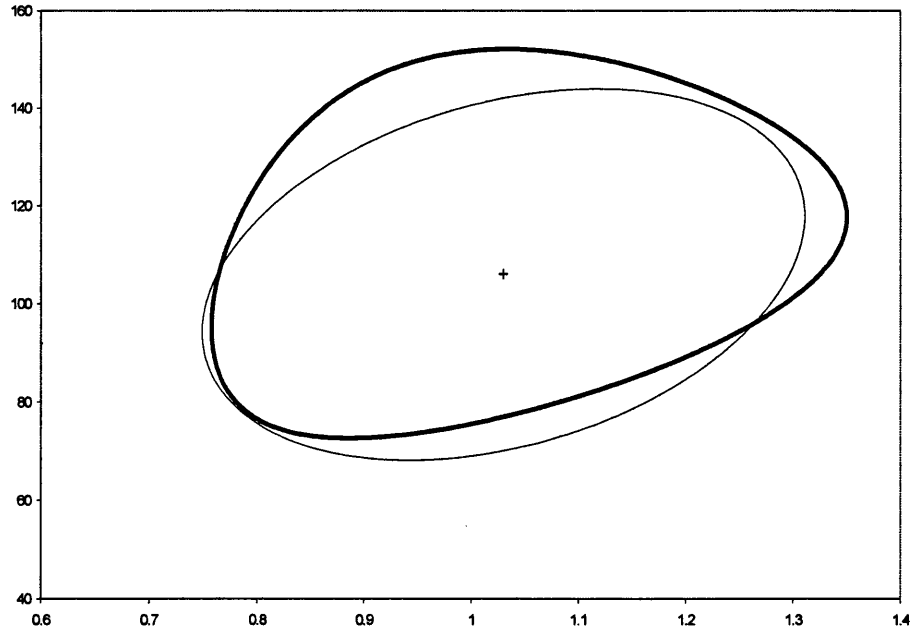

Figure 4.26: The MLE (+) together with 0.05 confidence regions based on asymptotic Normality and relative likelihood (bold line) for the 49 failures data from Epstein (1960), at $c = \infty$.

17.7245	26.8619	33.9372	40.0338	45.5588
50.7180	55.6346	60.3916	65.0497	69.6577
74.2572	78.8869	83.5849	88.3912	93.3502
98.5144	103.9482	109.7355	115.9900	122.8762
130.6478	139.7332	150.9559	166.2711	192.8568

Table 4.2: Idealised complete Weibull sample for $n = 25$

in section 3.3.1 We also point out that, due to their asymptotic equivalence, the difference between the two curves will disappear as $n \to \infty$.

The next section will investigate the use of relative likelihood contours in the general sampling distribution of $\left(\hat{\beta}_c, \hat{\theta}_c\right)$, with the usual combinations of varying n and c.

4.4 Expected Weibull Contours

So far we have used the relative likelihood function to obtain confidence regions based on a single set of example data. We now adapt the approach used to provide confidence regions for the sampling distribution of $\left(\hat{\beta}_c, \hat{\theta}_c\right)$. This involves identifying, for any (β, θ), sample size and censoring regime, an *idealised* sample, which can be produced via the corresponding order statistics as data values. We can then use the above algorithm with this idealised sample to calculate and plot the expected relative likelihood contours. For the Weibull distribution, David & Nagaraja (2003) gives the following formula for the expected order statistics

$$E\left[X_{i:n}\right] = \frac{n!}{(n-i)!\,(i-1)!}\theta \sum_{k=0}^{i-1} (-1)^{i-1-k} \binom{i-1}{k} \frac{\Gamma\left(\frac{1}{\beta}+1\right)}{(n-k)^{\frac{1}{\beta}+1}},$$

for $1 \leq i \leq n$. Using the Mathematica code below, we can produce these expected order statistics on which the idealised sample is based:

```
Ezip[n_,t_,b_,p_,i_]:=n!/(n-i)!(i-1)! *t^p*
                      Sum[(-1)^(i-1-k) Binomial[i-1,k]*Gamma[(p/b)+1]/(n-k)^((p/b)+1), {k,0,i-1}]
tEzip[n_,t_,b_,p_]:=Table[N[Ezip[n,t,b,p,i],10],{i,1,n}]
Block[{$MaxExtraPrecision=300000},tEzip[25,100,2,1]].
```

To illustrate, Table 4.2, shows the idealised sample for $\beta = 2$, $\theta = 100$, and $n = 25$.

We can then apply a censoring regime (as discussed in section 1.1) to produce our idealised sample under this regime. For example, the idealised sample in Table 4.2 with censoring time of $c = 100$, becomes that shown in Table 4.3.

17.7245	26.8619	33.9372	40.0338	45.5588
50.7180	55.6346	60.3916	65.0497	69.6577
74.2572	78.8869	83.5849	88.3912	93.3502
98.5144	100*	100*	100*	100*
100*	100*	100*	100*	100*

Table 4.3: Idealised Weibull sample for $n = 25$, censored at $c = 100$

We define

$$\hat{\beta}_e, \hat{\theta}_e$$

as the MLEs obtained from this idealised sample, and can produce the expected relative likelihood contours around $\left(\hat{\beta}_e, \hat{\theta}_e\right)$. We recall that bivariate Normality implies that the scatter plot of (β, θ) will be elliptical. However, investigations in Chapter 3 showed that this is not the case, particularly for small sample sizes or early censoring levels. We now evaluate the suitability of the relative likelihood contours as replacement confidence regions to the Normal theory intervals.

4.4.1 Small to moderate samples

For illustration, we assume $\rho = 0.05$, and show the contour maps for some ideal samples for various c and n; this yields the approximate 95% confidence regions for (β, θ). If we look specifically at data simulated from a Weibull distribution with $\beta = 2$ and $\theta = 100$, then we see for $n = 50$, we can superimpose the expected contour over the scatter plot of the 10,000 paired estimates $\left(\hat{\beta}_c, \hat{\theta}_c\right)$ obtained.

Figure 4.27 shows that the upward and rightward stretching strongly suggests non-Normality in $\left(\hat{\beta}_c, \hat{\theta}_c\right)$, which was confirmed in Chapter 3. Although Normality does not hold, the relative likelihood contour captures the shape of scatter plot very well.

We see in Figures 4.28 and 4.29 that the contours become more elliptical as c increases, while still maintaining to effectively portray the shape of the scatter plot. Intuitively, we can validate the measure of precision using the relative likelihood, by counting the number of MLEs included within each contour; this is considered below.

4.4.2 Large samples

Keeping $\beta = 2$ and $\theta = 100$, but changing the sample size to $n = 1000$, Figures 4.30, 4.31, and 4.32 show that, as expected, the shape of the relative likelihood contours mirrors the shape of the scatter plot, becoming more elliptical with increasing n and c.

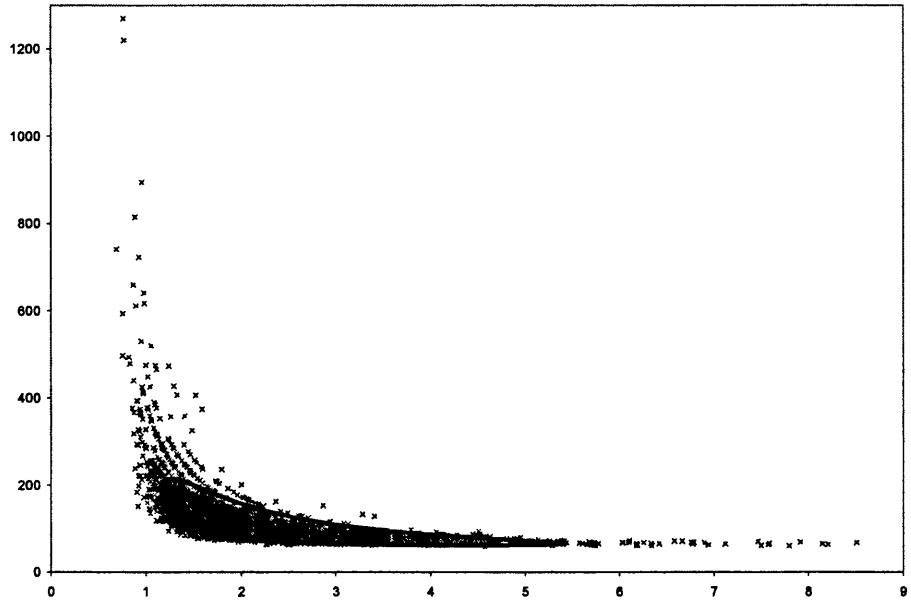

Figure 4.27: Relative likelihood contour superimposed over MLE scatterplot, for $\beta = 2$, $\theta = 100$, $n = 50$, $c = 50$; with $\left(\hat{\beta}_e, \hat{\theta}_e\right) = (2.24, 92.90)$.

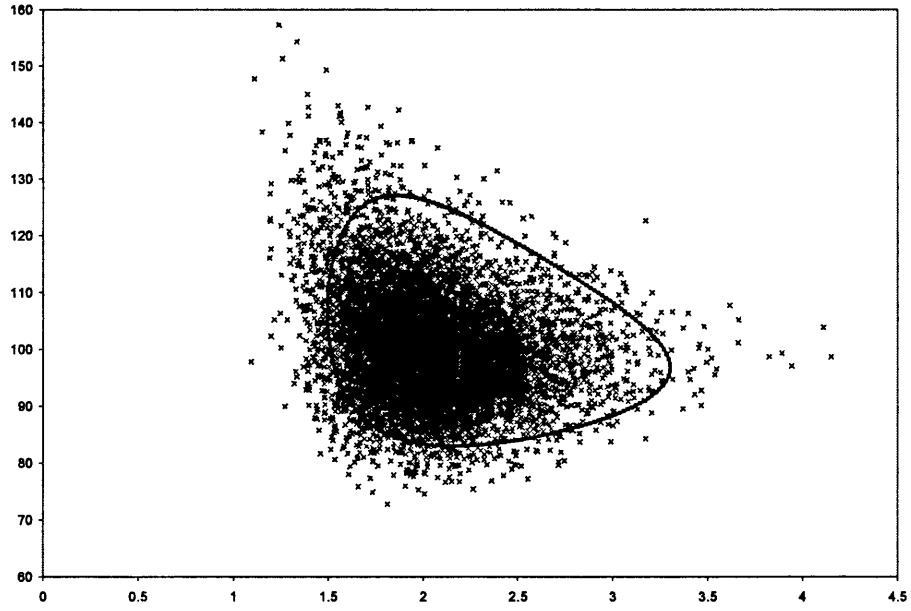

Figure 4.28: Relative likelihood contour superimposed over MLE scatterplot, for $\beta = 2$, $\theta = 100$, $n = 50$, $c = 100$; with $\left(\hat{\beta}_e, \hat{\theta}_e\right) = (2.11, 98.96)$.

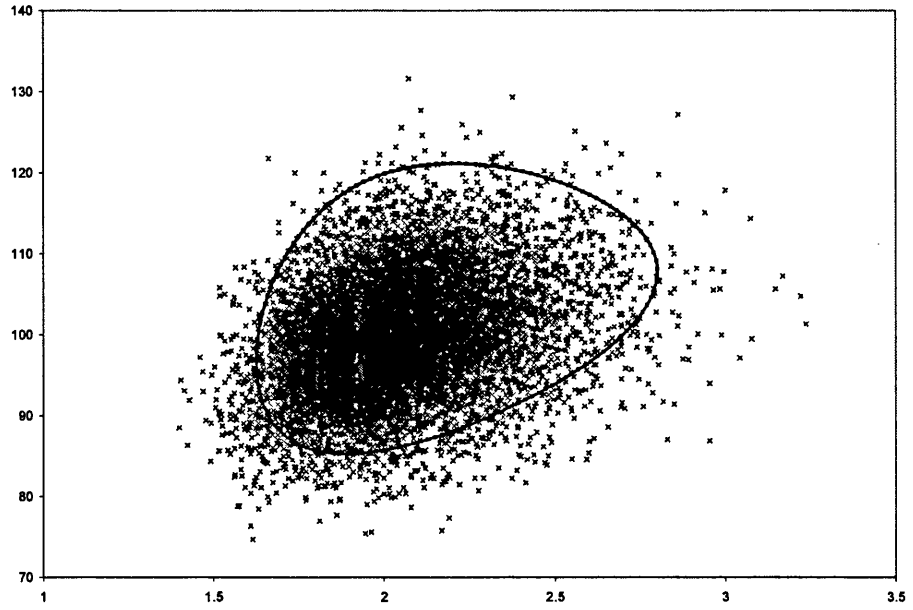

Figure 4.29: Relative likelihood contour superimposed over MLE scatterplot, for $\beta = 2$, $\theta = 100$, $n = 50$, $c = \infty$; with $\left(\hat{\beta}_e, \hat{\theta}_e\right) = (2.07, 200.18)$.

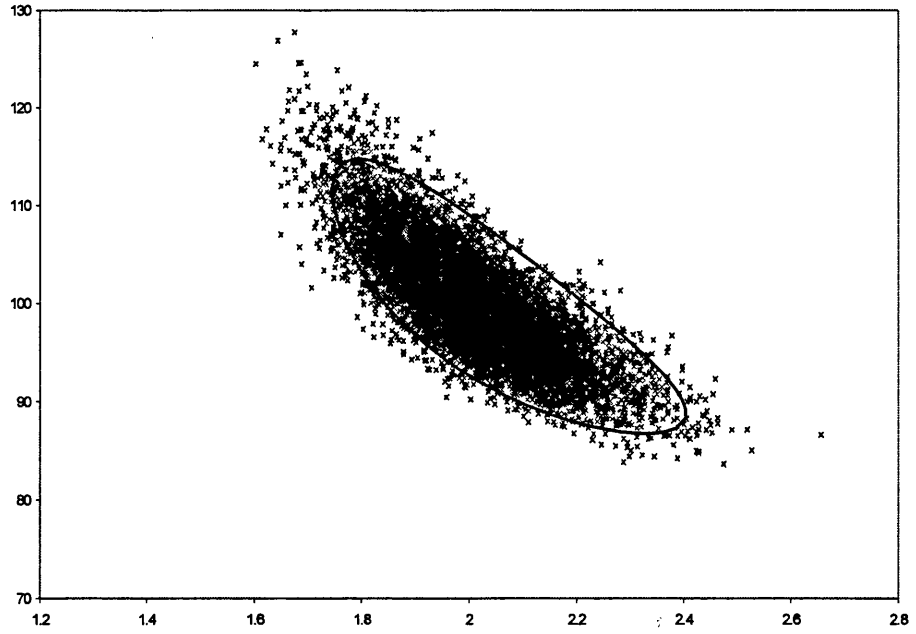

Figure 4.30: Relative likelihood contour superimposed over MLE scatterplot, for $\beta = 2$, $\theta = 100$, $n = 1000$, $c = 50$; with $\left(\hat{\beta}_e, \hat{\theta}_e\right) = (2.02, 99.48)$.

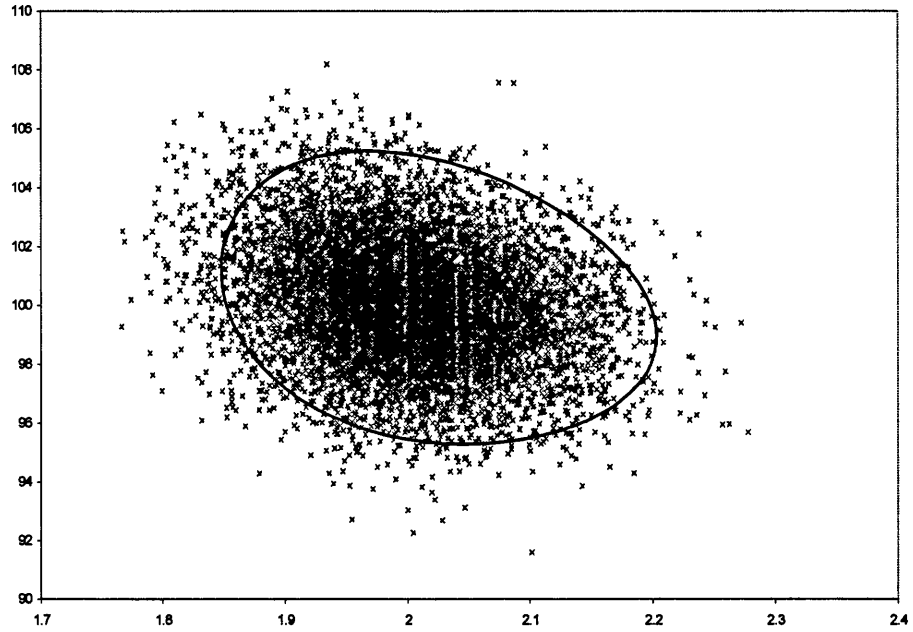

Figure 4.31: Relative likelihood contour superimposed over MLE scatterplot, for $\beta = 2$, $\theta = 100$, $n = 1000$, $c = 100$; with $\left(\hat{\beta}_e, \hat{\theta}_e\right) = (2.01, 99.98)$.

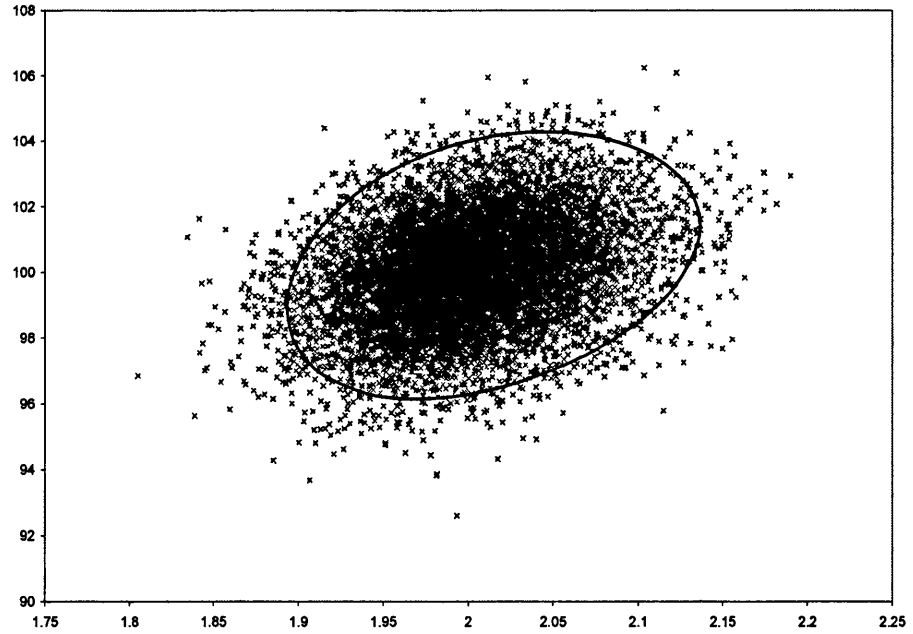

Figure 4.32: Relative likelihood contour superimposed over MLE scatterplot, for $\beta = 2$, $\theta = 100$, $n = 1000$, $c = \infty$; with $\left(\hat{\beta}_e, \hat{\theta}_e\right) = (2.01, 100.02)$.

c	n					
	25	50	100	300	500	1000
50	89.47	91.61	91.94	92.99	93.29	94.16
100	88.46	91.97	92.27	93.60	93.50	94.43
150	89.84	91.64	92.89	93.56	94.48	94.69
200	89.98	92.16	93.18	94.05	94.07	94.48
∞	88.93	91.91	92.79	94.03	94.32	94.34

Table 4.4: Percentage of $\left(\hat{\beta}_c, \hat{\theta}_c\right)$ covered by relative likelihood contour for simulated Weibull data with $(\beta, \theta) = (0.9, 100)$

4.5 Contour Validation

By definition, a simulated pair of MLEs, $\left(\hat{\beta}_c, \hat{\theta}_c\right)$, will be inside the relative likelihood contour if

$$R\left(\hat{\beta}_c, \hat{\theta}_c\right) = \frac{L\left(\hat{\beta}_c, \hat{\theta}_c\right)}{L\left(\hat{\beta}_e, \hat{\theta}_e\right)} < 0.05$$

or equivalently, if we take the natural logarithm

$$r\left(\hat{\beta}_c, \hat{\theta}_c\right) = \ln R\left(\hat{\beta}_c, \hat{\theta}_c\right) = l\left(\hat{\beta}_c, \hat{\theta}_c\right) - l\left(\hat{\beta}_e, \hat{\theta}_e\right) < \ln 0.05. \tag{4.8}$$

For various sample sizes and censoring levels, we can now simulate data values from a Weibull distribution, and obtaining the corresponding $r\left(\hat{\beta}_c, \hat{\theta}_c\right)$, (4.8), determine whether or not the expected relative likelihood contour contains the yielded $\left(\hat{\beta}_c, \hat{\theta}_c\right)$. We repeat this procedure 10,000 times, and anticipate that 95% of the simulated MLEs to be within the expected contour area. As usual, we are concerned with the effect of the shape parameter, and so in our simulation studies, fix $\theta = 100$, but vary β, including some values with $\beta < 1$ (a decreasing hazard function), $\beta = 1$ (constant hazard function), and $\beta > 1$ (increasing hazard function).

The results of each combination of β, n, and c replicated are shown in Tables 4.4, 4.5, 4.6, 4.7, and 4.8. The results compare favorably with expected values, and we see the agreement improves, approaching 95% as n and c increase. We also see that the results are reasonably consistent across the various values of the shape parameter considered here.

4.6 Summary

In this chapter we have proposed relative likelihood as an alternative method to asymptotic Normality to measure the precision of the Weibull MLEs. We have shown that in small samples, the relative likelihood and its contour plots best capture the behaviour of the Type I censored MLEs, where large sample Normal theory fails. We have also found that the relative likelihood results provide an accurate measure of precision, and on investigating the

c	n					
	25	50	100	300	500	1000
50	87.44	91.69	92.12	93.06	93.79	94.19
100	88.91	92.46	92.80	93.73	93.97	94.09
150	90.93	91.87	92.46	94.06	94.41	94.10
200	89.32	92.36	93.21	94.71	94.31	94.50
∞	89.33	91.95	93.16	94.21	94.47	94.45

Table 4.5: Percentage of $\left(\hat{\beta}_c, \hat{\theta}_c\right)$ covered by relative likelihood contour for simulated Weibull data with $(\beta, \theta) = (1, 100)$

c	n					
	25	50	100	300	500	1000
50	90.45	92.72	91.74	92.66	93.74	94.05
100	89.65	92.98	92.60	93.82	94.30	94.29
150	89.70	92.74	92.51	93.51	94.41	94.54
200	90.36	92.20	92.83	93.88	94.70	94.22
∞	89.59	92.33	93.00	93.91	94.50	94.33

Table 4.6: Percentage of $\left(\hat{\beta}_c, \hat{\theta}_c\right)$ covered by relative likelihood contour for simulated Weibull data with $(\beta, \theta) = (1.1, 100)$

c	n					
	25	50	100	300	500	1000
50	92.26	91.26	92.10	93.76	94.29	93.55
100	91.75	91.55	93.52	93.76	94.11	94.49
150	92.13	92.26	92.99	94.12	94.35	94.94
200	90.49	92.35	93.45	94.13	94.34	94.46
∞	91.39	92.43	93.38	94.28	94.24	94.55

Table 4.7: Percentage of $\left(\hat{\beta}_c, \hat{\theta}_c\right)$ covered by relative likelihood contour for simulated Weibull data with $(\beta, \theta) = (2, 100)$

c	n					
	25	50	100	300	500	1000
50	93.95	93.95	93.95	93.20	93.00	94.19
100	91.34	92.92	93.63	93.76	94.42	94.89
150	90.40	92.91	93.69	94.22	94.26	94.61
200	91.31	92.86	93.57	94.16	94.13	94.48
∞	91.31	92.86	93.57	94.16	94.13	94.49

Table 4.8: Percentage of $\left(\hat{\beta}_c, \hat{\theta}_c\right)$ covered by relative likelihood contour for simulated Weibull data with $(\beta, \theta) = (3.5, 100)$

expected Weibull contours in section 4.4, we see that the MLEs lying outside of the contour are fairly informally spread around the contour.

Despite there being more complicated computations involved in the relative likelihood approach to approximating confidence regions, with the use of the algorithm described, and the computational capabilities available today, we recommend the use of relative likelihood contours as an alternative measure of precision in small to moderate samples, where the asymptotic Normality assumption is implausible, as discussed in Chapter 3.

It is possible to repeat the process of finding and validating expected Weibull contours for the various ρ discussed earlier, such as 90%, or 99% confidence regions. There is also scope to extend this theory to other censoring regimes; for instance, Chua et al. (2007) outline the basic theory for ideal samples that have undergone Type II censoring.

Chapter 5

The Reliability Analyses of Censored Reliability Data

5.1 Introduction

In practice it may be possible to repeat the analysis described in Chapter 2 at each of a sequence $c_1, c_2, ...$ of times, until (at a sufficiently large value of c) all items have failed, and the data set is complete. In this chapter we will extend some results presented by Finselbach & Watkins (2006), which link the statistical analyses of reliability data arising from a sample of items at two or more points in time. For example, in the 49 failures data, we see in Table 2.6 that under Weibull analysis, the parameter MLEs at $c = 100$ are

$$\hat{\theta}_c = 122.4351, \ \hat{\beta}_c = 0.8709$$

but how useful is this in predicting the complete estimates

$$\hat{\theta} = 106.0505, \ \hat{\beta} = 1.0300$$

which are obtained if all items were left to fail? Intuitively, it is more informative to re-analyse the data at $c = 150$, when more items have failed, but it remains to quantify the increase in precision.

In practical terms, we are interested in gauging the earliest point c at which the experiment can be reasonably terminated while still yielding a close or reliable guide to the complete MLE, which in turn leads to a percentiles of item life. Or, we may be interested in studying the effects of an early censoring time, $c_1, c_2, ..., < c$, in comparison with censoring at c, as discussed in Peng & MacKenzie (2007).

For simplicity, we set $\beta = 1$, and consider the theory required for the negative exponential distribution, with pdf

$$1 - \exp\left(-\frac{x}{\theta}\right),$$

which follows immediately from (1.25), with $\beta = 1$.

5.2 Negative exponential distribution

We assume that the lifetimes of individual items follow the negative exponential distribution with mean θ, that a set of n items are put on test simultaneously, and that continual monitoring of these items is possible. Throughout this thesis, we require that there will be at least one failure, that is $M > 0$, and therefore, the discussion is conditional on this. The likelihood method for this distribution is well documented, for example Kalbfleisch (1979), and we can obtain estimates at consecutive censoring times, and then a final complete analysis when all items have failed.

5.2.1 Likelihood Theory

We stop the experiment at c, and have a random number M failures and $n - M$ values censored to time c. In notation previously introduced, we have

$$S_{M,0} = \sum_{i=1}^{M} X_i$$

and, from our discussion of the Weibull distribution in Chapter 2, with $\beta = 1$, we obtain the likelihood

$$L_c = \theta^{-M} \exp\left\{-\theta^{-1}\left[S_{M,0} + (n-M)c\right]\right\}.$$

On taking logarithms, we obtain

$$l_c = -M \ln\theta - \theta^{-1}\left[S_{M,0} + (n-M)c\right],$$

and

$$\frac{dl_c}{d\theta} = -\frac{M}{\theta} + \frac{1}{\theta^2}\left[S_{M,0} + (n-M)c\right], \tag{5.1}$$

as the log-likelihood and the score function respectively. Equating (5.1) to zero, it is now straightforward to obtain the MLE

$$\hat{\theta}_c = M^{-1}\left[S_{M,0} + (n-M)c\right].$$

We note here that (5.1) can now be written as

$$\frac{dl_c}{d\theta} = -\frac{M}{\theta} + \frac{1}{\theta^2}\left[M\hat{\theta}_c\right] = \frac{M}{\theta^2}\left[\hat{\theta}_c - \theta\right]. \tag{5.2}$$

We now introduce some examples of negative exponential data, and obtain the MLE of θ at various censoring levels, c. We will return to these examples throughout the chapter, in order to illustrate our theoretical work.

c	M	$\hat{\theta}_c$
25	12	88.0333
75	23	114.9696
125	30	124.4600
175	39	114.0667
225	44	108.6773
275	46	107.9217
325	47	108.3723
∞	49	104.8898

Table 5.1: $\hat{\theta}_c$ for various c for the $n = 49$ failure times, used in Epstein (1960)

4	5	8	11	20
29	35	40	66	70

Table 5.2: The failure times of 10 electronic components assumed to follow the negative exponential distribution, taken from Kalbfleisch (1979)

Example: 49 failures data

We return to the 49 failure times example, shown in Table 2.2. Using the above analysis, we can find $\hat{\theta}_c$ successively until all items fail when we find the complete estimate. These are shown in Table 5.1, and we see that the estimate appears to level off at $c = 225$. We need to know whether much more information about the complete estimate is gained by continuing the experiment after this time.

Example: Electronic components

A second example of data following the negative exponential distribution is the lifetimes of 10 electronic components, used by Kalbfleisch (1979). The data is given in Table 5.2.

We can find the MLE for the complete data set, and those for censoring times of $c = 15, 30$ and 45. These are shown in Table 5.3. With such a small sample, it is logical to ask whether any censoring will enable a good approximation to the complete estimate?

c	M	$\hat{\theta}_c$
14	4	28
28	5	37.6
42	8	29.5
56	8	33
∞	10	28.8

Table 5.3: $\hat{\theta}_c$ for various c for the $n = 10$ electrical component failure times

0.75	1.7	20.8	28.5	54.9
126	175	236	274	290
363	458	776	828	871
970	1278	1311	1661	1787

Table 5.4: 20 lifetimes of pressure vessels assumed to follow the negative exponential distribution, Ansell & Phillips (1994).

c	M	$\hat{\theta}_c$
100	5	321.3300
500	12	502.3875
1000	16	592.1031
1500	18	614.5917
∞	20	575.5325

Table 5.5: $\hat{\theta}_c$ for various c for the $n = 20$ presure vessels failure times

Example: Pressure vessels

Another example of negative exponential data we will use is the $n = 20$ times to failure (in hours) for pressure vessels, as discussed in Ansell & Phillips (1994). The data is reproduced in Table 5.4 and we look at the MLE calculated for the complete data set, and for the censored times of $c = 100, 500, 1000$ and 1500. The estimates obtained, including for the complete sample, are shown in Table 5.5. It is now unclear whether censoring at $c = 1000$ would in fact give a better guide to the complete estimate than censoring at $c = 1500$.

From each example discussed above, it is clear that we need to consider the relationship between the estimate $\hat{\theta}_c$, obtained at time c, and $\hat{\theta}$, obtained when all items have failed. The next sections show how we can use properties of $\hat{\theta}_c$ and the asymptotic relationships involved in the likelihood theory to gain a theoretical result for $Corr\left(\hat{\theta}, \hat{\theta}_c\right)$.

5.3 Link between $\hat{\theta}$ and $\hat{\theta}_c$

The discussion in chapter 2, noted that M is binomial with parameters n, q_c, where q_c is now simplified, with $\beta = 1$, to

$$q_c = 1 - \exp\left(-\frac{c}{\theta}\right).$$

Throughout, we denote the moments of M as follows

$$\begin{aligned} m_1 &= E[M] = nq_c \\ m_2 &= E[M^2] = nq_c^2 r_c + n^2 q_c^2 \end{aligned} \tag{5.3}$$

where we have defined r_c, (2.38), as the odds ratio of survival beyond c, to failure before c, in (2.38). This leads to the variance

$$Var(M) = nq_c^2 r_c.$$

5.3.1 Expectations involving failed items

Chapter 2 required expectations of a transformed variable Z, see (2.26); we know that X is equivalent to the Weibull distribution when $\beta = 1$, and therefore, we can express negative exponentially distributed lifetimes as

$$X = \theta Z.$$

It is now straightforward to obtain moments of the right truncated random variable X_f, with pdf

$$\frac{\exp\left(-\frac{x}{\theta}\right)}{\theta q_c},$$

for $0 \leq y \leq c$. Thus, for lifetimes of items failed before c, from (2.40), it follows that

$$E[X_f] = \theta(1 - z_c r_c)$$

where, for $\beta = 1$,

$$z_c = \frac{c}{\theta}.$$

Thus,

$$E[X_f] = \theta - cr_c.$$

Similarly we will need the second moment of the right truncated distribution, and, from (2.41) we can write this as

$$\begin{aligned} E[X_f^2] &= \theta^2(2 - 2z_c r_c - z_c^2 r_c) \\ &= 2\theta^2 - 2\theta c r_c - c^2 r_c. \end{aligned}$$

We note that as $c \to \infty$, and therefore $q_c \to 1$, the above expectations reach their complete counterparts $E[X] = \theta$ and $E[X^2] = 2\theta^2$.

5.3.2 Properties of $\hat{\theta}_c$

We can now proceed as the complete case, and obtain expressions for the expectations that will be needed for the analysis. Firstly, we note that, from the conditionality argument described in (2.39), that

$$E[S_{M,0}] = E[M]E[X_f] = nq_c E[X_f],$$

hence, we can show

$$\begin{aligned} E\left[\hat{\theta}_c\right] &= E\left[M^{-1}\left\{S_{M,0}+(n-M)c\right\}\right] \\ &= E\left[X_f\right]+E\left[M^{-1}(n-M)c\right] \\ &= E\left[X_f\right]+E\left[\frac{nc}{M}\right]-E\left[\frac{Mc}{M}\right] \\ &= (\theta-cr_c)+\frac{c}{q_c}-c \\ &= \theta-cr_c+cr_c \\ &= \theta. \end{aligned}$$

From (5.1), the expectation of the score is

$$\begin{aligned} E\left[\frac{dl_c}{d\theta}\right] &= E\left[-\frac{M}{\theta}+\frac{1}{\theta^2}\left[S_{M,0}+(n-M)c\right]\right] \\ &= -\frac{nq_c}{\theta}+\frac{1}{\theta^2}\left[nq_c\left(\theta-cr_c\right)+n\left(1-q_c\right)c\right] \\ &= -\frac{nq_c}{\theta}+\frac{nq_c}{\theta}+\frac{1}{\theta^2}\left[-nq_cr_cc+nq_cr_cc\right] \\ &= 0. \end{aligned} \tag{5.4}$$

We also know the asymptotic result between $Var\left(\hat{\theta}_c\right)$ and the expected Fisher information, given below, holds

$$Var(\hat{\theta}_c) \simeq -E\left[\frac{d^2l_c}{d\theta^2}\right]^{-1},$$

as specified in Lawless (1982). This is the Cramer-Rao lower bound of the variance of the maximum likelihood estimator. We can now use this approximation to find $Var(\hat{\theta})$. Following from (5.2), we have

$$\frac{d^2l_c}{d\theta^2}=\frac{M}{\theta^2}-\frac{2M\hat{\theta}_c}{\theta^3}$$

and so

$$\begin{aligned} -E\left[\frac{d^2l_c}{d\theta^2}\right] &= -E\left[\frac{M}{\theta^2}-\frac{2M\hat{\theta}_c}{\theta^3}\right] \\ &= -\frac{E\left[M\right]}{\theta^2}+\frac{2E\left[M\widehat{\theta}_c\right]}{\theta^3} \\ &= -\frac{nq_c}{\theta^2}+\frac{2nq_c\theta}{\theta^3} \\ &= -\frac{nq_c}{\theta^2}+\frac{2nq_c}{\theta^2} \\ &= \frac{nq_c}{\theta^2}. \end{aligned}$$

Therefore

$$Var(\hat{\theta}_c) \simeq -E\left[\frac{d^2 l_c}{d\theta^2}\right]^{-1} = \frac{\theta^2}{nq_c}. \tag{5.5}$$

5.3.3 Asymptotic results

From the above properties, it is possible to consider the usual asymptotic relationship between the MLE, the expected Fisher information and the score function, and from

$$\frac{dl_c}{d\theta} \simeq \frac{nq_c}{\theta^2}\left(\hat{\theta}_c - \theta\right),$$

we may write,

$$\sqrt{\frac{nq_c}{\theta^2}}\left(\hat{\theta}_c - \theta\right) \simeq \sqrt{\frac{\theta^2}{nq_c}}\left\{-\frac{M}{\theta} + \frac{1}{\theta^2}\left[S_{M,0} + (n-M)c\right]\right\}.$$

Since this relationship also covers the case $c \to \infty$ (when it becomes exact), we can now approximate

$$Corr\left(\hat{\theta}, \hat{\theta}_c\right) = Corr\left(\sqrt{\frac{nq_c}{\theta^2}}\left(\hat{\theta}_c - \theta\right), \sqrt{\frac{n}{\theta^2}}\left(\hat{\theta} - \theta\right)\right)$$

by

$$\begin{aligned} & Corr\left(\sqrt{\frac{\theta^2}{n}}\left\{-\frac{n}{\theta} + \frac{1}{\theta^2}S_0\right\}, \sqrt{\frac{\theta^2}{nq_c}}\left\{-\frac{M}{\theta} + \frac{1}{\theta^2}\left[S_{M,0} + (n-M)c\right]\right\}\right) \\ = & \frac{\theta^2}{n\sqrt{q_c}} Corr\left(\left\{-\frac{n}{\theta} + \frac{1}{\theta^2}S_0\right\}, \left\{-\frac{M}{\theta} + \frac{1}{\theta^2}\left[S_{M,0} + (n-M)c\right]\right\}\right), \end{aligned}$$

where

$$S_0 = \sum_{i=1}^{n} X_i$$

as defined in (2.3).

We can now use regularity conditions to write this correlation in terms of expectations, and hence obtain

$$\begin{aligned} & \frac{\theta^2}{n\sqrt{q_c}} E\left[\left\{-\frac{M}{\theta} + \frac{1}{\theta^2}\left[S_{M,0} + (n-M)c\right]\right\} \times \left\{-\frac{n}{\theta} + \frac{1}{\theta^2}S_0\right\}\right] \\ = & \frac{\theta^2}{n\sqrt{q_c}} E\left[\begin{array}{c} \frac{nM}{\theta^2} - \frac{M}{\theta^3}S_0 - \frac{n}{\theta^3}\left[S_{M,0} + (n-M)\,c\right] \\ + \frac{1}{\theta^4}S_0 S_{M,0} + \frac{(n-M)c}{\theta^4}S_0 \end{array}\right], \end{aligned} \tag{5.6}$$

as our approximation to $Corr\left(\hat{\theta}, \hat{\theta}_c\right)$.

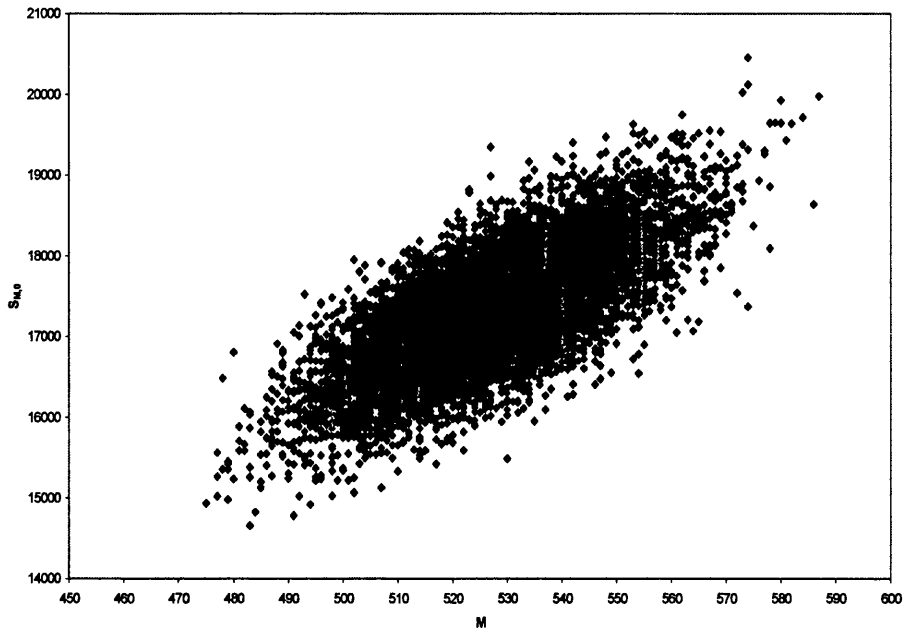

Figure 5.1: Scatter plot of M versus $S_{M,0}$ for simulated data with $\theta = 100$, $c = 75$, $n = 1000$, and 10,000 replications.

5.3.4 Some statistical considerations

Terms in the expectation (5.6) involving S_0 will be complicated, due to the inter-relationship between

$$M,\ S_{M,0},\ \text{and}\ S_0.$$

Figure 5.1 shows, using simulated data with $\theta = 100$, $c = 75$, and $n = 1000$, that there is strong positive correlation between M and $S_{M,0}$- intuitively, large M leads to large $S_{M,0}$, as the more items that fail, the more lifetimes there are to sum in $S_{M,0}$. Figure 5.2 shows strong negative correlation between M and S_0. Large M will lead to small S_0, as more items failing before $c = 75$ indicates that more early failures are occurring, and therefore the lifetimes contributing to S_0 are small in general. For the same reason, Figure 5.3 shows moderate negative correlation between S_0 and $S_{M,0}$.

So, some expectations needed in (5.6) require some care, but can be obtained using

$$S_0 = S_{M,0} + \sum_{i=M+1}^{n} X_i$$

in which the lifetimes $X_{M+1}, ..., X_n$ of the survivors censored at c follow the left truncated

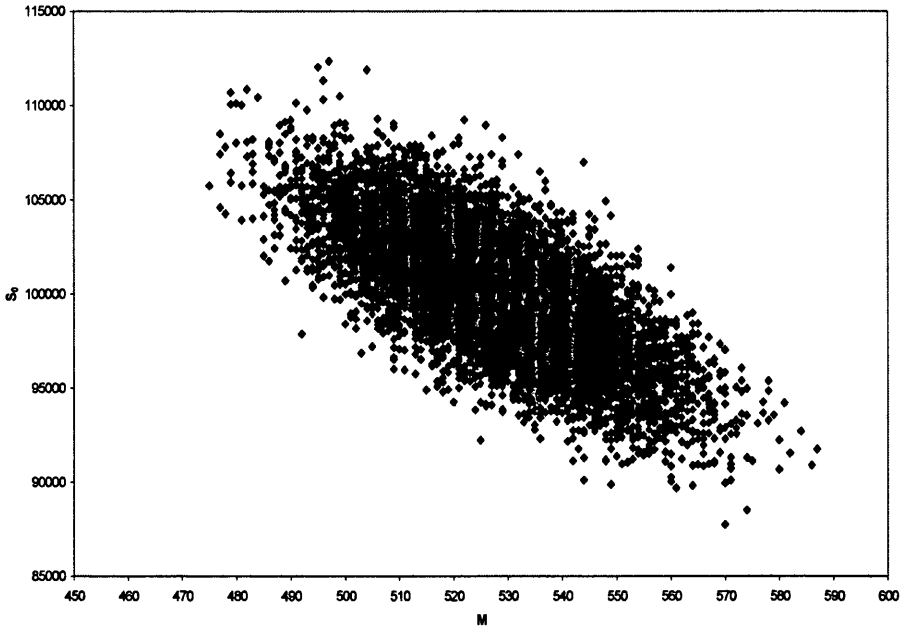

Figure 5.2: Scatter plot of M versus S_0 for simulated data with $\theta = 100$, $c = 75$, $n = 1000$, and $10,000$ replications.

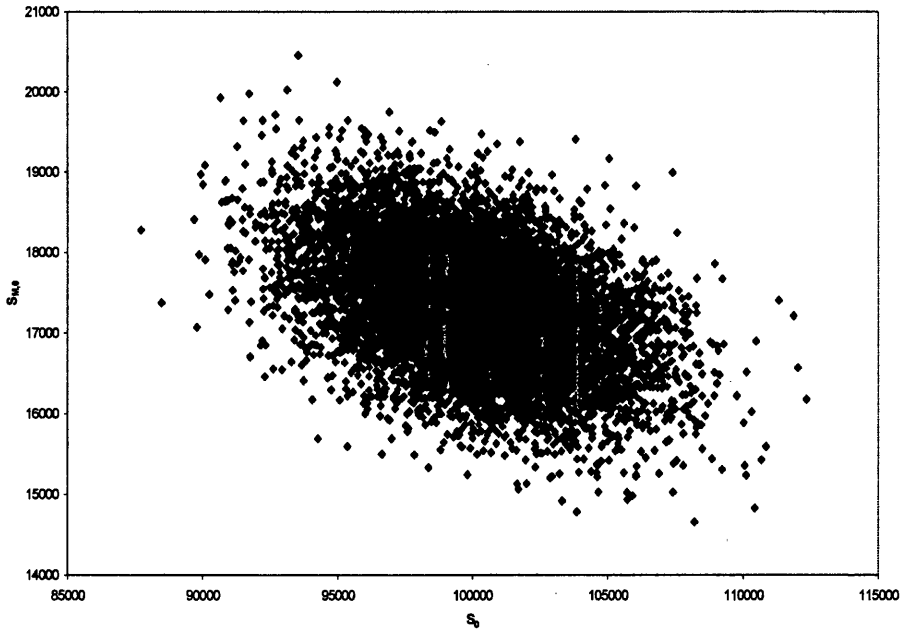

Figure 5.3: Scatter plot of S_0 versus $S_{M,0}$ for simulated data with $\theta = 100$, $c = 75$, $n = 1000$, and $10,000$ replications.

negative exponential distribution , with pdf

$$\frac{\exp\left(-\frac{(x+c)}{\theta}\right)}{\theta}.$$

The mean lifetimes of these surviving items can be found using the fact that $E[X] = \theta$ for the complete sample, and this must reflect both censored and surviving items. We have

$$q_c E[X_f] + (1 - q_c) E[X_c] = \theta,$$

where X_c is the left truncated random variable (lifetime of surviving items), and, from which we find the mean lifetime of the survivors,

$$\begin{aligned} E[X_c] &= \frac{\theta - q_c E[X_f]}{(1 - q_c)} \\ &= \frac{\theta - q_c(\theta - cr_c)}{(1 - q_c)} \\ &= \frac{\theta(1 - q_c)}{(1 - q_c)} + \frac{cq_c r_c}{(1 - q_c)} \\ &= \theta + c. \end{aligned} \tag{5.7}$$

5.3.5 Expectations required

Looking at the terms of the expectation (5.6) individually gives us

$$E\left[\frac{nM}{\theta^2}\right] = \frac{n^2 q_c}{\theta^2},$$

which cancels with

$$\begin{aligned} E\left[-\frac{n}{\theta^3}\{S_{M,0} + (n - M)c\}\right] &= -\frac{n}{\theta^3}\{m_1 E[X_f] + (n - m_1)c\} \\ &= -\frac{n}{\theta^3}\{nq_c(\theta - cr_c) + nq_c r_c c\} \\ &= -\frac{n}{\theta^3}\{nq_c\theta\} \\ &= -\frac{n^2 q_c}{\theta^2}. \end{aligned}$$

We are then left with

$$\begin{aligned} E\left[-\frac{M}{\theta^3}S_0\right] &= -\frac{1}{\theta^3}E[MS_0] \\ &= -\frac{1}{\theta^3}E\left[M\left(S_{M,0} + \sum_{i=M+1}^{n} X_i\right)\right] \\ &= -\frac{1}{\theta^3}\{m_2 E[X_f] + E[M(n - M)]E[X_c]\}. \end{aligned}$$

This can be simplified to

$$E\left[-\frac{M}{\theta^3}S_0\right] = -\frac{1}{\theta^3}\left\{\begin{array}{c}\left(nq_c^2r_c+n^2q_c^2\right)(\theta-cr_c)\\+\left(n^2q_c^2r_c-nq_c^2r_c\right)(c+\theta)\end{array}\right\} \quad (5.8)$$

$$= -\frac{1}{\theta^3}\left\{n^2q_c\theta-nq_cr_cc\right\}$$

$$= \frac{nq_cr_cc}{\theta^3}-\frac{n^2q_c}{\theta^2}.$$

We also have to simplify

$$E\left[\frac{1}{\theta^4}S_0S_{M,0}\right] = \frac{1}{\theta^4}E\left[S_{M,0}\left(S_{M,0}+\sum_{i=M+1}^{n}X_i\right)\right]$$

$$= \frac{1}{\theta^4}\left\{\begin{array}{c}m_1E\left[X_f^2\right]+E\left[M\left(M-1\right)\right]E\left[X_f\right]^2\\+E\left[M\left(n-M\right)\right]E\left[X_f\right]E\left[X_c\right]\end{array}\right\}.$$

This becomes

$$E\left[\frac{1}{\theta^4}S_0S_{M,0}\right] = \frac{1}{\theta^4}\times$$

$$\left\{\begin{array}{c}nq_c\left(2\theta^2-2\theta cr_c-c^2r_c\right)+\left(n^2q_c^2-nq_c^2\right)\left(\theta^2-2\theta cr_c+c^2r_c^2\right)+\\\left(n^2q_c^2r_c-nq_c^2r_c\right)\left(\theta^2+\theta c-\theta cr_c-c^2r_c\right)\end{array}\right\}$$

$$= \frac{1}{\theta^4}\left\{nq_c\theta^2-nq_cr_c\theta c-nq_cr_cc^2+n^2q_c\theta^2-n^2q_cr_c\theta c\right\}$$

$$= \frac{nq_c}{\theta^2}-\frac{nq_cr_cc}{\theta^3}-\frac{nq_cr_cc^2}{\theta^4}+\frac{n^2q_c}{\theta^2}-\frac{n^2q_cr_cc}{\theta^3}.$$

Finally we are left to simplify the remaining expectation

$$E\left[\frac{\left(n-M\right)c}{\theta^4}S_0\right] = \frac{c}{\theta^4}\left\{E\left[nS_0\right]-E\left[MS_0\right]\right\}$$

which from (5.8) can be written as

$$E\left[\frac{\left(n-M\right)c}{\theta^4}S_0\right] = \frac{c}{\theta^4}\left\{n^2\theta-\left(n^2q_c\theta-nq_cr_cc\right)\right\}$$

$$= \frac{c}{\theta^4}\left\{n^2q_cr_c\theta+nq_cr_cc\right\}$$

$$= \frac{n^2q_cr_cc}{\theta^3}+\frac{nq_cr_cc^2}{\theta^4}.$$

c	n					$\sqrt{q_c}$
	50	100	300	500	1000	
25	0.4027	0.4696	0.4734	0.4687	0.4769	0.4703
50	0.5966	0.6201	0.6305	0.6241	0.6325	0.6273
100	0.7784	0.7906	0.7931	0.7946	0.8016	0.7951
150	0.8714	0.8758	0.8808	0.8789	0.8849	0.8814
200	0.9238	0.9252	0.9312	0.9277	0.9320	0.9299
250	0.9537	0.9555	0.9582	0.9572	0.9592	0.9581
300	0.9724	0.9732	0.9747	0.9740	0.9757	0.9748

Table 5.6: $Corr\left(\hat{\theta}, \hat{\theta}_c\right)$ for negative exponential data generated with $\theta = 100$ and various c. Figures are based on 10,000 replications

It is clear that most of these terms in the expectation will cancel, as shown below

$$\begin{aligned} & \frac{nq_cr_cc}{\theta^3} - \frac{n^2q_c}{\theta^2} + \frac{nq_c}{\theta^2} - \frac{nq_cr_cc}{\theta^3} - \frac{nq_cr_cc^2}{\theta^4} + \frac{n^2q_c}{\theta^2} \\ & -\frac{n^2q_cr_cc}{\theta^3} + \frac{n^2q_cr_cc}{\theta^3} + \frac{nq_cr_cc^2}{\theta^4} \\ = & \frac{nq_c}{\theta^2}. \end{aligned}$$

On substituting this into (5.6), we obtain the approximate correlation of

$$\begin{aligned} Corr\left(\hat{\theta}, \hat{\theta}_c\right) &= \frac{\theta^2}{n\sqrt{q_c}}\left\{\frac{nq_c}{\theta^2}\right\} \\ &= \frac{q_c}{\sqrt{q_c}} \\ &= \sqrt{q_c}. \end{aligned} \tag{5.9}$$

This approximate correlation does not depend on n, and therefore holds across all sample sizes.

Checks for finite samples

Since the approximation (5.9) is asymptotically derived, we need to assess its agreement for finite samples. We do this for fixed $\theta = 100$, at a range of censoring times, $c = 25, 50, 100, 150, 200, 250$, and 300. Results of our simulation tests are given in Table 5.6; as always, our statistical summaries are based on 10,000 replications. We see that agreement between simulated correlations and the theoretical result improves as the sample size, n, and censoring level, c, increases.

5.3.6 Covariance properties

One consequence of (5.9) is that the covariance of the complete and censored MLE is equal to the variance of the complete MLE, that is,

$$Cov\left(\hat{\theta},\hat{\theta}_c\right) = Var\left(\hat{\theta}\right). \tag{5.10}$$

We will algebraically show that this is true, and, in the next chapter, prove that this result generalises to the Weibull distribution. From (5.9) we have

$$Cov\left(\hat{\theta},\hat{\theta}_c\right) = \sqrt{q_c}\sqrt{Var\left(\hat{\theta}\right)}\sqrt{Var\left(\hat{\theta}_c\right)}$$

and from (5.5), this can be expressed as

$$\begin{aligned} Cov\left(\hat{\theta},\hat{\theta}_c\right) &= \sqrt{q_c}\sqrt{\frac{\theta^2}{n}}\sqrt{\frac{\theta^2}{nq_c}} \\ &= \frac{\theta^2}{n} \\ &= Var\left(\hat{\theta}\right). \end{aligned} \tag{5.11}$$

Hence the covariance does not depend on the censoring MLE (and therefore the censoring level) at all. This result can be used to simplify expressions in the following section, where we discuss the use of $\hat{\theta}_c$ as an estimate of $\hat{\theta}$, and therefore θ.

5.4 What can $\hat{\theta}_c$ tell us about $\hat{\theta}$?

While most literature concerning MLE theory constructs confidence intervals as a measure of the precision of the estimate compared to the true parameter value, here, we are more interested in gauging the precision in $\hat{\theta}_c$ as an estimate of $\hat{\theta}$, and hence of θ. In other words, we want to know how reliable the censored MLE is as a guide to the complete MLE, since this will influence any decision on the worth of continuing the experiment.

We use

$$\Delta = \hat{\theta} - \hat{\theta}_c$$

and now assume that the MLEs follow the Normal distribution, and that we are dealing with unbiased estimators. Although Chapter 3 shows that Normality is not achieved in small to moderate samples of MLEs, we recall that asymptotic assumptions used for theoretical variance and EFI gave good approximations to simulation results in finite samples; see Tables 2.14 and 2.15.

We then have

$$E\left[\Delta\right] = E\left[\hat{\theta}\right] - E\left[\hat{\theta}_c\right] \simeq \theta - \theta \simeq 0$$

and

$$Var(\Delta) = Var\left(\hat{\theta} - \hat{\theta}_c\right) = Var\left(\hat{\theta}\right) + Var\left(\hat{\theta}_c\right) - 2Cov(\hat{\theta}, \hat{\theta}_c),$$

and from (5.11), we can write this as

$$\begin{aligned} Var(\Delta) &= Var\left(\hat{\theta}_c\right) - Var\left(\hat{\theta}\right) \\ &= \frac{\theta^2}{nq_c} - \frac{\theta^2}{n} \\ &= \frac{\theta^2}{n}\left(\frac{1}{q_c} - 1\right) \\ &= \frac{\theta^2 r_c}{n} \end{aligned}$$

Therefore, the asymptotic distribution of Δ is

$$N\left(0, \frac{\theta^2 r_c}{n}\right),$$

and from this, we have

$$\Pr\left\{-1.96 < \frac{\Delta}{\sqrt{\frac{\theta^2 r_c}{n}}} < 1.96\right\} = 0.95,$$

which yields the 95% confidence interval for $\hat{\theta}$, based on $\hat{\theta}_c$, as

$$\hat{\theta} = \hat{\theta}_c \pm 1.96\theta\sqrt{\frac{r_c}{n}}.$$

In practice, at censoring time c, we would estimate the true value of θ by the MLE $\hat{\theta}_c$, so we would have

$$\hat{\theta} = \hat{\theta}_c \pm 1.96\hat{\theta}_c\sqrt{\frac{\hat{r}_c}{n}}, \tag{5.12}$$

where

$$\hat{r}_c = \frac{1 - \hat{q}_c}{\hat{q}_c}$$

and

$$\hat{q}_c = \exp\left(-\frac{c}{\hat{\theta}_c}\right).$$

5.4.1 Lessons for experimental design

It is clear that the structure of the variance, and therefore the width of the interval obtained in (5.12) depends on the rate at which

$$\frac{r_c}{n} \to 0,$$

c	M	$\hat{\theta}_c$	95% CI for $\hat{\theta}$
25	12	88.0333	(45.0207, 131.0460)
75	23	114.9696	(81.4084, 148.5308)
125	30	124.4600	(97.9657, 150.9543)
175	39	114.0667	(97.3207, 130.8127)
225	44	108.6773	(97.1160, 120.2385)
275	46	107.9217	(99.1187, 116.7248)
325	47	108.3723	(101.4226, 115.3221)
375	49	104.8898	

Table 5.7: Confidence limits of $\hat{\theta}$ at each successive censoring level, c for the 49 failure times data

c	M	$\hat{\theta}_c$	95% CI for $\hat{\theta}$
14	4	28	(6.4531, 49.5469)
28	5	37.6	(15.4379, 59.7621)
42	8	29.5	(19.2022, 39.7978)
56	8	33	(23.3121, 42.6879)
∞	10	28.8	

Table 5.8: Confidence limits of $\hat{\theta}$ at each successive censoring level, c for the electrical component data

and so the width of the confidence interval can be established during the design process of an experiment. A smaller interval, and therefore a more precise estimate to the complete MLE will be obtained if the number of items tested, n, increases, or if the number of items allowed to fail increases, by extending the censoring time, c. Either option to tighten the confidence interval will add expense to the experiment, and so the importance of the precision in the interval must be weighed up against the costs involved. We will now test this using published examples of negative exponential distributed data.

Example: 49 failure times

Using (5.12) we can then find the confidence limits corresponding to each censoring level. These are shown in Table 5.7 and displayed in Figure 5.4. There is a clear improvement in the precision of the estimate as c increases, but even at late censoring, $c = 225$, when almost 90% of items have failed, we have a large interval, approximately ± 12 around θ_c, and, if possible, it is now better to wait until the last failure occurs.

Example: Electronic components

Table 5.8 shows the MLEs obtained at each censoring level, and also the confidence interval found via 5.12. Figure 5.5 shows these limits. Again, from a practical perspective, it appears that the intervals obtained may be too large to have any certainty regarding the final estimates, and the best option is to wait until all items have failed.

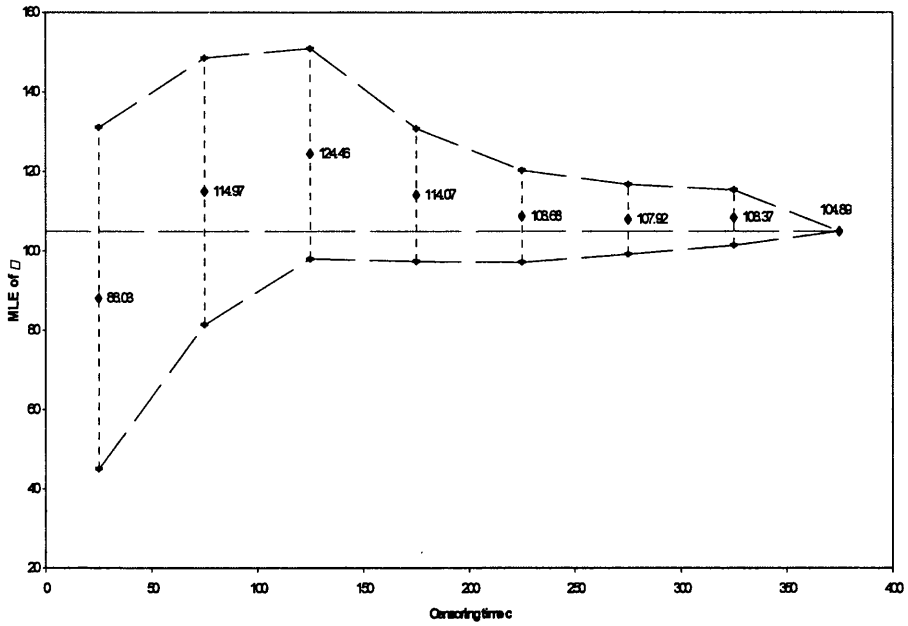

Figure 5.4: 95% confidence interval for $\hat{\theta}$ at successive censoring levels for the 49 failure times data.

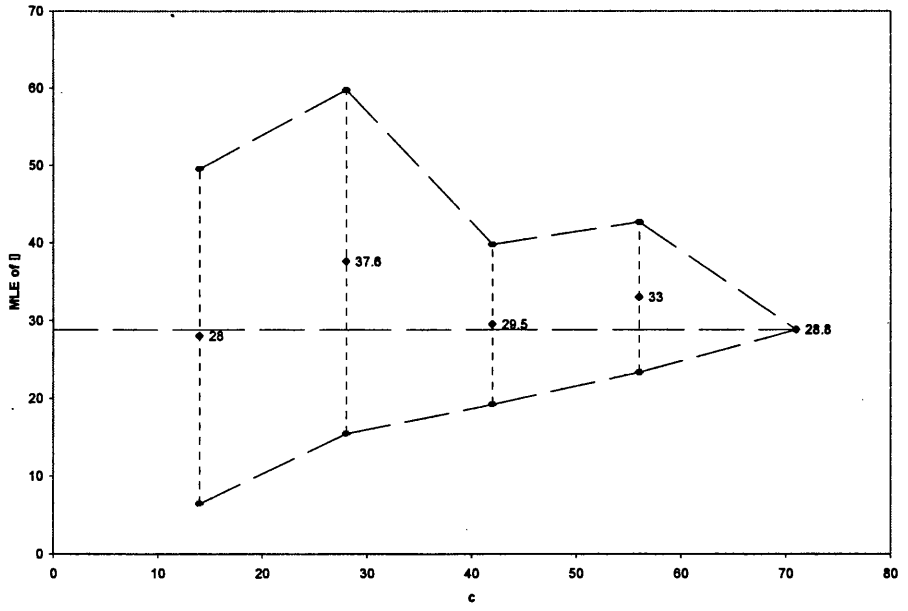

Figure 5.5: 95% confidence interval of $\hat{\theta}$ at successive censoring levels for the electronic components data.

c	M	$\hat{\theta}_c$	95% CI for $\hat{\theta}$
100	5	321.3300	(88.2508, 554.4092)
500	12	502.3875	(333.7837, 670.9913)
1000	16	592.1031	(468.5803, 715.6259)
1500	18	614.5917	(531.3889, 697.7945)
∞	20	575.5325	

Table 5.9: Confidence limits of $\hat{\theta}$ at each successive censoring level, c for the pressure vessels data

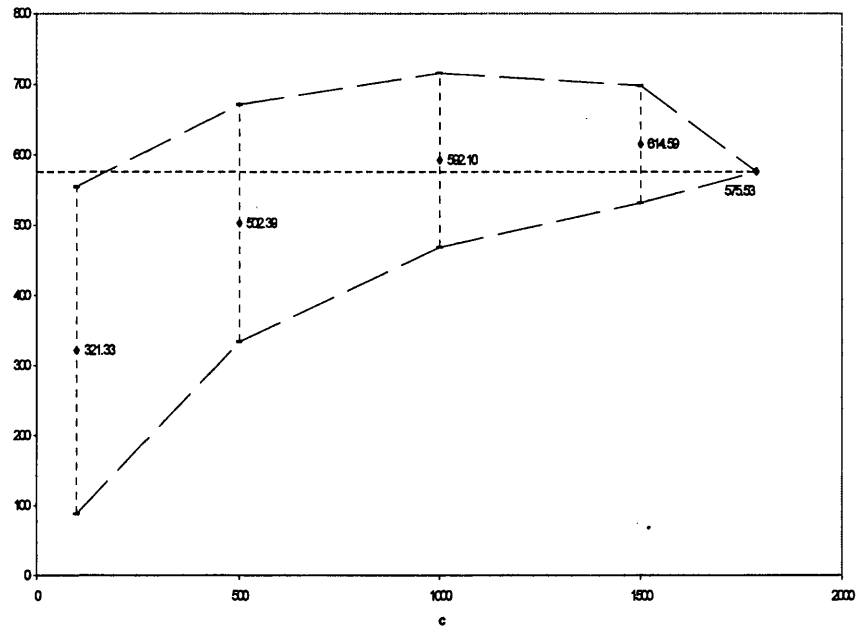

Figure 5.6: 95% confidence interval of $\hat{\theta}$ at successive censoring levels for the pressure vessel failure times data.

Example: Pressure vessels

The results are shown in Table 5.9, and the 95% confidence interval limits can be seen in Figure 5.6. We see that, at the early censoring level $c = 100$, the limits do not contain the complete estimate. As c increases we see the confidence limits narrow, but as for the other examples, the width is too large to provide any reasonable guide to the final estimate, even with only 2 items left to fail. We note that, although the intervals are quite large, the estimates do "flatten" off.

The outcome of these examples seem rather disappointing, in that there is no indication of a optimum level of censoring to stop an experiment which would provide an adequate guide to the complete estimate. We can conclude however that increasing the sample size of items being tested is likely to help identify a plateau in the estimates obtained at successive c, at which time it seems reasonable to stop the experiment, providing the precision of the

	n				
c	50	100	300	500	1000
25	95.25	95.24	95.59	94.77	95.10
50	95.22	94.99	95.84	94.87	95.10
100	94.76	94.75	95.31	95.19	95.28
150	94.51	94.79	95.04	95.09	95.01
200	94.52	94.36	95.37	94.88	94.95
250	94.50	94.48	95.48	94.86	95.00
300	94.30	94.54	95.31	94.90	95.44

Table 5.10: negative exponential data, with $\theta = 100$.

estimate is satisfactory.

5.4.2 Simulations

Using SAS we simulate MLEs from a negative exponential distribution at different censoring levels, for a number of different sample sizes. We then use (5.12) to find the proposed 95% confidence interval from each censored MLE generated, and then we can find the percentage of these intervals from the 10,000 repetitions that actually contain the corresponding complete MLE, $\hat{\theta}$. Table 5.10 gives the results for various sample sizes, $n = 50, 100, 300, 500$ and $n = 1000$; in all cases, samples were censored successively at $c = 25, 50, 100, 150, 200, 250$ and 300.

There is good agreement between theory and practice, even for small sample sizes and early censoring, where the correlation approximations were less accurate; see Table 5.6. These simulation experiments again confirm that, despite the lack of Normality in MLEs bases on data in samples with n smaller than 1000, the approximations obtained from asymptotic Normal theory still leads to reliable inference for small to moderate sample sizes.

5.5 Summary

We have detailed an approach summarised in Finselbach & Watkins (2006), which considers interim analysis of negative exponential data, and uses these to obtain confidence intervals for $\hat{\theta}$, the estimate yielded at the final analysis, when all items have failed. We note that the single parameter θ can easily be interpreted as a quantile, using a linear function of θ, see (1.24).

The negative exponential distribution however is not the most versatile reliability distribution, and we next extend these results to the popular Weibull distribution in the chapter 6. This analysis not only has the complications of an extra parameter, but also requires a more careful consideration of the quantile function B_{10}.

Chapter 6

Interim Analysis of Weibull Reliability Data

We can now show how the results for the negative exponential distribution, in Chapter 5, generalise to the Weibull distribution. As discussed in Chapter 2, the likelihood theory now involves two parameters, and the algebra becomes much more involved than that discussed in the previous chapter. We will use the same asymptotic relationships as discussed for the negative exponential distribution, and use the interim analysis, based on Type I censored information, to determine the precision with which we can make statements on final estimates, based on these interim estimates. We exploit the notation used in Chapter 2, and will use the same examples therein to illustrate any theoretical results developed.

6.1 Asymptotic relationships of MLEs

It is straightforward to show that the asymptotic relationship between the MLEs, the EFI and the score function is

$$\begin{pmatrix} \hat{\beta}_c - \beta \\ \hat{\theta}_c - \theta \end{pmatrix} \simeq \mathbf{A}_c^{-1} \begin{pmatrix} \frac{\partial l_c}{\partial \beta} \\ \frac{\partial l_c}{\partial \theta} \end{pmatrix}.$$

We refer to (2.48) for the elements of the EFI for a Type I censored sample, but can express the above in general as

$$\begin{aligned} \begin{pmatrix} \hat{\beta}_c - \beta \\ \hat{\theta}_c - \theta \end{pmatrix} &= \begin{pmatrix} Var\left(\hat{\beta}_c\right) & Cov\left(\hat{\beta}_c, \hat{\theta}_c\right) \\ Cov\left(\hat{\theta}_c, \hat{\beta}_c\right) & Var\left(\hat{\theta}_c\right) \end{pmatrix} \begin{pmatrix} \frac{\partial l_c}{\partial \beta} \\ \frac{\partial l_c}{\partial \theta} \end{pmatrix} \\ &= \begin{pmatrix} Var\left(\hat{\beta}_c\right) \frac{\partial l_c}{\partial \beta} + Cov\left(\hat{\beta}_c, \hat{\theta}_c\right) \frac{\partial l_c}{\partial \theta} \\ Cov\left(\hat{\theta}_c, \hat{\beta}_c\right) \frac{\partial l_c}{\partial \beta} + Var\left(\hat{\theta}_c\right) \frac{\partial l_c}{\partial \theta} \end{pmatrix}. \end{aligned}$$

Since this relationship also covers the case $c \to \infty$, we now have, for example

$$\begin{aligned} Corr(\hat{\beta}, \hat{\beta}_c) &= Corr\left\{\left(\hat{\beta}-\beta\right), \left(\hat{\beta}_c-\beta\right)\right\} \\ &\simeq Corr\left\{\begin{pmatrix} Var\left(\hat{\beta}\right)\frac{\partial l}{\partial \beta}+ \\ Cov\left(\hat{\beta},\hat{\theta}\right)\frac{\partial l}{\partial \theta}\end{pmatrix}, \begin{pmatrix} Var\left(\hat{\beta}_c\right)\frac{\partial l_c}{\partial \beta}+ \\ Cov\left(\hat{\beta}_c,\hat{\theta}_c\right)\frac{\partial l_c}{\partial \theta}\end{pmatrix}\right\} \end{aligned}$$

Initially we can consider the covariance, and it follows that,

$$Cov(\hat{\beta}, \hat{\beta}_c) \simeq Cov\left(\left\{\begin{array}{l} Var\left(\hat{\beta}\right)\frac{\partial l}{\partial \beta}+ \\ Cov\left(\hat{\beta},\hat{\theta}\right)\frac{\partial l}{\partial \theta}\end{array}\right\}, \left\{\begin{array}{l} Var\left(\hat{\beta}_c\right)\frac{\partial l_c}{\partial \beta}+ \\ Cov\left(\hat{\beta}_c,\hat{\theta}_c\right)\frac{\partial l_c}{\partial \theta}\end{array}\right\}\right),$$

and due to regularity conditions, this can be written in terms of expectations

$$\begin{aligned} Cov(\hat{\beta}, \hat{\beta}_c) &\simeq E\left[\begin{array}{l}\left(Var\left(\hat{\beta}\right)\frac{\partial l}{\partial \beta}+Cov\left(\hat{\beta},\hat{\theta}\right)\frac{\partial l}{\partial \theta}\right) \\ \times\left(Var\left(\hat{\beta}_c\right)\frac{\partial l_c}{\partial \beta}+Cov\left(\hat{\beta}_c,\hat{\theta}_c\right)\frac{\partial l_c}{\partial \theta}\right)\end{array}\right] \\ &= Var\left(\hat{\beta}\right)Var\left(\hat{\beta}_c\right)Cov\left(\frac{\partial l}{\partial \beta}, \frac{\partial l_c}{\partial \beta}\right) \\ &\quad +Var\left(\hat{\beta}\right)Cov\left(\hat{\beta}_c,\hat{\theta}_c\right)Cov\left(\frac{\partial l}{\partial \beta}, \frac{\partial l_c}{\partial \theta}\right) \\ &\quad +Cov\left(\hat{\beta},\hat{\theta}\right)Var\left(\hat{\beta}_c\right)Cov\left(\frac{\partial l}{\partial \theta}, \frac{\partial l_c}{\partial \beta}\right) \\ &\quad +Cov\left(\hat{\beta},\hat{\theta}\right)Cov\left(\hat{\beta}_c,\hat{\theta}_c\right)Cov\left(\frac{\partial l}{\partial \theta}, \frac{\partial l_c}{\partial \theta}\right). \end{aligned} \tag{6.1}$$

Similarly we obtain

$$\begin{aligned} Cov(\hat{\beta}, \hat{\theta}_c) &= Var\left(\hat{\beta}\right)Cov\left(\hat{\beta}_c,\hat{\theta}_c\right)Cov\left(\frac{\partial l}{\partial \beta}, \frac{\partial l_c}{\partial \beta}\right) \\ &\quad +Var\left(\hat{\beta}\right)Var\left(\hat{\theta}_c\right)Cov\left(\frac{\partial l}{\partial \beta}, \frac{\partial l_c}{\partial \theta}\right) \\ &\quad +Cov\left(\hat{\beta},\hat{\theta}\right)Cov\left(\hat{\beta}_c,\hat{\theta}_c\right)Cov\left(\frac{\partial l}{\partial \theta}, \frac{\partial l_c}{\partial \beta}\right) \\ &\quad +Cov\left(\hat{\beta},\hat{\theta}\right)Var\left(\hat{\theta}_c\right)Cov\left(\frac{\partial l}{\partial \theta}, \frac{\partial l_c}{\partial \theta}\right), \end{aligned} \tag{6.2}$$

$$\begin{aligned} Cov(\hat{\theta}, \hat{\theta}_c) &= Cov\left(\hat{\beta},\hat{\theta}\right)Cov\left(\hat{\beta}_c,\hat{\theta}_c\right)Cov\left(\frac{\partial l}{\partial \beta}, \frac{\partial l_c}{\partial \beta}\right) \\ &\quad +Cov\left(\hat{\beta},\hat{\theta}\right)Var\left(\hat{\theta}_c\right)Cov\left(\frac{\partial l}{\partial \beta}, \frac{\partial l_c}{\partial \theta}\right) \\ &\quad +Var\left(\hat{\theta}_c\right)Cov\left(\hat{\beta}_c,\hat{\theta}_c\right)Cov\left(\frac{\partial l}{\partial \theta}, \frac{\partial l_c}{\partial \beta}\right) \\ &\quad +Var\left(\hat{\theta}\right)Var\left(\hat{\theta}_c\right)Cov\left(\frac{\partial l}{\partial \theta}, \frac{\partial l_c}{\partial \theta}\right), \end{aligned} \tag{6.3}$$

and

$$\begin{aligned} Cov(\hat{\theta},\hat{\beta}_c) &= Cov\left(\hat{\beta},\hat{\theta}\right) Var\left(\hat{\beta}_c\right) Cov\left(\frac{\partial l}{\partial \beta},\frac{\partial l_c}{\partial \beta}\right) \\ &\quad + Cov\left(\hat{\beta},\hat{\theta}\right) Cov\left(\hat{\beta}_c,\hat{\theta}_c\right) Cov\left(\frac{\partial l}{\partial \beta},\frac{\partial l_c}{\partial \theta}\right) \\ &\quad + Var\left(\hat{\theta}\right) Var\left(\hat{\beta}_c\right) Cov\left(\frac{\partial l}{\partial \theta},\frac{\partial l_c}{\partial \beta}\right) \\ &\quad + Var\left(\hat{\theta}\right) Cov\left(\hat{\beta}_c,\hat{\theta}_c\right) Cov\left(\frac{\partial l}{\partial \theta},\frac{\partial l_c}{\partial \theta}\right). \end{aligned} \tag{6.4}$$

6.1.1 Details of the score functions

We write the score functions in terms of the transformed variable Z, see (2.26), which follows the standard negative exponential distribution. It follows from (2.4), (2.5), (2.19) and (2.20) that

$$\frac{\partial l}{\partial \beta} = \beta^{-1}\left\{n + \sum_{i=1}^{n} \ln Z_i - \sum_{i=1}^{n} Z_i \ln Z_i\right\} \tag{6.5}$$

$$\frac{\partial l}{\partial \theta} = \beta\theta^{-1}\left\{-n + \sum_{i=1}^{n} Z_i\right\} \tag{6.6}$$

$$\frac{\partial l_c}{\partial \beta} = \beta^{-1}\left\{M + \sum_{i=1}^{M} \ln Z_i - \sum_{i=1}^{M} Z_i \ln Z_i - (n-M) z_c \ln z_c\right\} \tag{6.7}$$

and

$$\frac{\partial l_c}{\partial \theta} = \beta\theta^{-1}\left\{-M + \sum_{i=1}^{M} Z_i + (n-M) z_c\right\}. \tag{6.8}$$

6.2 Failure times and expectations involved

It is clear from the above that we require expectations of the form

$$E[Z],\ E[\ln Z], \text{ and } E[Z \ln Z].$$

As in the preceding chapter, we know that the items that fail before c follow the right truncated negative exponential distribution; see (2.34). We recall from Chapter 2 that the expectations required from this distribution are given in equations (2.40) to (2.47).

We also need some expectations of the surviving items, *i.e.* the lifetimes of those items that have survived past the censored time c. To do this we can use the expectations for the complete sample and draw on the fact that this must reflect both the censored items and the survivors, as done for the negative exponential distribution, see (5.7). So we have, for Z_c following the left truncated negative exponential distribution,

$$E[Z_c] = \tilde{\mu}_{10},$$

say. Therefore

$$q_c\mu_{10} + (1 - q_c)\,\tilde{\mu}_{10} = 1,$$

and so from (2.28),

$$\begin{aligned}\tilde{\mu}_{10} &= \frac{1 - q_c\mu_{10}}{(1 - q_c)} \\ &= \frac{1 - q_c\,(1 - z_c r_c)}{r_c q_c} \\ &= \frac{1 - q_c + z_c r_c q_c}{r_c q_c} \\ &= 1 + z_c. \end{aligned} \tag{6.9}$$

We will also need

$$E[\ln Z_c] = \tilde{\mu}_{01},$$

say, where, from (2.29)

$$q_c\mu_{01} + (1 - q_c)\,\tilde{\mu}_{01} = -\gamma.$$

This leads us to evaluate

$$\tilde{\mu}_{01} = \frac{-\,(\gamma + q_c\mu_{01})}{(1 - q_c)} = \frac{-\left(\gamma + \gamma^{(1)}\,(1, z_c)\right)}{r_c q_c}. \tag{6.10}$$

Finally we want

$$E[Z_c \ln Z_c] = \tilde{\mu}_{11}$$

say, where, from (2.30), we know

$$q_c\mu_{11} + (1 - q_c)\,\tilde{\mu}_{11} = 1 - \gamma,$$

and so

$$\begin{aligned}\tilde{\mu}_{11} &= \frac{(1 - \gamma - q_c\mu_{11})}{(1 - q_c)} \\ &= \frac{1 - \gamma - \left(\gamma^{(1)}\,(1, z_c) + q_c - z_c \ln z_c r_c q_c\right)}{(1 - q_c)} \\ &= 1 + z_c \ln z_c - \frac{\gamma + \gamma^{(1)}\,(1, z_c)}{r_c q_c}. \end{aligned} \tag{6.11}$$

6.2.1 Expectations involved

Our calculations of the covariance of the score functions, in (6.1) to (6.4), will require the following expectations, which we provide in terms of the incomplete gamma function, see

(1.8), and recall the moments of M, m_1 and m_2, given in (5.3).

$$\begin{aligned} E_1 &= E\left[M\sum_{i=1}^{n} z_i\right] = E\left[M\left(\sum_{i=1}^{M} z_i + \sum_{i=M+1}^{n} z_i\right)\right] \\ &= m_2\mu_{10} + (nm_1 - m_2)\,\tilde{\mu}_{10} \\ &= n^2 q_c - n z_c r_c q_c \end{aligned}$$

$$\begin{aligned} E_2 &= E\left[\sum_{i=1}^{n} z_i \sum_{i=1}^{M} z_i\right] = E\left[\left(\sum_{i=1}^{M} z_i + \sum_{i=M+1}^{n} z_i\right)\sum_{i=1}^{M} z_i\right] \\ &= (nm_1 - m_2)\,\mu_{10}\tilde{\mu}_{10} + m_1 m_c + (m_2 - m_1)\,\mu_{10}^2 \\ &= n\,(n+1)\,q_c\,(1 - z_c r_c) - n z_c^2 r_c q_c \end{aligned}$$

$$\begin{aligned} E_3 &= E\left[\sum_{i=1}^{n} z_i \sum_{i=1}^{M} \ln z_i\right] = E\left[\left(\sum_{i=1}^{M} z_i + \sum_{i=M+1}^{n} z_i\right)\sum_{i=1}^{M} \ln z_i\right] \\ &= m_1\mu_{11} + (m_2 - m_1)\mu_{10}\mu_{01} + (nm_1 - m_2)\,\tilde{\mu}_{10}\mu_{01} \\ &= n^2\gamma^{(1)}\,(1, z_c) + nq_c - n z_c \ln z_c r_c q_c \end{aligned}$$

$$\begin{aligned} E_4 &= E\left[\sum_{i=1}^{n} z_i \sum_{i=1}^{M} z_i \ln z_i\right] = E\left[\left(\sum_{i=1}^{M} z_i + \sum_{i=M+1}^{n} z_i\right)\sum_{i=1}^{M} z_i \ln z_i\right] \\ &= m_1\mu_{21} + (m_2 - m_1)\mu_{10}\mu_{11} + (nm_1 - m_2)\,\tilde{\mu}_{10}\mu_{11} \\ &= n\,(n+1)\,\gamma^{(1)}\,(1, z_c) + n^2 q_c + 2nq_c - n z_c r_c q_c - n\,(n + 1 + z_c)\,z_c \ln z_c r_c q_c \end{aligned}$$

Regarding the left truncated random variable Z_c, these first four expectations only involve

$$\sum_{i=M+1}^{n} z_i,$$

and therefore use $\tilde{\mu}_{10}$, (6.9). The remaining expectations, below, will involve

$$\sum_{i=M+1}^{n} \ln z_i$$

or

$$\sum_{i=M+1}^{n} z_i \ln z_i$$

and thus require the expectations $\tilde{\mu}_{01}$, (6.10), and $\tilde{\mu}_{11}$, (6.11), respectively.

$$\begin{aligned} E_5 &= E\left[M\sum_{i=1}^{n}\ln z_i\right] = E\left[M\left(\sum_{i=1}^{M}\ln z_i + \sum_{i=M+1}^{n}\ln z_i\right)\right] \\ &= m_2\mu_{01} + (nm_1 - m_2)\,\tilde{\mu}_{01} \\ &= n\gamma^{(1)}(1, z_c) - n(n-1)\,q_c\gamma \end{aligned}$$

$$\begin{aligned} E_6 &= E\left[M\sum_{i=1}^{n} z_i\ln z_i\right] = E\left[M\left(\sum_{i=1}^{M} z_i\ln z_i + \sum_{i=M+1}^{n} z_i\ln z_i\right)\right] \\ &= m_2\mu_{11} + (nm_1 - m_2)\,\tilde{\mu}_{11} \\ &= n\gamma^{(1)}(1, z_c) + n^2 q_c(1-\gamma) + nq_c\gamma - nz_c\ln z_c r_c q_c \end{aligned}$$

We note that the algebra becomes considerably lengthy for these more complex expectations.

$$\begin{aligned} E_7 &= E\left[\sum_{i=1}^{n}\ln z_i\sum_{i=1}^{M} z_i\right] = E\left[\left(\sum_{i=1}^{M}\ln z_i + \sum_{i=M+1}^{n}\ln z_i\right)\sum_{i=1}^{M} z_i\right] \\ &= m_1\mu_{11} + (m_2 - m_1)\,\mu_{10}\mu_{01} + (nm_1 - m_2)\,\mu_{10}\tilde{\mu}_{01} \\ &= n\gamma^{(1)}(1, z_c) + nq_c - nz_c\ln z_c r_c q_c - n(n-1)\,q_c(1 - z_c r_c)\,\gamma \end{aligned}$$

$$\begin{aligned} E_8 &= E\left[\sum_{i=1}^{n} z_i\ln z_i\sum_{i=1}^{M} z_i\right] = E\left[\left(\sum_{i=1}^{M} z_i\ln z_i + \sum_{i=M+1}^{n} z_i\ln z_i\right)\sum_{i=1}^{M} z_i\right] \\ &= m_1\mu_{21} + (m_2 - m_1)\,\mu_c\mu_{11} + (nm_1 - m_2)\,\mu_c\tilde{\mu}_{11} \\ &= 2n\gamma^{(1)}(1, z_c) + n^2 q_c(1 - z_c r_c) + 2nq_c - 2nz_c\ln z_c r_c q_c \\ &\quad -nz_c^2\ln z_c r_c q_c - n(n-1)\,q_c(1 - z_c r_c)\,\gamma \end{aligned}$$

$$\begin{aligned} E_9 &= E\left[\sum_{i=1}^{n}\ln z_i\sum_{i=1}^{M}\ln z_i\right] = E\left[\left(\sum_{i=1}^{M}\ln z_i + \sum_{i=M+1}^{n}\ln z_i\right)\sum_{i=1}^{M}\ln z_i\right] \\ &= m_1\mu_{02} + (m_2 - m_1)\,\mu_{01}^2 + (nm_1 - m_2)\,\mu_{01}\tilde{\mu}_{01} \\ &= n\gamma^{(2)}(1, z_c) - n(n-1)\,\gamma^{(1)}(1, z_c)\,\gamma \end{aligned}$$

$$\begin{aligned} E_{10} &= E\left[\sum_{i=1}^{n}\ln z_i\sum_{i=1}^{M} z_i\ln z_i\right] = E\left[\left(\sum_{i=1}^{M}\ln z_i + \sum_{i=M+1}^{n}\ln z_i\right)\sum_{i=1}^{M} z_i\ln z_i\right] \\ &= m_1\mu_{12} + (m_2 - m_1)\,\mu_{01}\mu_{11} + (nm_1 - m_2)\,\mu_{11}\tilde{\mu}_{01} \\ &= n\gamma^{(2)}(1, z_c) + 2n\gamma^{(1)}(1, z_c) - n(n-1)\,\gamma^{(1)}(1, z_c)\,\gamma - nz_c(\ln z_c)^2 r_c q_c \\ &\quad -n(n-1)\,q_c\gamma + n^2 z_c\ln z_c r_c q_c\gamma \end{aligned}$$

Expectation	Theoretical	Simulated
$E1$	6284.42	6289.61
$E2$	2632.05	2635.82
$E3$	−7902.78	−7906.24
$E4$	−1634.81	−1635.91
$E5$	−3691.87	−3690.36
$E6$	2629.33	2638.17
$E7$	−1526.44	−1526.62
$E8$	1099.53	1104.17
$E9$	4730.36	4727.66
$E10$	958.83	958.33
$E11$	−3315.30	−3324.67
$E12$	−683.49	−685.59

Table 6.1: Numerical checks of expectations E1 to E12

$$\begin{aligned} E_{11} &= E\left[\sum_{i=1}^{n} z_i \ln z_i \sum_{i=1}^{M} \ln z_i\right] = E\left[\left(\sum_{i=1}^{M} z_i \ln z_i + \sum_{i=M+1}^{n} z_i \ln z_i\right) \sum_{i=1}^{M} \ln z_i\right] \\ &= m_1\mu_{12} + (m_2 - m_1)\,\mu_{01}\mu_{11} + (nm_1 - m_2)\,\mu_{01}\tilde{\mu}_{11} \\ &= n\gamma^{(2)}(1, z_c) + n(n+1)\,\gamma^{(1)}(1, z_c) - n(n-1)\,\gamma^{(1)}(1, z_c)\,\gamma - nz_c(\ln z_c)^2 r_c q_c \end{aligned}$$

$$\begin{aligned} E_{12} &= E\left[\sum_{i=1}^{n} z_i \ln z_i \sum_{i=1}^{M} z_i \ln z_i\right] = E\left[\left(\sum_{i=1}^{M} z_i \ln z_i + \sum_{i=M+1}^{n} z_i \ln z_i\right) \sum_{i=1}^{M} z_i \ln z_i\right] \\ &= m_1\mu_{22} + (m_2 - m_1)\,\mu_{11}^2 + (nm_1 - m_2)\,\mu_{11}\tilde{\mu}_{11} \\ &= 2n\gamma^{(2)}(1, z_c) + n^2\gamma^{(1)}(1, z_c) + 5n\gamma^{(1)}(1, z_c) + n(n+1)\,q_c - n(n+1)\,z_c \ln z_c r_c q_c \\ &\quad -n(2 + z_c)\,z_c(\ln z_c)^2 r_c q_c - n(n-1)\left(\gamma^{(1)}(1, z_c) + q_c - z_c \ln z_c r_c q_c\right)\gamma \end{aligned}$$

We can use Mathematica to compute these expectations and compare these to their corresponding simulated values. Table 6.1 shows this comparison for $\beta = 2$, $\theta = 100$, $c = 100$, and $n = 100$. We see good agreement between the theoretical and simulated values.

6.2.2 Covariances of the score functions

Using the above expectations, and from (6.5) to (6.8), we can obtain the covariance of the score functions for all combinations of the censored and complete MLEs. Some of the algebra and cancellation of terms is very detailed, and so have been omitted. We use Mathematica to calculate numerical values of the following expressions; we set $\beta = 2$, $\theta = 100$, $c = 100$, and $n = 100$.

$Cov\left(\frac{\partial l}{\partial \theta}, \frac{\partial l_c}{\partial \theta}\right)$

$$\begin{aligned} Cov\left(\frac{\partial l}{\partial \theta}, \frac{\partial l_c}{\partial \theta}\right) &= E\left[\frac{\partial l}{\partial \theta} \times \frac{\partial l_c}{\partial \theta}\right] \\ &= E\left[\left(\beta\theta^{-1}\left\{-n + \sum_{i=1}^{n} z_i\right\}\right) \times \frac{\partial l_c}{\partial \theta}\right] \\ &= -n\beta\theta^{-1}E\left[\frac{\partial l_c}{\partial \theta}\right] + E\left[\left(\beta\theta^{-1}\left\{\sum_{i=1}^{n} z_i\right\}\right) \times \frac{\partial l_c}{\partial \theta}\right] \end{aligned}$$

and since $E\left[\frac{\partial l_c}{\partial \theta}\right] = 0$, we have

$$\begin{aligned} Cov\left(\frac{\partial l}{\partial \theta}, \frac{\partial l_c}{\partial \theta}\right) &= E\left[\left(\beta\theta^{-1}\left\{\sum_{i=1}^{n} z_i\right\}\right) \times \left(\beta\theta^{-1}\left\{-M + \sum_{i=1}^{M} z_i + (n-M)z_c\right\}\right)\right] \\ &= \beta^2\theta^{-2}E\left[M\sum_{i=1}^{n} z_i + \sum_{i=1}^{n} z_i \sum_{i=1}^{M} z_i + (n-M)z_c \sum_{i=1}^{n} z_i\right] \\ &= \beta^2\theta^{-2}\left[E_2 - E_1\left(1 + z_c\right) + n^2 z_c q_c\right] \\ &= \beta^2\theta^{-2} n q_c \end{aligned}$$

We refer back to (2.52) for the relevant Mathematica code for our required functions, and obtain the following output

```
In[1] :=Covtt1=beta*beta/theta*theta * n* qc]
Out[1] :=0.0252848
```

This compares favorably with our simulated value

$$Cov\left(\frac{\partial l}{\partial \theta}, \frac{\partial l_c}{\partial \theta}\right) = 0.0256,$$

which (throughout) is based on 10,000 replications.

$Cov\left(\frac{\partial l}{\partial \theta}, \frac{\partial l_c}{\partial \beta}\right)$

$$
\begin{aligned}
Cov\left(\frac{\partial l}{\partial \theta}, \frac{\partial l_c}{\partial \beta}\right) &= E\left[\frac{\partial l}{\partial \theta} \times \frac{\partial l_c}{\partial \beta}\right] \\
&= E\left[\beta\theta^{-1}\left\{-n + \sum_{i=1}^{n} z_i\right\} \times \frac{\partial l_c}{\partial \beta}\right] \\
&= E\left[\begin{array}{c} \beta\theta^{-1}\left\{-\sum_{i=1}^{n} z_i\right\} \times \\ \beta^{-1}\left\{M + \sum_{i=1}^{M} \ln z_i - \sum_{i=1}^{M} z_i \ln z_i - (n-M) z_c \ln z_c\right\} \end{array}\right] \\
&= \theta^{-1} E\left[\begin{array}{c} -M\sum_{i=1}^{n} z_i + \sum_{i=1}^{n} z_i \sum_{i=1}^{M} \ln z_i - \sum_{i=1}^{n} z_i \sum_{i=1}^{M} z_i \ln z_i \\ -(n-M) z_c \ln z_c \sum_{i=1}^{n} z_i \end{array}\right] \\
&= \theta^{-1}\left[E_1\left(1 + z_c \ln z_c\right) + E_3 - E_4 - n^2 z_c \ln z_c\right] \\
&= -n\theta^{-1}\left(q_c + \gamma^{(1)}\left(1, z_c\right)\right)
\end{aligned}
$$

This leads to the theoretical value

```
In[1]:=Covtb1=-n/theta * (qc+g1)]
Out[1]:=0.164479
```

and simulated value

$$Cov\left(\frac{\partial l}{\partial \theta}, \frac{\partial l_c}{\partial \beta}\right) = 0.1687. \tag{6.12}$$

$Cov\left(\frac{\partial l}{\partial \beta}, \frac{\partial l_c}{\partial \theta}\right)$

$$
\begin{aligned}
Cov\left(\frac{\partial l}{\partial \beta}, \frac{\partial l_c}{\partial \theta}\right) &= E\left[\frac{\partial l}{\partial \beta} \times \frac{\partial l_c}{\partial \theta}\right] \\
&= E\left[\beta^{-1}\left\{n + \sum_{i=1}^{n} \ln z_i - \sum_{i=1}^{n} z_i \ln z_i\right\} \times \frac{\partial l_c}{\partial \theta}\right] \\
&= E\left[\begin{array}{c} \beta^{-1}\left\{\sum_{i=1}^{n} \ln z_i - \sum_{i=1}^{n} z_i \ln z_i\right\} \\ \times \beta\theta^{-1}\left\{-M + \sum_{i=1}^{M} z_i + (n-M)z_c\right\} \end{array}\right] \\
&= \theta^{-1} E\left[\begin{array}{c} -M\sum_{i=1}^{n} \ln z_i + \sum_{i=1}^{n} \ln z_i \sum_{i=1}^{M} z_i + (n-M)z_c \sum_{i=1}^{n} \ln z_i \\ +M\sum_{i=1}^{n} z_i \ln z_i - \sum_{i=1}^{n} z_i \ln z_i \sum_{i=1}^{M} z_i - (n-M)z_c \sum_{i=1}^{n} z_i \ln z_i \end{array}\right] \\
&= \theta^{-1}\left[(E_6 - E_5)(1 + z_c) + E_7 - E_8 - n^2 z_c\right] \\
&= -n\theta^{-1}\left(q_c + \gamma^{(1)}(1, z_c)\right)
\end{aligned}
$$

We note that this is equal to $Cov\left(\frac{\partial l}{\partial \theta}, \frac{\partial l_c}{\partial \beta}\right)$, and our simulated figure, given below, is suitably close to (6.12),

$$Cov\left(\frac{\partial l}{\partial \beta}, \frac{\partial l_c}{\partial \theta}\right) = 0.1674.$$

$Cov\left(\frac{\partial l}{\partial \beta}, \frac{\partial l_c}{\partial \beta}\right)$

$$
\begin{aligned}
Cov\left(\frac{\partial l}{\partial \beta}, \frac{\partial l_c}{\partial \beta}\right) &= E\left[\frac{\partial l}{\partial \beta} \times \frac{\partial l_c}{\partial \beta}\right] \\
&= E\left[\beta^{-1}\left\{n + \sum_{i=1}^{n} \ln z_i - \sum_{i=1}^{n} z_i \ln z_i\right\} \times \frac{\partial l_c}{\partial \beta}\right] \\
&= E\left[\begin{array}{c} \beta^{-1}\left\{\sum_{i=1}^{n} \ln z_i - \sum_{i=1}^{n} z_i \ln z_i\right\} \\ \times \beta^{-1}\left\{M + \sum_{i=1}^{M} \ln z_i - \sum_{i=1}^{M} z_i \ln z_i - (n-M) z_c \ln z_c\right\} \end{array}\right] \\
&= \beta^{-2} E\left[\begin{array}{c} M \sum_{i=1}^{n} \ln z_i + \sum_{i=1}^{n} \ln z_i \sum_{i=1}^{M} \ln z_i - \sum_{i=1}^{n} \ln z_i \sum_{i=1}^{M} z_i \ln z_i \\ -(n-M) z_c \ln z_c \sum_{i=1}^{n} \ln z_i - M \sum_{i=1}^{n} z_i \ln z_i \\ - \sum_{i=1}^{n} z_i \ln z_i \sum_{i=1}^{M} \ln z_i + \sum_{i=1}^{n} z_i \ln z_i \sum_{i=1}^{M} z_i \ln z_i \\ +(n-M) z_c \ln z_c \sum_{i=1}^{n} z_i \ln z_i \end{array}\right] \\
&= \beta^{-2}\left[\begin{array}{c} (E_5 - E_6)(1 + z_c \ln z_c) + E_9 - E_{10} - E_{11} + E_{12} \\ +n^2 z_c \ln z_c \end{array}\right] \\
&= n\beta^{-2}\left(\gamma^{(2)}(1, z_c) + 2\gamma^{(1)}(1, z_c) + q_c\right)
\end{aligned}
$$

Using Mathematica, this gives

```
In[1] :=Covbb1=-n/(beta*beta) * (g2+2*g1+qc)]
Out[1] :=20.5337
```

which agrees well with the corresponding simulated value

$$Cov\left(\frac{\partial l}{\partial \beta}, \frac{\partial l_c}{\partial \beta}\right) = 20.5834.$$

6.2.3 Simplification of the covariances

We can now use the results above to simplify the covariances of the complete and censored MLEs. We know that (2.25) and (2.33) are symmetrical matrices, and so we can write

$$
\begin{aligned}
Cov\left(\hat{\beta},\hat{\beta}_c\right) &= Var\left(\hat{\beta}\right) Var\left(\hat{\beta}_c\right) Cov\left(\frac{\partial l}{\partial \beta},\frac{\partial l_c}{\partial \beta}\right) \\
&\quad + Var\left(\hat{\beta}\right) Cov\left(\hat{\beta}_c,\hat{\theta}_c\right) Cov\left(\frac{\partial l}{\partial \beta},\frac{\partial l_c}{\partial \theta}\right) \\
&\quad + Cov\left(\hat{\beta},\hat{\theta}\right) Var\left(\hat{\beta}_c\right) Cov\left(\frac{\partial l}{\partial \theta},\frac{\partial l_c}{\partial \beta}\right) \\
&\quad + Cov\left(\hat{\beta},\hat{\theta}\right) Cov\left(\hat{\beta}_c,\hat{\theta}_c\right) Cov\left(\frac{\partial l}{\partial \theta},\frac{\partial l_c}{\partial \theta}\right) \\
&= 6n^{-2}\pi^{-2}\left[q_c\gamma^{(2)}(1,z_c) - \left\{\gamma^{(1)}(1,z_c)\right\}^2\right]^{-1} \times \\
&\quad \begin{bmatrix} \beta^2\beta^2 q_c\left\{n\beta^{-2}\left(\gamma^{(2)}(1,z_c) + 2\gamma^{(1)}(1,z_c) + q_c\right)\right\} \\ -\beta^2\theta\left\{q_c + \gamma^{(1)}(1,z_c)\right\}\left\{n\theta^{-1}\left(q_c + \gamma^{(1)}(1,z_c)\right)\right\} \\ -\theta(1-\gamma)\beta^2 q_c\left\{n\theta^{-1}\left(q_c + \gamma^{(1)}(1,z_c)\right)\right\} \\ +\theta(1-\gamma)\theta\left\{q_c + \gamma^{(1)}(1,z_c)\right\}\left\{\beta^2\theta^{-2}nq_c\right\} \end{bmatrix} \\
&= 6n^{-2}\pi^{-2}\left[q_c\gamma^{(2)}(1,z_c) - \left\{\gamma^{(1)}(1,z_c)\right\}^2\right]^{-1} \times \\
&\quad \begin{bmatrix} n\beta^2 q_c\left(\gamma^{(2)}(1,z_c) + 2\gamma^{(1)}(1,z_c) + q_c\right) \\ -n\beta^2\left\{q_c + \gamma^{(1)}(1,z_c)\right\}^2 \\ -n\beta^2 q_c(1-\gamma)\left\{q_c + \gamma^{(1)}(1,z_c)\right\} \\ +n\beta^2 q_c(1-\gamma)\left\{q_c + \gamma^{(1)}(1,z_c)\right\} \end{bmatrix} \\
&= 6n^{-2}\pi^{-2}\left[q_c\gamma^{(2)}(1,z_c) - \left\{\gamma^{(1)}(1,z_c)\right\}^2\right]^{-1} \times \\
&\quad \left[n\beta^2\left\{q_c\gamma^{(2)}(1,z_c) - \left\{\gamma^{(1)}(1,z_c)\right\}^2\right\}\right] \\
&= 6n^{-1}\pi^{-2}\beta^2 \\
&= Var\left(\hat{\beta}\right) \qquad (6.13)
\end{aligned}
$$

The same process of simplification leads to

$$
\begin{aligned}
Cov(\hat{\beta},\hat{\theta}_c) &= Var\left(\hat{\beta}\right) Cov\left(\hat{\beta}_c,\hat{\theta}_c\right) Cov\left(\frac{\partial l}{\partial \beta},\frac{\partial l_c}{\partial \beta}\right) \\
&\quad + Var\left(\hat{\beta}\right) Var\left(\hat{\theta}_c\right) Cov\left(\frac{\partial l}{\partial \beta},\frac{\partial l_c}{\partial \theta}\right) \\
&\quad + Cov\left(\hat{\beta},\hat{\theta}\right) Cov\left(\hat{\beta}_c,\hat{\theta}_c\right) Cov\left(\frac{\partial l}{\partial \theta},\frac{\partial l_c}{\partial \beta}\right) \\
&\quad + Cov\left(\hat{\beta},\hat{\theta}\right) Var\left(\hat{\theta}_c\right) Cov\left(\frac{\partial l}{\partial \theta},\frac{\partial l_c}{\partial \theta}\right) \\
&= 6n^{-2}\pi^{-2}\left[q_c\gamma^{(2)}(1,z_c) - \left\{\gamma^{(1)}(1,z_c)\right\}^2\right]^{-1} \times \\
&\quad \begin{bmatrix} \beta^2\theta\left\{q_c+\gamma^{(1)}(1,z_c)\right\}\left\{n\beta^{-2}\left(\gamma^{(2)}(1,z_c)+2\gamma^{(1)}(1,z_c)+q_c\right)\right\} \\ -\beta^2\beta^{-2}\theta^2\left\{\gamma^{(2)}(1,z_c)+2\gamma^{(1)}(1,z_c)+q_c\right\}\left\{n\theta^{-1}\left(q_c+\gamma^{(1)}(1,z_c)\right)\right\} \\ -\theta(1-\gamma)\theta\left\{q_c+\gamma^{(1)}(1,z_c)\right\}\left\{n\theta^{-1}\left(q_c+\gamma^{(1)}(1,z_c)\right)\right\} \\ +\theta(1-\gamma)\beta^{-2}\theta^2\left\{\gamma^{(2)}(1,z_c)+2\gamma^{(1)}(1,z_c)+q_c\right\}\left\{\beta^2\theta^{-2}nq_c\right\} \end{bmatrix} \\
&= 6n^{-2}\pi^{-2}\left[q_c\gamma^{(2)}(1,z_c) - \left\{\gamma^{(1)}(1,z_c)\right\}^2\right]^{-1} \times \\
&\quad \left[n\theta(1-\gamma)\begin{bmatrix} q_c^2+\gamma^{(2)}(1,z_c)q_c+2\gamma^{(1)}(1,z_c)q_c-q_c^2 \\ -2\gamma^{(1)}(1,z_c)q_c-\left\{\gamma^{(1)}(1,z_c)\right\}^2 \end{bmatrix}\right] \\
&= 6n^{-1}\pi^{-2}\theta(1-\gamma) \\
&= Cov\left(\hat{\beta},\hat{\theta}\right) \qquad (6.14)
\end{aligned}
$$

$$
\begin{aligned}
Cov(\hat{\theta},\hat{\beta}_c) &= Cov\left(\hat{\beta},\hat{\theta}\right) Var\left(\hat{\beta}_c\right) Cov\left(\frac{\partial l}{\partial \beta},\frac{\partial l_c}{\partial \beta}\right) \\
&\quad + Cov\left(\hat{\beta},\hat{\theta}\right) Cov\left(\hat{\beta}_c,\hat{\theta}_c\right) Cov\left(\frac{\partial l}{\partial \beta},\frac{\partial l_c}{\partial \theta}\right) \\
&\quad + Var\left(\hat{\theta}\right) Var\left(\hat{\beta}_c\right) Cov\left(\frac{\partial l}{\partial \theta},\frac{\partial l_c}{\partial \beta}\right) \\
&\quad + Var\left(\hat{\theta}\right) Cov\left(\hat{\beta}_c,\hat{\theta}_c\right) Cov\left(\frac{\partial l}{\partial \theta},\frac{\partial l_c}{\partial \theta}\right) \\
&= 6n^{-2}\pi^{-2}\left[q_c\gamma^{(2)}(1,z_c) - \left\{\gamma^{(1)}(1,z_c)\right\}^2\right]^{-1} \times \\
&\quad \left[\begin{array}{c}
\theta(1-\gamma)\beta^2 q_c\left\{n\beta^{-2}\left(\gamma^{(2)}(1,z_c) + 2\gamma^{(1)}(1,z_c) + q_c\right)\right\} \\
+\theta(1-\gamma)\theta\left\{q_c + \gamma^{(1)}(1,z_c)\right\}\left\{-n\theta^{-1}\left(q_c + \gamma^{(1)}(1,z_c)\right)\right\} \\
+\beta^{-2}\theta^2\left[\frac{\pi^2}{6} + (\gamma-1)^2\right]\beta^2 q_c\left\{-n\theta^{-1}\left(q_c + \gamma^{(1)}(1,z_c)\right)\right\} \\
+\beta^{-2}\theta^2\left[\frac{\pi^2}{6} + (\gamma-1)^2\theta\left(q_c + \gamma^{(1)}(1,z_c)\right)\beta^2\theta^{-2}nq_c\right]
\end{array}\right] \\
&= 6n^{-2}\pi^{-2}\left[q_c\gamma^{(2)}(1,z_c) - \left\{\gamma^{(1)}(1,z_c)\right\}^2\right]^{-1} \times \\
&\quad \left[n\theta(1-\gamma)\left[\begin{array}{c}
q_c^2 + \gamma^{(2)}(1,z_c)\,q_c + 2\gamma^{(1)}(1,z_c)\,q_c - q_c^2 \\
-2\gamma^{(1)}(1,z_c)\,q_c - \left\{\gamma^{(1)}(1,z_c)\right\}^2
\end{array}\right]\right] \\
&= 6n^{-1}\pi^{-2}\theta(1-\gamma) \\
&= Cov\left(\hat{\theta},\hat{\beta}\right) \qquad (6.15)
\end{aligned}
$$

and

$$
\begin{aligned}
Cov(\hat{\theta},\hat{\theta}_c) &= Cov\left(\hat{\beta},\hat{\theta}\right) Cov\left(\hat{\beta}_c,\hat{\theta}_c\right) Cov\left(\frac{\partial l}{\partial \beta},\frac{\partial l_c}{\partial \beta}\right) \\
&\quad + Cov\left(\hat{\beta},\hat{\theta}\right) Var\left(\hat{\theta}_c\right) Cov\left(\frac{\partial l}{\partial \beta},\frac{\partial l_c}{\partial \theta}\right) \\
&\quad + Var\left(\hat{\theta}\right) Cov\left(\hat{\beta}_c,\hat{\theta}_c\right) Cov\left(\frac{\partial l}{\partial \theta},\frac{\partial l_c}{\partial \beta}\right) \\
&\quad + Var\left(\hat{\theta}\right) Var\left(\hat{\theta}_c\right) Cov\left(\frac{\partial l}{\partial \theta},\frac{\partial l_c}{\partial \theta}\right) \\
&= 6n^{-2}\pi^{-2}\left[q_c\gamma^{(2)}(1,z_c) - \left\{\gamma^{(1)}(1,z_c)\right\}^2\right]^{-1} \times \\
&\quad \left[\begin{array}{c}
\left[\begin{array}{c} \theta(1-\gamma)\,\theta\left\{q_c+\gamma^{(1)}(1,z_c)\right\} n\beta^{-2}\times \\ \left(\gamma^{(2)}(1,z_c)+2\gamma^{(1)}(1,z_c)+q_c\right)\end{array}\right] \\
+\left[\begin{array}{c} \theta(1-\gamma)\,\beta^2\theta^{-2}\left(\gamma^{(2)}(1,z_c)+2\gamma^{(1)}(1,z_c)+q_c\right)\times \\ \left\{-n\theta^{-1}\left(q_c+\gamma^{(1)}(1,z_c)\right)\right\}\end{array}\right] \\
+\left[\begin{array}{c} \beta^{-2}\theta^2\left[\frac{\pi^2}{6}+(\gamma-1)^2\right]\beta^{-2}\theta^2\theta\left(q_c+\gamma^{(1)}(1,z_c)\right)\times \\ \left\{-n\theta^{-1}\left(q_c+\gamma^{(1)}(1,z_c)\right)\right\}\end{array}\right] \\
+\left[\begin{array}{c} \beta^{-2}\theta^2\left[\frac{\pi^2}{6}+(\gamma-1)^2\right]\times \\ \beta^{-2}\theta^2\left(\gamma^{(2)}(1,z_c)+2\gamma^{(1)}(1,z_c)+q_c\right)\beta^2\theta^{-2}nq_c\end{array}\right]
\end{array}\right] \\
&= 6n^{-2}\pi^{-2}\left[q_c\gamma^{(2)}(1,z_c) - \left\{\gamma^{(1)}(1,z_c)\right\}^2\right]^{-1} \times \\
&\quad \left[n\beta^{-2}\theta^2\left[\frac{\pi^2}{6}+(\gamma-1)^2\right]\left(q_c\gamma^{(2)}(1,z_c) - \left\{\gamma^{(1)}(1,z_c)\right\}^2\right)\right] \\
&= 6n^{-1}\pi^{-2}\beta^{-2}\theta^2\left[\frac{\pi^2}{6}+(\gamma-1)^2\right] \\
&= Var(\hat{\theta}). \qquad (6.16)
\end{aligned}
$$

We therefore have the general result,

$$
\begin{pmatrix} Cov\left(\hat{\beta},\hat{\beta}_c\right) & Cov(\hat{\beta},\hat{\theta}_c) \\ Cov(\hat{\theta},\hat{\beta}_c) & Cov(\hat{\theta},\hat{\theta}_c)\end{pmatrix} = \mathbf{A}^{-1},
$$

which we note is an extension of the relationship found for the one parameter negative exponential distribution, (5.10). The relationship is probably a consequence of the lack-of-memory property, and we assume therefore that it only holds for the negative exponential and Weibull distributions. Further research is needed to prove this result holds for data following these distributions under alternative censoring regimes. We use this result to simplify the calculation of the corresponding correlations, given below.

6.3 Correlations of censored and complete MLEs

The covariance of the score functions are then used to find the required covariances, see for example (6.1). This in turn yields the correlation between censored and complete MLEs, since, for example,

$$\begin{aligned}
Corr\left(\hat{\beta},\hat{\beta}_c\right) &= \frac{Cov\left(\hat{\beta},\hat{\beta}_c\right)}{\sqrt{Var\left(\hat{\beta}\right)Var\left(\hat{\beta}_c\right)}} \\
&= \frac{Var\left(\hat{\beta}\right)}{\sqrt{Var\left(\hat{\beta}\right)Var\left(\hat{\beta}_c\right)}} \\
&= \sqrt{\frac{Var\left(\hat{\beta}\right)}{Var\left(\hat{\beta}_c\right)}} \\
&= \sqrt{\frac{6n^{-1}\pi^{-2}\beta^2}{n^{-1}\left[q_c\gamma^{(2)}(1,z_c)-\left\{\gamma^{(1)}(1,z_c)\right\}^2\right]^{-1}\beta^2 q_c}} \\
&= \sqrt{\frac{6\pi^{-2}\left[q_c\gamma^{(2)}(1,z_c)-\left\{\gamma^{(1)}(1,z_c)\right\}^2\right]}{q_c}}
\end{aligned}$$

again, with similar expressions obtained for $Corr\left(\hat{\beta},\hat{\theta}_c\right)$, $Corr\left(\hat{\theta},\hat{\beta}_c\right)$, and $Corr\left(\hat{\theta},\hat{\theta}_c\right)$.

$$\begin{aligned}
Corr\left(\hat{\beta},\hat{\theta}_c\right) &= \frac{Cov\left(\hat{\beta},\hat{\theta}_c\right)}{\sqrt{Var\left(\hat{\beta}\right)Var\left(\hat{\theta}_c\right)}} \\
&= \frac{Cov\left(\hat{\beta},\hat{\theta}\right)}{\sqrt{Var\left(\hat{\beta}\right)Var\left(\hat{\theta}_c\right)}} \\
&= \frac{6n^{-1}\pi^{-2}\theta(1-\gamma)}{\sqrt{\begin{array}{l}6n^{-2}\pi^{-2}\left[q_c\gamma^{(2)}(1,z_c)-\left\{\gamma^{(1)}(1,z_c)\right\}^2\right]^{-1}\times \\ \beta^2\beta^{-2}\theta^2\left\{q_c+\gamma^{(2)}(1,z_c)+2\gamma^{(1)}(1,z_c)\right\}\end{array}}} \\
&= \sqrt{\frac{6\pi^{-2}(1-\gamma)^2\left[q_c\gamma^{(2)}(1,z_c)-\left\{\gamma^{(1)}(1,z_c)\right\}^2\right]}{\left\{q_c+\gamma^{(2)}(1,z_c)+2\gamma^{(1)}(1,z_c)\right\}}}
\end{aligned}$$

$$
\begin{aligned}
Corr\left(\hat{\theta},\hat{\beta}_c\right) &= \frac{Cov\left(\hat{\theta},\hat{\beta}_c\right)}{\sqrt{Var\left(\hat{\theta}\right)Var\left(\hat{\beta}_c\right)}} \\
&= \frac{Cov\left(\hat{\theta},\hat{\beta}\right)}{\sqrt{Var\left(\hat{\theta}\right)Var\left(\hat{\beta}_c\right)}} \\
&= \frac{6n^{-1}\pi^{-2}\theta\left(1-\gamma\right)}{\sqrt{6n^{-2}\pi^{-2}\left[q_c\gamma^{(2)}\left(1,z_c\right)-\left\{\gamma^{(1)}\left(1,z_c\right)\right\}^2\right]^{-1}\beta^{-2}\theta^2\left[\frac{\pi^2}{6}+\left(\gamma-1\right)^2\right]\beta^2 q_c}} \\
&= \sqrt{\frac{6\pi^{-2}\left(1-\gamma\right)^2\left[q_c\gamma^{(2)}\left(1,z_c\right)-\left\{\gamma^{(1)}\left(1,z_c\right)\right\}^2\right]}{\left[\frac{\pi^2}{6}+\left(\gamma-1\right)^2\right]q_c}}
\end{aligned}
$$

$$
\begin{aligned}
Corr\left(\hat{\theta},\hat{\theta}_c\right) &= \frac{Cov\left(\hat{\theta},\hat{\theta}_c\right)}{\sqrt{Var\left(\hat{\theta}\right)Var\left(\hat{\theta}_c\right)}} \\
&= \frac{Var\left(\hat{\theta}\right)}{\sqrt{Var\left(\hat{\theta}\right)Var\left(\hat{\theta}_c\right)}} \\
&= \sqrt{\frac{Var\left(\hat{\theta}\right)}{Var\left(\hat{\theta}_c\right)}} \\
&= \sqrt{\frac{6n^{-1}\pi^{-2}\beta^{-2}\theta^2\left[\frac{\pi^2}{6}+\left(\gamma-1\right)^2\right]}{n^{-1}\left[q_c\gamma^{(2)}\left(1,z_c\right)-\left\{\gamma^{(1)}\left(1,z_c\right)\right\}^2\right]^{-1}\left\{q_c+\gamma^{(2)}\left(1,z_c\right)+2\gamma^{(1)}\left(1,z_c\right)\right\}}} \\
&= \sqrt{\frac{6\pi^{-2}\left[\frac{\pi^2}{6}+\left(\gamma-1\right)^2\right]\left[q_c\gamma^{(2)}\left(1,z_c\right)-\left\{\gamma^{(1)}\left(1,z_c\right)\right\}^2\right]}{\left\{q_c+\gamma^{(2)}\left(1,z_c\right)+2\gamma^{(1)}\left(1,z_c\right)\right\}}}
\end{aligned}
$$

As for the negative exponential case, these approximate correlations do not depend on n, and therefore hold across all sample sizes.

6.3.1 Finite sample checks of Weibull MLE correlations

Tables 6.2, 6.3, and 6.4, compare the theoretical and simulated correlations for varying censoring levels and $n = 1000$. We do this for three values of β; $\beta = 0.8$, which represents a decreasing hazard function, $\beta = 1$, a constant hazard function, and $\beta = 2$, an increasing hazard function. By checking each value, we hope to assess whether the theory holds for all types of Weibull failure data. We see that there is strong agreement between the theoretical and simulated results. These can now be used to obtain confidence intervals for $\hat{\beta}$ and $\hat{\theta}$

c	$Corr\left(\hat{\beta},\hat{\beta}_c\right)$	$Corr\left(\hat{\beta},\hat{\theta}_c\right)$	$Corr\left(\hat{\theta},\hat{\beta}_c\right)$	$Corr\left(\hat{\theta},\hat{\theta}_c\right)$
50	0.5499	0.1820	0.1722	0.5814
	0.5570	0.1787	0.1701	0.5859
100	0.6880	0.2552	0.2154	0.8150
	0.6904	0.2461	0.2118	0.8134
150	0.7715	0.2852	0.2415	0.9109
	0.7681	0.2818	0.2344	0.9087
200	0.8283	0.2983	0.2593	0.9529
	0.8259	0.2998	0.2552	0.9524

Table 6.2: Theoretical (above) and simulated (below) correlation of complete and censored MLEs obtained from a generated Weibull distribution with $\beta = 0.8$ and $\theta = 100$.

c	$Corr\left(\hat{\beta},\hat{\beta}_c\right)$	$Corr\left(\hat{\beta},\hat{\theta}_c\right)$	$Corr\left(\hat{\theta},\hat{\beta}_c\right)$	$Corr\left(\hat{\theta},\hat{\theta}_c\right)$
50	0.5179	0.1634	0.1621	0.5219
	0.5220	0.1613	0.1667	0.5214
100	0.6880	0.2552	0.2154	0.8150
	0.6868	0.2554	0.2285	0.8066
150	0.7919	0.2905	0.2479	0.9280
	0.7929	0.2894	0.2603	0.9253
200	0.8603	0.3035	0.2693	0.9695
	0.8601	0.3042	0.2779	0.9683

Table 6.3: Theoretical (above) and simulated (below) correlation of complete and censored MLEs obtained from a generated Weibull distribution with $\beta = 1$ and $\theta = 100$.

based on their censored counterparts, and are also needed to extend this analysis to the quantile function B_{10}. These tables show good agreement between theory and practice for all values of β considered, even at early censoring levels.

6.4 The reliability of censored MLEs

Following the same methodology as in the negative exponential case in Section 5.4, we can now measure the effectiveness of $\hat{\beta}_c$ and $\hat{\theta}_c$ as estimates of $\hat{\beta}$ and $\hat{\theta}$. We use

$$\Delta_\beta = \hat{\beta} - \hat{\beta}_c$$

and assume that the MLEs follow the normal distribution, and that we are dealing with unbiased estimators. We then have the mean,

$$E\left[\Delta_\beta\right] = E\left[\hat{\beta}\right] - E\left[\hat{\beta}_c\right] \simeq \beta - \beta \simeq 0$$

and variance

$$V_\beta = Var\left(\Delta_\beta\right) = Var\left(\hat{\beta} - \hat{\beta}_c\right) \simeq Var\left(\hat{\beta}\right) + Var\left(\hat{\beta}_c\right) - 2Cov(\hat{\beta},\hat{\beta}_c) \qquad (6.17)$$

c	$Corr\left(\hat{\beta},\hat{\beta}_c\right)$	$Corr\left(\hat{\beta},\hat{\theta}_c\right)$	$Corr\left(\hat{\theta},\hat{\beta}_c\right)$	$Corr\left(\hat{\theta},\hat{\theta}_c\right)$
50	0.3778	0.0898	0.1183	0.2869
	0.3865	0.0799	0.1076	0.2979
100	0.6880	0.2552	0.2154	0.8150
	0.6921	0.2420	0.2135	0.8110
150	0.8855	0.3067	0.2772	0.9795
	0.8895	0.2980	0.2778	0.9796
200	0.9728	0.3125	0.3045	0.9983
	0.9736	0.3064	0.2966	0.9982

Table 6.4: Theoretical (above) and simulated (below) correlation of complete and censored MLEs obtained from a generated Weibull distribution with $\beta = 2$ and $\theta = 100$.

and from (6.13) this becomes

$$\begin{aligned} V_\beta &\simeq Var\left(\hat{\beta}\right) + Var\left(\hat{\beta}_c\right) - 2Var\left(\hat{\beta}\right) \\ &\simeq Var\left(\hat{\beta}_c\right) - Var\left(\hat{\beta}\right) \end{aligned}$$

where both variances are given earlier, in (2.32) and (2.48), respectively. Under the same assumptions, we can obtain similar expressions for the expectations and variance of

$$\Delta_\theta = \hat{\theta} - \hat{\theta}_c.$$

Thus we have

$$\Delta_\beta \sim N\left(0, V_\beta\right),$$

and

$$\Delta_\theta \sim N\left(0, V_\theta\right).$$

So we have

$$\Pr\left\{-1.96 < \frac{\Delta_\beta}{\sqrt{V_\beta}} < 1.96\right\} = 0.95,$$

from which we can obtain the 95% confidence interval for $\hat{\beta}$, based on $\hat{\beta}_c$, as

$$\hat{\beta} = \hat{\beta}_c \pm 1.96\theta\sqrt{V_\beta}.$$

In practice we would then estimate the true value of β with the MLE $\hat{\beta}_c$ calculated at censoring time c, so we would have

$$\hat{\beta} = \hat{\beta}_c \pm 1.96\theta\sqrt{\hat{V}_\beta}.$$

where $\hat{V}_\beta$ is the variance of Δ_β calculated at $\beta = \hat{\beta}_c$. We have omitted the lengthy expressions of these variances, and instead kept the notation simple for ease of reading.

c	M	$\hat{\beta}_c$	$\hat{\theta}_c$	95% CI for $\hat{\beta}$	95% CI for $\hat{\theta}$
50	7	3.0866	69.4707	(1.1268, 5.0467)	(47.1535, 91.7855)
75	15	2.7634	72.8142	(1.8879, 3.6392)	(65.5866, 80.0416)
100	18	2.2398	80.3151	(1.7288, 2.7512)	(70.8859, 85.7459)
125	20	2.0731	82.4301	(1.7461, 2.4006)	(79.2384, 85.6246)
150	22	2.1268	81.5604	(1.9388, 2.3149)	(80.3327, 87.7889)
∞	23	2.1021	81.8783		

Table 6.5: Confidence Interval of $\hat{\beta}$ and $\hat{\theta}$ for the Ball Bearings data

The same process can be followed to obtain confidence intervals for $\hat{\theta}$, based on $\hat{\theta}_c$. We can now move on to look at some published examples and the perform some validation checks on the numerous asymptotic approximations, to discover the suitability of using such inference in finite samples.

6.4.1 Example: Ball bearings data

Applying the theoretical confidence intervals for β and θ to the censored ball bearings data MLEs, we obtain the numerical limits shown in Table 6.5. We notice that, as we increase the stopping time, and more items are allowed to fail, these confidence limits get smaller. As expected, the precision of the censored estimates increase as more information is collected.

Plotting these intervals with the MLEs, see Figure 6.1 for β and Figure 6.2 for θ, we clearly see the effect of extending the censoring time. There is much benefit to be gained from increasing c, but even at $c = 125$, when all but three items have failed, the confidence limits are still quite wide. We also point out that when censoring at $c = 75$, the confidence interval around $\hat{\theta}_c$ does not contain the complete estimate, and so does not provide a reliable guide to the estimate yielded at the end of the experiment.

6.4.2 Example: 49 failure times

Repeating the process for the 49 failure times data in Table 2.2, leads to the following 95% confidence intervals for $\hat{\beta}$ (Figure 6.3) and $\hat{\theta}$ (Figure 6.4). We again see the same pattern of very wide intervals, even when 90% of the items have failed. We note that $\hat{\beta} \simeq 1$, and so the analysis in Chapter 5 is still useful.

6.4.3 Simulation: Confidence intervals for $\hat{\beta}$ and $\hat{\theta}$

We have made checks throughout the theory development in the chapter, to ensure that the asymptotic theory is a good enough approximation to what we obtain in finite samples. Now we can validate the resulting confidence intervals using our simulation experiment set up. Again we simulate 10,000 MLEs yielded from failures following the Weibull distribution, with various n and c. We fix the scale parameter $\theta = 100$, but vary the shape parameter β, as we have already discussed the influence this has on the nature of the data. We count

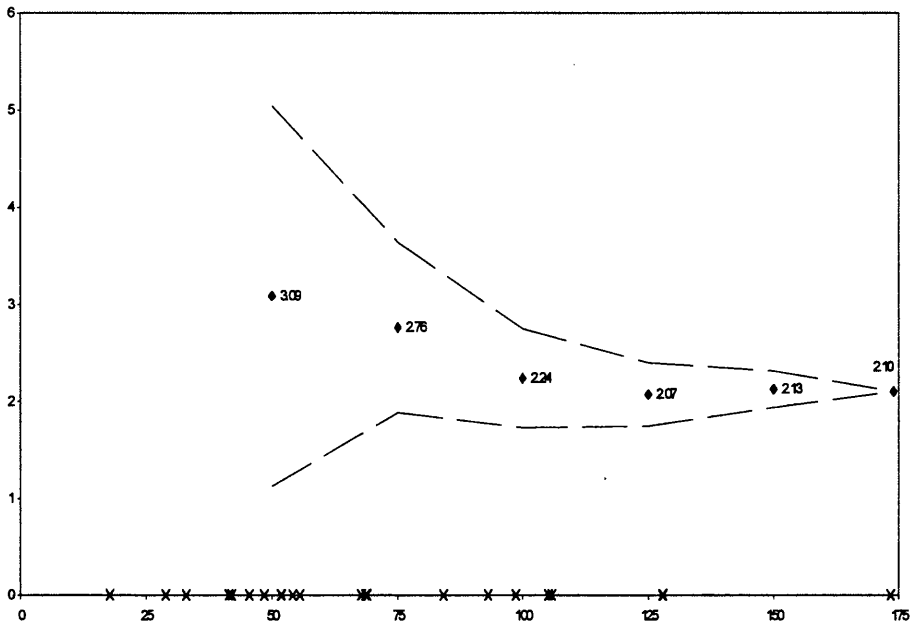

Figure 6.1: $\hat{\beta}_c$ and 95% confidence limits for $\hat{\beta}$ for various c for the ball bearings failure data ($\times$).

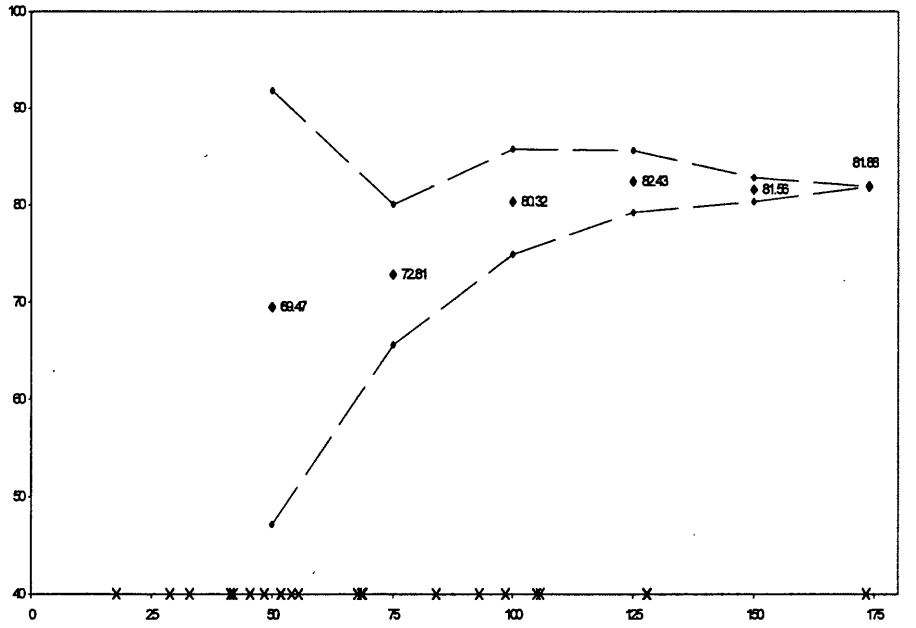

Figure 6.2: $\hat{\theta}_c$ and 95% confidence limits for $\hat{\theta}$ for various c for the ball bearings failure data ($\times$).

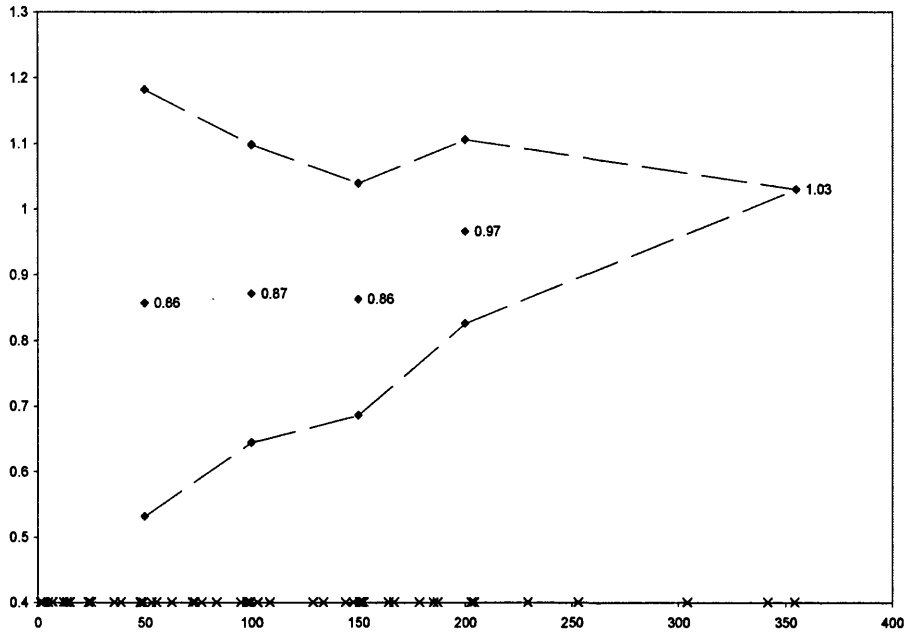

Figure 6.3: $\hat{\beta}_c$ and 95% confidence limits for $\hat{\beta}$ for various c for the 49 failure times data ($\times$).

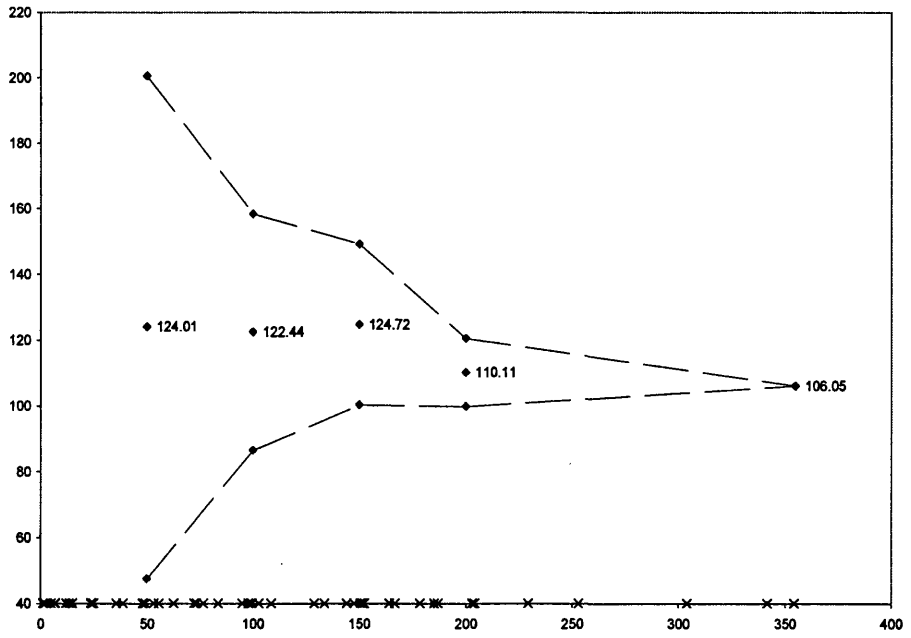

Figure 6.4: $\hat{\theta}_c$ and 95% confidence limits for $\hat{\theta}$ for various c for the 49 failure times data ($\times$).

c	n				
	50	100	300	500	1000
50 : $\hat{\beta}$	92.89	93.98	93.80	94.62	95.10
: $\hat{\theta}$	90.67	92.49	93.80	93.98	94.82
100 : $\hat{\beta}$	93.92	94.35	94.30	94.99	94.91
: $\hat{\theta}$	91.73	92.88	93.91	94.67	94.75
150 : $\hat{\beta}$	94.17	94.51	94.92	94.95	94.82
: $\hat{\theta}$	91.64	93.20	94.07	94.45	94.63
200 : $\hat{\beta}$	94.77	95.12	95.18	95.26	94.65
: $\hat{\theta}$	91.97	93.09	94.35	94.90	94.35

Table 6.6: Percentage of $\hat{\beta}$ (top line), and $\hat{\theta}$ (bottom line) covered by Confidence Interval for simulated Weibull data with $\beta = 0.9$ and $\theta = 100$

c	n				
	50	100	300	500	1000
50 : $\hat{\beta}$	92.49	94.04	94.52	94.57	94.40
: $\hat{\theta}$	90.88	92.71	93.81	94.52	94.34
100 : $\hat{\beta}$	93.77	94.55	94.66	94.67	94.86
: $\hat{\theta}$	91.31	93.19	93.83	94.22	94.65
150 : $\hat{\beta}$	94.69	94.68	94.75	95.14	94.32
: $\hat{\theta}$	91.87	93.04	94.15	94.65	94.47
200 : $\hat{\beta}$	95.34	94.93	94.76	94.99	94.67
: $\hat{\theta}$	92.13	93.30	94.05	94.55	94.46

Table 6.7: Percentage of $\hat{\beta}$ covered by Confidence Interval for simulated Weibull data with $\beta = 1$ and $\theta = 100$

the number of complete MLEs are within the confidence intervals that have been fitted to our corresponding 10,000 censored estimates.

Tables 6.6 to 6.9 display these results in percentages at $\beta = 0.9, 1, 1.1$, and 2. This again covers a wide range of failure rates, and ensures that the changing hazard function around $\beta = 1$ does not have a detrimental effect on the coverage power of the confidence interval. We see that the results agree well with theory, particularly for increasing n and c.

6.5 Correlation of lifetime quantile estimates

We can also assess the correlation between MLEs of linear relationships of $\hat{\beta}$ and $\hat{\theta}$, by computing the theoretical correlation between the complete and censored lifetime quantiles. For a simulation we know that the true value of B_{10} is

$$B_{10,0} = \theta_0 \times \lambda^{1/\beta_0}, \tag{6.18}$$

c	n				
	50	100	300	500	1000
50 : $\hat{\beta}$	92.63	94.07	94.72	94.51	95.38
: $\hat{\theta}$	90.92	91.79	94.20	94.60	94.72
100 : $\hat{\beta}$	93.97	94.59	94.79	94.42	95.40
: $\hat{\theta}$	91.61	92.91	94.24	94.42	94.84
150 : $\hat{\beta}$	94.50	95.00	94.79	94.90	95.44
: $\hat{\theta}$	91.93	93.17	94.22	94.32	95.01
200 : $\hat{\beta}$	95.22	95.26	94.75	94.98	95.19
: $\hat{\theta}$	91.90	93.15	93.98	94.46	95.13

Table 6.8: Percentage of $\hat{\beta}$ covered by Confidence Interval for simulated Weibull data with $\beta = 1.1$ and $\theta = 100$

c	n				
	50	100	300	500	1000
50 : $\hat{\beta}$	90.56	92.27	94.18	94.59	94.58
: $\hat{\theta}$	91.01	92.19	94.20	94.27	94.35
100 : $\hat{\beta}$	93.76	93.98	94.71	95.27	94.82
: $\hat{\theta}$	93.04	93.68	94.43	94.61	94.55
150 : $\hat{\beta}$	95.16	94.95	95.34	95.10	94.98
: $\hat{\theta}$	92.37	93.36	94.37	94.72	94.90
200 : $\hat{\beta}$	96.55	95.74	95.59	95.38	95.01
: $\hat{\theta}$	91.94	92.48	94.48	94.33	94.52

Table 6.9: Percentage of $\hat{\beta}$ covered by Confidence Interval for simulated Weibull data with $\beta = 2$ and $\theta = 100$

where $\lambda = -\ln(0.9)$, as in (2.53). Via a Taylor Series expansion we have

$$\begin{aligned}\hat{B}_{10} &\doteqdot B_{10,0} + \left(\hat{\theta} - \theta_0\right)\frac{\partial B_{10}}{\partial \theta}|_{\beta=\beta_0,\theta=\theta_0} + \left(\hat{\beta} - \beta_0\right)\frac{\partial B_{10}}{\partial \beta}|_{\beta=\beta_0,\theta=\theta_0} \\ &\doteqdot B_{10,0} + \lambda^{\frac{1}{\beta_0}}\left(\hat{\theta} - \theta_0\right) - \beta_0^{-2} B_{10,0}\left(\ln\lambda\right)\left(\hat{\beta} - \beta_0\right)\end{aligned}$$

and using (6.18), this becomes

$$\hat{B}_{10} \doteqdot B_{10,0}\left[1 + \theta_0^{-1}\left(\hat{\theta} - \theta_0\right) - \left(\ln\lambda\right)\beta_0^{-2}\left(\hat{\beta} - \beta_0\right)\right].$$

This approximation agrees with simulations, and we can also assume the following for the censored estimate,

$$\hat{B}_{10,c} \doteqdot B_{10,0}\left[1 + \theta_0^{-1}\left(\hat{\theta}_c - \theta_0\right) - \left(\ln\lambda\right)\beta_0^{-2}\left(\hat{\beta}_c - \beta_0\right)\right]$$

which also agrees with simulations, but the strength of the approximation appears to decrease with early censoring times.

From this we can obtain the covariance between the complete and censored MLEs of B_{10},

$$\begin{aligned}Cov\left(\hat{B}_{10}, \hat{B}_{10,c}\right) &= B_{10}^2\left\{\begin{array}{l}\theta^{-2}Cov\left(\hat{\theta}, \hat{\theta}_c\right) + \left(\ln\lambda\right)^2\beta^{-4}Cov\left(\hat{\beta}, \hat{\beta}_c\right) \\ -\left(\ln\lambda\right)\theta^{-1}\beta^{-2}\left[Cov\left(\hat{\theta}, \hat{\beta}_c\right) + Cov\left(\hat{\beta}, \hat{\theta}_c\right)\right]\end{array}\right\} \qquad (6.19) \\ &= B_{10}^2\left\{\frac{6}{n\pi^2\beta^2}\left[\left(\ln\lambda\right)^2 - 2\left(\ln\lambda\right)(1-\gamma) + \left[\frac{\pi^2}{6} + (\gamma-1)^2\right]\right]\right\} \\ &= \frac{6\theta^2\left\{\lambda^{\frac{1}{\beta}}\right\}^2}{n\pi^2\beta^2}\left[\left(\ln\lambda\right)^2 - 2\left(\ln\lambda\right)(1-\gamma) + \left[\frac{\pi^2}{6} + (\gamma-1)^2\right]\right]\end{aligned}$$

and from (2.54) and (2.55), it is straightforward to establish

$$Cov\left(\hat{B}_{10}, \hat{B}_{10,c}\right) = Var\left(\hat{B}_{10}\right).$$

From this we can obtain the correlation using

$$\begin{aligned}Corr\left(\hat{B}_{10}, \hat{B}_{10,c}\right) &= \frac{Cov\left(\hat{B}_{10}, \hat{B}_{10,c}\right)}{\sqrt{Var\left(\hat{B}_{10}\right)Var\left(\hat{B}_{10,c}\right)}} \\ &= \sqrt{\frac{Var\left(\hat{B}_{10}\right)}{Var\left(\hat{B}_{10,c}\right)}}.\end{aligned}$$

where the variances are given in (2.54) and (2.55). We can then compare this theoretical correlation with a simulated counterpart with varying c and n. We see from Table 6.10

c	β		
	0.8	1	2
50	0.8671	0.8632	0.8585
	0.8683	0.8636	0.8613
100	0.8952	0.8952	0.8952
	0.8950	0.8948	0.8965
150	0.9186	0.9248	0.9558
	0.9170	0.9249	0.9572
200	0.9364	0.9471	0.9883
	0.9357	0.9469	0.9883

Table 6.10: Theoretical (above) and Simulated (below) correlation of complete and censored estimates of B_{10} obtained from a generated Weibull distribution with various β, $\theta = 100$, and $n = 1000$.

that the theoretical and simulated results are in good agreement.

6.6 The Reliability of $\hat{B}_{10,c}$

Statistical and reliability literature provides numerous methods and opinions on calculating confidence intervals of distribution parameters, see for example Meeker & Nelson (1977), or Thoman et al. (1969). We however, wish to obtain a confidence interval of the estimated lifetime percentile, $\hat{B}_{10}$ of a complete sample, given that we know the value of censored $\hat{B}_{10,c}$ at time c. We use

$$\Delta_{B10} = \hat{B}_{10} - \hat{B}_{10,c}$$

and assume both Normality and that we are dealing with unbiased estimators.

We then have

$$E\left[\Delta_{B10}\right] = E\left[\hat{B}_{10}\right] - E\left[\hat{B}_{10,c}\right] \simeq B_{10} - B_{10} \simeq 0$$

and

$$\begin{aligned} V_{B10} &= Var\left(\hat{B}_{10} - \hat{B}_{10,c}\right) \\ &= Var\left(\hat{B}_{10}\right) + Var\left(\hat{B}_{10,c}\right) - 2Cov(\hat{B}_{10}, \hat{B}_{10,c}) \\ &= Var\left(\hat{B}_{10,c}\right) - Var\left(\hat{B}_{10}\right) \end{aligned}$$

which are given in (2.54). Therefore, under the above assumptions we have $\Delta \sim N\left(0, V_{B10}\right)$.

So we have the probability

$$\Pr\left\{-1.96 < \frac{\Delta_{B10}}{\sqrt{V_{B10}}} < 1.96\right\} = 0.95$$

c	Items failed	$\hat{B}_{10,c}$	95% Confidence Interval
50	7	33.5100	(30.3951, 36.6249)
75	15	32.2525	(29.6285, 34.8766)
100	18	29.4100	(26.9381, 31.8819)
125	20	27.8427	(25.9415, 29.7440)
150	22	28.3120	(27.1735, 29.4504)
∞	23	28.0694	

Table 6.11: Confidence Interval of $\hat{B}_{10}$ for Ball Bearings data

From which we can obtain the 95% confidence interval for $\hat{B}_{10}$ below

$$\hat{B}_{10} = \hat{B}_{10,c} \pm 1.96\sqrt{V_{B10}} \tag{6.20}$$

As for $\hat{\beta}$ and $\hat{\theta}$, in practice we would then estimate the variance of Δ_{B10} using the MLEs in place of the true parameter values.

6.6.1 Example: Ball bearings data

We recall the Ball Bearing example, lifetimes given in Table 1.2, and censored MLEs given in Table 2.5. Using a SAS program we calculate the 95% confidence interval, (6.20), of $\hat{B}_{10}$ at censoring times $c = 50, 100, 150$, and 200. Table 6.11 displays the results, and we can observe the confidence interval in Figure 6.5.

We see a different message here compared to the intervals for $\hat{\beta}$ and $\hat{\theta}$ discussed in the previous section. The interval width does not change as much when c increases, and in fact, there appears to little more benefit waiting until time $c = 125$, compared to the precision obtained at $c = 50$. This may have a positive impact on the experimental design process, depending on what level of precision is acceptable. The best option would be to allow all items to fail, but if this was not feasible, then early censoring would possibly provide a reasonable guide to the final analysis estimate.

6.6.2 Example: 49 failure times

Fitting the confidence intervals to the 49 failure times data leads to the confidence interval for B_{10} in Figure 6.6. Again we do not see vast improvement in the precision of the estimate as the censoring level increases from $c = 50$ to $c = 200$.

6.6.3 Simulations

We use our generated MLEs calculated from a Weibull distribution, with various shape parameters β, $\theta = 100$, again at different censoring levels, and for a number of different sample sizes. We then use equation (6.20), given above, to find the proposed 95% confidence interval from each censored $\hat{B}_{10,c}$ generated, and then the percentage of these intervals from the 10,000 repetitions that actually contain the corresponding complete MLE, $\hat{B}_{10}$ is

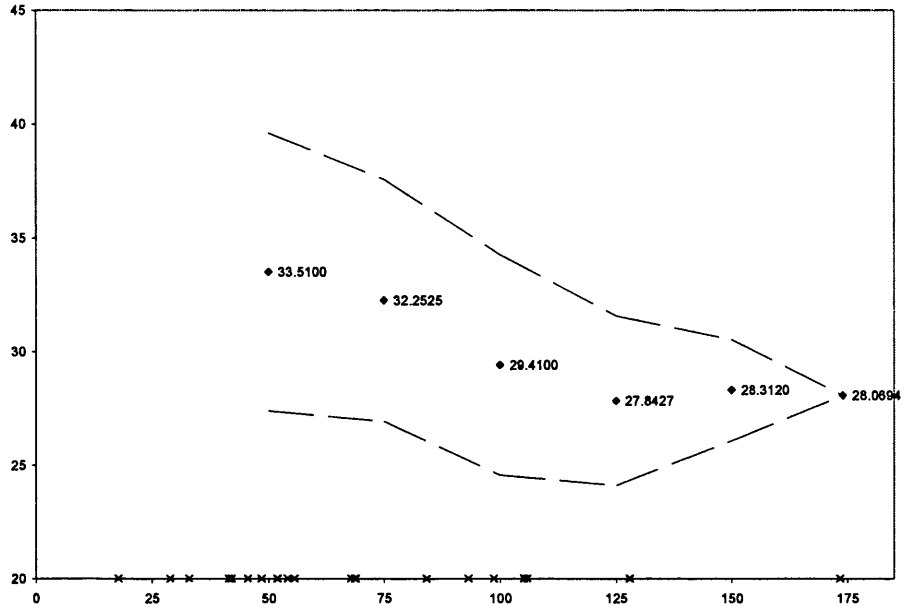

Figure 6.5: $\hat{B}_{10,c}$ and 95% confidence limits for $\hat{B}_{10}$ for various c for the ball bearings data ($\times$).

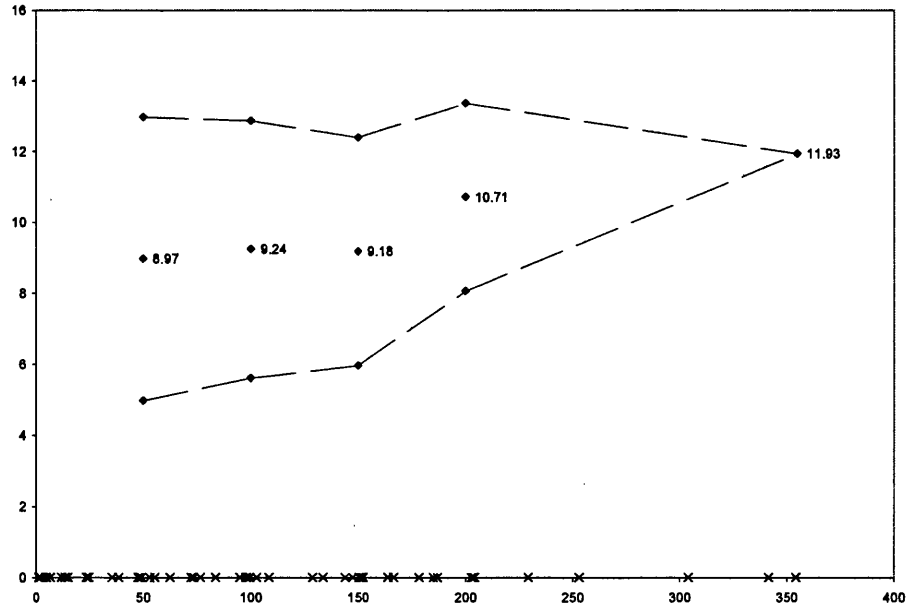

Figure 6.6: $\hat{B}_{10,c}$ and 95% confidence limits for $\hat{B}_{10}$ for various c for the 49 failure times data ($\times$).

c	n				
	50	100	300	500	1000
50	92.90	93.83	94.45	94.87	94.97
100	93.05	93.69	94.43	94.85	94.84
150	93.08	93.53	94.51	94.89	94.67
200	93.68	94.15	94.92	94.93	94.67

Table 6.12: Percentage of $\hat{B}_{10}$ covered by Confidence Interval for simulated Weibull data with $\beta = 0.9$ and $\theta = 100$

c	n				
	50	100	300	500	1000
50	93.54	94.30	94.48	94.57	94.61
100	93.32	94.28	94.62	94.92	94.79
150	93.66	94.10	94.73	94.95	94.42
200	94.28	94.42	94.49	94.80	94.60

Table 6.13: Percentage of $\hat{B}_{10}$ covered by Confidence Interval for simulated Weibull data with $\beta = 1$ and $\theta = 100$

calculated. Tables 6.12 to 6.15 summarises these percentages, and we see the simulations agree with our theoretical 95% confidence interval of $\hat{B}_{10}$ obtained using the $\hat{B}_{10,c}$ estimate for all combinations of β, c, and n tried.

6.7 Summary

We have obtained general expressions for the correlations between the two sets of maximum likelihood estimates of Weibull parameters β and θ, and the percentile B_{10}. These, in turn, yield approximate 95% confidence limits for the final estimate given the interim estimate. Our formulae are relatively straightforward and computationally tractable. The correlations follow immediately from the EFI matrix, presented in Chapter 2. We have also shown that these asymptotic results agree with the behavior observed in simulation experiments for various combinations of censoring time c and (finite) sample size n.

In practical terms, we have established a link between censored and complete estimates, and have provided a method for a data user, or experiment manager, to quickly analyse

c	n				
	50	100	300	500	1000
50	94.37	94.38	94.95	94.79	95.58
100	94.11	94.32	94.82	94.58	95.42
150	94.03	94.59	94.78	94.79	95.36
200	94.51	94.64	94.61	95.15	95.14

Table 6.14: Percentage of $\hat{B}_{10}$ covered by Confidence Interval for simulated Weibull data with $\beta = 1.1$ and $\theta = 100$

c	n				
	50	100	300	500	1000
50	93.89	94.99	94.95	95.22	95.19
100	95.68	95.55	94.93	95.02	95.15
150	96.03	95.38	94.79	95.42	95.64
200	96.63	95.88	95.50	95.65	95.37

Table 6.15: Percentage of $\hat{B}_{10}$ covered by Confidence Interval for simulated Weibull data with $\beta = 2$ and $\theta = 100$

interim experiment results, and decide using a measure of precision if that interim estimate is sufficient to provide inference from, or whether the experiment should continue and allow more items to fail. Clearly there will have to be some loss in precision of the parameter estimates in order to cap experimental costs, but now these are more quantifiable and easier to compare.

Chapter 7

Practical Implications and Conclusions

In this final chapter, we discuss the work completed in previous chapters, outline the practical implications of our work, and consider further areas of investigation.

7.1 Discussion

The aim of this thesis is to develop the theory already used in reliability analysis. The requirement for sound methods in reliability is essential, and as discussed in chapter one, reliability analysis is used to provide inference, and address problems in a variety of disciplines; for example, engineering, biology, and economics. The specific areas of research considered throughout this thesis are of a more practical nature, and we have provided more detailed information and solutions for the methods and techniques that are most often used in practice, rather than develop more sophisticated theory, that consequently would rarely be used by practitioners.

The main focus of this thesis has been on the effect censoring has on the properties and precision of the Weibull MLEs, and to establish some guidelines on an optimal time to stop an experiment, which maximises the practical benefits while minimising the loss of statistical information. The decision to concentrate on Weibull MLEs was made early, and was based both on their widespread use in practice, and favorable theoretical properties.

The Weibull distribution is the most commonly used lifetime distribution in practice, due to the flexibility it has in modelling a variety of life characteristics, achieved via the shape parameter. There are a number of estimation methods available to obtain parameter estimates for lifetime models, and as discussed in chapter one, we chose ML (maximum likelihood), which have desirable asymptotic properties. We concentrate on Type I censoring, as a fixed experiment time means that it may often be easier to plan, and therefore it is more regularly implemented in practice.

Chapter two was concerned with fitting the Weibull distribution to data sets via ML, and

we illustrated our techniques on the ball bearings data, and the 49 failure times data from Epstein (1960). We began by fitting the Weibull distribution to complete data, then moved on to Type I censored data. Simulation studies investigated factors such as the sample size, and true shape parameter value β, in addition to censoring time, that may affect the bias and precision of MLEs and the quantile B_{10}. We then considered the theoretical EFI matrix for complete and censored data, which leads to asymptotically valid variances and covariance of the Weibull parameters and quantile function.

Throughout it has been our intention to assess the extent to which asymptotic results held for small to moderate samples, particularly when considering the role of censoring. Numerous simulation studies were carried out, and, in addition, theoretical values were obtained. For various sample sizes, we were then able to observe the agreement between the asymptotic results and practical (simulated) results. This check on moments was done for various values of the shape parameters, covering decreasing, increasing and constant hazard functions.

We found generally good agreement between simulated and theoretical results, and this improved as the sample size and censoring time increased. For the estimates of β and θ, large sample sizes will generally yield more precise estimates, but, when using a censoring regime, gains can be made in the precision of our estimates if we reduce the sample size, as long as the censoring time is then increased. For example, the estimates obtained at $n = 500$ and $c = 100$, are more precise than those at $n = 1000$ and $c = 50$. However, this is not the case for B_{10}, where the sample size is the main factor affecting the precision of the estimates. Thus, it may be more beneficial to increase the sample size being tested, but reduce the censoring time, as this would generally yield a more precise estimate of B_{10}. In circumstances where the cost of the items being tested are not excessively greater than the cost of running the experiment, this would also help to reduce the total cost of an experiment. We now review the three main problems regarding ML estimation under a type I censoring regime that this thesis considered.

7.1.1 Tests for Asymptotic Normality of MLEs

The general property of asymptotic Normality of MLEs is widely known, and is used in practice to obtain approximate confidence regions around parameters. We investigated the distribution of the MLEs, with particular emphasis on the rate at which the MLEs approach Normality, for increasing n. We also demonstrated the effect Type I censoring has on the progress towards Normality. Using numerical simulations, we have also ascertained the extent to which large sample Normality theory applies to smaller sample sizes. Similar studies have been carried out previously by researchers, but their result were commonly based on as few as 500 simulations, and complicated calculations were often done by hand. This thesis updates such research, using the computational resources that are available today.

Despite chapter two showing strong agreement between practical and asymptotic vari-

ances of Weibull MLEs, formal tests showed that Normality was not reached until samples were very large, and censoring only impaired this progress. Univariate tests on estimates for the two distributional parameters showed that both $\hat{\beta}_c$ and $\hat{\theta}_c$ were skewed to the right, but $\hat{\theta}_c$ reached Normality quicker than $\hat{\beta}_c$. The rate at which Normality is approached by increasing sample size depends on the true shape parameter, β, and this seems to affect the distribution of $\hat{\beta}_c$ and $\hat{\theta}_c$ differently, with the distribution of $\hat{\theta}_c$ reaching Normality much faster than $\hat{\beta}_c$, particularly when the true shape parameter $\beta > 2$. Formal tests of Normality on the simulated $B_{10,c}$ MLEs showed that the assumption of Normality is implausible in sample sizes less than $n = 1000$.

Despite these poor approximations to the Normal distribution, precision and confidence intervals obtained in the simulation studies still provided good coverage of the MLEs, but the shape of the distribution of $\left(\hat{\beta}_c, \hat{\theta}_c\right)$ is not well represented, particularly for early censoring. This resulted in the investigation of an alternative method to measure precision.

7.1.2 An Alternative Measure of Precision - Relative Likelihood

Chapter 4 considered an alternative method for quantifying the precision in the estimates of Weibull parameters. We investigated factors affecting the precision of MLEs, such as sample size and censoring levels, using relative likelihood theory. Relative likelihood methods are discussed in most reliability text books, but, due to the computational burden involved, is used less often in practice.

We outlined an algorithm to compute contours at various levels of relative likelihood, and displayed these for the ball bearings and Epstein's failure times examples. As we would expect, the contours generally tend to become smaller when the censoring time increases, and became more elliptical implying bivariate Normality when the value of the contour increases. When comparing with Normal theory confidence regions, we have shown that the two curves overlap, and as the censoring time c increases, the overlap increases, with the relative likelihood contour moving towards the asymptotic Normal ellipse. For large samples the two confidence regions would be quite similar, as the methods are asymptotically equivalent.

We then extended this to the general sampling distribution of $\left(\hat{\beta}_c, \hat{\theta}_c\right)$, with the usual investigation of various n and c. We then used the expected order statistics as data values for an idealised Weibull sample, and on applying a type I censoring regime to this sample, obtained relative likelihood contours for that sample. These gave much better representative to the multivariate distribution of the Weibull MLEs.

Despite the more complicated computations involved in the relative likelihood approach to approximating confidence regions, with the computational capabilities available today, we can reasonably recommend the use of relative likelihood contours as an alternative measure of precision in small to moderate samples, as discussed above, where the asymptotic Normality assumption is not valid.

7.1.3 Interim Analysis - The Reliability of Censored Reliability Analyses

Finally, we investigate the problem of identifying an optimum time to censor. We started by setting $\beta = 1$, and therefore simplifying to the negative exponential distribution, and using the usual asymptotic relationship between the MLE, the expected Fisher information and the score function, we calculated the correlation between the censored and complete estimate. This approximate correlation does not depend on n, and therefore holds across all sample sizes. This correlation then provided a measure of precision of the censored estimate $\hat{\theta}_c$, as an estimate of $\hat{\theta}$. Confidence intervals were presented for published examples, and some practical issues of experimental design were identified. A smaller interval, and therefore a more precise estimate to the complete MLE, will be obtained if the number of items tested, n, increases, or if the number of items allowed to fail increases, by extending the censoring time, c. Either option to tighten the confidence interval will add expense to the experiment, and so the importance of the precision in the interval must be weighed against the costs involved.

Such confidence intervals were validated using simulation studies, and, again, this was undertaken for various sample sizes, censoring levels and shape parameters. The simulation experiments again confirmed that, despite the lack of Normality in MLEs based on data in samples with n smaller than 1000, the approximations obtained from asymptotic Normal theory still leads to reliable inference for small to moderate sample sizes.

Next, we generalised the results from the negative exponential distribution to the Weibull distribution. The analysis proved to be more detailed, but the same concepts held, and the corresponding relationships between censored and complete estimates were found. The correlations followed immediately from the EFI matrix, with the theory presented in Chapter 2. We also showed that these asymptotic results agree with the behaviour observed in simulation experiments for various combinations of censoring time c and sample size n.

By exploiting the asymptotic relationships between the MLEs, transforming a Weibull random variable to a negative exponential random variable thereby simplifying the calculations, and using the truncated negative exponential distributions to handle complicated relationships between the number of failures and expectations involving failure and survivor times, this thesis has used a novel approach, which has contributed some new knowledge to the field of reliability. We have established a link between censored and complete Weibull MLEs, thus providing a method for a data user, or experimental manager, to analyse interim experiment results, and decide, using a measure of precision, whether that interim estimate is sufficient to provide inference from, or whether the experiment should continue and allow more items to fail.

7.2 Areas for Future Research

As discussed in section 1.6, the algorithms, simulations and numerical calculations were developed in SAS or Mathematica. We could consider other available packages such as *R*,

which, due to its wide availability and extensibility, is a popular choice for many statisticians today. We refer to Chambers (2007) for further details on programming in *R*.

Throughout our work, we have generally considered the Weibull distribution, and, naturally, it would be of interest to extend this research to alternative reliability distributions, such as the Burr XII distribution mentioned in chapter 1. We considered Type I censoring to speed up the running time of experiments, but alternative censoring regimes, such as Type II censoring could also be investigated. Though it has been shown that the Fisher information matrices for Type I and Type II censored data are asymptotically equivalent, see, for example, Escobar & Meeker (2001), it would be of some interest to compare the two regimes, and see how the results differ in finite sample sizes.

An alternative, or additional, approach to the efficient testing of experimental items is the use of accelerated life testing (ALT). In this process, we would exert an item to one or more external stresses - such as temperature, current or humidity - above and beyond those found in normal operating conditions, in an attempt to induce early failure. Nelson (1990) provides practical details on ALT, which could initiate further research to the analysis of Weibull reliability data.

Chapter 3 gave an in-depth investigation into the suitability of assumption of Normality of MLEs, generated from small to moderate samples of failure data. Tests were chosen on the basis of their power properties and ease in computation, but there are other tests for Normality, or transformations to Normality, that we could have used and displayed, if space and time had allowed. We refer to Thode (2002) for details on such alternative tests.

In chapter 4 we considered the overlap between the confidence regions obtained from Normal theory and relative likelihood, but the extent to which they agree, and how they differ could be examined in much further detail. To investigate the use of relative likelihood contours for the general sampling distribution of $\left(\hat{\beta}_c, \hat{\theta}_c\right)$ we used the expected order statistics of the Weibull distribution to obtain our *idealised* sample. Alternative methods of creating such a Weibull sample are available, and would be worthy of further investigation.

In our study of interim analysis, we proved a general relationship between the covariances of complete and censored MLEs ($\hat{\beta}$, $\hat{\beta}_c$, $\hat{\theta}$, and $\hat{\theta}_c$), and the complete EFI matrix. The relationship seems to be a consequence of the lack-of-memory property, and we should not assume that it holds more generally. Thus, further research is needed to generalise our work for data following other distributions, using a conditioning argument on M (random in Type I censored experiments), as well as data under alternative censoring regimes.

Finally, in several places, we have mentioned the objective of exploiting finite resources in an optimal way, and, in this regard, the evaluation of a cost model to provide structured information for a data user or experimental manager, weighing up the financial cost versus the loss in precision, would be of great practical use.

Bibliography

Abramowitz, M. & Stegun, I. A. (1972), *Handbook of Mathematical Functions with Formulas, Graphs and Mathematical Tables.* Wiley-Interscience.

Ansell, J. I. & Phillips, M. J. (1994), *Practical Methods for Reliability Data Analysis.* Oxford Statistical Science Series, Oxford University Press.

Balakrishnan, N. & Rao, C. R. (editors) (1997), *Order Statistics-Theory and Methods*, volume 16 of *Handbook of Statistics.* Elsevier Science B.V.

Burr, I. W. (1942), Cumulative Frequency Function. *Annals of Mathematical Statistics*, **13**: 215–232.

Caroni, C. (2002), The Correct "Ball Bearings" Data. *Lifetime Data Analysis*, **8**(4): 395–399.

Chambers, J. M. (2007), *Software for Data Analysis: Programming with.* Springer, New York.

Chua, S. J., Finselbach, H. K. & Watkins, A. J. (2007), Small Sample Properties of Maximum Likelihood Estimators for Type II Censored Data. *Proceedings of the 22nd International Workshop on Statistical Modelling, Barcelona.*

Cohen, A. C. (1991), *Truncated and Censored Samples - Theory and Applications.* Marcel Dekker.

Cox, D. R. & Hinkley, D. V. (1974), *Theoretical Statistics.* Chapman and Hall.

Cramer, H. (1946), *Mathematical Methods of Statistics.* Princeton University Press.

Crowder, M. J., Kimber, A. C., Smith, R. L. & Sweeting, T. J. (1991), *Statistical Analysis of Relaibility Data.* Chapman and Hall / CRC.

D'Agostino, R. & Pearson, E. S. (1973), Tests for Departure from Normality. Empirical Results for the Distributions of b_2 and $\sqrt{b_1}$. *Biometrika*, **60**(3): 613–622.

D'Agostino, R. B. (1971), An Omnibus Test of Normality for Moderate and Large Size Samples. *Biometrika*, **58**(2): 341–348.

D'Agostino, R. B., Belanger, A. & D'Agostino Jr, R. B. (1990), A Suggestion for Using Powerful and Informative Tests of Normality. *The American Statistician*, **44**(4): 316–321.

D'Agostino, R. B. & Stephens, M. A. (1986), *Goodness-of-Fit Techniques*. Marcel Dekker.

David, H. A. & Nagaraja, H. N. (2003), *Order Statistics*. John Wiley and Sons, 3rd edition.

Der, G. & Everitt, B. S. (2002), *A Handbook of Statistical Analyses Using SAS*. Chapman and Hall / CRC.

Epstein, B. (1960), Tests for the Validity of the Assumption That the Underlying Distribution of Life is Exponential: Part II. *Technometrics*, **2**(2): 167–183.

Escobar, L. A. & Meeker, W. Q. (2001), The Asymptotic Equivalence of the Fisher Information Matrices for Type I and Type II Censored Data from Location-Scale Families. *Communications in Statistics- Theory and Methods*, **30**(10): 2211–2225.

Farnum, N. R. & Booth, P. (1997), Uniqueness of Maximum Likelihood Estimators of the 2-Parameter Weibull Distribution. *IEEE Transactions on Reliability*, **46**(4): 523–525.

Finselbach, H. K. & Watkins, A. J. (2006), The Reliability of Censored Reliability Analyses. *Proceedings of the 21st International Workshop on Statistical Modelling, Galway*: 182–189.

Gradshteyn, I. & Ryzhik, I. (2000), *Table of Integrals, Series, and Products*. Academic Press, SanDiego, sixth edition.

Gross, A. J. & Clark, V. A. (1975), *Survival Distributions: Reliability Applications in the Biomedical Sciences*. John Wiley and Sons.

Healy, M. J. R. (1968), Multivariate Normal Plotting. *Applied Statistics*, **17**: 157–161.

Kalbfleisch, J. D. & Prentice, R. L. (1980), *The Statistical Analysis of Failure Time Data*. John Wiley and Sons.

Kalbfleisch, J. G. (1979), *Probability and Statistical Inference II*. Springer-Verlag.

Khattree, R. & Rao, C. R. (editors) (2003), *Statistics in Industry*, volume 22 of *Handbook of Statistics*. Elsevier Science B. V.

Lawless, J. F. (1982), *Statistical Models and Methods for Lifetime Data*. John Wiley and Sons.

Leech, D. J. & Watkins, A. J. (1990), Some Factors Affecting Precision in Estimators of Parameters of Lifetime Distributions. *Reliability Engineering and System Safety*, **29**: 249–260.

Lieblein, J. & Zelen, M. (1956), Statistical Investigation of the Fatigue Life of Deep Groove Ball Bearings. *Journal of Research of the National Bureau of Standards*, **57**: 273–316.

Mann, N. R., Schafer, R. E. & Singpurwalla, N. D. (1974), *Methods for Statistical Analysis of Reliability and Life Data.* John Wiley and Sons.

Mardia, K. V. & Foster, K. (1983), Omnibus Tests of Multinormality Based on Skewness and Kurtosis. *Communications in Statistics- Theory and Methods*, **12**(2): 207–221.

Mardia, K. V., Kent, J. T. & Bibby, J. M. (1979), *Multivariate Analysis.* Academic Press Ltd.

Meeker, W. Q. & Escobar, L. A. (1995), Teaching About Approximate Confidence Regions Based on Maximum Likelihood Estimation. *The American Statistician*, **49**(1): 48–53.

Meeker, W. Q. & Nelson, W. (1977), Weibull Variances and Confidence Limits by Maximum Likelihood for Singly Censored Data. *Technometrics*, **19**(4): 473–476.

Montgomery, D. C. & Runger, G. C. (1994), *Applied Statistics and Probability for Engineers.* John Wiley and Sons.

Murdoch, J. & Barnes, J. A. (1974), *Statistical Tables for Science, Engineering, Management and Business Sciences.* Macmillan Ltd, 2nd edition.

Nelson, W. (1982), *Applied Life Data Analysis.* John Wiley and Sons.

Nelson, W. (1990), *Accelerated Testing: Statistical Models, Test Plans, and Data Analyses.* John Wiley Sons.

Peng, D. & MacKenzie, G. (2007), On the Analysis of Censored Reliability Data. *Proceedings of the 22nd International Workshop on Statistical Modelling, Barcelona*: 481–484.

Richards, D. O. & McDonald, J. B. (1987), A General Methodology for Determining Distributional Forms with Applications in Reliability. *Journal of Statistical Planning and Inference*, **16**: 365–376.

Ross, R. (1996), Bias and Standard Deviation Due to Weibull Parameter Estimation for Small Data Sets. *IEEE Transactions on Dielectrics and Electrical Insulation*, **3**(1): 28–42.

Royston, J. P. (1982), An Extension of Shapiro and Wilk's W Test for Normality to Large Samples. *Applied Statistics*, **31**(2): 115–124.

SAS (2004), SAS/IML 9.1 Users Guide. Technical report, SAS Institute Inc.

Shapiro, S. S. & Francia, R. S. (1972), An Approximate Analysis of Variance Test Normality. *Journal of the American Statistical Association*, **67**: 215–216.

Shapiro, S. S. & Wilk, M. B. (1965), An Analysis of Variance Test for Normality (Complete Samples). *Biometrika*, **52**: 591–611.

Shapiro, S. S., Wilk, M. B. & Chen, H. J. (1968), A Comparative Study of Various Tests for Normality. *Journal of the American Statistical Association*, **63**: 1343–1372.

Shenton, L. R. & Bowman, K. O. (1977), *Maximum Likelihood Estimation in Small Samples.* Charles Griffin Company Ltd.

Slater, L. J. (1966), *Generalised Hypergeometric Functions.* Cambridge Universtiy Press.

Stephens, M. A. (1974), EDF Statistics for Goodness of Fit and Some Comparisons. *Journal of the American Statistical Association*, **69**: 730–737.

Thode, H. C., Jr. (2002), *Testing for Normality.* Marcel Dekker.

Thoman, D. R., Bain, L. J. & Antle, C. E. (1969), Inferences on the Parameters of the Weibull Distribution. *Technometrics*, **11**(3): 445–460.

Watkins, A. J. (1998), On Expectations Associated with Maximum Likelihood Estimationin the Weibull Distribution. *Journal of the Italian Statistical Society*, **7**(1): 15–26.

Watkins, A. J. (2001), On the Likelihood Function for the Three Parameter Burr XII Distribution. *International Journal of Reliability, Quality and Safety Engineering*, **8**(2): 173–188.

Watkins, A. J. (2004), On Precision in Maximum Likelihood Estimates for the Weibull Distribution. *International Journal of Pure and Applied Mathematics*, **17**(2): 175–180.

Watkins, A. J. & John, A. M. (2004), On the Expected Fisher Information for the Weibull Distribution with Type I Censored Data. *International Journal of Pure and Applied Mathematics*, **15**(3): 401–412.

Watkins, A. J. & John, A. M. (2008), On Constant Stress Accelerated Life Tests Terminated by Type II Censoring at One of the Stress Levels. *Journal of Statistical Planning and Inference*, **138**: 768–786, forthcoming.

Watkins, A. J. & Leech, D. J. (1989), Towards Automatic Assessment of Reliability for Data from a Weibull Distribution. *Reliability Engineering and System Safety*, **24**: 343–350.

Weibull, W. (1951), A Statistical Distribution Function of Wide Applicability. *Journal of Applied Mechanics*, **18**: 293–297.

Wolstenholme, L. C. (1999), *Reliability Modelling: A Statistical Approach.* Chapman and Hall / CRC.

Appendix A : SAS Code: Fitting Weibull MLEs to Ball Bearing data

```
proc iml;

start weibmle2;
    n=nrow(wdata);
    m=sum(ind);
    c=n-m;
    cdata=(ind#wdata);
    maxc=max(cdata);
    lnx=log(wdata);
    lncx=(ind#lnx);
    lncx2=lncx#lncx;
    se=sum(lncx);
    v=log(t) - se/m;
    beta=1/(v*(1-m/(2*n)));
    *print n t m c v beta maxc;
    do iter = 1 to 10;
        lnt=log(t);
        s0=sum(ind#(exp(beta*lncx)));
        s1=sum(ind#(lncx#exp(beta*lncx)));
        s2=sum(ind#(lncx2#exp(beta*lncx)));
        f1=s0 + (c*(t**beta));
        f2=s1 + (c*(t**beta)*lnt);
        f3=s2 + (c*(t**beta)*lnt*lnt);
        ratio=f2/f1;
        pl= m * log(beta) - m * log(f1) + m*(log(m)) + (beta-1)*se - m;
```

```
        plb= m/beta - m*(ratio) + se;
        plbb= -m/(beta**2) - m * (f3/f1) + m * (ratio**2);
        beta = beta - plb/plbb;
        *print beta plb plbb;
    end;
        theta=exp((log(f1/m))/beta);
        lw=m*log(m*beta/s0) + (beta-1)*se -m;
        b10=theta*((-log(0.9))**(1/beta));
        print t beta theta b10 s0 lw;
finish weibmle2;
do;
    data={    17.88, 28.92, 33.00, 41.52, 42.12, 45.60,
            48.48, 51.84, 51.96, 54.12, 55.56, 67.80,
            68.64, 68.64, 68.88, 84.12, 93.12, 98.64,
            105.12, 105.84, 127.92, 128.04, 173.40};
    wdata=data;
    t=50;
    ind=wdata<t;

    run weibmle2;
end;
do;
    data={    17.88, 28.92, 33.00, 41.52, 42.12, 45.60,
            48.48, 51.84, 51.96, 54.12, 55.56, 67.80,
            68.64, 68.64, 68.88, 84.12, 93.12, 98.64,
            105.12, 105.84, 127.92, 128.04, 173.40};
    wdata=data;
    t=max(wdata)+0.001;
    ind=wdata<t;

    run weibmle2;
end;
quit;
```

Appendix B : SAS Code: Drawing Relative Likelihood Contours for Ball Bearing data

```
proc iml;
    /*locate MLEs*/
start weibmle2;
    n=nrow(wdata);
    m=sum(ind);
    c=n-m;

    cdata=(ind#wdata);
    lnx=log(wdata);
    lncx=(ind#lnx);
    lncx2=lncx#lncx;
    se=sum(lncx);
    v=log(max(cdata)) - se/m;
    beta=1;
    print n t m v se beta;
    do iter = 1 to 15;
        lnt=log(t);
        s0=sum(ind#(exp(beta*lncx)));
        s1=sum(ind#(lncx#exp(beta*lncx)));
        s2=sum(ind#(lncx2#exp(beta*lncx)));
        f1=s0 + (c*(t**beta));
        f2=s1 + (c*(t**beta)*lnt);
        f3=s2 + (c*(t**beta)*lnt*lnt);
        ratio=f2/f1;
        pl= m * log(beta) - m * log(f1) + m*(log(m)) + (beta-1)*se - m;
        plb= m/beta - m*(ratio) + se;.
```

```
        plbb= -m/(beta**2) - m * (f3/f1) + m * (ratio**2);
        beta = beta - plb/plbb;
        *print beta;
    end;
        theta=exp((log(f1/m))/beta);
        maxl=m*log(m*beta/f1) + (beta-1)*se -m;
        maxlike=exp(maxl);
        b10=theta*((-log(0.9))**(1/beta));
        print beta theta b10 maxl;
finish weibmle2;
do;
    data={    17.88, 28.92, 33.00, 41.52, 42.12, 45.60,
            48.48, 51.84, 51.96, 54.12, 55.56, 67.80,
            68.64, 68.64, 68.88, 84.12, 93.12, 98.64,
            105.12, 105.84, 127.92, 128.04, 173.40};
    wdata=data;
    t=75;
    lnt=log(t);
    ind=wdata<t;

    run weibmle2;
end;
/*end of locating MLEs*/
    /*defining the drawing area*/
do i=1 to 100;
j=i*0.05;
minb=beta*(1-j);
s0minb=sum((exp(minb*lncx)))+(c*(t**minb));
minbtheta=(s0minb/m)**(1/minb);
lminb=m*log(m*minb/s0minb) + (minb-1)*se -m;
likeminb=exp(lminb);
relminb=likeminb/maxlike;
print i minb likeminb relminb;
if relminb < 0.01 then stop;
*print minb;
end;
do i=1 to 100;
k=i*0.05;
maxb=beta*(1+k);
s0maxb=sum((exp(maxb*lncx)))+(c*(t**maxb));
```

```
maxbtheta=exp((log(s0maxb/m))/maxb);
lmaxb=m*log(m*maxb/s0maxb) + (maxb-1)*se -m;
likemaxb=exp(lmaxb);
relmaxb=likemaxb/maxlike;
print i maxb likemaxb relmaxb;
if relmaxb < 0.01 then stop;
*print maxb;
end;
do i=1 to 100;
j=i*0.01;
mint=theta*(1-j);
mintbeta=beta;
do iter=1 to 50;
    s0mint=sum((exp(mintbeta*lncx)))+(c*(t**mintbeta));
    s1mint=sum((lncx#exp(mintbeta*lncx)))+(c*(t**mintbeta)*lnt);
    s2mint=sum((lncx#lncx#exp(mintbeta*lncx)))+(c*(t**mintbeta)*lnt*lnt);
    lnmint=log(mint);
        d1= - m *lnmint + m/mintbeta + se +((mint**(-mintbeta))*
                  ((s0mint*lnmint)-s1mint));
        d2= (-m/(mintbeta**2))-((mint**(-mintbeta))*((s0mint*(lnmint**2))
                  -(2*s1mint*lnmint)+s2mint));
    mintbeta = mintbeta - d1/d2;
    /*print mintbeta;*/
end;
mintl=(-m*mintbeta*lnmint)+(m*log(mintbeta))+((mintbeta-1)*se)
                  -((mint**(-mintbeta))*s0mint);
mintlike=exp(mintl);
relmint=mintlike/maxlike;
print i mint mintlike relmint;
if relmint < 0.01 then stop;
*print mint;
end;
do i=1 to 100;
k=i*0.01;
maxt=theta*(1+k);
maxtbeta=beta;
do iter=1 to 50;
    s0maxt=sum((exp(maxtbeta*lncx)))+(c*(t**maxtbeta));
    s1maxt=sum((lncx#exp(maxtbeta*lncx)))+(c*(t**maxtbeta)*lnt);
    s2maxt=sum((lncx#lncx#exp(maxtbeta*lncx)))+(c*(t**maxtbeta)*lnt*lnt);
```

```
    lnmaxt=log(maxt);
        d11= - m *lnmaxt + m/maxtbeta + se +((maxt**(-maxtbeta))
                  *((s0maxt*lnmaxt)-s1maxt));
        d12=(-m/(maxtbeta**2))-((maxt**(-maxtbeta))*((s0maxt*(lnmaxt**2))
                  -(2*s1maxt*lnmaxt)+s2maxt));
    maxtbeta = maxtbeta - d11/d12;
    /*print maxtbeta;*/
end;
maxtl=(-m*maxtbeta*lnmaxt)+(m*log(maxtbeta))+((maxtbeta-1)*se)
                  -((maxt**(-maxtbeta))*s0maxt);
maxtlike=exp(maxtl);
relmaxt=maxtlike/maxlike;
print i maxt maxtlike relmaxt;
if relmaxt < 0.01 then stop;
*print maxt;
end;
/*Area defined with min & max beta and theta*/
    /*Define p and distance moved*/
p=0.99;
delta=0.01;
    /*find initial point on contour*/
x=1;
y=maxt/theta;
    do until (abs(fxy)<0.0000009);
        s0=sum(ind#(exp(beta*lncx)))+(c*(t**beta));
        s1=sum(ind#(lncx#exp(beta*lncx)))+(c*(t**beta)*lnt);
        s2=sum(ind#(lncx#lncx#exp(beta*lncx)))+(c*(t**beta)*lnt*lnt);
            s0xb=sum(ind#(exp(x*beta*lncx)))+(c*(t**(x*beta)));
            s1xb=sum(ind#(lncx#exp(x*beta*lncx)))+(c*(t**(x*beta))*lnt);
            s2xb=sum(ind#(lncx#lncx#exp(x*beta*lncx)))
                  +(c*(t**(x*beta))*lnt*lnt);
    fxy=(-m*x*beta*log(y*theta))+(m*log(x*beta))+(((x*beta)-1)*se)
           -(((y*theta)**(-(x*beta)))*s0xb)+(m*beta*log(theta))-
            (m*log(beta))-((beta-1)*se)+((theta**(-beta))*s0)-log(p);
    fxyy=((-m*x*beta)/y)+((x*beta*((y*theta)**(-(x*beta)))*s0xb)/y);
    y=y-(fxy/fxyy);
    end;
betap=x*beta;
thetap=y*theta;
fxyx=(-m*beta*log(y*theta))+(m/x)+(beta*se)+(((y*theta)**(-(x*beta)))
```

```
                    *beta*((s0xb*log(y*theta))-s1xb));
xnew= x + ((delta*fxyy)/SQRT((fxyx**2)+(fxyy**2)));
ynew= y - ((delta*fxyx)/SQRT((fxyx**2)+(fxyy**2)));
x1=x1//x; y1=y1//y; xnew1=xnew1//xnew; ynew1=ynew1//ynew;
betap1=betap1//betap; thetap1=thetap1//thetap;
x11=x1[1:nrow(x1)]; y11=y1[1:nrow(y1)]; xnew11=xnew1[1:nrow(xnew1)];
ynew11=ynew1[1:nrow(ynew1)];
betap11=betap1[1:nrow(betap1)]; thetap11=thetap1[1:nrow(thetap1)];
matrixp=x11||xnew11||betap11||y11||ynew11||thetap11;
varnames='x'//'xnew'//'betap'//'y'//'ynew'//'thetap';
create filecontour1 from matrixp[colname=varnames];
append from matrixp;
close filecontour1;
    /*moving along contour*/
/*down and left-anticlockwise*/
do i=1 to 3000;
x=xnew;
y=ynew;
    do until (abs(fxy)<0.0000009);
        s0=sum(ind#(exp(beta*lncx)))+(c*(t**beta));
        s1=sum(ind#(lncx#exp(beta*lncx)))+(c*(t**beta)*lnt);
        s2=sum(ind#(lncx#lncx#exp(beta*lncx)))+(c*(t**beta)*lnt*lnt);
            s0xb=sum(ind#(exp(x*beta*lncx)))+(c*(t**(x*beta)));
            s1xb=sum(ind#(lncx#exp(x*beta*lncx)))+(c*(t**(x*beta))*lnt);
            s2xb=sum(ind#(lncx#lncx#exp(x*beta*lncx)))+(c*(t**(x*beta))
                        *lnt*lnt);
    fxy=(-m*x*beta*log(y*theta))+(m*log(x*beta))+(((x*beta)-1)*se)
           -(((y*theta)**(-(x*beta)))*s0xb)+(m*beta*log(theta))-
            (m*log(beta))-((beta-1)*se)+((theta**(-beta))*s0)-log(p);
    fxyy=((-m*x*beta)/y)+((x*beta*((y*theta)**(-(x*beta)))*s0xb)/y);
    y=y-(fxy/fxyy);
    end;
betap=x*beta;
thetap=y*theta;
fxyx=(-m*beta*log(y*theta))+(m/x)+(beta*se)+(((y*theta)**(-(x*beta)))
                    *beta*((s0xb*log(y*theta))-s1xb));
xnew= x + ((delta*fxyy)/SQRT((fxyx**2)+(fxyy**2)));
ynew= y - ((delta*fxyx)/SQRT((fxyx**2)+(fxyy**2)));
x1=x1//x; y1=y1//y; xnew1=xnew1//xnew; ynew1=ynew1//ynew;
betap1=betap1//betap; thetap1=thetap1//thetap;
```

```
x11=x1[1:nrow(x1)]; y11=y1[1:nrow(y1)]; xnew11=xnew1[1:nrow(xnew1)];
ynew11=ynew1[1:nrow(ynew1)];
betap11=betap1[1:nrow(betap1)]; thetap11=thetap1[1:nrow(thetap1)];
matrixp=x11||xnew11||betap11||y11||ynew11||thetap11;
varnames='x'//'xnew'//'betap'//'y'//'ynew'//'thetap';
create filecontour2 from matrixp[colname=varnames];
append from matrixp;
close filecontour2;
end;
/*down and right*/
do i=1 to 3000;
x=xnew;
y=ynew;
    do until (abs(fxy)<0.00001);
        s0=sum(ind#(exp(beta*lncx)))+(c*(t**beta));
        s1=sum(ind#(lncx#exp(beta*lncx)))+(c*(t**beta)*lnt);
        s2=sum(ind#(lncx#lncx#exp(beta*lncx)))+(c*(t**beta)*lnt*lnt);
            s0xb=sum(ind#(exp(x*beta*lncx)))+(c*(t**(x*beta)));
            s1xb=sum(ind#(lncx#exp(x*beta*lncx)))+(c*(t**(x*beta))*lnt);
            s2xb=sum(ind#(lncx#lncx#exp(x*beta*lncx)))+(c*(t**(x*beta))
                        *lnt*lnt);
    fxy=(-m*x*beta*log(y*theta))+(m*log(x*beta))+(((x*beta)-1)*se)
           -(((y*theta)**(-(x*beta)))*s0xb)+(m*beta*log(theta))-
            (m*log(beta))-((beta-1)*se)+((theta**(-beta))*s0)-log(p);
    fxyx=(-m*beta*log(y*theta))+(m/x)+(beta*se)+(((y*theta)**(-(x*beta)))
                    *beta*((s0xb*log(y*theta))-s1xb));

    x=x-(fxy/fxyx);
    end;
betap=x*beta;
thetap=y*theta;
fxyy=((-m*x*beta)/y)+((x*beta*((y*theta)**(-(x*beta)))*s0xb)/y);
xnew= x + ((delta*fxyy)/SQRT((fxyx**2)+(fxyy**2)));
ynew= y - ((delta*fxyx)/SQRT((fxyx**2)+(fxyy**2)));
x1=x1//x; y1=y1//y; xnew1=xnew1//xnew; ynew1=ynew1//ynew;
betap1=betap1//betap; thetap1=thetap1//thetap;
x11=x1[1:nrow(x1)]; y11=y1[1:nrow(y1)]; xnew11=xnew1[1:nrow(xnew1)];
ynew11=ynew1[1:nrow(ynew1)];
betap11=betap1[1:nrow(betap1)]; thetap11=thetap1[1:nrow(thetap1)];
matrixp=x11||xnew11||betap11||y11||ynew11||thetap11;
```

```
varnames='x'//'xnew'//'betap'//'y'//'ynew'//'thetap';
create filecontour3 from matrixp[colname=varnames];
append from matrixp;
close filecontour3;
end;
/*up and right*/
do i=1 to 3000;
x=xnew;
y=ynew;
    do until (abs(fxy)<0.00001);
        s0=sum(ind#(exp(beta*lncx)))+(c*(t**beta));
        s1=sum(ind#(lncx#exp(beta*lncx)))+(c*(t**beta)*lnt);
        s2=sum(ind#(lncx#lncx#exp(beta*lncx)))+(c*(t**beta)*lnt*lnt);
            s0xb=sum(ind#(exp(x*beta*lncx)))+(c*(t**(x*beta)));
            s1xb=sum(ind#(lncx#exp(x*beta*lncx)))+(c*(t**(x*beta))*lnt);
            s2xb=sum(ind#(lncx#lncx#exp(x*beta*lncx)))+(c*(t**(x*beta))
                        *lnt*lnt);
         fxy=(-m*x*beta*log(y*theta))+(m*log(x*beta))+(((x*beta)-1)*se)
           -(((y*theta)**(-(x*beta)))*s0xb)+(m*beta*log(theta))-
            (m*log(beta))-((beta-1)*se)+((theta**(-beta))*s0)-log(p);
    fxyy=((-m*x*beta)/y)+((x*beta*((y*theta)**(-(x*beta)))*s0xb)/y);
    y=y-(fxy/fxyy);
    end;
betap=x*beta;
thetap=y*theta;
fxyx=(-m*beta*log(y*theta))+(m/x)+(beta*se)+(((y*theta)**(-(x*beta)))
                    *beta*((s0xb*log(y*theta))-s1xb));
xnew= x + ((delta*fxyy)/SQRT((fxyx**2)+(fxyy**2)));
ynew= y - ((delta*fxyx)/SQRT((fxyx**2)+(fxyy**2)));
x1=x1//x; y1=y1//y; xnew1=xnew1//xnew; ynew1=ynew1//ynew;
betap1=betap1//betap; thetap1=thetap1//thetap;
x11=x1[1:nrow(x1)]; y11=y1[1:nrow(y1)]; xnew11=xnew1[1:nrow(xnew1)];
ynew11=ynew1[1:nrow(ynew1)];
betap11=betap1[1:nrow(betap1)]; thetap11=thetap1[1:nrow(thetap1)];
matrixp=x11||xnew11||betap11||y11||ynew11||thetap11;
varnames='x'//'xnew'//'betap'//'y'//'ynew'//'thetap';
create filecontour4 from matrixp[colname=varnames];
append from matrixp;
close filecontour4;
end;
```

```
/*up and left*/
do i=1 to 3000;
x=xnew;
y=ynew;
    do until (abs(fxy)<0.00001);
        s0=sum(ind#(exp(beta*lncx)))+(c*(t**beta));
        s1=sum(ind#(lncx#exp(beta*lncx)))+(c*(t**beta)*lnt);
        s2=sum(ind#(lncx#lncx#exp(beta*lncx)))+(c*(t**beta)*lnt*lnt);
            s0xb=sum(ind#(exp(x*beta*lncx)))+(c*(t**(x*beta)));
            s1xb=sum(ind#(lncx#exp(x*beta*lncx)))+(c*(t**(x*beta))*lnt);
            s2xb=sum(ind#(lncx#lncx#exp(x*beta*lncx)))+(c*(t**(x*beta))
                        *lnt*lnt);
    fxy=(-m*x*beta*log(y*theta))+(m*log(x*beta))+(((x*beta)-1)*se)
           -(((y*theta)**(-(x*beta)))*s0xb)+(m*beta*log(theta))-
            (m*log(beta))-((beta-1)*se)+((theta**(-beta))*s0)-log(p);
    fxyx=(-m*beta*log(y*theta))+(m/x)+(beta*se)+(((y*theta)**(-(x*beta)))
                    *beta*((s0xb*log(y*theta))-s1xb));

    x=x-(fxy/fxyx);
    end;
betap=x*beta;
thetap=y*theta;
fxyy=((-m*x*beta)/y)+((x*beta*((y*theta)**(-(x*beta)))*s0xb)/y);
xnew= x + ((delta*fxyy)/SQRT((fxyx**2)+(fxyy**2)));
ynew= y - ((delta*fxyx)/SQRT((fxyx**2)+(fxyy**2)));
x1=x1//x; y1=y1//y; xnew1=xnew1//xnew; ynew1=ynew1//ynew;
betap1=betap1//betap; thetap1=thetap1//thetap;
x11=x1[1:nrow(x1)]; y11=y1[1:nrow(y1)]; xnew11=xnew1[1:nrow(xnew1)];
ynew11=ynew1[1:nrow(ynew1)];
betap11=betap1[1:nrow(betap1)]; thetap11=thetap1[1:nrow(thetap1)];
matrixp=x11||xnew11||betap11||y11||ynew11||thetap11;
varnames='x'//'xnew'//'betap'//'y'//'ynew'//'thetap';
create filecontour5 from matrixp[colname=varnames];
append from matrixp;
close filecontour5;
end;
/*last*/
do i=1 to 3000;
x=xnew;
y=ynew;
```

```
    do until (abs(fxy)<0.00001);
        s0=sum(ind#(exp(beta*lncx)))+(c*(t**beta));
        s1=sum(ind#(lncx#exp(beta*lncx)))+(c*(t**beta)*lnt);
        s2=sum(ind#(lncx#lncx#exp(beta*lncx)))+(c*(t**beta)
                    *lnt*lnt);
            s0xb=sum(ind#(exp(x*beta*lncx)))+(c*(t**(x*beta)));
            s1xb=sum(ind#(lncx#exp(x*beta*lncx)))+(c*(t**(x*beta))*lnt);
            s2xb=sum(ind#(lncx#lncx#exp(x*beta*lncx)))+(c*(t**(x*beta))
                    *lnt*lnt);
    fxy=(-m*x*beta*log(y*theta))+(m*log(x*beta))+(((x*beta)-1)*se)
           -(((y*theta)**(-(x*beta)))*s0xb)+(m*beta*log(theta))-
            (m*log(beta))-((beta-1)*se)+((theta**(-beta))*s0)-log(p);
    fxyy=((-m*x*beta)/y)+((x*beta*((y*theta)**(-(x*beta)))*s0xb)/y);
    y=y-(fxy/fxyy);
    end;
betap=x*beta;
thetap=y*theta;
fxyx=(-m*beta*log(y*theta))+(m/x)+(beta*se)+(((y*theta)**(-(x*beta)))
                *beta*((s0xb*log(y*theta))-s1xb));
xnew= x + ((delta*fxyy)/SQRT((fxyx**2)+(fxyy**2)));
ynew= y - ((delta*fxyx)/SQRT((fxyx**2)+(fxyy**2)));
x1=x1//x; y1=y1//y; xnew1=xnew1//xnew; ynew1=ynew1//ynew;
betap1=betap1//betap; thetap1=thetap1//thetap;
x11=x1[1:nrow(x1)]; y11=y1[1:nrow(y1)]; xnew11=xnew1[1:nrow(xnew1)];
ynew11=ynew1[1:nrow(ynew1)];
betap11=betap1[1:nrow(betap1)]; thetap11=thetap1[1:nrow(thetap1)];
matrixp=x11||xnew11||betap11||y11||ynew11||thetap11;
varnames='x'//'xnew'//'betap'//'y'//'ynew'//'thetap';
create filecontour6 from matrixp[colname=varnames];
append from matrixp;
close filecontour6;
end;
quit;
```